UNIVERSIDADE DE LISBOA
INSTITUTO SUPERIOR TÉCNICO

TESSEE - Tool for Early Stem Cells Economic Evaluation

Cátia Filipa Medina Bandeiras

Supervisor: Doctor Frederico Castelo Alves Ferreira
Co-Supervisor: Doctor Stan Neil Finkelstein

Thesis approved in public session to obtain the PhD Degree in

Bioengineering

Jury final classification: Pass with Distinction

2019

UNIVERSIDADE DE LISBOA
INSTITUTO SUPERIOR TÉCNICO

TESSEE - Tool for Early Stem Cells Economic Evaluation

Cátia Filipa Medina Bandeiras

Supervisor: Doctor Frederico Castelo Alves Ferreira
Co-Supervisor: Doctor Stan Neil Finkelstein

Thesis approved in public session to obtain the PhD Degree in

Bioengineering

Jury final classification: Pass with Distinction

Jury

Chairperson: Doctor Joaquim Manuel Sampaio Cabral, Instituto Superior Técnico, Universidade de Lisboa

Members of the Committee:

Doctor Suzanne Farid, Faculty of Engineering Science, University College London, UK

Doctor Joaquim Manuel Sampaio Cabral, Instituto Superior Técnico, Universidade de Lisboa

Doctor Mónica Duarte Correia de Oliveira, Instituto Superior Técnico, Universidade de Lisboa

Doctor Robert Abraham Gabbay, Harvard Medical School, USA

Doctor Frederico Castelo Alves Ferreira, Instituto Superior Técnico, Universidade de Lisboa

Funding Institution

FCT - Fundação para a Ciência e Tecnologia

2019

To my father, José Bandeiras, for always saying ”Every problem has a solution”, making him the first informal engineer and doctor of philosophy of the family way before me.

To my mother, sister and grandmothers, for being amazing female role models.

Acknowledgments

This four-year project was an immense adventure, shared between two countries and two cities, which challenged me professionally but, most of all, in a personal level.

First, I would like to acknowledge the funding from Fundação para a Ciência e Tecnologia (FCT), through the PhD grant PD/BD/105868/2014.

When acknowledging the people whom I worked with during the PhD, the first word of gratitude comes to my supervisors, Prof. Frederico Ferreira (iBB-IST) and Dr. Stan Finkelstein (MIT and BIDMC-HMS). I learned a lot from you, not only academically, but on how to be an independent researcher with broad interests, and I am also grateful for the support in times of struggle. You gave me the opportunity to pursue and test my (various) professional ambitions and encouraged me to be always aware of my career development, both inside and outside this project. Thank you as well for all the trust you put in me.

I want to thank Prof. Joaquim Sampaio Cabral, the PI of the Stem Cell Engineering Research Group (SCERG - iBB - IST) for welcoming me there and to all the group for helping me better understand cell culture in the lab, providing feedback on my model, and for the fun moments in the first year of thesis. Special mentions come to the people I worked the closest with: Lígia Figueiredo for being a trailblazer on early technology assessment in the field and mentorship; Prof. Cláudia Lobato da Silva, Dr. Carlos Rodrigues, Dr. Diogo Pinto, and Miguel Fuzeta, for the joint project on expansion of MSCs on the vertical wheel bioreactor, and additionally Prof. Tiago Fernandes, Dr. Carlos Rodrigues, Diogo Nogueira and João Cotovio for the collaboration on the SCERG website and social media, a side project I vastly enjoyed doing.

During my time in the US, I was a member of two research units: IDSS-MIT, where I want to thank Prof. Richard Larson and his group, and also to our Fran Marone, for the ”science salon” fun group meetings, and DCI-BIDMC-HMS, where a special word of mention comes to Dr. Charles Safran for welcoming me there and to all the group, with a special mention to Maya Molaei for the fun conversations and guidance on Python modeling, and also to Ava Atkinson for always being such a welcoming face to the division.

Regarding the cystic fibrosis project, I want to acknowledge Dr. James Chmiel and Dr. Jane Reese (Case Western Reserve University) and Dr. Greg Sawicki (Boston Children’s Hospital), with a word as well to Compass Biomedical (Ahalya Selvaraj, Yiwei Ma, Meghan Samberg and Caitlin Smith).

The diabetes project was made possible by the kind feedback of Dr. Robert Gabbay (Joslin Diabetes Center). Pertaining to this project, Dr. Jerry Ritz and Dr. Helene Negre (Dana Farber Cancer Institute) and Dr. Ramona Pop and Dr. Laurence Daheron (Harvard Stem Cell Institute) are also acknowledged for feedback on pluripotent stem cell modeling and for showing me the cell therapy core facility.

Finally, I also want to thank all the experts interviewed in this thesis. With their feedback, I had a better grasp of the market needs for cost effectiveness of stem cell manufacturing and reimbursement. A special word comes as well to Dr. Brock Reeve (Harvard Stem Cell Institute) for kindly providing several introductions.

I would like to thank to the selection committee and program coordination of the MIT Portugal Program (MPP) in Bioengineering, for the opportunity to start the PhD in 2015 with a fellowship. The first year was quite intensive and shaped what my PhD project would be. I want to thank all the professors and colleagues of the 2015 cohort, as well as my supervisors of the lab rotations: Prof. Rui Oliveira (FCT-UNL), for the opportunity to work on a startup related project, and again Prof. Frederico Ferreira, for the opportunity to get involved in a project that would become my PhD thesis. José Silva Lopes (now at REQUIMTE - FCT-UNL) was fundamental for a successful first year with all his support to the Bioengineering students. From the structure of MPP at MIT, I want to thank Flavia Cardarelli and Christian Prothman in particular.

Professionally, I would like to also thank the people who started me on research after I graduated in 2011: Dr. Gabriela Gomes (then at Instituto Gulbenkian de Ciência), Prof. António Completo (Universidade de Aveiro) and all the members of these groups for teaching me so much about being a scientist and shaping my computational skills, and also for helping me guide toward my path on computational regenerative medicine.

Somewhat unrelated to this work, but also an important experience during this PhD Thesis, was becoming an Editor of IEEE Potentials in 2018. I thank all the editorial board who trusted me and found my expertise of use to the journal. It has been a great way to also develop my editing and writing skills, something that is of great use to everyone writing a thesis.

Such an intensive work is not possible without the help of dear people on a personal level as well. I would need a much larger document to thank everyone involved in my life during these 4 years who provided some fun moments and some serious discussions about career and life goals. Here are a few special acknowledgements: - To the MPP Bioengineering cohort of 2015; - To the MPP cohort of 2017 and 2018 in Boston, for all the fun moments, trips and lunch hours; - To Renee Aird, my flatmates, and our dogs Toby and Darwin, for being a home and a family during my time in Brookline; - To the people I met online and in person through the blogging and social media science community; - To Grupo de Jovens de Mem Martins for being an ever-present influence in my life and teaching me community service and mentorship; - To my old friends for keeping in touch and offering encouragement, even when I have been in Portugal for very short periods of time during half of my PhD.

A word to Carlos, for all his support and much needed reality checks in hard times, but most of all for his love, kindness, fun spirit, and patience. It has been great to share this journey with you as we are both becoming PhDs and moving on to new chapters in our lives. You taught me more than you could ever imagine.

Finally, I want to address my close family: my uncles, aunt and cousins (with a special word to my godson Gonçalo, whom I hope to be an example to), my grandmothers and the biggest mention to my parents, Alexandra and José Bandeiras, and to my sister Carolina. Thank you for always being there for me.

Resumo

O uso terapêutico de células estaminais é promissor para várias aplicações clínicas. No entanto, são diversos os desafios a nível da produção e da adoção pelo mercado. TESSEE surge como uma nova ferramenta de avaliação económica prévia (eHTA) do uso terapêutico de células estaminais. Modelos computacionais foram desenvolvidos incorporando incerteza biológica, de processo e económica. TESSEE é personalizável para diferentes casos de estudo e está disponível gratuitamente. Nesta tese, foi aplicada a quatro casos de estudo de relevância industrial e clínica. O primeiro caso de estudo consiste na escolha do suplemento para o meio de cultura usado na produção de células estaminais/estromais mesenquimatosas (MSC). Os resultados indicam que o uso de lisado plaquetário humano reduz os custos de produção em 97% dos dadores avaliados, em comparação com o uso de soro fetal bovino. Um caso de estudo, focado na implementação de um reator de roda vertical para expansão de MSC em *microcarriers*, mostra que o uso deste sistema aumentou o número de células por lote e reduziu os custos de produção até 48% relativamente à utilização de sistemas de cultura em monocamada 2D. Foi realizada a eHTA de dispositivos contendo células beta derivadas de células estaminais pluripotentes, com o objetivo de dispensar a injeção de insulina em pacientes com diabetes tipo 1. Concluiu-se que, apesar de estes dispositivos serem muito eficazes na melhoria da qualidade de vida, uma redução do preço atual de 75% seria necessária para atingir custo-efetividade para mais de 50% da população. A produção de MSC como agentes anti-inflamatórios na fibrose quística foi estudada. Os resultados do modelo sugerem custo-efetividade quando a aplicação de MSC resulta numa redução de 50% da taxa de complicações em relação à terapêutica atual. Esta tese demonstra a utilidade da TESSEE no desenvolvimento e adoção de terapias baseadas em células estaminais.

Palavras-chave: Células estaminais, economia de bioprocessos, modelos de código aberto, medicina regenerativa, avaliação económica prévia de tecnologias de saúde

Abstract

Stem cell therapies are promising for diverse clinical indications. However, there are manufacturing and reimbursement challenges that must be addressed towards widespread adoption. This thesis presents TESSEE, a new tool for Early Health Technology Assessment (eHTA), supported on bioprocess and/or health economics models. TESSEE is developed specifically for stem cell therapies, incorporating biological, process, clinical, and economic uncertainty. Unlike other eHTA, TESSEE is an open source tool, freely available and customizable to several case studies. In order to develop and demonstrate the different features of TESSEE, four industrially and clinically relevant case studies are presented. These case studies involve mesenchymal stem/stromal cell (MSC) and pluripotent stem cell (PSC) based therapies. A study on the selection of a culture media supplement for autologous MSC therapy manufacturing determined that human platelet lysate reduced the cost of goods CoG, in comparison to fetal bovine serum, for 97% of donors. An expansion system focused case study assessed the implementation of a new vertical wheel reactor for the microcarrier-based culture of MSC. The use of this system increases the number of cells per batch, and reduces CoG/dose by up to 48% of costs of typical two-dimensional flasks for expansion. An eHTA of devices containing PSC-derived beta cells, aiming at insulin independence in type 1 diabetes patients, was performed. While these devices were very effective at improving the quality of life, a price reduction of 75% is required to achieve widespread cost-effectiveness. MSC manufacturing as anti-inflammatory agents in cystic fibrosis was modeled. The results suggest that cost-effectiveness can be reached when a reduction of pulmonary exacerbation and function decay of over 50% from the standard of care is observed. TESSEE highlights innovative strategies, aiming at reducing the manufacturing CoG. Importantly, it also quantifies the long-term value of prospective stem cell therapies, in order to secure reimbursement.

Keywords: Stem cells, bioprocess economics, open source tools, regenerative medicine, early health technology assessment

Contents

List of Figures

List of Tables

List of Abbreviations

2D	Two-dimensional
3D	Three-dimensional
AT	Adipose Tissue
ATMP	Advanced Therapeutic Medical Products
ATPS	Aqueous Two-Phase Separation
BM	Bone Marrow
BSC	Biosafety Cabinet
CAPEX	Capital Expenditure
CAGR	Compound Annual Growth Rate
CAR-T	Chimeric Antigen Receptor T-cells
CoG	Cost of Goods
CRISPR	Clustered Regularly Interspaced Short Palindromic Repeats
CBA	Cost-Benefit Analysis
CEA	Cost-Effectiveness Analysis
CF	Cystic Fibrosis
CFTR	Cystic Fibrosis Transmembrane Conductance Regulator
CHF	Congestive Heart Failure
CMA	Cost-Minimization Analysis
CUA	Cost-Utility Analysis
DALY	Disability-Adjusted Life-Years
DE	Definitive Endoderm
DES	Discrete Event Simulation

DMEM Dulbecco's Modified Eagle medium

DMSO Dimethyl Sulfoxide

DSP Downstream Processing

eHTA Early Health Technology Assessment

ESC Embryonic Stem Cells

ESRD End-Stage Renal Disease

EMA European Medicines Agency

FACS Fluorescence Activated Cell Sorting

FBC Fluidized Bed Centrifugation

FBS Fetal Bovine Serum

FCI Fixed Capital Investment

FDA Food and Drug Administration

FEV_1 Forced Expiratory Volume in 1 second

FTE Full-time Equivalent

GBP Pound Sterling

GMP Good Manufacturing Practice

GPL General Public License

GvHD Graft vs Host Disease

HLA Human Leukocyte Antigen

HCT/P Human Cells, Tissues, and Cellular and Tissue-Based Products

hPL Human Platelet Lysate

HSC Hematopoietic Stem Cells

HTA Health Technology Assessment

HVAC Heating, Ventilation, and Air Conditioning

HYE Healthy-Years Equivalent

ICER Incremental Cost-Effectiveness Ratio

IIT Intensive Insulin Therapy

iPSC Induced Pluripotent Stem Cells

LY Life Years

MACS Magnetic Activated Cell Sorting

MCB Master Cell Bank

MCDA Multiple-Criteria Decision Analysis

MEA Managed Entry Agreements

MNC Mononuclear Cells

MSC Mesenchymal Stem/Stromal Cells

NICE National Institute for Health and Care Excellence

OPEX Operational Expenditure

PBM Preference-Based Measures

PBRSA Performance-Based Risk Sharing Agreements

PEx Pulmonary Exacerbation

PP Pancreatic Progenitors

PSA Probabilistic Sensitivity Analysis

PSC Pluripotent Stem Cells

QA Quality Assurance

QALY Quality-Adjusted Life-Years

QC Quality Control

QP Qualified Person

RMAT Regenerative Medicine Advanced Therapies

SAVE Saved Young Life Equivalents

SCM Serum-containing media

SF Serum-free

SFM Serum-free media

SVF Stromal Vascular Fraction

STR Stirred Tank Reactor

T1D Type 1 Diabetes

TFF Tangencial Flow Filtration

UCM Umbilical Cord Matrix

UK United Kingdom

USD United States Dollars

WCB Working Cell Bank

WTP Willingness to Pay

VOI Value of Information

VWR Vertical-Wheel Reactor

XF Xeno-free

Chapter 1

Introduction

1.1 Motivation

1.1.1 Computational Decision Support Tools for Stem Cell Bioprocessing

Stem cell based therapies may be a breakthrough for several unmet medical needs. Their efficacy has already been proven for graft vs host disease, osteoarthritis, acute myocardial infarction and diabetic retinopathy, and clinical trials on several other prospective indications on the field of neurological diseases, diabetes and autoimmune diseases are also being explored [1, 2, 3]. The global market for cell based therapies currently generates annual profits of more than $ 1 billion, with an estimated revenue of $ 20 billion in 2025 [1, 3]. In particular, stem cells have regenerative and immunomodulatory potential to address a diverse number of unmet medical needs. Over 5400 clinical trials related to stem cells as an intervention have been reported until now, with the majority of the trials being related with adult stem cells, like the Hematopoietic Stem Cells (HSC) (1763 trials) and Mesenchymal Stem/Stromal Cells (MSC) (811). Pluripotent Stem Cells (PSC), like the Induced Pluripotent Stem Cells (iPSC) (50 trials) and Embryonic Stem Cells (ESC) (34 trials) are in an earlier stage of development [4]; despite the large interest, regulatory approval for these therapies has been difficult. However, currently, there are six approved products in specific countries and three reimbursed products, with the price of one course of therapy rising up to dozens or even hundreds of thousands of dollars [2].

The widespread application of stem cell based therapies would benefit from reducing reimbursement price, while maintaining product profitability. Moreover, the set reimbursement price must cover the research and development and clinical trials costs, but also the manufacturing costs of such therapies, which are still extremely high when compared with conventional pharma or biotherapeutic products. These large costs are due to largely manual product handling and manipulation [3], product and process variability, impractical scaling-up of production [5], use of xenogeneic materials, high culture media costs [6] and high costs of quality control [7]. Commonly used small scale planar expansion platforms, with cells cultivated in Two-dimensional (2D) surfaces, such as T-flasks, are not enough to meet market demands and ensuring maintenance of the therapeutic potential of the product. Apart from difficult scaling-up, they do not allow control and monitoring of culture parameters, lead to development of con-

centration gradients and require a lot of incubation space and manual operation [7]. Therefore, other manufacturing methods need to be adopted in order to provide more cost competitive therapies [3] and with higher possibilities of being lucrative upon the thresholds for reimbursement that the payers from several countries impose on the therapies [8].

Current process design is guided by the envisioned demand and compliance with regulatory requirements. However, design of manufacturing processes streamlining for cost efficiency, while preparing a new therapy for approval and reimbursement, is often neglected. After initial regulatory approval, further process manufacturing changes are usually administrative and their validation is cost prohibitive. In order to have a more thorough and less time consuming risk assessment of changes in process design, computational modeling of bioprocessing and bioeconomics is of great value to consider the impact of those changes on the process costs and quality of the final products given biological and technological parameters informed by past experiments. Computational decision support tools can contribute to faster, safer and less expensive production of therapies. Namely, through design of logical processes and optimization of several manufacturing parameters to achieve the lowest Cost of Goods (CoG) for a given demand of doses and lots of the therapy, as well as providing recommendations on which unit operations have higher impact on the process costs and need to be further optimized. These tools can also allow to select, for a given demand of therapeutic doses, the production configuration that ensures manufacture profitability and reimbursement prices accessible to relevant payers.

The area of computational modeling for stem cell manufacturing is a recent one and there are a few academic contributions in the field, either using commercial flowsheeting software, like Superpro Designer [9] or on custom-made code [5, 6, 10, 11]. The published models are focused on either the simulation of bioprocessing of allogeneic mesenchymal stem cell based therapies [5, 10, 11] or the simulation of manufacturing of induced pluripotent stem cell derived differentiated cells, such as cardiomyocytes [9], neurons [6] and pancreatic progenitors [12]. In terms of manufacturing challenges, the limitations of 2D culture systems were addressed in terms of cost of goods of expansion and the inability to meet high dose demands for doses containing high numbers of cells. The process strategies for overcoming these limitations, include the automation for processing of large multi stack systems as opposed to regular T-flasks, and the use of stirred tank bioreactors with microcarriers to increase expansion area. Process modeling allows to evaluate cost-effectiveness of stem cell production in suspension over planar technologies, as well as the selection of the best combinations between upstream and downstream technologies [10, 11]. While most of these studies focused on deterministic parameters and employed sensitivity analysis to determine the impact of key model parameters on final costs, stochasticity was also considered with appropriate statistical distributions through the Monte Carlo method [6, 11]. These tools can be employed for a multitude of manufacturing problems and ultimately propose technological and pricing changes in materials employed in cell manufacturing. Ongoing research is related with the evaluation of the impact of different culture medium formulations on the growth rates of cells across multiple passages and technologies to allow a more biologically based evaluation of the impact of process changes on the economics of the process [13].

Modeling frameworks that are able to integrate stem cell manufacturing bioeconomics and reim-

bursement are interesting to answer and adapt reimbursement and cost structure of stem cell therapies. Previous works mentioned the need to reduce costs of goods in manufacturing of allogeneic MSC for those to become commercially viable [10]. Biological and economic effects of using xenogeneic culture media vs xeno-free media were discuss to support a logical decision, beyond safety considerations, to move towards xeno-free media. Additional ongoing studies discuss together effects of required cell dosage and cell source considering clinical trial data and stem cell biological behavior [13]. Previous studies considered the use of planar vs Three-dimensional (3D) suspension cultures [13], again this discussion is readdressed to quantitatively highlight the key process innovations need to ensure profitability of scaled-up stem cell manufacture processes. These are critical examples illustrating the use of computing modeling results potential use to process design decision making. Computational modeling can be particularly useful as well to assess the payers' benefit when comparing conventional and regenerative therapeutic approaches.

Computational models for bioeconomics of stem cell therapy manufacturing and reimbursement are still in their early stages and have been proven to be useful to evaluate the impact of technological changes in bioprocessing in the economics of manufacturing of different types of stem cells, and to evaluate the profitability of manufactured therapies against a specific reimbursement threshold. More contributions in the field would be welcome, particularly the ones connecting manufacturing and cost-effectiveness models including stochastic processes for a more complete and risk based approach to stem cell therapies project management.

1.1.2 Early Health Technology Assessment of Stem Cell Therapies

Traditionally, health economics evaluation methods focus on the determination of value of therapies that already underwent clinical trials. Recently, it has become increasingly common to start these evaluations in the early clinical development of new therapies and devices. These approaches, called early health technology assessment (eHTA), will help to determine the commercial viability of a new therapy or technology, create guidelines for the design of the clinical trial and data to inform the models, provide uncertainty ranges that are acceptable for prospective cost-effectiveness of a new therapy, or to stop the project early and reduce costs associated with failed clinical trials or products that are not compatible with reimbursement after approval [14, 15].

While the concept of eHTA is more frequently associated with medical devices [14], there are some published approaches on cell, tissue and gene therapies [16].

Decision making tools evaluating costs, probability and quality of life outcomes are used to choose the most appropriate therapy for a given patient or population. The most simple is a decision tree method, where a decision between multiple alternatives is determined by choosing the option with the highest value, given a payoff from each alternative, that can be either monetary, quality of life, avoidance of complications, or mortality/morbility. cost-effectiveness analysis in stem cell therapies using decision trees is well established for making decisions on treatments involving HSC [17, 18].

A more complex method, encompassing different transitions between states of disease, is the dis-

ease state Markov model, using probabilities of state transition to create individual values of healthcare utilization costs and quality of life outcomes. For prospective stem cell therapy applications, this method would require establishing a cost similar to an analogous therapy, or conducting uncertainty analysis to the prospective reimbursement price. This method was used in combination with a previously implemented disease state Markov model of type 1 diabetes progression to determine the maximum difference in direct medical costs incurred by the transplantation of stem cell derived beta cells for insulin secretion allowable to have the new therapy become cost-effective in comparison with intensive insulin therapy, under the typical threshold of Pound Sterling (GBP) 20,000/Quality-Adjusted Life-Years (QALY) ($25,750/QALY) used in the United Kingdom [19]. In this study, considering a fixed utility gain per patient after a 20 year follow up period after a single transplant of 1.5 QALY, a new stem cell based therapy would be cost saving against insulin in a range of 9 to 11 years after the transplant, with costs of transplant between $100,000 and $200,000. Additionally, another way to quantify uncertainty around therapies under development is by estimating a reimbursement price and varying the effectiveness of the treatment. A recent approach taking into account stem cell based Advanced Therapeutic Medical Products (ATMP) for heart failure in France, under a Willingness to Pay (WTP) threshold of $50,000/QALY, and varying curative effectiveness of the new therapy between 0 and 100%, allowed to estimate budget impacts of the prospective new therapy on the national healthcare system between 2 and 348 billion euros [20]. Another approach to study the early economic impact of these therapies was proposed through evaluating the costs of stem cell based airway transplants under a compassionate care setting, and estimating what would be the long term effectiveness required to meet the ”end-of-life” cost-effectiveness threshold in the United Kingdom (UK) (approximately $75,000/QALY) [21].

A method that is often used in the evaluation of costs of prospective early stage therapies is the headroom method. This is a simple multiplicative method that allows to set a maximum price the prospective therapy would have based on clinical effectiveness, as assessed by health utility weights, given a threshold of willingness to pay (price the healthcare payer is willing to pay above the standard to care therapy to gain an additional unit of the chosen utility measure). While this method was used to evaluate early stage tissue engineering based therapies [22, 23, 24], there are only a few contributions in the stem cell therapy field, combined with disease state Markov models, on prospective therapies for the treatment of sepsis [25] and neurological disorders [26].

This methods has some drawbacks, such as being over simplistic and does not take into account how much manufacturing of each dose would cost, as well as being dependent on utility measures and being only directly applicable to countries that use a price appraisal system based on cost-effectiveness measures, QALY [16].

As mentioned in Section 1.1.1 of this thesis, the prospective costs of stem cell based therapies are very high in comparison to small drugs, devices and biologics. Methods to estimate the CoG, such as bioprocess economics modeling tools combining the biological growth characteristics of cells with the length and costs of the process, aid in deriving initial estimates of the costs per dose of prospective new products under considerable uncertainty [16]. Previous studies concerning cost of goods modeling and evaluating the probability of reimbursement carried a probabilistic sensitivity analysis to the reimburse-

ment price, under an United Kingdom payer perspective [27, 28]. However, these studies did not include an explicit health economics model of disease progression.

The combination of cost of goods modeling and health economics modeling using disease state Markov models for prospective stem cell therapies is a very recent field. From our knowledge, before the studies performed in the scope of this thesis, the only reported study was performed by Wallner and colleagues, where a bioprocessing protocol for allogeneic ESC based Pancreatic Progenitors (PP) manufacturing toward transplantation for Type 1 Diabetes (T1D) treatment was modeled, considering cell encapsulation to avoid immunosuppression, together with a disease state Markov model of disease progression, assuming up to four transplants throughout the follow-up period [12]. They determined that the stem cell based therapy would have a possibility of cost-effectiveness at a willingness to pay threshold of $100,000/QALY, under Canadian healthcare utilization resources. However, only therapies that are produced at a mass scale of 500 doses per year either with a scale out or scale up approach could be cost effective, and that undergoing further research in the topic would increase the likelihood of cost-effectiveness, as determined by Value of Information (VOI) analysis. However, in this work, the cost of goods calculation was simplified in comparison with other works in the field of PSC cost of goods modeling, due to the oversimplification of downstream processing bottlenecks that limit the scale of production of these therapies [9, 6].

Under the scope of this thesis, for the results chapters combining bioprocess economics with disease state transition models for cost-effectiveness analysis of prospective stem cell therapies, the aim is to provide a more complete scenario of bioprocess costs, with the inclusion of biologically determined cell growth parameters. The two results chapters combining bioprocess and health economics aim at providing guidance toward the possible effectiveness parameters that a clinical trial must accomplish to have a possibility of reimbursement, and also at providing technological improvements to reduce the costs of manufacturing together with maintaining or improving clinical outcomes.

1.2 Original Contributions

As stated in Section 1.1.1, the published works thus far in the field of bioprocess and bioeconomic modeling of stem cell therapies have focused either on commercial flowsheeting software, like Superpro Designer [9] or BioSolve Process [29] or on custom-made code, developed using the C# language within the .NET framework linked to Microsoft Access databases [5, 6, 10]. These frameworks, albeit valuable, have several pitfalls. The SuperPro Designer approach offers a more rigid framework in terms of the building blocks, has a limited number of blocks per sheet (25 in the academic version) and generally overestimates the costs of production in an industrial setting (as assessed by expert opinion), apart from being only available for Windows platforms and having license costs. Regarding the C# environment, it has discrete event simulation packages as required to accomplish these simulations and is a powerful language that can be used in several operating systems but is not an open-source language. The open-source implementation is an interesting point for the project due to the ease that interested partners or students would have to install the tool without having to pay a license for the source programming

language. Bearing this in mind, in this project we will innovate in comparison to the previous works and implement the tool using the open-source programming language Python, freely available for several operating systems and enabling discrete event simulation through the SimPy library.

The bioprocess economics studies currently published in the field of stem cell therapies, aiming at solving problems on the expansion side, are focused on the comparison of cell throughput and costs using established expansion technologies, such as T-flasks and cell factories, with new 3D, suspension platforms, such as stirred tank bioreactors [5, 30, 28, 9], packed bed and hollow fiber bioreactors [30], and the impact of automation to manipulate high volumes of cell factories [5] for different doses, cell number, and lot demands. However, up to date, there are no studies comparing different sources of MSC from the cost-effectiveness standpoint, the replacement of animal serum-containing culture media with animal component-free culture media, or the impact of Vertical-Wheel Reactor (VWR), a new bioreactor configuration aimed at providing a more homogeneous fluid mixing than Stirred Tank Reactor (STR) and generate higher cell throughputs at lower power inputs and agitations speeds [31, 32, 33]. Chapter 4 is focused on the economic feasibility of a transition toward a xeno free culture media for MSC, while chapter 5 is related to the transition from a planar expansion process of Adipose Tissue (AT) and Umbilical Cord Matrix (UCM)-MSC to a VWR expansion using xeno-free culture media.

The concept of connection of the cost of goods with the reimbursement potential is recent and is under the scope of eHTA [14, 24]. Hassan et al have determined an estimated target reimbursement value and stipulated that, for a therapy to become commercially viable, the costs of goods needed to be below 15% of the maximum reimbursement value [10]. However, in real case-scenarios, the maximum reimbursement values are not constant and depend on a myriad of factors such as the direct medical costs, indirect costs related with loss or gain of productivity through the new therapy, cost of complications averted, gains in life years or quality of life for the patients, and budget impact on health care systems [34, 35, 36]. Based on cost-effectiveness analysis, considering QALY as the clinical effectiveness outcome, a recently published analysis combined cost of goods of prospective stem cell derived type 1 diabetes therapies with a disease state transition Markov model for disease progression [12]. While one of the clinical case studies of this PhD thesis is the manufacturing and cost-effectiveness analysis of stem cell therapies for type 1 diabetes as well, the aim is to innovate by addressing banking and downstream process contributions more explicitly, as these are factors that limit the throughput of these therapies. The other clinical case study is the first study on cost-effectiveness of stem cell therapies as anti inflammatory agents for Cystic Fibrosis (CF), as they are currently in a phase 1 clinical trial [37]. This study aims to provide cues on how to improve manufacturing costs and to drive possible clinical effectiveness ranges to ensure the viability of the clinical trial toward approval and reimbursement.

1.3 Aim and Research Questions

A gap in the literature in bioprocessing and early health assessment tools for stem cells was identified. Up until now, there were no reported open source models for bioprocess and health economics modeling in the stem cell field. Additionally, the works on eHTA, combining bioprocess and health eco-

nomics modeling for a specific therapeutic challenge that can be solved by stem cells, were very scarce. An assessment of prospective effectiveness and healthcare costs, in combination with current cost of goods and manufacturing supply, can provide cues on where to improve manufacturing and effectiveness towards a more likely reimbursement of these expensive therapies. This thesis aims to answer four research questions in this field as applications of TESSEE. These applications helped promote the development of all different modules and capabilities of the tool and framework:

1. **Cost-effective process transfer from an animal-based culture media supplement (Fetal Bovine Serum (FBS)) to a xeno-free culture media supplement (Human Platelet Lysate (hPL)) for manufacturing autologous Bone Marrow (BM)-MSC** (Chapter 4).

   (i) How can experimental data on multi passage growth of BM-MSC with an animal containing culture media supplement (FBS) or with a xeno-free culture media supplement (hPL) provide information for the calculation of the cost of goods of autologous BM-MSC therapies?

   (ii) How does donor-to-donor variability in the isolation and expansion process impact the distribution of the total costs of goods per dose?

   (iii) For what ranges of cost, process, and biological parameters, is the process transfer to a more expensive xeno-free media cost-effective?

2. **Cost-effective process transfer of expansion of adipose tissue MSC (AT-MSC) and umbilical cord matrix MSC (UCM-MSC) from two-dimensional cell culture flasks to a vertical wheel bioreactor** (Chapter 5).

   (i) How can experimental data on the expansion of AT-MSC and UCM-MSC on two-dimensional flasks or a new microcarrier-based system with a vertical wheel bioreactor provide information for the calculation of the cost of goods of allogeneic AT-MSC or UCM-MSC therapies?

   (ii) How does the process transfer to a bioreactor based system affect the number of cells and doses per batch and the total number of batches obtained from a single AT or UCM donor?

   (iii) How do the batch size and the total number of batches drive changes in the cost of goods per dose?

   (iv) What are the process components that are affected by the process transfer to the bioreactor based system?

3. **Early health technology assessment, combining bioprocess and health economics modeling, of stem cell-based devices containing pluripotent stem cell (PSC) derived beta cells as an implantable therapy for type 1 diabetes (T1D)** (Chapter 6).

   (i) To what extent does an increase in the annual production of stem-cell based devices containing PSC derived beta cells reduce the costs of goods?

   (ii) What are the process resources and stages that are affected the most by an increase in the number of patients treated per batch, and the number of patients treated per year?

(iii) What process factors need to be optimized for the most impact in the reduction in the cost of goods of the devices?

(iv) Assuming that cost of goods are 25% of the final price of the devices, and that clinical effectiveness of the stem cell-based devices is similar to what is known for cadaveric islet transplantation, to what extent are the stem cell-based therapies cost-effective, in comparison with insulin intensive therapy, for T1D patients?

(v) Based on willingness to pay thresholds associated with healthcare payers and the prevention of diabetes-related complications, to which patients should the stem cell-based therapy be administered first?

4. **Early health technology assessment, combining bioprocess and health economics modeling, of BM-MSC as an anti-inflammatory therapy for cystic fibrosis** (Chapter 7).

(i) Given the current manufacturing setting for a Phase I clinical trial of allogeneic, fresh BM-MSC as anti-inflammatory agents for cystic fibrosis, what are the costs of goods per dose?

(ii) For what rate of reduction Pulmonary Exacerbation (PEx) and decay of pulmonary function is the annual infusion of BM-MSC, paired with daily disease modulator therapy, cost-effective in comparison with modulator therapy only?

(iii) Assuming that cost of goods per dose of BM-MSC is 20% of the final product price, to what combinations of clinical effectiveness and willingness to pay thresholds is the BM-MSC annual administration cost-effective?

1.4 Research Strategy

There are diverse strategies that could be followed in the development of the eHTA tool and in terms of case studies to be addressed. However, in the scope of the thesis, a finite set of strategies was employed for the best results, taking into account key desired attributes for modeling bioprocess and health economics of stem cell therapies under considerable uncertainty:

- Provide a platform to simulate the operation of a facility for stem cell bioprocessing and enable the calculation of the cost of goods. This platform should be flexible enough to allow modeling of allogeneic and autologous bioprocesses. Additionally, in order to mimic the biological variability of inputs and outputs, the modeling and simulation approaches should allow easy implementation of probabilistic distributions and random sampling of input values from these distributions. This will allow to derive probabilistic distributions of outputs, such as the number of cells per batch, and the cost of goods per dose.

- Use the CoGs to derive acceptable prices for scenarios in an individual simulation of disease progression.

- Allow fast and parallel simulation of facility operations, replicating the real cases where several operations in a facility can be performed at the same time, and enabling scale-out manufacturing.
- Easy and fast handling and processing of large volumes of data, generated by a sizeable number of individual simulations.
- Compliance with recent literature in pharmacoeconomics, recommending improved transparency of cost-effectiveness analyses and open source development in economic evaluation [38, 39].

1.4.1 Choice of programming language for development of the open source assessment tool

Aiming at free distribution for educational purposes, it was important that the programming language for development was open source as well. Furthermore, for faster simulation running times, discrete event simulation is a practical paradigm for advancing computational times in events with fixed duration, such as the manufacturing operations in stem cell culture. Two of the most widely used open source programming languages in biomedical research, R and Python, were considered for this purpose. Ultimately, Python was chosen for the following reasons:

- R is a language following the functional programming paradigm, while Python is an object oriented programming language. Functional programming languages focus on the computation of functions with defined inputs and outputs. Object oriented programming focuses on the creation of objects from instances called classes (e.g. a car is a class that can generate objects with multiple attributes, such as color, number of seats, type of fuel, etc). Object oriented programming makes it easier to specify different attributes in a stem cell manufacturing facility, such as the flasks where cells are contained, the cell donors, and the equipment where cells are processed.
- While both R and Python have libraries (in the former) and modules (in the latter) for discrete event simulation (Simmer in R and SimPy in Python), due to the previously mentioned motivation, SimPy was the discrete event simulator of choice.
- Python has very well developed models for data analysis and transfer of files via CSV and text files, such as Pandas and NumPy, that are widely used by the data science community.

1.4.2 Types of stem cells

Since this work is aimed at eHTA, the goal would be to address innovative therapies that are not approved yet in a widespread manner, as opposed to traditional cost-effectiveness analysis to therapies that already underwent a clinical trial and were approved for commercialization by regulatory agencies. For this reason, hematopoietic stem cells (HSC) were excluded from this analysis, as they are widespread treatments for hematologic malignancies in several countries. Two types of stem/stromal cells were addressed in the scope of this thesis:

- Mesenchymal stem/stromal cells (MSC) due to their versatility as addressed by many clinical trials in diverse applications and anti-inflammatory properties, and the ease of collection and expansion from different sources. Analyses using the most traditional MSC source, bone marrow (BM), were performed, but the culture of adipose stem/stromal cells (ASC) and umbilical cord matrix (UCM) was also modeled, as they are seen as more sustainable MSC niches, involving less invasive collection methods.
- Pluripotent stem cells (PSC), either embryonic (ESC) or induced pluripotent (iPSC), due to the possibility of being differentiated into any type of terminal cell for regenerative medicine purposes, as well as for drug screening and toxicology assays. Due to the differentiation and reprogramming (when required) protocols, these cells are much more expensive than MSC to manufacture.

1.4.3 Types of culture media

In the studies involving mesenchymal stem/stromal cells, the type of culture media was assessed in order to address the cost-effectiveness of a process transfer from an animal original based culture media supplement (fetal bovine serum – FBS) to an animal component free culture media supplement, based on human platelet lysate (hPL). The process transfer is driven by regulatory agency recommendations for minimization of the use of animal derived components in human cell culture. As hPL is currently more expensive than FBS, modeling studies involving the tradeoff between improved cell yields and a more costly culture media supplement address the total cost per dose to determine if the investment in an animal free culture media is a cost effective investment. In the studies involving pluripotent stem cells, the culture media formulation for PSC expansion is based on mTeSR, in agreement with the modeled experimental protocols. For differentiation, custom made media with different costs for each stage of differentiation will be modeled for a more specific range of full manufacturing costs.

1.4.4 Types of expansion platforms

Since high numbers of stem cells (or stem cell derived differentiated cells) are required, in the order of millions to billions of cells per dose per patient, the supply of “off-the-shelf” stem cell products in limited by the expansion areas and volumes and the downstream processing volume bottlenecks. Additionally, traditional 2D culture flasks do not allow in line monitoring and control of metabolite and nutrient gradients that might impair cell potency. Higher culture yields can be reached by using 3D expansion platforms, such as spinner flasks and bioreactors. In the case of adherent cell types, such as MSC, microcarriers for cell adhesion are required. While, in the genesis of this work, stirred tank bioreactors were modeled and data from cell expansion in stirred tank bioreactors was used for a preliminary conference work. Building from this setup in the model, a new type of bioreactor, the Vertical Wheel Reactor^{TM} (VWR) by PBS, was modeled since it is a more innovative approach that can be scaled up to higher culture volumes and allows a more efficient stirring than traditional impellers, avoiding shear stress and nutrient gradients that are detrimental to cell quality attributes (Chapter 5). However, three of the four results chapters (Chapters 4, 6, and 7) were modeled using data from 2D technologies, as

it was challenging to find published experimental multi passage expansion data of stem cells using 3D expansion and differentiation platforms.

1.4.5 Type of health economics modeling

In order to address the value of prospective stem cell therapies against a standard of care, at the current high cost of manufacturing, it is impossible to have profitable products that would cost the same per dose as a small drug or a biologic. Furthermore, it is expected that the new therapies would have a higher clinical effectiveness than standards of care to be used. Therefore, an analysis that combines cost and effectiveness would be ideal. A typical measure of clinical effectiveness used by the academic community and recommendations for reimbursement in countries with single payer healthcare systems is the quality-adjusted life-years (QALY). These analysis adjust the life expectancy by the perceived quality of life in a scheme of life utility between 0 and 1. The difference in costs and QALY between the new stem cell therapy and the standard of care will provide an Incremental Cost-Effectiveness Ratio (ICER) that must be compared with a willingness to pay threshold used for reimbursement recommendations.

1.4.6 Clinical Applications

With the aim of connecting manufacturing with clinical delivery and prospective reimbursement of cost-effective stem cell based therapies, specific clinical applications were derived for a combined bioprocess and cost-effectiveness analysis:

- Type 1 diabetes, due to the establishment with a clinical collaboration involved in the stem cell consortium for encapsulated beta cells derived from pluripotent stem cells for implantation in type 1 diabetes patients. These therapies aim at restoring glucose dependent insulin secretion and a phase I/II clinical trial was recently completed in the field. The standard of care for comparison in the cost-effectiveness analysis for this therapy is the intensive administration of insulin.
- Cystic fibrosis, due to the establishment of a collaboration for modeling manufacturing of MSC for a pioneer phase I clinical trial aiming at reducing inflammation in cystic fibrosis patients infected with opportunistic pathogens. The cost-effectiveness analysis of disease modulators with MSC as adjuvant anti inflammatory agents was performed against a standard of care of disease modulators alone.

1.4.7 Modeling of biological uncertainty

Stem cell from different donors have different growth and potency attributes. Apart from the intrinsic donor to donor differences in stem cell growth, cells also respond differently to different culture media supplements, expansion technologies, nutrient concentrations, duration of expansion, and purification technologies. Additionally, the impact of a new therapy in the quality of life of patients is related to the probability of mortality and/or morbidity when managing the disease. Complications from the disease also increase direct medical costs due to additional hospital visits and ancillary care. The modeling

of a combination of intrinsic cell, bioprocessing, and patient variability is modeled through stochastic simulation. The stochastic simulation is made possible by the Monte Carlo approach where, at each run of the model, values of key parameters are randomly sampled from an appropriate probabilistic distribution derived from real world cell and patient data.

In the bioprocess models, parameters for which there is information from more than one donor (or multiple expansion runs from the same donor) are those from which published experimental data allows to extract either a mean and a minimum-maximum parameters range, or a mean and a standard deviation. In order to avoid the existence of negative parameters in the parametric space, a triangular distribution, using a mean, minimum and maximum value was input using the experimental values. For each run of the model, the code samples randomly a parameter value from within the range specified in the triangular distribution for that parameter. With that, each run will provide different outputs in terms of number of cells per passage, total process time, and total cost of goods per dose, as inputs that drive the calculation of these outputs are changed.

In the health economics models, the annual probability of each patient having a state transition, or suffering from a disease related complication, is kept fixed. In each year, the sampling of the ocurrence of an event of transition or complication is mediated by a binomial distribution with the probability of event as specified. Whenever the coded binomial distribution yields an event (i.e, the output of the binomial distribution is 1), the patient undergoes a state transition.

In the beginning of the health economics model, the initial state of each patient is sampled from appropriate distributions. The age and weight (when applicable) of the cohort are sampled from uniform distributions within a range of maximum and minimum values for that parameter. An uniform distribution assumes that, within the range of values this parameter can have, the probability of each value ocurring is the same. When calculating the initial state of the patient in terms of disease severity, the initial health state is sampled from a multinomial distribution. A multinomial distribution is the probability of the parameter (in this case, health state) having more than two possible values. The total probabilities of these events sum to 1.

1.5 Thesis Outline

The following main chapters organize the work conducted in the scope of this thesis:

- State of the Art (Chapter 2), covering the concepts analyzed in this thesis: stem cells, with considerations on applications, market, bioprocessing and manufacturing; bioprocess modeling, covering the methodologies, technical and cost drivers; and an introduction on health economics for the contextualization of decision making models and cost-effectiveness analysis.

- Model Implementation (Chapter 3), detailing the modular structure of the bioprocess economics and health economics model, the most relevant equations used for modeling the results chapters, and validation examples of works from published literature using other softwares/proprietary code.

- Results and Discussion (Chapters 4-6), describing the results on the process transfer to a xeno-free culture media for manufacturing of MSC based therapies (Chapter 4), the process transfer from a planar to a 3D, vertical wheel reactor based manufacturing of MSC therapies (Chapter 5), the evaluation of process bottlenecks and cost-effectiveness acceptance in a population of patients with type 1 diabetes (T1D) that could be subject to a pluripotent stem cell (PSC) based beta cell loaded device for independent insulin secretion and glucose control (Chapter 6), and the optimization of manufacturing and clinical effectiveness of a MSC therapy with anti inflammatory action in cystic fibrosis patients (Chapter 7).
- Conclusions and Future Work, summarizing the main assumptions, providing thoughts on how the implemented model can contribute for raising awareness in technological, clinical and reimbursement issues hindering development and deployment of stem cell based therapies, and suggesting future applications and development of the modeling approaches.

Chapter 2

State of the Art

2.1 Stem Cells

2.1.1 Definition of stem cells

Stem cells are defined by their ability for self-renewal and production of differentiated progeny comprised of several cell types. With every cell division, either two new stem cells are generated, or two differentiated cells, or one stem cell and one differentiated. The differentiation is dependent on signaling mechanisms that induce cell maturation into a given lineage. Due to these properties, these cells are seen as very versatile. Therefore, they are an attractive clinical candidate for the regeneration of damaged tissues or the treatment of degenerative diseases, disease modeling, and drug screening [40, 41, 42].

According to their differentiation potential, stem cells can be classified into one of four types [43]:

- **Totipotent cells:** Potential to give rise to any and all human cells that compose an entire functional organism. The only human totipotent cells are the fertilized egg (zygote) and the cells produced by its division in the first four days;
- **Pluripotent cells:** Cells that can generate all tissue types but not an entire functional organism. Embryonic stem cells and induced pluripotent stem cells belong to this category;
- **Multipotent cells:** Progenitor cells that give rise to a limited range of cells within a tissue type;
- **Unipotent cells:** Precursor cells that differentiate into only one type of cells. The testis stem cells are an example of unipotent cells.

Regarding the source of stem cells, the following groups are defined [43]:

- **Embryonic stem cells (ESC):** Pluripotent stem cells derived from the inner mass of the blastocyst;
- **Induced pluripotent stem cells (iPSC):** Pluripotent stem cells originated from a non-pluripotent cell, generally an adult somatic cell, by cell reprogramming;

- **Adult stem cells:** Originate from the three primary germ layers of the human embryo. Clinically relevant stem cells, like the hematopoietic and mesenchymal, belong to this category;
- **Cancer stem cells:** Responsible for the maintenance of cancers, have been detected in most of the cancers.

2.1.2 Applications of stem cells

The most typical applications of stem cells are therapeutic product development, research, and drug screening/disease modeling. However, there are other applications not necessarily related to human stem cells. Examples are wildlife preservation or restoration of extinct species, improvement of crops, and enhancement of cosmetic products [44].

Therapeutic applications

Human stem cells used in therapeutic applications come either from autologous or allogeneic sources. In autologous therapies, the cells from the patient are multiplied (i.e., expanded) and then administered back into the patient. Allogeneic therapies involve one universal donor that is expanded over a larger scale to provide therapies to multiple patients [45].

Autologous therapies are preferable in cases where immunosuppression from an allogeneic transplant is a serious health concern. Since each batch of doses will only be administered to one patient, not many doses are required. These therapies are amenable to parallel processing (i.e, scale-out), and quality controls are performed on a donor-to-donor basis [45, 46].

Allogeneic therapies are helpful when the cells of the patient have abnormalities that impair their therapeutic ability, and when costs of goods (COG) need to be reduced. Since one donor fits several patients, allogeneic therapies benefit from economies of scale through a scale-up approach of manufacturing. However, they involve more complex logistics than the autologous therapies, due to the establishment of intermediate banking steps, and the possibility of a higher impact of batch failure in quality controls, as the batch sizes are higher than for autologous therapies [45, 47].

Stem cell-based therapies have been researched for a very diverse number of indications due to their regenerative, immunomodulatory, pro-angiogenic and potential gene delivery properties [1, 48, 49]. The first clinical application was accomplished in 1968 when the first transplant of human hematopoietic stem cells was successful and has since become a routine procedure for bone marrow regeneration [3]. It is estimated that more than 50,000 hematopoietic stem cell transplants occur every year worldwide. More than 1500 hospitals or centers perform this procedure, a number expected to grow [50].

The first approval of a mesenchymal stem/stromal cell (MSC) based product was granted to Cellgram-AMI (formerly HeartiCellGram), produced by Pharmicell in South Korea [49] for the treatment of post-acute myocardial infarction. This therapy is based on autologous bone marrow-derived MSC. However, phase II/III clinical trials were performed after marketing approval and did not manage to prove a significant improvement on the primary endpoints in comparison with the placebo [51].

Also in South Korea, Cartistem by Medipost was approved in 2012 as an allogeneic umbilical cord blood-MSC therapy for the treatment of osteoarthritis [49] and is currently undergoing clinical trials for possible market approval by FDA in the United States. In 2015, Medipost reported good safety and efficacy results 7 years after Cartistem injection [52].

The first autologous AT-MSC based therapy approved is Cupistem by Anterogen, having been granted market approval in South Korea in 2012 for the treatment of Crohn's fistula. For Cupistem, clinical trial data was not made public [53].

In countries other than South Korea, two MSC-based products were approved. TEMCELL (formerly known as Prochymal), an allogeneic BM-MSC based product for the treatment of acute Graft vs Host Disease (GvHD) in children, was manufactured by Osiris and granted approval in Canada and New Zealand in 2012 and is available in the US for compassionate use [53]. However, the therapy was never commercially launched in those countries. Since Osiris was acquired by Mesoblast and the product was renamed as TEMCELL, approval was granted in Japan in 2016 through its licensee JCR Pharma and was approved for reimbursement [54].

In 2018, Alofisel, a product by TiGenix for complex perianal fistulas related to Crohn's disease, was the first allogeneic adipose stromal cell-based therapy approved in Europe [55].

Currently, there are no adult stem cell suspension therapeutic products approved in the USA apart from hematopoietic stem cell transplants. However, there are two combination products approved by the Food and Drug Administration (FDA) which consist of the combination of MSC with an allogeneic bone matrix for orthopedics applications: Allostem, by AlloSource, is a cellular bone allograft with AT-MSC and Trinity Evolution, by Orthofix, contains MSC from an unspecified source and osteogenic precursor cells (OPCs) [56].

In the human pluripotent stem cell space, the first clinical trial with ESC was performed in 2010 for the treatment of spinal cord injury, without adverse events, but also without any relevant improvement in motor or sensory function [57]. Since then, trials aiming at treating retina macular degeneration [57], type 1 diabetes [57] and heart conditions have been conducted with varying degrees of success [57]. With the advent of iPSC, an experimental procedure was performed in 2014 with iPSC-derived retinal pigment epithelial cells for the treatment of macular degeneration. The clinical trial was planned to continue in other patients but it was suspended in 2015 due to genomic instability of iPSC, raising concerns about the reprogramming procedure used and turning the procedure from autologous based to allogeneic based [48, 57, 58]. More recently, authorizations for trials involving iPSC for cardiac regeneration [59] and Parkinson's disease [60, 61] were granted in Japan.

Despite the fact that there are few currently approved products based on stem cells for clinical application, significant research and clinical trials have also been conducted for autoimmune diseases, such as Crohn's disease [62], type 1 diabetes [63] and rheumatoid arthritis, as well as for neurological conditions like spinal cord injury [64], multiple sclerosis (MS) and amyotrophic lateral sclerosis (ALS) [65], Alzheimer's [66] and Parkinson's disease [67].

Drug screening and disease modeling

Drug screening and disease modeling in pre-clinical stages rely on animal models. However, there is a poor correlation between effectiveness and toxicity events in pre-clinical animal models and the events in clinical trials [68]. Therefore, human-based, patient-specific, *in vitro* pre-clinical assays for drug screening and toxicity are invaluable for improving the targeting of drugs in the tissues and populations of interest.

The advent of reprogramming technology to generate iPSC allowed to improve the study and targeting of therapies for genetically associated diseases, in the context of precision medicine. The differentiation of these patient-specific cells in cell types related to the disease enables the study of more specific drug effects and toxicity events in pre-clinical studies [69, 40]. Such 2D platforms are useful in creating high throughput screenings to assess the therapeutic and toxicological profile of different compounds on cells of interest [68].

Additionally, a more sophisticated method of disease modeling is the establishment of tridimensional tissue-like structures, called organoids, resembles spatial organization of tissues, cell-cell interactions, and interactions with external molecules and pathogens more thoroughly [40, 70]. Organoids were successfully generated from iPSC for a variety of tissues and organs: retina [71], kidney [72], central nervous system [73], heart [74], liver [75], and gastrointestinal tract [76]. They can be integrated into organ-on-a-chip devices and mimic a circulatory, multi-organ environment through microfluidic channels [77].

2.1.3 Market Landscape

Stem cells constitute a highly valued market. In 2016, the market value was estimated in $6.7 billion and it is estimated to reach a value of $12.3 billion in 2021, with a Compound Annual Growth Rate (CAGR) of 13.1%. The most relevant applications of stem cells are the establishment of therapeutic products, drug screening, and disease modeling and research purposes [78, 79].

The therapeutic perspectives for stem cells are growing at a very fast pace, with a CAGR of 39.5% from 2015 to 2020, with an expected value of $330 million by 2020. This growth is powered by the increasing number of late-stage clinical trials using mesenchymal stem cells (MSC), induced pluripotent stem cells (iPSC) and embryonic stem cells (ESC) [78, 79, 80, 81].

The global stem cell market is generally segmented geographically into North America, Europe, Asia Pacific and rest of the world. North America has currently the highest market share of 25% of the total and a market value of $2.0 billion in 2013. Europe was valued as a market to $1.4 billion in 2013 and is expected to grow at a CAGR of 13.4% until $2.4 billion in 2018. However, Asia-Pacific is the market with the fastest growth, with a CAGR of 25% mostly due to contract research outsourcing in this area and medical tourism [78, 79, 80, 81].

The stem cell research product market is also highly valuable and includes culture media and reagents, growth factors, tools for identification, purification and analysis, isolation, expansion and differentiation methods and the establishment of stem cell lines. This market is a part of the global cell

expansion market, valued at $8.34 billion in 2016 with a CAGR of 17.6% through 2021, with an expected market value of $18.76 billion [82, 83].

In terms of market value for each type of stem cells, some considerations may be drawn from recent reports. As of 2013, adult stem cells largely dominated the market with 80% of market share. However, induced pluripotent stem cells are a fast-growing market, with an estimated market value of $1.2 billion in 2013 and an expected market value of $2.9 billion in 2018 at a CAGR of 19.7% [80].

The major industrial players in the field of stem cell therapies are Mesoblast Ltd. (Australia), Aastrom Biosciences, Inc., Celgene Corporation and StemCells, Inc. (USA). In the market of stem cell research products, the industry leaders are Thermo Fisher Scientific, BD Biosciences, Merck KGaA, Miltenyi Biotec, STEMCELL Technologies, Lonza, Clontech and GE Healthcare [78, 79, 80, 81].

Another very attractive application for stem cells is the establishment of drug screening platforms, toxicity testing, and disease modeling. These platforms are obtained by controlled differentiation of PSC and may allow screening more compounds in less time and with fewer costs than what is currently possible by using cell lines and model organisms. The fact that the screening is done in human cells and, in some cases, in patient-specific cells for personalized treatments, may reduce the failure rates of compounds that go through the clinical trial phase because of biological differences between humans and model organisms. This application is integrated into the high throughput screening (HTS) market, with an expected market value of $M 19.6 in 2018 at a CAGR of 7.4% and is dominated by pharmaceutical companies [82, 83].

While this technology has gathered industrial interest, it is still in a very early phase of development and most of the approaches have been related to basic research. The therapeutic areas where stem cells for disease modeling and drug screening have been used the most are cancer research, diabetes, and neurological disorders. The key industrial players in this market segment are BD Biosciences, Cellular Dynamics International, EMD Millipore, GE Healthcare, Life Technologies and Lonza [82, 83].

2.1.4 Regulatory landscape

Europe

Stem cell-derived therapeutic products fall under the scope of the advanced therapy medicinal products (ATMP) category of the European Medicines Agency (EMA), through Regulation EC No. 1394/2007. ATMPs are medicinal products based on cells or genes, for which the cells, genes or tissues are the product. While the manufacturing of these products is, at the moment, in a considerably lower scale than those of small molecule drugs and biologics, the same quality control requirements are imposed, including compliance with Good Manufacturing Practice (GMP). Like other therapeutic products, ATMPs are subjected to clinical trials before approval, a process that generally takes 10-15 years [84]. However, some products may receive a conditional marketing authorization, in the case a seriously life-threatening unmet medical need is fulfilled, the product is aimed at emergency situations, or treats an orphan disease (incidence below 5 in 10,000 individuals). Under the conditional marketing authorization, while the clinical data is incomplete, the access to the therapy is provided when the risk-benefit profile is promis-

ing. The marketing authorization is granted for one year and may be converted into a full marketing authorization once post-marketing clinical data is positive [85, 84, 86, 87].

However, some therapies are exempt from a full clinical trial. The Hospital Exemption rule allows an ATMP, prepared on a non-routine basis and adhering to specific quality standards, and exclusively administered in a hospital by a medical practitioner, to be administered without a prior marketing authorization. As of 2017, Hospital Exemptions in member states are only granted in situations of high unmet medical need, when no treatment alternatives exist [88].

When approved, ATMPs are authorized for commercialization in the European Union (EU) due to the centralized approval procedure by EMA. However, distribution and reimbursement in individual EU countries are dependent on governmental agencies [86].

United States

Stem cells therapies fall in the scope of Human Cells, Tissues, and Cellular and Tissue-Based Products (HCT/P). They can be regulated either by the Center for Biologics Evaluation and Research (CBER) or by the Center for Devices and Radiological Health (CDRH) depending on the nature of the product. The products regulated by CBER are regulated by different sections [89]:

- **Section 351:** More than minimally manipulated therapies, requires clinical trials for market approval (e.g. unrelated allogeneic hematopoietic stem cells)
- **Section 361:** Minimally manipulated, does not require a clinical trial and pre-market approval but needs to guarantee prevention of transmission of infectious diseases (e.g. hematopoietic stem cells from donor's umbilical cord blood)

For most stem cell therapies, section 351 applies. In order to streamline the approval of Regenerative Medicine Advanced Therapies (RMAT), the 21st Century Cures Act, enacted December 13rd, 2016, provided guidelines for expedited development of these therapies. The designation grants similar benefits to breakthrough therapy designation to sponsors of a clinical trial, as long as preliminary clinical evidence indicates that therapy addresses unmet medical needs. There are two specific benefits of the breakthrough therapy designation of major relevance to stem cell therapy development. First, the possibility of frequent meetings with the FDA for efficient drug development, starting from Phase 1 of the clinical trial. Second, the therapy in development can be eligible for accelerated approval (approved on the basis of a surrogate endpoint) and for priority review (a process of application review of 6 months, instead of the usual 10 for New Drug Applications) [89].

Other regions

Besides the EU and USA, it is important to mention the regulatory landscape in Japan and Korea.

The regulatory schemes in these two countries are considerably fast-tracked, favoring expedited marketing approval, conditional on a period of post-marketing surveillance.

Japan introduced a fast track for regenerative medicine therapeutics in 2014. Regenerative medicines include human cell and tissue-based biologics. Conditional, limited-term marketing approval of up 7 years for these therapies was introduced. This marketing approval is granted as long as early-stage clinical trials demonstrate safety and good indications for efficacy. Additionally, these products are eligible for reimbursement at the national healthcare system. The payer would cover for 70% of the therapy costs [90]. However, this legislation is controversial, due to the possibility of products of unknown efficacy being approved and made profitable at very high costs due to payments by the healthcare system and patients [90, 91].

Korea was the first country to implement conditional approval for cell and tissue-based therapies [92, 93]. Under this scheme, as of 2015, 16 cell therapies had been approved, including 4 stem cell therapies. However, the lack of peer-reviewed data and demonstrated clinical effectiveness led to concerns [94].

2.1.5 Pricing and reimbursement landscape

Building from the regulatory framework presented in the previous section, this section aims at providing a context on the traditional reimbursement pathways for cell therapies, with a focus on the American and European jurisdictions. Herein, the challenges and limitations of traditional reimbursement pathways will be highlighted and new reimbursement and payment schemes will be showcased, taking into account specific considerations of pricing and reimbursement for stem cell based therapies.

In order to start the framing of pricing and reimbursement, it is important to highlight key differences between the American and European jurisdictions. In the United States, there is more freedom to manufacturers and producers to set the pricing and determine value of a new therapy for reimbursment. However, monetary standards for specific procedures and therapies are put in place by private insurance companies and government agencies, namely Medicare and Medicaid. While there is not an explicit cost-effectiveness threshold in the form of $/QALY, interventions under WTP thresholds of $50,000 to $150,000/QALY are regarded by academic evaluations and public pricing committees, such as the Institute for Clinical and Economic Review (ICER), as cost-effective [95, 96, 97].

More stringent control of pricing and reimbursement is put in place in countries where public health care is the standard with National Healthcare Systems, and where market access is dependent on positive recommendations by Health Technology Assessment (HTA) agencies, like several European countries. In the United Kingdom, explicit cost-effectiveness thresholds, in the form of cost per quality-adjusted life-years (QALY) are put in place by the National Institute for Health and Care Excellence (NICE) [98, 99], with a threshold of GBP 30,000/QALY ($38,650/QALY) being the norm [99, 96]. In Germany, the main health economic analysis is budget impact analysis and this is used for pricing negotiation, in combination with international price potential. Cost-effectiveness analysis, in contrast to the UK, plays a limited role [99, 100].

For cell, tissue, and gene therapies, recent recommendations for increasing these cost-effectiveness thresholds have been reported. In the case of rare and orphan diseases, for which some cell and gene therapy approvals were achieved, ICER has performed cost-effectiveness evaluations up to a threshold

of $500,000/QALY, and NICE has considered thresholds of up to GBP 300,000/QALY ($389,047/QALY). Furthermore, the value of one-time treatments has been deemed hard to assess with additional QALY, so other evaluation methods, taking into account the value of prolonging survival and risk-sharing agreements for reimbursement have been discussed [101, 102].

Reimbursement of cell, tissue and gene therapeutic products

Past approvals in cell, tissue, and gene products with therapeutic applications can inform on the historical background of the reimbursement landscape. While the prices for approved products are country, indication, and context dependent, these products have generally high prices per treatment. Table 2.1 describes the lower and upper bounds for prices, converted to US Dollars, of the prices per treatment of 18 cell therapies, 23 tissue engineered products, and 13 gene therapies that were granted regulatory approval in 14 countries or jurisdictions [103, 104, 105, 106, 107]:

Table 2.1: Lower and upper bounds of prices per treatment of approved cell, tissue, and gene therapeutic products, Prices converted to US Dollars.

Product type	Lower bound	Upper bound
Allogeneic cell therapy	$2,150 (India)	$200,000 (Canada)
Autologous cell therapy	$3,000 (South Korea)	$425,000 (United States)
Tissue engineered products	$400 (South Korea)	$123,154 (Japan)
Gene therapy	$5,501 (South Korea)	$2,501,000 (United States)

These prices are a considerable barrier to entry of these therapies into market and their commercialization. In the near future, it is assumed that these therapies will continue to be high priced as the manufacturing costs are high and the scale of production is small in comparison with small molecules and biologics [98, 100]. It is challenging for public and private health care systems to provide coverage of these products [106, 100]. Some of these therapies were never marketed in the countries where regulatory approval was granted due to lack of reimbursement. This is the case of Prochymal, an allogeneic MSC-based therapy for acute graft vs host disease, that was granted conditional regulatory approval by Health Canada in 2012. Osiris, the manufacturer of this therapy at the time of approval in Canada, never submitted the therapy for evaluation by The Canadian Agency for Drugs and Technologies in Health, an agency that provides recommendations for drug reimbursement based on cost-effectiveness for the provinces with publicly funded health plans. As a result, the product was not granted full approval and was not reimbursed [55, 108].

Additionally, in countries where public health care systems exist, unability to reimburse these therapies may lead to market withdrawals. One example is Glybera, a gene therapy approved by the EMA in the European Union for treatment of lipoprotein lipase deficiency, an ultrarare disease in Europe. At the time of approval in 2012, Glybera cost 1.1 million euros [109]. Health technology assessment agencies in Germany and France rejected public health coverage, and the therapy was not assessed in other European countries. Due to lack of demand, uniQure, the manufacturer of Glybera, did not renew the marketing authorization of the product and its manufacturing was discontinued [106].

While there were several cell, tissue and gene therapeutic products that were granted reimbursement, these therapies are vulnerable to competition by possible lower cost alternatives, such as generics, biosimilars, and medical devices [105]. For some indications, payers have cellular and small drugs/biologics products under the same reimbursement category and under the same budget constraints [110]. These issues lead to market discontinuation of these products. One example was Provenge, a cell-based immunotherapy for prostate cancer, approved by the FDA in the United States. The list price for Provenge was $93,000 for a full course of treatment. The lack of sound clinical effectiveness data, the appearance of a lower cost small-drug competitor, and a budget reduction for cell therapies of 60% by Medicare and Medicaid resulted on the removal of this product from the market [111, 112, 113].

Another additional barrier to market entry and reimbursement of the aforementioned cell, tissue, and gene products, is the fact that they after often one-time treatments, providing a cure or remission of a condition. Cell and gene therapies are key examples showcasing the limitations of payment schemes.

In the American regulatory and payer framework, cell therapies are approved as biologics and reimbursed as drugs, and drugs are priced per-use [114, 98]. Traditionally, this means that payments to manufacturers correlate with outcomes and manufacturers would continue to receive revenue only if patients stay on the therapy. Therefore, paying for the therapy over time or a one time upfront payment, regardless of future outcomes, is a critical choice for payers. In the United States, 20-30% of patients change insurance carriers and plans every year, providing a large risk to individual insurers to pay for such large one-time upfront prices [114]. As the outcomes and value of these therapies are often only demonstrated in a long-term fashion, which is hard to estimate from initial clinical trial data [99, 100], and may be realized by the prevention of costly complications of conditions [98]. Another considerable risk for the reimbursement of one-time costly therapies is the rate of non responders. Non-responder rates of 30-40%, and even of 60-70%, have been reported [98].

Traditional reimbursement schemes can also limit the accessibility to cell and gene therapies to patients by hospitals and clinical centers. Hospital reimbursement varies on whether the drug is administered on an outpatient or inpatient setting. In outpatient hospital admissions, the patient goes to the hospital for a medical appointment, but does not stay overnight. On the other hand, an inpatient hospital admission requires an overnight stay, generally associated with an intervention or surgery [115].

On top of the price of the drug, a charge-to-cost ratio, or markup, is generally applied by hospitals in the United States on top of the Medicare list prices [116]. Outpatient drug reimbursement is based on the average selling price plus a small outpatient drug price markup. For inpatient procedure reimbursement, all costs are grouped into the diagnosis-related groups (DRGs) that do not include the costs of new cell therapies. Additionally, inpatient administration has larger hospital price markups than outpatient procedures [117]. For this reason, in the case of inpatient procedures, hospitals are negotiating reimbursement of cell therapy administration directly with payers for each patient as a means to not lose significant amounts of money per patient [114]. This is a cumbersome process as the number of patients that could benefit from these therapies grows.

The limitations and challenges herein stated provided the background for new reimbursement schemes

to handle the sizable uncertainty involving efficacy and payment of cell, tissue, and gene therapeutic products. An increasingly common way to deal with these uncertainties is through Managed Entry Agreements (MEA), or Performance-Based Risk Sharing Agreements (PBRSA). These agreements involve tracking the performance of the therapies over a specific time period, with the continuation of reimbursement being dependent on the achieved outcomes. These agreements have been suggested as well for ATMP [118, 119, 99].

Two forms of PBRSA used to spread the reimbursement of one-time treatments over a longer time period are [119, 99]:

- Outcomes-based payments involve the payer making annual payments to the manufacturer, upon continued achievement of clinical outcomes by following up the patients. If the treatment fails, the manufacturer no longer receives further payments.
- Amortization requires the payers to make annual payments to the manufacturer as long as the patient is alive, irrespective of the efficacy of the therapy.

A key example of the use of PBRSAs to enable the accessibility of cell therapies in the United States and the European Union is the market entry of therapies based on Chimeric Antigen Receptor T-cells (CAR-T). In 2017, two CAR-T based therapies were first approved by the FDA for the treatment of two cancers and made available by state and private healthcare payers [120, 121]: Kymriah, a therapy for pediatric acute lymphoblastic leukemia (ALL), is manufactured by Novartis; and Yescarta, a therapy for adult non-Hodgkin lymphoma, manufactured by Kite Pharma (now owned by Gilead) [120, 121] (Table 2.2) [122, 106, 123, 124, 125, 126, 127, 128, 129].

Novartis entered an outcomes-based contract strategy in the United States for Kymriah for treating relapsed or refractory pediatric ALL, as a route toward value-based pricing. In the outcomes-based contract, the manufacturer will only be paid for the treatment if the patient has a positive response to the treatment. The value-based pricing strategy would link the price of the treatment to a sliding scale according to the magnitude of benefits showed by the therapy. Additionally, if Kymriah is approved for more clinical indications, the manufacturer would set differential pricing according to the specific indication [130, 121]. Medicare, the program covering health services for US citizens over the age of 65, recently recommended national coverage for CAR-T therapies, instead of the usual state and plan varied coverage [131].

Recent recommendations on a pricing strategy for CAR-T therapy suggest price competition between manufacturers, or case-rate payment, for which physicians or hospitals would take financial responsibility for the use of the therapy and respective complications, regardless of its outcomes. This strategy could drive cost reduction at the manufacturer level [113]. In fact, when Kymriah was approved for adult lymphoma, the same indication for which Yescarta had already been approved, Novartis matched the list price of Yescarta ($373,000), despite the fact that outcomes-based payments would not be sought after for this second indication [124].

In countries other than the United States, in order to enter the market, Novartis provided price discounts [123, 132, 125, 126, 127, 128]. In the United Kingdom, Gilead offered a confidential list price

Table 2.2: Indications, list prices, and risk-sharing agreements for market entry of CAR-T therapies.

Product	Clinical Indication	Country	List price	Risk-sharing agreement
Kymriah	Relapsed or refractory pediatric ALL	United States	$475,000	Outcomes-based
Kymriah	Relapsed or refractory adult lymphoma	United States	$373,000	N/A
Kymriah	Relapsed or refractory pediatric ALL	Canada	Confidential	Managed access
Kymriah	Relapsed or refractory adult lymphoma	Canada	Confidential	Managed access
Kymriah	Relapsed or refractory pediatric ALL	Germany	EUR 320,000 ($354,176)	Outcomes-based
Kymriah	Relapsed or refractory adult lymphoma	United Kingdom	GBP 282,000 ($365,552)	Managed access
Kymriah	Relapsed or refractory pediatric ALL	United Kingdom	GBP 282,000 ($365,552)	Managed access
Kymriah	Relapsed or refractory pediatric ALL	Switzerland	CHF 370,000 ($374,576)	Outcomes-based
Kymriah	Relapsed or refractory adult lymphoma	Switzerland	CHF 370,000 ($374,576)	Outcomes-based
Kymriah	Relapsed or refractory pediatric ALL	Australia	AUD 598,000 ($407,028)	Outcomes-based
Kymriah	Relapsed or refractory adult lymphoma	Australia	AUD 598,000 ($407,028)	Outcomes-based
Kymriah	Relapsed or refractory pediatric ALL	Japan	JPY 33,500,000 ($308,434)	N/A
Kymriah	Relapsed or refractory adult lymphoma	Japan	JPY 33,500,000 ($308,434)	N/A
Yescarta	Relapsed or refractory adult lymphoma	United States	$373,000	Case-by-case outcomes-based
Yescarta	Relapsed or refractory adult lymphoma	Canada	N/A	N/A
Yescarta	Relapsed or refractory adult lymphoma	United Kingdom	Confidential	Managed access

discount on Yescarta as well [132]. In the United Kingdom, where both Kymriah and Yescarta received appraisals by the local HTA agency [132], the risk-sharing agreement is based on managed access. Under a managed access agreement, the continuation of commercialization of the new therapy is conditional on the collection of additional data to resolve clinical uncertainties, and a new cost-effectiveness analysis after the 5-year follow-up period [132]. An outcomes-based agreement for reimbursement was not reported. Research suggests that such outcomes-based agreements would increase the 10-year financial burden to hospitals in comparison with CAR-T entry without an outcomes-based agreement because of the additional costs of data collection to compensate for uncertainty [133].

Pricing and reimbursement of MSC-based products

The list prices of MSC therapies in specific countries are shown in Table 2.3 [134, 135, 136, 104, 106].

Table 2.3: Pricing of approved MSC based therapies. AMI - Acute myocardial infarction. GvHD - Graft vs Host Disease. CLI - Critical limb ischemia

Product	Indication	Country	Price ($)	Reimbursement status
Cartistem	Osteoarthritis	South Korea	19,000-21,000	In market
Cupistem	Crohn's fistula	South Korea	3,000-5,000	In market
Hearticellgram	AMI	South Korea	19,000	In market
Stempeucel	CLI	India	2,150	Limited access
Prochymal	Acute GvHD	Canada New Zealand	200,000	Never marketed
TEMCELL	Acute GvHD	Japan	115,000-170,000	In market
Alofisel	Crohn's fistula	European Union	60,000-120,000	Not recommended

The reason why there are more approvals and marketing authorizations in South Korea and Japan is related to the regulatory landscape, granting approval once safety studies are completed, on the condition of post-marketing surveillance. To the best of current knowledge, there were no performance-based risk-sharing agreements put in place for the appraisal and reimbursement of MSC-based therapies. However, in India, Stempeucel was approved and marketed under a limited release of 200 patients on a cost-recovery basis, and post-marketing surveillance studies were required [104], a strategy that is more similar to the managed access agreements put in place in the United Kingdom for CAR-T cells [132]. However, Takeda proposed outcomes-based pricing in the European Union for expensive drugs. This decision is expected to impact Alofisel [137]. In the United Kingdom, NICE did not recommend Alofisel for public healthcare reimbursement, on the basis of modest benefits in the clinical outcomes and large uncertainty on the long-term cost-effectiveness outcomes [135].

Pricing and reimbursement of PSC-based products

Currently, PSC-based therapies have not been administered outside clinical trials. On early 2019, a treatment involving iPSC-derived sheets to treat damaged corneas was granted conditional approval in Japan [138], while clinical trials with iPSC-derived products for treating Parkinson's disease [139] and repairing damaged heart tissue [140] in Japan as well have attracted attention. In the United States, trials involving ESC or iPSC-derived cell therapies for type 1 diabetes [141], solid tumors [142] or age-related macular degeneration (AMD) [143] started recently. In Europe, a trial for iPSC-derived therapies for AMD was also conducted [143], and a phase 1 trial using MSC derived from iPSC was also completed [142].

The cost of goods estimated through bioprocess modeling for PSC-derived products range from $75 - $605/million terminally differentiated cells, for the case of an off-the-shelf, ESC-derived therapy [12], to $6,330 - $8,656/million terminally differentiated cells, for the case of patient-specific, iPSC-derived cell lines for drug screening [6]. List prices of $1,000 - $2,000/million cells for off-the-shelf iPSC-derived

cell lines and of $5,000/million cells for patient-specific iPSC-derived cell lines were reported [6]. These costs are considerably higher than the costs of goods per million cells estimated for off-the-shelf MSC-based therapies, in the range of $5 - $350/million cells [144, 27, 10], and also higher than the list price per million cells proposed by Takeda for Alofisel in the European Union (approximately $581/million cells) [135]. This means that, under the current manufacturing landscape, possible prices proposed for reimbursement of PSC will be closer to the prices of CAR-T cell therapies and gene therapies than the prices of adult stem cell-based therapies.

A factor driving the cost of goods of PSC-based therapies up, common to both ESC and iPSC-based therapies, is the long expansion and differentiation process times, expensive cell culture components, frequent and costly quality controls, limited differentiation and purification yields, and labor intensive tasks [143, 145, 146, 147, 148]. For iPSC, the reprogramming process is long and add significant costs. For research, reprogramming of an iPSC cell line takes 3-5 months to complete and costs approximately $3,000 [149]. For one patient, costs of $10,000 - $20,000/iPSC cell line were reported as well [150].

The cost issue is even more noticeable for patient-specific iPSC-derived therapies. While these therapies could be interesting for long-term cost-effectiveness from a clinical point of view, by reducing the need for immunosuppression due to Human Leukocyte Antigen (HLA) mismatch in a cell transplant [151, 150], the costs and time associated with cell reprogramming and generating a patient-specific PSC cell bank, combined with the expensive quality controls required for a therapy with such a small scale make the costs prohibitive. For the autologous transplant of iPSC-derived retinal epithelial cell (RPE) sheets for AMD treatment in a clinical trial setting in Japan, costs of generating the therapy were approximately $1 million [151]. The generation of off-the-shelf, HLA matched haplobanks of iPSC is seen as a cost-saving approach, by offsetting estimated to offset the costs of cell banking by more doses of PSC-derived products [150]. Currently, the costs of generating a GMP-compliant iPSC cell bank are estimated to be in the range of $800,000 - $1 million [152]. These HLA haplobanks are mostly feasible in countries with relatively homogeneous HLA haplotypes, such as Japan, where a cell bank storing the most common 100 haplotypes would cover approximately 90% of the population. In more heterogeneous populations, the establishment of an HLA haplobank is more challenging. Covering the 20 most common haplotypes would cover 50% of the European population and 22% of the African population. The establishment of an HLA also involves significant screening costs [151, 150]. Another potentially cost-reducing alternative that has been investigated is the development of immunocompatible iPSC lines with Clustered Regularly Interspaced Short Palindromic Repeats (CRISPR)-based HLA engineering [153].

In light of these process hurdles for cost-effective manufacturing of PSC-based therapies, the prospective evaluation of the long-term cost-effectiveness of these therapies is key to determine how reimbursement of these potentially expensive therapies can be supported.

2.2 Stem Cell Bioprocessing and Manufacturing

Stem cell therapies, while very promising, face several hurdles in order to reach widespread availability as products. One of these hurdles lies in the numbers of cells necessary to treat a patient, which are

generally way higher than the cells available from isolation and harvest from a donor. Therefore, isolation and processing of cells and tissues are not sufficient to obtain clinically relevant numbers of cells. An engineering and manufacturing technological effort is required to reach large-scale production of cells. A successful bioprocessing and manufacturing approach for stem cells needs to guarantee compliance with Good Manufacturing Practices (GMP), the robustness of the manufactured doses, the safety of clinical application and cost-effectiveness for the manufacturer and the relevant stakeholders [154, 155]. In order to achieve this goal, intrinsic cell and process parameters, such as donor heterogeneity, produced factors and microenvironmental cues need to be contained into an acceptable variation range. GMP-compliant processes involve expensive quality controls, qualification and calibration of the facility, and current cell culture systems are labor intensive and have expensive components, and the annual scale of production is small in comparison with small drugs and biologics [156].

2.2.1 Process Components

The main process components and key considerations to be accounted for in bioprocess modeling of stem cell manufacturing are depicted in Figure 2.1:

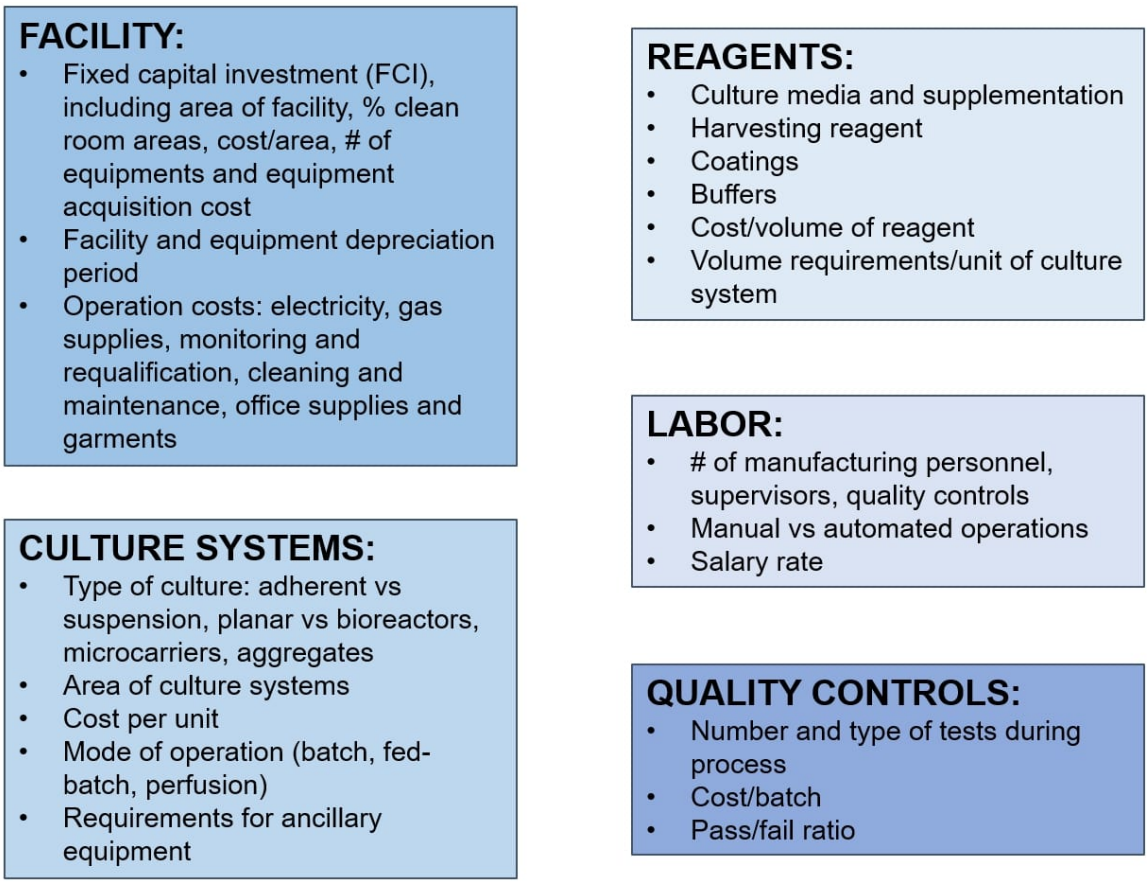

Figure 2.1: Main process components in stem cell manufacturing.

In the following sections, the specific characteristics and challenges of each process component are showcased.

Facility

The main intrinsic issues to consider when setting up a facility for stem cell manufacturing are related to the possible risk of infection derived from uncontrolled tissue isolation and the risk of contamination and detrimental cell quality when carrying continuous stem cell cultures for long periods. Therefore, concerns with reproducibility of the protocols and maintenance of aseptic cultures are paramount [157].

Good manufacturing practices (GMP) refer to the procedures and protocols adopted to meet a set of standards required for the stem cell product to be used in medicinal products. In line with this, all the procedures of isolation, processing, preservation, and storage have to be well documented and thoroughly tested for quality and compliance with these norms. Since, in order to avoid contamination of the products, clean rooms are necessary to process and manufacture the cells, the costs of setting up a GMP facility are very high and can easily surpass $1M depending on the dimension of the facility. Apart from the high setup costs, the cost of running production in these facilities is equally high, since validation of processes and equipment, clean room single use consumables and quality assurance are constant concerns and require extensive time and monetary investment [157].

The reasoning behind the requirement for clean rooms is that they are advantageous for the performance of cell culture work and are desired to operate at desired standards of air quality. In a clean room, careful attention to laboratory furniture and finishing materials is required to avoid the growth of microorganisms [158].

In light of these requirements for operation in a laboratory, when modeling the cost structure for the setup of operation of a GMP facility for stem cell manufacturing, the following costs need to be considered [159]:

- **Building costs:** construction materials of clean-rooms and non-clean rooms, Heating, Ventilation, and Air Conditioning (HVAC) system, accounting for depreciation;
- **Equipment acquisition costs:** Biosafety Cabinet (BSC), cell culturing systems (incubators or bioreactor control systems with heating equipment), centrifuges or filtration systems, refrigerators, freezers, cryopreservation systems (such as liquid nitrogen freezers and supply) and quality control equipment (microscopes, flow cytometer, ELISA, etc). Depreciation costs to all these types of equipment need to be accounted;
- **Labor costs:** management personnel costs that are independent of production volume;
- **Qualification costs:** include both initial qualification and annual requalification costs associated with design, installation, operations, and performance of the facility and associated equipment.
- **Cleaning and environmental monitoring:** Procedures associated with the maintenance of the microbiologically clean environment required for manufacturing. Generally, monthly procedures that need to be carried out even if a manufacturing room is not in use.
- **Energy consumption:** The highest amount of energy spent for the functioning of the facility is related to the operation of the HVAC system, while smaller portions are required for laboratory equipment operation and to the lighting systems and office equipment.

- **Gas supply costs:** Related to the volume of N_2, O_2 and CO_2 for the maintenance and operation of the equipments.
- **Clean room garment costs:** the cost of disposable or reusable garments added to the cost of sterilization required.

Some contributions regarding the modeling of the cost structure for cell therapies are available. Denault et al [160] presented a case study in which a 10000 ft^2 (929 m^2) GMP facility for regenerative medicine therapeutical products has about 20% of the area occupied by GMP rooms, with a cost of construction of \$600/ft^2, while the non-GMP rooms cost \$350/ft^2, resulting in a \$4 million building cost. Equipment acquisition and installation costs total over \$1 million in this setting. The costs for setting up a 400 m^2 GMP facility for manufacturing of T cells in Germany included building costs of €1.62 million (\$M 1.83) and equipment acquisition and installation costs of €620,000 (\$ 700,000) [159]. Labor and maintenance and validation costs are also considerable cost contributors in both cases.

Culture systems

Stem cells are found in relatively low numbers in vivo and need to be expanded in order to generate sufficient numbers for therapeutic doses (in the order of 1-2 million cells/kg). The traditional culture methodologies employ flat two-dimensional flasks or cell stacks that support adherent cell culture. The advantages of such 2D technologies lie on their simplicity, ease of handling and low cost. However, issues related to the labor-intensive manipulation, the lack of online control of the culture conditions, mass transport limitations and the limited surface-to-volume ratio impair the scaling up of cell numbers [161].

In order to overcome the limitations of 2D technologies, 3D based technologies have been developed with increased surface area and mass transport. For this goal, spinner flasks and bioreactors have been developed. Dynamic culture conditions are fundamental to overcome the mass transport limitations and may be achieved through perfusion and stirring typically [161].

Stirred tank reactors (STR) have been used for 3D MSC culture and require a careful impeller design to avoid the occurrence of high shear stresses that cause cell damage.

Stirred tank bioreactors can be modeled at a lower volume scale by the use of spinner flasks with volumes until 3L but do not support inline control of the culture parameters [161]. Benchtop bioreactors with volumes of 1-5L were tested for research purposes with good results, yielding 5 x 10^5 cells/ml after 7 days in suspension culture and comparable with the results obtained with spinner flasks [162, 163, 164]. Pilot-scale bioreactors have volumes up until 300L and are commonly used in cultures of other animal cell types. However, for the culture of MSC, results have only been published for a 50L bioreactor with 35L working volume for the culture of adipose stem cells. Scaling up from the spinner flask and benchtop reactor to the pilot reactor was proven [165]. Industrial scale single-use reactors have volumes up to 2000L. Currently, there is no reported successful culture of MSC in such volumes. A mechanical limiting factor for the culture in such scale is the amount of shear stress that the cells are subjected to, having detrimental effects in the multipotency of MSC [166]. Other limiting factors include the high volume of

expensive reagents, such as culture media, the high seeding density required to start cultures, and the rates of batch failure.

The packed or fluidized bed bioreactors have been used for large scale expansion of stem cells. They offer some advantages relatively to STR, since they provide a surface area for cell growth that is interconnected, allowing for a more homogeneous seeding, and reducing the need for mixing and nutrient gradients. However, they have limitations in the perfusion flow velocity, which poses limits on scalability due to nutrient and oxygen shortage [167, 168].

Hollow-fiber bioreactors have also been used with success, achieving a low shear stress environment with enhanced mass transport. The hollow fibers carry nutrients and oxygen by passing through a selective membrane that shields cells from the shear stress. The membranes have a greatly increased expansion area relatively to T-flasks, but have limitations in mass transfer once the cells grow in sufficient number in the periphery of the membranes [161, 168].

Rotating wall vessels are a system of suspension culture adapted for lower shear stresses. However, this is a complex system, and not easily scalable [168]. The WAVE bioreactor (GE Healthcare Life Sciences) is an inexpensive, single-use system that uses a rocking motion to provide good nutrient distribution with low shear stresses. While this system is easily scalable, the in-line parameter control is not as simple as with other bioreactor configurations, leading to undesired nutrient and oxygen gradients [168].

In 3D cultures, cell culture support systems, such as microcarriers, aggregates or spheroids are required. Microcarriers are most common for the 3D culture of adherent cell types, such as MSC. Microcarriers are generally spherical in shape and were initially manufactured with xenogeneic materials, like gelatin and collagen. Cultispher and Cytodex are examples of such xenogeneic microcarriers. However, animal-free materials, such as glass and polystyrene with animal-free coating have been employed as well. Examples of xeno-free microcarriers are Synthemax II and SoloHill Plastic microcarriers with laminin or fibronectin based coatings [162]. The surface structure of the microcarriers has a great influence on the surface area per volume and the attachment and proliferation and differentiation response for each cell type.

Culture media

For stem cell culture, most culture media formulations consist of a basal medium formulation, supplemented with either undefined serum containing supplements, or with chemically defined supplements. This section will focus on the culture media used for MSC and PSC culture since those are the cell types evaluated in the scope of this thesis.

In the case of adult stem cells, the most common formulations are Dulbecco's Modified Eagle medium (DMEM), Iscove's modified Dulbecco's medium (IMDM) and α-minimal essential medium (α-MEM). The most common formulations of those media used for culture of MSC are the low glucose formulations. These media generally contain L-Glutamine, essential to energy production, or Glutamax, a more stable formulation [169].

The complete growth factors requirements for optimal MSC expansion are still unknown and depend

on the type of MSC, despite the recent attempts of producing chemically defined culture media. However, the most effective growth factors and cytokines include the platelet-derived growth factor (PDGF), epidermal growth factor (EGF), transforming growth factor (TGF-β), insulin-like growth factor and fibroblast growth factor-2 (FGF-2). In order to provide these supplements, fetal bovine serum (FBS) has been the most used formulation, since it contains all the required growth factors, generally at a 10% concentration. However, FBS has a very high batch-to-batch variation, has safety issues associated with transmission of prion or viral diseases, possibility of immune response by the host and ethics problems regarding animal cruelty. For good manufacturing practice for clinical applications, it is required to use FBS from countries free of bovine spongiform encephalopathy (BSE). The only recognized countries for this standard are Australia or New Zealand [169].

The risks of using xenogeneic culture medium supplements may be averted by using human serum (hS) or human platelet lysate (hPL). Recently, hPL has been preferred since it is easier to collect and pool from healthy donors, along with showing improved proliferation abilities. Some data also show that medium supplemented with 5% hPL has superior proliferative capacity than with 10% FBS. However, hPL has limitations in terms of chemical definition and batch-to-batch variation and can be prone to the transmission of pathogens when not detected by screening [169].

Higher reproducibility and safety could be achieved with Serum-free (SF) and Xeno-free (XF) chemically defined media. The first FDA-approved medium is StemPro SFM XF and studies have shown comparability with medium supplemented with serum. The main disadvantage of the chemically defined medium is the cost, along with possible modification of MSC stemness and potency [169].

For pluripotent stem cell culture, the first versions of culture media contained FBS and secretory components from mouse embryonic fibroblasts (MEF). However, alternative xeno-free solutions have emerged. These solutions contain chemically defined growth factors and proteins free from animal components. One of the most commonly used xeno-free media to support PSC growth is mTeSR. While this medium supports the expansion of PSC, the inclusion of human serum albumin and human-sourced matrix proteins increases the costs of production. Additionally, the presence of these proteins results in a medium that is not completely defined [170]. A further step toward reproducibility and safety was promoted by serum-free and xeno-free media, such as the E8 formulation. The E8 formulation is similar to mTeSR but does not contain serum albumin or β-mercaptoethanol [170, 171, 172]. Differentiation of PSCs into one of the three germinative layers (ectodermal, mesodermal and endodermal lineages) starts by replacement of PSC growth media to specific induction media. These media compositions are tailored and optimized throughout differentiation stages to obtain efficient differentiation in the cell types of interest [172].

Other reagents

For adherent cell types, the cells are passaged when they reach sub-confluence or confluence (i.e., they occupy approximately, or completely, the expansion surface area available to cells). Since adherent cell types are defined by plastic adherence, harvesting reagents are required to break down the attachment of cells to plastic, and to break down a cell monolayer into single cells. Enzymatic dissociation, using

trypsin, is effective for this goal. However, trypsin is an animal-derived component. With guidelines for minimization of the use of animal components for added safety, xeno-free alternatives were developed. TrpyLE is an alternative, in which recombinant trypsin-like proteolytic enzymes are present [173, 174]. In pluripotent stem cell culture, the use of trypsin or TrypLE is discouraged, as trypsin induces chromosomal aberrations in PSC lines and reduces the plating efficiency [175]. For the dissociation of PSC aggregates and sequential passaging, or for starting the differentiation process, Accutase is also a commonly used enzymatic reagent. Consisting of a mixture of proteolytic and collagenolytic enzymes, it supports better plating efficiency than trypsin [176, 175]. However, Accutase dissociation also may lead do karyotypic aberrations and, due to the low rate of survival, expensive differentiation inhibitors, such as the Rho-associated protein kinase (ROCK) inhibitor, are necessary to promote sequential cell expansion [176, 177].

Enzymatic harvesting might be detrimental to cell viability and structural protein integrity. This latter factor might affect ligand based downstream processing yields. Therefore, non-enzymatic alternatives were developed. These reagents work through the principle of chelating calcium and magnesium ions, important to promote cell adhesion [173]. Non-enzymatic harvesting methods are particularly relevant for PSC culture. Among these methods, plate scraping with an Ethylenediamine tetraacetic acid (EDTA) solution is notable by dissociating aggregates in small clusters, guaranteeing better survival than enzymatic methods [176].

Pluripotent stem cells need an ancillary group of cells that can provide growth and proliferation support, or an extracellular matrix (ECM) to support their fixation. One of the commonly used feeder cell types is mouse embryonic fibroblasts (MEF) [178, 179]. In order to avoid co-culture with murine cells, culture systems have been plated with Matrigel, a mixture of ECM proteins, conditioned with MEF culture media [179]. While Matrigel does not solve the issue of the use of xenogeneic materials, solutions such as recombinant ECM proteins (laminin, fibronectin, collagen, and vitronectin) became available. Furthermore, a matrix produced by human MSC can also support the growth of PSC in vitro [180].

Equipment

The basic equipment for stem cells culture is analogous to equipment used for culture of other cells and tissues. The main equipment for cell processing is Biosafety Cabinets (BSC), CO_2 incubators, and centrifuges. For cell product storage, fridges, freezers and low-temperature freezers based on liquid nitrogen are also necessary. Cell characterization involves equipment such as microscopes, flow cytometers, and real-time polymerase chain reaction (RT-PCR) [181].

Additionally, specific purification equipment needs to be employed, in particular for pluripotent stem cells. The most commonly used solutions to separated terminally differentiated cells or early committed populations from residual PSC are Magnetic Activated Cell Sorting (MACS) and Fluorescence Activated Cell Sorting (FACS). MACS is based on coupling magnetic beads with antibodies that will bind against specific cell-surface markers. The cells linked to the antibody will be retained in a matrix, while non-marked cells will be washed [182, 147]. FACS works by labeling target cells with a fluorescent tag. The liquid stream containing the cells is irradiated with a laser and, as cells pass, droplets of cells acquire

different electrostatic charges, depending on if they contain labeled cells or not [182, 147, 183]. Labeling free purification methods, such as SpheriTech, have recently been proposed, with good results for affinity separation of iPSC-derived photoreceptors [147].

For process scalability, when bioreactors are employed, control systems are required to mediate the supply of nutrients and oxygen and the removal of waste products. The control systems also provide energy supply and agitation necessary for 3D dynamic culture [172]. Additionally, scalable downstream processing equipment needs to be employed. As benchtop centrifuges become quickly impractical with high cell volumes, scalable, sterile systems, such as Tangencial Flow Filtration (TFF) and Fluidized Bed Centrifugation (FBC), were proposed for volume reduction with good results [10, 184, 162].

Labor

Labor is a key cost contributor for stem cell manufacturing. Currently, most process steps require manual, open manipulation of cell culture flasks, performed at biosafety cabinets to minimize the probability of cell product contamination. Most personnel in a GMP facility is highly trained. While there is always the possibility of manual operator variability, frequent requalification and verification of manual processes can reduce this. However, as processes are scaled up, the volumes and numbers of culture systems to be manipulated simultaneously become a process bottleneck [103, 185, 186]. Overcoming safety, sterility, and labor-intensive tasks can be achieved by the implementation of fully closed, integrated and automated manufacturing systems [103, 186, 187]. Automation has been promoted at the level of inline control, nutrient and oxygen supply at bioreactors for cell expansion, handling of flasks and multi-layer cell factories, reprogramming of differentiated cells into iPSCs, purification steps with MACS, the downstream processing with TFF or FBC devices, and in the fill-finish step by automated aseptic vial filling [188, 183, 189].

Quality Controls

The main quality controls across different stem cell types are [190]:

- **Identity.** Testing for identity aims at avoiding inadvertent switching of cell lines and cross-contamination with other lines. This can be performed through genotyping.
- **Sterility.** Avoiding contamination with mycoplasma, bacteria, fungi, virus, and endotoxin is paramount for safe product administration. Culture methods to detect colonies are performed to obtain detectable levels of pathogens.
- **Characterization.** Marker analysis to identify stemness is performed across different stem cell types. The most common analysis are flow cytometry, immunocytochemistry, rt-PCR, and functional assays. In some cases, differentiation analysis into the specific germinative layers (in case of PSC) or into specific cell lineages for adult stem cells are required.
- **Viability.** The alive cell counts after preservation should be addressed to guarantee a particular cell dose will be indeed administered to the patients.

- **Potency.** The biological activity of the cells is linked to the therapeutic action of the product.

In the case of pluripotent stem cells, the maintenance of long-term passage with genomic stability needs to be assessed by karyotyping analysis. It is common to accumulate culture-driven mutations, hence this factor is critical in the establishment of PSC banks [190].

Induced pluripotent stem cells (iPSCs) require reprogramming. Testing for residual reprogramming viral vectors is mandatory since there are safety issues with potential vector integration into the host genome. Seed and master cell banks of iPSCs should contain below 1 plasmid copy per 100 cells to pass the test. Plasmid detection is done through RT-PCR [190].

2.2.2 Process Unit Operations

In order to obtain cells in clinically relevant numbers, they need to first be collected from the biological sample, an unit operation called isolation. In the case of iPSC, as the biological sample contains differentiated cells and it is necessary to revert them back to a pluripotent-like state, a operation known as reprogramming.

Since the number of cells after isolation are not sufficient for clinical efficacy upon administration, or are not sufficient for differentiation into the cell population of interest at relevant numbers, the stem cells need to be multiplied, in sequential passages, to obtain the target number of cells. This operation is known as expansion. In the case of PSC, this operation is followed by a differentiation operation with several sequential steps to obtain the population of interest.

Finally, the cells need to be captured from the cell culture vessels where they were expanded, in an operation named harvesting. Finally, the cells need to be purified from the culture media and possible contaminants, so that the cells are ready for a final product formulation, either fresh or cryopreserved.

The process flowsheets for both the MSC and PSC derived products are shown in Figure 2.2.

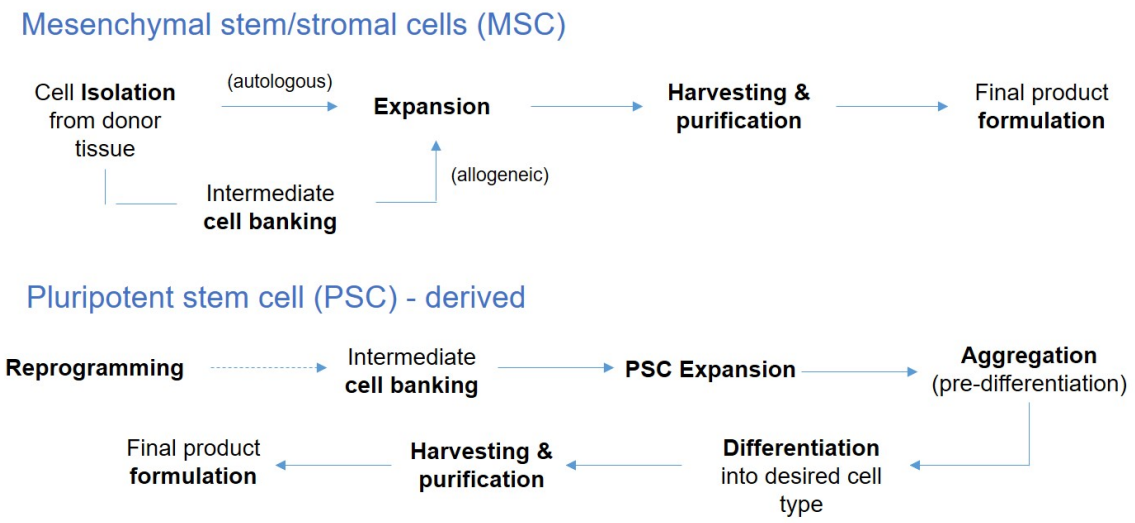

Figure 2.2: Process flowsheets with the main unit operations for bioprocessing of mesenchymal stem/stromal cells (MSC) and pluripotent stem cells (PSC)-derived products

Isolation and Reprogramming

Due to the plastic adherence of MSC, cell plating density to obtain the initial population of MSC from a donor is highly relevant. The initial seeding density of Mononuclear Cells (MNC), from which the adherent MSC will be selected, has shown a large variation between studies, from 50 to 170 x 10^3 MNC/cm^2 [155]. The adherent MSC form colonies and it is assumed that the contaminants are eliminated from the culture after several culture medium exchanges [191]. After this first plating, the initial population, named as passage zero (P0) cells, is obtained and subsequent passages are done at a lower density. The use of a low seeding density, below 1000 cells/cm^2, was shown to yield a higher proliferation rate and multipotency potential than higher seeding densities since most MSC show contact inhibition. However, for clinical scale manufacturing, a low seeding density requires very high culture surfaces and culture times, with high costs of culture media exchange and intensive manual labor [155].

The first step for acquiring bone marrow MSC is the extraction from the bone marrow, generally in the form of an aspirate. The aspirate is obtained through a needle operated by a physician to extract bone marrow from the iliac crest of the donor. Harvesting can also be done from the subchondral knee [192]. Despite the fact that a local anesthetic is administered, the procedure is quite cumbersome for the patient. Generally, volumes of 15-20 ml of bone marrow are aspirated per side, yielding a total of 30-40 ml per donor [193].

The typical isolation procedures involve density centrifugation, using an appropriate density medium, to separate the mononuclear cell (MNC) fraction from other marrow components, such as red blood cells, plasma, and lipids. The MNC fraction contains T-cells, B-cells, monocytes, HSC, endothelial progenitor cells (EPC) and MSC [191]. The MSC fraction in the MNC is very small, of only about 0.0001% of the total MNC content [191, 194]. The MNC fraction is then plated generally at a very high seeding density onto tissue culture flasks and the MSC represent the adherent cell population that forms colonies.

The yield of MSC from the bone marrow is highly variable from donor-to-donor sourced, collection site and per protocol. Successive aspirations of MSC from the same donor show a decreased yield compared to the first aspiration [195]. Reported yields of BM-MSC from bone marrow aspirates range from 1 to 317400 cells/ml [192].

The isolation protocols used for MNCs may have a lot of influence in the phenotype of MNCs and the isolated MSC, which may then influence the functional characteristics for clinical use. Some of the factors that influence this outcome are the methods for bone marrow aspiration, processing of aspirate, density medium, washing and centrifugation steps, duration of MSC attachment during P0 and the culture medium used. This has been shown in two different clinical trials for acute myocardial infarction that differed in the density medium and centrifugation steps, with one of the trials showing positive results and the other showing no improvement of the clinical condition compared to the placebo administration [191].

Adipose stem cells (AT-MSC) are found in the perivascular region of white adipose tissue, including subcutaneous fat deposits [196]. Adipose tissue is collected by a needle biopsy or liposuction aspiration [197]. These methods are particularly attractive since adipose tissue is considered biological waste, therefore this source is less invasive than the collection of bone marrow. Furthermore, it has the advan-

tage that AT-MSC have a 100-1000 fold higher frequency on a volume basis comparatively to BM-MSC [198]. Additionally, yields per volume of AT-MSC range between 4,737 cells/ml and 1,550,000 cells/ml [192].

The initial source for AT-MSC is the Stromal Vascular Fraction (SVF) of the adipose tissue. This is a processed population of fibroblasts, endothelial cells, smooth muscle cells, pericytes, immune cells and preadipocytes. The adherent cells are the preadipocytes, with the successive exchange of the culture medium enabling the removal of the contaminant cell types. The first method developed for isolation of cells from the adipose tissue is the enzymatic digestion, where washed tissue fragments are digested with enzymes, like collagenase, trypsin or dispase [198]. After centrifugation of the digested mixture, the SVF cells make a pellet, while mature adipocytes are floating and can be removed [196, 197]. However, enzymes are very expensive and might have an impact on the safety and efficacy of the stem cell products. Therefore, non-enzymatic methods have been developed. These methods focus on shear force, centrifugal force, radiation and pressure. The purpose of these mechanical treatments is to replace the enzymatic digestion and separate the cells from the adipose tissue [198]. While both enzymatic and non-enzymatic methods show high variation in yields between protocols, non-enzymatic methods generally have a lower yield of nucleated SVF cells per volume of adipose tissue (100,000 – 1,300,000 cells/ml for enzymatic digestion vs 10,000 – 240,000 cells/ml for non-enzymatic digestion) [199]. Additionally, non-enzymatic methods yield a higher frequency of peripheral blood mononuclear cells. Despite these shortcomings, non-enzymatic methods pose significant advantages in terms of cost and processing time in comparison with enzymatic methods [199].

The umbilical cord is an attractive cell source since it is usually discarded after labor, its collection is non-invasive, and allows easy MSC isolation. Since these MSC are from a neonatal source, they have less risk of genomic modifications due to aging present in the adult source MSC and have a more primitive origin. While the umbilical cord blood is also a source of MSC, the low yield hinders its utilization as a scalable source of MSC. For this reason, the umbilical cord matrix, or Wharton's Jelly, is a more attractive tissue for isolation [200]. The yield of MSC from the umbilical cord matrix varies from 10,000 cells/cm to 4,700,000 cells/cm [192].

There are two main methods for isolation of MSC from the umbilical cord matrix. The explants method has the principle of making the tissue size small enough to allow the cells to contact with gases and nutrients and migrate to the plastic adherence surface. The other method is enzymatic digestion, using collagenase, hyaluronidase, and trypsin to dissociate the cells from the tissue. The duration of the enzymatic treatment is very important since it can degrade the ECM and cell membrane, impairing the adhesion of cells to the plastic surface [201]. The explants method was reported to have similar culture times until reaching P0 to the enzymatic method but higher cell yield/cm of cord than the enzymatic treatment [201].

Other methods of isolation to complement or replace the selection by plastic adherence, such as magnetically-activated cell sorting (MACS) or fluorescent activated cell sorting (FACS) can be used to further enrich the MSC population. However, these methods also may come at the expense of modifying the functional activity of MSC [202], possible cell damage, expensive costs and labor-intensive tasks

[169]. Due to these drawbacks, the cell sorting methods are rarely used in clinical trials and production.

Human ESC are generally extracted from the inner cell mass (ICM) of blastocysts during early embryonic expansion. ICM can be isolated by mechanical pressure, laser dissection or immunosurgery. These methods require the destruction of human embryos. This fact raised serious ethical concerns. More recent methods involve isolation of ESC from a single blastomere, without destruction of human embryos [203, 204].

In order to solve the ethical problems from ESC, iPSC are generated by somatic cell reprogramming. This procedure is related to the delivery of genes expressing reprogramming factors, such as Oct4, Sox2, Klf4, and Myc, to the differentiated cells, in order to revert them back to a pluripotent-like state. The most commonly used cell types used for reprogramming are fibroblasts and blood cells from either cord or peripheral blood. Regardless, in theory, every somatic cell can be reprogrammed [205]. As a result, large pools of cells would be generated in a more ethical way than ESC collection, allowing terminal differentiation of cells to be used in therapies, disease modeling, and drug screening. Furthermore, immunosuppression of allogeneic therapies could be overcome, as autologous iPSC can be generated by reprogramming cells from the patients themselves [206].

In order to ensure that the generated PSC would be suitable for clinical application, the delivered genes should not integrate the genome and have to be delivered through non-integrative methods. The methods used to reprogram differentiated cells are non-integrating (Sendai or adeno) viruses, episomal vectors, or direct transfection with mRNA or proteins for the pluripotency factors [206, 205, 207].

Despite the promise of reprogramming technology, leading to therapeutic approaches derived from iPSC in experimental procedures and early-stage clinical trials, safety and reproducibility is still a concern. There is high variability on the ability of individual iPSC lines in the differentiation into certain lineages. Age, tissue, and state of differentiation of the cells used for reprogramming also have a significant impact on the efficiency of reprogramming. Additionally, there is evidence of DNA damage and genomic instability. These facts lead to high rates of rejection of reprogrammed cell lines [206, 208, 209, 207].

Master and Working Cell Banking

The typical methodology to establish stem cell therapies has been a one-donor – one-batch approach, where one patient is treated with cells from a single donor and the next patient is treated with cells from a different donor, promoting high batch-to-batch variability due to the different donor properties. An alternative to increase the number of cells available and reduce the batch-to-batch variability would be to pool isolated cells from different donors together and then expand them to P0 to select for the plastic adherent cells [210].

When the production of an allogeneic therapy is sought after, it is fundamental to establish a Master Cell Bank (MCB) and a Working Cell Bank (WCB) for further expansion. When a reasonable yield of MSC at P0 is accomplished, it is possible to cryopreserve concentrated vials of cells and then use one of those vials for further expansion. However, it is common to establish the MCB after one passage of MSC, obtaining passage one (P1) cells, since cells collected at P0 often contain monocytes and macrophages in the mixture as well and they need to be further eliminated with another adherent passage [202].

The cryopreservation of cells generally occurs at a high concentration of 1-5 million cells/ml and in small cryovials [56]. Cooper et al reported the establishment of an MCB from UCM-MSC at P1 where 10-15 vials per donor were obtained at a concentration of 1-2 million cells/ml, stored in liquid nitrogen containers. From the whole bank, one vial is allocated for the quality control studies [211].

The quality controls for MCB involve cell counting and enumeration, immunophenotype characterization with antibodies, cell viability assays and microbiology safety tests, such as sterility, endotoxin and mycoplasma assays [211].

While a master cell bank may be the starting point for the availability of an “off-the-shelf” product, it has the disadvantage of very high development costs [210]. The estimated costs for the generation of an MCB of MSC with 500-1000 cryovials at 1-5 million cells/vial include $10k-20k expenses in serum-containing medium + $10k-15k in quality controls, reaching a value of $100 per vial. When using serum-free cultures, the costs can rise to $150-500 per vial [56].

The preparation of a working cell bank begins after the MCB underwent quality control and is released for the expansion process. The process begins by thawing a single vial from the MCB and expanding the cells for one or two passages. Therefore, the WCB is generally established with MSC at P2-P3. The WCB also undergoes quality controls to release the cells for expansion. The main factors that influence the quality of the WCB are the seeding density and the quality of reagents such as culture media and growth factors [202].

Expansion

MSC generally show contact inhibition [212, 213], meaning that proliferation of cells is inhibited when the expansion technology used is approaching confluency. Therefore, in order to optimize cell quality, cells are harvested and passaged when reaching 70-80% confluency. When looking to scale up the number of cells, which is fundamental for allogeneic therapies, the cells are passaged to a higher surface area, generally maintaining the same seeding density used in the initial passages.

Cells behave differently across passages and also show variations in growth and size depending on the cell source, biological age, the initial seeding density, and the culture medium.

The proliferation potential of MSC from different sources varies. In general, neonatal based sources have higher proliferation rates and numbers of cells at confluence than adult based sources. Several studies reported that umbilical cord blood or cord matrix MSC have higher proliferative potential, life span, and differentiation potential compared to BM-MSC. Regarding the comparison of the two main adult sources, growth of adipose-derived stem cells in media containing FBS was reported to be lower than the growth of BM-MSC [214]. However, AT-MSC are more positively affected by cultures with hPL than BM-MSC, surpassing the proliferative potential of the latter [215, 216].

It is known that sequential passages affect the quality attributes of MSC. While some MSC types show a proliferation peak around P2-P3, successive passages slow growth down, accompanied by loss of multipotency. For safety reasons, it has been recommended that expanded cells for a clinical application have less than 20 population doublings and about 75% of reported clinical trials have focused in expansion with less than 6 passages [155, 217, 169]. However, due to the creation of master and

working cell banks for allogeneic cell therapies, products submitted to clinical trials for the FDA have already reported passage numbers close to 10 [218].

Regarding the initial seeding density in 2D cultures, it has been shown that low seeding densities maintain better the multipotency of MSC and promote a higher proliferation rate due to lower contact inhibition. However, for clinical expansion, very low seeding densities are impractical, since it would take longer to reach confluency, with higher culture medium exchanges and more expansion technology units spent. Therefore, it has been hypothesized that a seeding density of 1000 cells/cm^2 offers the optimal compromise [155]. However, clinical trials attempt to reduce the cost/labor compromise even further, therefore 75% of recent clinical trials use a seeding density of 3000 cells/cm^2.

Relatively to the seeding densities in 3D cultures with microcarriers, more cells have to be seeded to reach an effective seeding density similar to the 2D cultures due to imperfect adhesion to microcarriers. Adhesion to microcarriers is influenced by factors such as the cell source, the topography, and microstructure of the microcarriers, the coating used for adhesion of the cells and the culture medium components, as well as the adhesion time and agitation protocols in the initial 24h of culture. Reported adhesion rates range between 20 and 100% in stirred spinner flasks and benchtop bioreactors [219]. The usefulness of microcarriers is also limited by the ability to promote, at a similar seeding density, the same growth rates as in 2D cultures. It was previously reported that microcarrier cultures of BM-MSC in FBS showed lower proliferation rates than with T-flasks, but with hPL as a culture medium supplement, the reported growth rates are similar [220].

When performing expansion with microcarriers, generally the 3D expansion step occurs at the last passage, after which the cells are harvested and separated from the microcarriers. However, there has been evidence, in some studies, that cells can migrate to freshly added empty microcarriers, making it possible to increase the surface available for the cells to grow without subjecting the cells to the stress related with harvesting. This migration is named bead-to-bead transfer and depends on a complex interaction between the MSC source, media composition, and microcarrier surface [162].

Since PSC do not survive as single cells, they need to be grown as aggregates. These cells can either be grown in adherent or suspension culture, in static or dynamic conditions. Since harvesting processes associated with adherent cultures are detrimental to cell yield, suspension cultures should be preferred [221, 222]. Culture in aggregates mimics better the *in vivo* microenvironment of PSC. However, the size of aggregates needs to be controlled and optimized to find the best compromise between the number of cells and avoiding nutrient, oxygen and soluble factor gradients [223, 224]. The fact that culture in aggregates does not require separation from a carrier during the downstream processing makes it a practical approach for large-scale culture of PSC [225].

Two-dimensional cultures can be performed in well plates, in T-flasks, or cell stacks. At a higher scale, aiming at scale-out or scale-up studies, cell factories may be used as well [222]. However, cultures in 3D platforms, such as spinner flasks and bioreactors, have also been performed for added scalability. Culture of PSC has been performed in stirred spinners, rotating wall vessels, rocking motion reactors, and stirred-tank bioreactors [221, 226, 227, 225]. Recently, a new vertical wheel reactor was used successfully for expansion of iPSC [33].

Similar to MSC, in 3D culture, PSC can also be expanded using microcarriers as adherence support. The use of microcarriers can provide advantages in comparison to suspension aggregates in terms of the surface to area ratios for cell growth, protection from shear stress, and through a more easy transition from 2D monolayer cultures [228, 229, 230]. Microcarriers, similarly to the adherent 2D culture of PSC, require coatings, such as Matrigel and vitronectin, to promote cell adhesion [222, 228, 229]. In comparison with aggregate cultures, the downstream processing of microcarrier based cultures could be more cumbersome due to the detachment of cells from the carriers. This limitation was recently overcome experimentally by using dissolvable microcarriers to promote the expansion of PSC [230].

Differentiation

Differentiation is the unit operation aiming at obtaining partially or terminally differentiated cells from stem cells. Differentiation protocols can be performed in the same vessels used for expansion of pluripotent stem cells [231, 232, 233]. However, they involve different culture media, with specific growth factors that will induce sequential differentiation, starting by the germinative layer from where the cells of interest come from. Depending of the cell type aimed as the differentiation target, reported differentiation protocols can last from 2 weeks up to 4 months [234, 235, 236, 237, 238, 239]. However, the differentiation process itself, even at a high efficiency, does not fully eliminate PSC with tumorigenic potential from the cell population. Teratomas have been shown to arise from transplants with as low as 0.2% of PSC content [240]. Tumorigenic assays have currently a high variability on the detection limit [241, 242]. This fact makes it critical to establish effective purification protocols to remove the PSC from the cell populations of interest.

Downstream Processing

Downstream Processing (DSP) equipment and protocols were discussed briefly in section 2.2.1. Building up from this section, it is important to notice that downstream processing of cell therapies is more difficult than for small drug molecules or biologics since the cells are the product itself. Therefore, DSP techniques should guarantee the highest cell viability possible, while preserving other quality attributes [10, 3, 243].

Two-dimensional culture, followed by harvesting and benchtop centrifugation for volume reduction, becomes impractical and slow as the scale of operation and the expansion volumes increase. Therefore, a key bottleneck of processing is on the volumes and cell numbers handled by DSP equipment. Additionally, these systems should be closed, scalable, use single-use components with easy disposable and, ideally, automated. Large scale systems currently addressed, such as TFF and FBC, are derived from blood processing [10, 244]. Affinity purification systems, such as MACS and FACS, are not scalable yet with the same ease as TFF and FBC. These systems are of key relevance in the downstream processing of therapies derived from PSC, as it is important to reduce the PSC content to a very low value to prevent the formation of teratomas and other tumors *in vivo*. Additionally, the detachment from the antibody binding results in loss of cell viability. For this reason, label-free purification systems are

being developed to allow scalable purification of cell therapies [245].

Finally, fully integrated upstream and downstream processing platforms would ensure more safety and sterility for closed processing [244].

Final Product Formulation

After washing and purification from culture contaminants, like culture medium supplements and cells that are not a part of the population of interest, the stem cell therapy needs to be preserved, either as a cell bag for fresh infusion or as a cryopreserved product. The fresh formulation has been the preferred route since it has been shown that cryopreservation affects stem cell potency and viability after thawing. However, other studies involving MSC showed no significant difference in quality attributes *invitro* and *invivo* after thawing in comparison with fresh products [246]. Furthermore, cryopreservation agents, such as Dimethyl Sulfoxide (DMSO) can induce undesired differentiation of stem cells [247].

2.3 Bioprocess Modeling

Computational and mathematical tools have been used in manufacturing frequently as a means to simulate the scale up, optimization and control of product and process development. These methodologies are code or software instruments driving structured decision-making in diverse fields. Decision support tools allow to design the best process configurations for economical manufacturing of the envisioned products in complex operations. These tools can be developed under several process optimization frameworks. There are commercial and proprietary code tools, and good data visualization is also a good requisite for possible widespread utilization and commercialization [248, 249]. The body of work in bioprocess economics modeling up to date with applications to stem cell manufacturing is summarized in Table 2.4.

The bioprocess modeling tools used for cell therapies nowadays were derived from tools used for the production of biologics, namely monoclonal antibodies. For the extension of these approaches to the modeling of cell therapy bioprocesses, some modifications need to be performed, as the cells are the product. Furthermore, stem cells can be differentiated into specific tissue cells, and the specifics of these operations need to be accounted for [253].

There are flowsheet and spreadsheet-based solutions for bioprocess modeling. The latter is based on Microsoft Excel spreadsheets and are simple to use, including solvers to estimate cell growth parameters. Excel spreadsheets are often combined with Visual Basic for Applications (VBA) to include iterative algorithms and multiple scenario analysis [254]. However, these tools are not practical to model operation queues for facility equipment, or to model parameters that are time-sensitive, such as cell growth rates [249]. Additionally, Visual Basic and Excel codes are susceptible to updates or changes in the spreadsheet formatting inputs [254]. Also, these tools work well on their own for deterministic modeling and parametric sensitivity analysis. For Monte Carlo method based stochastic simulations, plugins to make this process easier, such as @Risk, are required [254, 27].

Table 2.4: Stem cell bioprocess economics modeling approaches. DES - Discrete Event Simulation. QC - Quality Control

Reference	Cell type	Unit operations	Simulation method	Simulation environment
Darkins et al, 2014 [9]	Autologous iPSCs	Expansion, Differentiation, DSP	Biomechatronic analysis	SuperPro Designer
Simaria et al, 2014 [5]	Allogeneic MSC	Expansion, QC	DES	C#, .NET, Microsoft Access
Hassan et al, 2015 [10]	Allogeneic MSC	Expansion, DSP, QC	DES	C#, .NET, Microsoft Access
Jenkins et al, 2016 [6]	Autologous iPSCs	Reprogramming, Expansion, Differentiation	DES	Microsoft Excel VBA
Weil et al, 2017 [147]	Autologous iPSCs	Reprogramming, Expansion, Differentiation, DSP, QC	DES	Microsoft Excel VBA
Pereira Chilima et al, 2018 [27]	Allogeneic MSC	Expansion, DSP, QC	DES + MCDA	Microsoft Excel VBA + @Risk
Mizukami et al, 2018 [30]	Allogeneic MSC	Expansion, DSP, QC	DES	N/A
Misener et al, 2018 [250]	HSCs	Expansion, Differentiation	Robust Optimization, NPV	N/A
Harrison et al, 2018 [186]	Allogeneic MSC	Expansion, DSP, Fill-finish, QC	DES	C#, .NET, Microsoft Access
Ng et al, 2018 [251]	Allogeneic MSC derived exosomes	Expansion, DSP	DES	N/A
Wallner et al, 2018 [12]	Allogeneic ESCs	Expansion Differentiation	DES	Microsoft Excel
Glen et al, 2018 [252]	HSCs	Expansion, Differentiation	ODE	C#

The utilization of custom made code with general use programming languages, such as C#, allows a more versatile experience and a more straightforward inclusion of stochastic analysis. It has discrete event simulation packages as required to accomplish these simulations and is a powerful language that can be used in several operating systems but is not an open-source language. Therefore, the utilization of this programming language requires the payment of a license. Custom-made code with C# was paired with Microsoft Access databases to scale for larger volumes of data and high dose/lot demands [5, 10].

Traditionally used flowsheeting software, such as SuperPro Designer, was also applied to stem cell manufacturing process design [9]. The SuperPro Designer approach offers a more rigid framework in terms of the building blocks, has a limited number of blocks per sheet (25 in the academic version), apart from being only available for Windows platforms and having license costs.

The modeling approach for bioprocesses in cell therapies often use mass balances to determine the yields of certain unit operations, and/or Discrete Event Simulation (DES) to model the flow of process components over time and unit operations [249]. The focus of this background review is on discrete event simulation, since this is a more dynamically flexible framework to include uncertainty associated with cell therapies and was the chosen one for implementing the model.

Discrete event simulation models manufacturing as a series of queues for unit operations, depending on the available equipment. Each cell culture flask takes a certain amount of time to be processed and the processing time advances in a discrete fashion [255, 249, 256, 257]. The key components of DES

models are systems (in the case of stem cell manufacturing, the system is the GMP facility and their components), the variables (e.g., the number of doses produced) describing the state of the system (e.g. annual demand reached/not reaches, donor fully processed/under processing) at a given point in time. Throughout the simulation time, events (e.g. cell expansion, purification, passing/failing quality controls) will update the state of that system [258]. In DES, several operations might occur at the same time, allowing to mimic processes at a GMP facility. This type of framework is characteristic of parallel programming [257].

While DES-based modeling approaches have been used for biologics and cell therapy manufacturing successfully [5, 10, 11, 144, 253], when applied to bioprocess economics, they highlight the cost and process yield outputs only. For a more comprehensive inclusion of qualitative factors that influence cell therapy decision making, Multiple-Criteria Decision Analysis (MCDA) has been combined with bioprocess economics models [27, 156]. While several methods can be used to combine quantitative and qualitative attributes, the weighted sum method was used in the work by Chilima and colleagues. For the manufacturing of allogeneic MSC, the qualitative attributes used were the ease of process development, validation, setup, operation, and scale-up. These factors were applied with different rankings to aid in the choice between multi-layer flasks (i.e., cell stacks) and different types of bioreactors for MSC expansion [27].

2.4 Health Economics Modeling

An economic evaluation of therapies is fundamental to determine the value of a new therapy, as well as the budget impact of the administration of such therapy. It is advised to perform this analysis early on the drug development process. Such analysis will avoid pitfalls from the selection of clinical trial endpoints that are not aligned with effectiveness demonstration. From the manufacturing standpoint, the early economic evaluation can avoid manufacturing and scalability plans resulting in manufacturing costs incompatible with a prospective reimbursement price. These considerations are especially relevant in a scenario where cell therapies can face competition from less expensive alternatives, such as small drugs and biologics.

There are four types of economic evaluation [259]:

- **Cost-Minimization Analysis (CMA):** This analysis aims at comparing two therapies of similar effectiveness and choosing the least expensive alternative.

- **Cost-Benefit Analysis (CBA):** This analysis estimates the benefits of a new therapy through comparison with the cost. The benefits are also converted to monetary units using “willingness to pay” (WTP, the value an individual would pay to reduce illness severity) or “risk of death” or “human capital” (the value of the individual to a society based on productivity of future income). However, this analysis has limitations on the practical and ethical difficulties of converting the value of human life to monetary units.

- **Cost-Effectiveness Analysis (CEA):** This analysis is used to report costs relative to a given clinical outcome that cannot be translated into monetary benefits.
- **Cost-Utility Analysis (CUA):** This is a particular type of cost-effectiveness analysis, where the effectiveness measure is translated into health utilities. For instance, cost-effectiveness analysis might focus on cost per cases of disease prevented, or severe complications, while cost-utility analysis is directly related to the life years gained and, eventually, the quality of these years.

Typically, a cost-effectiveness analysis is performed with data from a clinical trial to compare the costs related to an outcome at the end of the treatment. The patients may be subjected to several clinical alternatives and move through different health states with probabilities that are determined by the incidences of these states in treatment [259].

The first step to conduct the analysis is to identify the perspective from which the analysis will be conducted since that influences beforehand the costs to include. The different perspectives possibly included are [259]:

- **Payer perspective:** includes all the costs associated with providing the health care service.
- **Societal perspective:** costs that affect society, such as time away from work and out-of-pocket expenses.
- **Patient/family perspective:** the costs directly affecting the patient, such as out-of-pocket costs, a copayment of health utilization, time away from work.
- **Clinical perspective:** direct costs to hospital budget, costs of learning new skills for utilization of the new procedure, office time.

The time frame in which the analysis should be conducted is also relevant to know the health outcome and economic impact of the study. Finally, the comparator treatments should be chosen, and the kind of pathways to conduct [259].

The choice between possible outcomes will lead to drawing a decision tree to decide on the best treatment option with prospective alternatives. In a decision tree, the decision node is placed to the left and then the possible outcomes and probabilities in which they occur are constructed to the right. Decision trees are best used for one-time treatments, with a short timespan of analysis. Therefore, they are best suited to decisions on acute interventions and short-term diagnostic or treatment decisions. For a continuous timespan, the complexity involved in adding more subnodes to each state to replicate the probability of flowing through different health states makes this modeling approach cumbersome. For chronic conditions of long timespan of analysis, Markov models are more practical, as they represent disease processes evolving over time with individuals migrating across different health states [260, 261]. This can be performed with a probabilistic analysis with a Monte Carlo analysis, where each patient and outcome will have probabilities of different outcomes calculated repeatedly [259].

There are recommendations from the Panel of Cost-Effectiveness in Health and Medicine on how to conduct these analyses, as well as from the International Society for Pharmacoeconomics and Out-

comes Research (ISPOR) and the Society for Medical Decision Making (SMDM). The most recent recommendations claim that both a payer (direct costs) and societal (indirect costs) should be used, in order to account not only for healthcare utilization but also for the loss of productivity and income of people undergoing a clinical challenge [262, 263]. For simplicity of the definition of the cost-effectiveness ratio, the analyses in this thesis will consider the direct medical costs only.

The costs associated with a health care intervention are grouped in three main categories [259]:

- **Direct:** costs associated with inpatient and outpatient services, supplies used for administration of the intervention, equipment, and utilization of health professionals, medication, and costs of management of possible associated complications. These costs are typically determined by accessing medical claims databases.
- **Indirect:** loss of income for the patient or its family. They are typically associated with productivity losses, typically quantified by annual wages.
- **Intangible costs:** monetary value of pain and possible mental health complications associated with the disease in question. These costs are generally hard to determine and are left out of the analyses most of the time.

The estimation of effectiveness of a new intervention might come from different studies, such as randomized controlled trials, observational studies, uncontrolled experiments, and descriptive series. These provide a framework to evaluate how the new therapy could, for instance, prevent additional complications associated with a disease [262]. In the case of eHTA, since the clinical trials were not yet performed, this kind of analysis is based on assumptions derived from analogous therapies.

When the value of an intervention cannot be translated into monetary benefits, other units come into play. It is important that a measure of health would be comparable across clinical areas, reflecting the benefits but also the possible caveats on the application of the new intervention as additional costs, changes in survival and/or quality of life, be sensitive to changes in quality of life, and reflect trade-offs between different aspects of health [264]. The most straightforward way to measure the effectiveness of an intervention is by the number of Life Years (LY) Gained. However, this measure does not account for the quality of life of the patient during the additional number of years of life. For that reason, quality-adjusted life years (QALY) were introduced.

QALY are measured by introducing the notion of quality of life by utilities. Utilities are health state classifications, ranging from 0 (death) to 1 (perfect health). The use of QALY in the reference case cost-effectiveness analysis has been recommended by past panels [262, 263]. Utilities can be measured with Preference-Based Measures (PBM), using questionnaires to guide the patient through the classification of the health state. Some questionnaires that are used to evaluate utilities are:

- EuroQoL
- Health Utility Index
- Quality of Well-Being Scale

- Years of Healthy life measure

However, in particular, for model-based analysis, evaluation of clinical trials, and even of utility for the eHTA approaches being implemented, mapping approaches are used to estimate utility values from non-utility measures are used. These approaches are used to derive a relationship between clinical explanatory variables and PBM [265]. In the end of a cost-utility analysis, the total QALY of each individual are simply obtained by adding the quality-adjusted years, given that an individual is in a given health state during a period of the simulation, and this health state has a specific associated utility.

QALY is a more comprehensive measure than LY due to the capture of morbidity and mortality. In an intervention, each life year gained is multiplied by the corresponding health utility. This analysis is largely used in academic settings and also used by several public healthcare systems to evaluate the value of new therapies introduced in the market and guide their approval and reimbursement.

However, this effectiveness measure comes with several hurdles. First of all, it is a simplified model of health and there would need added research to provide a better weighing system for how different challenges change the quality of life. Second, it is considered a flawed indicator of the quality of life [266]. For instance, 2 years with a health utility of 0.5 are not the same as 5 years with a health utility of 0.2 in qualitative terms, but both yield the same number of QALY (1), possibly leading to wrong reimbursement decisions. A recent study from the European Commission [267], in a healthcare reimbursement space where cost/QALY are widely used, concluded that the QALY multiplicative model is flawed and would be scientifically invalid, and should be deprecated [267]. However, a better alternative to evaluate the quality of life was not found yet. Another caveat is the fact that there are varying instruments for utility assessment and there is not a standard method. The adoption of a standardized method would have some impact on the estimates. Also, the fact that utility determination is based on patient-reported measures, there could be a degree of bias in response that would flaw the outcomes [262].

One of the other main hurdles is related to ethical questions. While QALY shows a positive ethical stance on evaluating people at different stages of life with the same perceived health quality as equal [97, 268], there is the reverse of considering a disabled person less valuable in terms of quality of life than a non-disabled person.

In addition to QALY, other metrics combining quality of life and survival are:

- Disability-Adjusted Life-Years (DALY)
- Healthy-Years Equivalent (HYE): conjectured number of years in perfect health lived that would be equivalent to the precise number of years spent in imperfect health
- Saved Young Life Equivalents (SAVE): equivalence between health gains by the program to be equivalent to save and restore one young life to full health

Modeling the progression of disease in response to intervention over a given timespan gives a good foundation to estimate effectiveness. Several data sources are combined to predict utilities and also derive a structure of the model. The types of models used in these approaches are:

- Logistic regression, for the estimation of the incidence of disease in response to risk factors

- Bayesian analysis, to estimate the probability of disease in response to a given probabilistic distribution of inputs
- Life expectancy model from survival curves

In terms of methodologies for structure [262]:

- Population vs cohort models, to determine cost-effectiveness either across the whole population or in a subgroup that could benefit the most from the intervention.
- Deterministic, for a base case with average values, vs stochastic/probabilistic models, for a full overview of how different likelihoods of an outcome affect decision making
- Decision analysis
- State-transition models, to have the patients migrate through different health states associated with the clinical case of interest with a given annual (or another time step) probability.

In order to account for possible variations in key model parameters and check for robustness of the model, Probabilistic Sensitivity Analysis (PSA) is required. Recommendations are that univariate sensitivity analysis should be performed, but the multivariate analysis should be conducted as well to investigate if key parameters are correlated and have a joint impact on the results. The costs should be discounted at a rate compatible with net inflation per year. Many studies use 3% [262].

2.5 Conclusions

This chapter highlighted the key characteristics of stem cells that make them interesting for clinical applications, the current market landscape, and pricing and reimbursement considerations. The steps and components required to achieve the numbers of cells compatible with clinical application were also depicted. Finally, the methodologies for long-term economic evaluation of new therapies were also presented and connected to the prospective long-term evaluation of new stem cell therapies.

There is considerable body of work in developing new systems for culture of stem cells that could reduce process time, minimize manual labor, and comply with regulatory trends. Decision support tools have been developed in the past to evaluate possible savings in the cost of goods per dose, or per million cells, when investing in innovative approaches for stem cell bioprocessing. These models were developed for both adult and pluripotent-derived cell products, and also showcase feasibility bottlenecks in terms of annual demands and number of doses per lot. To date, only one of these models was combined with a long-term cost-effectiveness model to inform more on the feasibility of the current manufacturing configurations to achieve therapies with prices compatible with reimbursement by health care payers.

Since there are very few approved stem cell therapies, and most of the prospective therapies are still in clinical trials, the body of work in HTA of these therapies is very limited. Early health technology assessment models could inform, from the early Research and Development stage, on the clinical and

commercial potential of the therapy under development. Given the large uncertainties associated with early preclinical and clinical research, these models could highlight ranges of parameters of manufacturing and clinical efficacy that are compatible with prospective reimbursement.

Furthermore, the high list prices proposed for other cell, tissue and gene therapies are highlighting the need for new reimbursement agreements, like the performance-based risk sharing agreements that include outcomes-based payments. Given that outcomes-based payments are linked to the continued efficacy of the therapy, approaches that highlight the groups of individuals to which the therapy might be more effective are desired, as a means of containing the prospective high budget impact of new cell therapies. The challenges of reimbursement of adult and pluripotent stem cell-based therapies were also differentiated, with PSC-based products being estimated to have prices closer to gene therapies than to adult cell therapies, due to the long process times, limited yield, and expensive manufacturing associated with reprogramming and differentiation of PSC.

While the contributions in the field have been invaluable, there is room for innovation. First, the use of a more comprehensive early HTA, including bioprocess variability as well, is an interesting approach to be fostered more frequently. Also, the majority of the case studies evaluated simulate prospective industrial-scale applications. However, innovation at the level of public research is done at a lab scale, where there is room for passage and donor specific variability to be showcased in a more specific manner. Finally, all the modeling contributions use either commercial spreadsheet and flowsheeting software. In order to comply with recent recommendations, asking for more transparency in economic modeling and the use of open source modeling platforms, the development of open source codes in this field is encouraged.

The next chapter focuses on the implementation of TESSEE, an open source framework for early health technology assessment of prospective stem cell therapies. The model architecture, and the key assumptions, process flowsheets, and equations are highlighted.

Chapter 3

Model Conception and Implementation

3.1 Introduction

The previous sections of this thesis (Chapter 1 - Introduction and Chapter 2 - State of the Art) outline the different concepts required to understand the need for implementation decision-making support tools in the field stem cell-based therapies and manufacture, in a fully comprehensive way. Such systems will contribute to more adequate planning of manufacturing systems, and respective scale optimization, as well as for reimbursement; thus, improving therapies adoption as pricing and effectiveness become better aligned with robust values that incorporate for inherent systems uncertainty. While health economics challenges are disease-specific, manufacturing challenges, for both current and prospective manufacturing technologies, are transversal to different therapeutic applications. Such challenges include the selection of the optimal bioprocess components (namely culture media, expansion technology, stem cell source), the selection of the process planning (autologous vs allogeneic, made-to-order vs off-the-shelf), the forecast of the annual demand and the decision on the number of doses per batch to be produced. Additionally, from the cost-utility analysis standpoint, given that stem cell therapies have a high associated cost, questions such as the frequency of administration of the therapy, prevention of disease complications, and improvement of overall quality of life, also need to be addressed when translating these therapies to the clinical setting.

This chapter is concerned with the technical aspects of the bioprocess economics and health economics models for early health technology assessment of prospective stem cell therapies. The model was developed considering analogous models in the literature [5, 6, 12, 10], as well as experts' opinions after several interviews.

The chapter is organized as follows. In Section 3.2, the overall model architecture for both the bioprocess economics and the disease state models is presented, as well as the linkage between the two models. Sections 3.3 and 3.4 describe the equations and components of the bioprocess economics model and of the health economics model, respectively. The methods used for the collection of the data

used in the results chapters are explained in Section 3.5. Finally, the rationale behind the choice of the case studies presented in the results chapters is presented in Section 3.6.

3.2 Tool architecture

TESSEE - Tool for Early Stem cellS Economic Evaluation (`https://github.com/catiabandeiras/TESSEE`) was developed as a new versatile free solution for driving economical and biological innovation to the development of stem cell based therapies and research tools. The code is licensed under a General Public License (GPL). The model is open source and cross platform, implemented in the open source programming language Python. Python is a widely used programming language, with widely documented freely available modules for data analysis, such as Numpy and Pandas, and ordinary differential equations and statistical analysis (SciPy). The model outputs can be easily stored as CSV files. Since the core of the model is the discrete event simulation, in order to advance time in discrete steps, the Simpy module was used.

The model modules allow for both deterministic and stochastic simulation, either in the bioprocess economics or health economics modules. Stochastic simulation, when applicable, is applied through the Monte Carlo method, through sampling, per model run, of parameters from an adequate parametric distribution, using the ”random” submodule of the Numpy module. The ranges and shape of parametric distributions, when applicable, are determined from experimental data.

The decisional tool has the following main components: a database, a Fixed Capital Investment (FCI) model, a bioprocess economics model, and a health economics model. The database contains general input parameters and assumptions, which may vary according to the case studies.

Two FCI models described in Section 3.3 were employed in the case studies presented in this thesis: a cost-per-area model and a Lang factor based model. The utilization of each model is dependent on the most appropriate choice for the specific case study.

The FCI model and the bioprocess specific database components are used by the bioprocess economics model to evaluate the cost of goods (COG) per dose, per batch, or per donor. This model optimizes the choice of the number of cell culture systems (either cell culture flasks or bioreactors) in order to minimize equipment occupation and reduce facility footprint. The components of COG are hereby divided into direct and indirect costs as follows:

- **Direct Costs:**
  - *Consumables* for cell culture, storage, and final product formulation
  - *Reagents* for cell and tissue sourcing/acquisition, cell culture, storage, and final product formulation
  - *Quality controls* in intermediate banking steps (when applicable) and final product release testing.
- **Indirect Costs:**

- *Depreciation* of facility and equipment
- *Operating costs* of facility and equipment
- *Labor* for manufacturing, supervision, quality controls and assurance.

The health economics model (Section 3.4) calculates, using an appropriate time span, the total direct medical costs related with managing the disease using a stem cell therapy vs management with the current standard of care, combined with the clinical effectiveness as quality-adjusted life-years (QALY). The difference in total costs is divided by the difference in QALY to provide an incremental cost-effectiveness ratio (ICER) of the stem cell therapy. The ICER per patient is then compared with the willingness to pay threshold (WTP) of a particular payer to determine cost-effectiveness for a specific patient.

In order to run TESSEE on each computer, the following technical requirements are suggested:

- **Python 3** (`https://www.python.org/download/releases/3.0/`). It is recommended that the Anaconda implementation of Python 3 (`https://www.anaconda.com/distribution/`) is used, as it contains most of the data science, parameter estimation, and ordinal differential equation modeling modules by default. It is not recommended that the browser-based Jupyter implementation of Python is used, as it generated inconsistencies with the discrete event simulation scheme across different dependent modules, as the one that was used in this work.
- **A text editor for code.** The development of this code was performed using Sublime Text (`https://www.sublimetext.com/`).
- **A CSV file reader**, such as Microsoft Excel or Libre Office.

3.3 Bioprocess Economics Model

3.3.1 Model workflow

The model structure for the bioprocessing economics builds from several prior contributions on the field for cell therapies, with some adaptations [5, 6, 12, 10]. In cases where applicable, the results from the manufacturing models are used to drive the costs of stem cell based therapies to input in the health technology assessment model.

The basic flowchart of the bioprocess model is shown in Figure 3.1 and is flexible enough to be adapted to any autologous or allogeneic stem cell therapy, and also can include differentiation unit operations for PSC-derived products. The sequence of operations is as follows:

1. Briefly, the model receives several inputs, following the components shown in Section 2.2.1. The inputs fall in the general categories of costs, installed capacity, mass balances, unit operations, cell growth, number of donors to be processed and target doses per simulation run.
2. Then, the scenario is initialized and a specific donor is processed, after its biological parameters were sampled from probabilistic distributions.

3. As long as there are free incubators, or other limiting equipment capacity, the donor is processed, starting the unit operations involved in the stem cell bioprocessing flowsheet. If all units of limiting equipment are occupied, the donor remains in a queue, waiting for its processing to start.

4. For each unit operation, the number of cell culture vessels and equipment to be used for processing this donor is minimized according to cell culture area and equipment constraints.

5. In the end of each expansion passage, the model evaluates if the target number of cells for this donor were achieved. If yes, the downstream processing and release testing are initiated so that, if the doses pass the release testing, the number of doses produced from a donor are added to the total number of doses produced in the facility, and the costs associated to this donor are stored.

6. If all donors were processed, or if the total number of doses to produce in this run was reached, the simulation stops and the cost of goods per dose are computed, taking into account the separate contributions from each process resource and unit operation. The costs of failed batches are spread by the doses that passed the release testing.

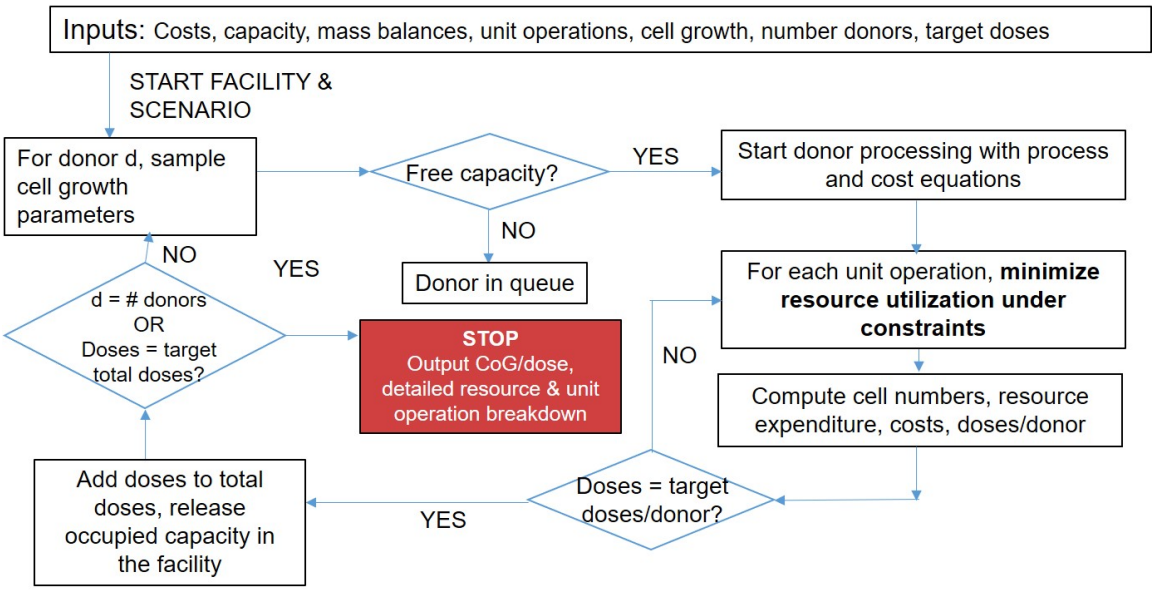

Figure 3.1: Generic Bioprocess Economics model flowchart.

The model follows a specific workflow between modules and classes (in agreement with general object-oriented programming syntax) as depicted below, and in agreement with the workflow presented above. Note that the contents of each module and file can be found on the GitHub repository (`https://github.com/catiabandeiras/TESSEE`):

1. The model receives as inputs both user specified values and database values from literature search and expert opinion (Section 3.5):

    - Database values include costs of facility management, equipment operation and maintenance costs, names, areas and costs of expansion technologies, and unit operation process times.

All the database values are stored as attributes of the **Database()** class in the module file **"database.py"**

- User specified inputs are related to the unit step initial and final cell yields, the number of passages per expansion operation, the number of differentiation stages and their times (when applicable) and the demand for number of cells per dose and number of donors to simulate. All these inputs are stored into the **Database()** class. The inputs have the option to be either deterministic or stochastic, when applicable. When the second option holds, for each run of the model, different values of the parameters are sampled.

2. In order to start the process, an instance of the **Facility()** class is called, to mimic the operation of a facility, using a discrete event simulation scheme to advance the times of operation. For each facility, a set of donors is simulated and processed. Therefore, the facility class has an attribute to call for initialization of different donors. The facility operational code is found in the **"facility.py"** file.

3. The facility recruits new donors until all the doses required are processed (for an allogeneic scheme) or until all required donors are processed (for an autologous scheme). When a new donor is initialized, the donor processing time is initialized and, according to the type of cells and specifications of the process, different sub methods for processing are called representing the unit operations: isolation (for adult stem cell processing), reprogramming (in the case of induced pluripotent stem cells), expansion (with or without intermediate cell banking stages), differentiation (in the case where a final product with a differentiated cell type is required), downstream processing and final release testing. In each one of these stages, depending on the initial number of cells per stage of the process, different cell culture flasks or reactors are recruited, based on the type of expansion (2D or 3D), the seeding densities of the culture process, and the number of cells available. The methods associated with processing of each donor are contained in the **"donor.py"** module.

4. Finally, each flask or reactor behaves as a unique instance that contains an initial number of cells, undergoes culture media changes, has a culture finite period, when the final collection of the cells (in a process called harvesting) with a certain yield occurs. The flasks undergo different processes whether it is an expansion or differentiation protocol. The methods and operations are described in **"flask.py"**.

5. When the facility finished running, either due to reaching the final number of donors to process, or reached the number of doses demanded, the costs of each category are stored as outputs. The outputs are saved as CSV files for easy manipulation, statistical analysis and data visualization. Examples of relevant outputs are the total process times, final cells per donor, total cost of goods per donor and per dose, and cost of goods breakdowns per process unit operation and resource category (consumables, reagents, labor, facility, quality controls).

3.3.2 Model equations

Fixed Capital Investment

In this work, two models were implemented to determine the total initial investment in the installation of a GMP facility for stem cell manufacturing: a cost-per-area model, and a Lang factor based model. These costs form the basis of the Capital Expenditure (CAPEX) with the GMP facility for stem cell bioprocessing.

- **Cost-per-area model:**

  In this model, it is assumed that, for a known GMP facility area, the total facility costs are dependent on the ratio of the GMP facility occupied by clean rooms, with a fixed cost per area of clean room and non-clean room areas. This method was presented in a case study of a GMP facility for manufacturing of tissue engineering products [160] and was the method of choice whenever a fixed capacity was installed. The results of this model were validated with interviews with operators of GMP facilities. The total investment in the facility construction is then calculated as follows:

$$C_{fi} = C_{cr/a} * r_{cr} + C_{ncr/a} * (1 - r_c r) \tag{3.1}$$

  where C_{fi} is the total facility installation costs ($), $C_{cr/a}$ is the cost of clean room space per unit area ($/m^2), r_{cr} is the ratio of the total GMP facility area that is occupied by clean rooms, and $C_{ncr/a}$ is the average cost per area of the facility except clean rooms.

  The FCI is determined by adding the facility installation costs by the equipment installation costs (C_{ei}):

$$FCI = C_{fi} + C_{ei} \tag{3.2}$$

- **Lang factor model:**

  This model is based on the Lang factor, a method typically used in manufacturing facility. Here, the total FCI is determined by multiplying the total equipment acquisition and installation costs by a cost factor (L):

$$FCI = L * C_{ei} \tag{3.3}$$

  In biopharmaceuticals production, this factor typically ranges from 4 to 8 [269]. For facilities for production of regenerative medicine products, values in the range of 2.6 - 23.7 were either reported by other studies [10, 27, 6], estimated from published data on GMP facilities [270, 16, 160], or acquired through validation with industry experts.

  The Lang factor model was the method of choice whenever equipment sizing was dynamically changed in order to supply a given annual demand.

Equipment sizing

In this section, main equipment used in stem cell bioprocessing is considered the following: incubators, bioreactor systems and ancillary equipment for bioreactor culture, biosafety cabinets, centrifuges and specific purification/downstream processing equipment when applicable.

In the cases where a fixed installed capacity was installed and the number of batches processed in parallel is already limited by the installed capacity (Chapters 4, 5, and 7), the costs of the installed equipment are simply determined by multiplying the acquisition cost of each equipment by the number of equipment in this facility. When the facility is being used in parallel for other projects, an occupancy ratio below 1 is multiplied to reflect the percentage of direct utilization of the equipment for the stem cell therapy project.

$$C_{ei} = C_{BSC} * N_{BSC} + C_{inc} * N_{inc} + C_{bioreact_eq} * N_{bioreact_eq} + C_{centrif} * N_{centrif} + C_{DSP} * N_{DSP} \quad (3.4)$$

Where the equipment sizing is changed in order to supply a given annual demand and number of batches being processed in parallel, the number of dedicated equipment for cell expansion (incubators and bioreactor systems) is calculated as:

$$N_{equip,i} = \frac{N_{vessels/batch}}{N_{vessels/equip,i}} * N_{batches,parallel} \quad (3.5)$$

In the equation above, $N_{equip,i}$ represents the number of units of equipment i, $N_{vessels/batch}$ is the number of cell culture vessels (either T-flasks, cell stacks, or single use bioreactor vessels) required, in the last expansion step, to obtain enough cells for a batch, $N_{vessels/equip,i}$ is the maximum number of vessels that fit in each unit of dedicated equipment, and $N_{batches,parallel}$ is the number of batches processed in parallel per campaign.

For labor requirement purposes, the number of clean rooms that the GMP facility will have is calculated as a function of the numbers of each dedicated equipment, given a specified maximum number of incubators or bioreactor systems per clean room:

$$N_{cr} = \frac{N_{equip,i}}{N_{maxequip,i/cr}} \quad (3.6)$$

In agreement with published literature and expert opinion, for the relatively small dimension case studies evaluated on this thesis, a maximum number of incubators per clean room ($N_{maxequip,i/cr}$) between 2 and 4 [270] were considered.

The number of shared equipment (biosafety cabinets, centrifuges, DSP equipment, fill-finish) used is dimensioned assuming that there is a maximum allowable time for each process operation. Hence, there is a need to use several units of the same type of equipment in parallel. For instance, for purification system, the maximum allowable time for DSP is 4h. After this, cell death starts to become significant [147, 10]. In this sense, the number of units of shared equipment are calculated as:

$$N_{equip,i} = \frac{N_{vessels/batch}}{N_{vessels/equip,i}} * \frac{t_{batch}}{t_{max,op/batch}} * N_{batches,parallel} \tag{3.7}$$

Where t_{batch} is the total time the unit operation would take per batch if a single equipment would be used, and $t_{max,op/batch}$ is the total admissible time of the unit operation per batch.

Equipment and Facility Depreciation

The costs related with equipment and facility depreciation for a cell culture campaign are obtained by simply dividing the acquisition costs of these assets by the time of depreciation of these assets, assuming linear depreciation. Since there are campaigns with variable length, instead of the usual annual demand, in some of the results chapters, the operation time length and depreciation time are measured in days.

$$COG_{fe,dep} = (\frac{C_{fi}}{t_{f,dep}} + \frac{C_{ei}}{t_{e,dep}}) * t_{operation} \tag{3.8}$$

In the equation above, $COG_{fe,dep}$ represents the total cost of goods associated with the facility and equipment depreciation, $t_{f,dep}$ and $t_{e,dep}$ represent the time (in days) over which the GMP facility and the installed cell culture equipment are depreciated, respectively, and $t_{operation}$ is the total time (in days) spent in the cell culture campaign.

Equipment and Facility Operation Costs

The costs related with the facility and equipment also have an additional component related with the operations necessary to keep the facility running. Daily rates of the following operational components were considered, in agreement with costs reported in published literature [270] and expert opinion.

$$COG_{fe,op} = (C_{gases} + C_{add,supplies} + C_{requalif} + C_{maintenance} + C_{cleaning} + C_{garment}) * t_{operation} \tag{3.9}$$

The cost components are [270]:

- C_{gases} include the supply of necessary gases for cell culture in the incubators and bioreactors. These gases include oxygen, carbon dioxide, liquid nitrogen, and water vapour.
- $C_{add,supplies}$ include the disposable office supplies, laboratory supplies not related to manufacturing, and utilities.
- $C_{requalif}$ is an annual process for new testing of air quality and compliance with GMP manufacturing norms.
- $C_{maintenance}$ is related with the predicted costs of preventive and corrective procedures in the equipment and facility. The costs are derived from annual estimates.
- $C_{cleaning}$ is related with the annual costs of cleaning and disinfection of the clean rooms.

- $C_{garment}$ include all materials used in clean room gowning.

The total facility and equipment cost contribution is simply obtained by adding the depreciation and operation contributions.

$$COG_{fe} = C_{fe,dep} + C_{fe,op} \tag{3.10}$$

Labor Requirements

The number of manufacturing operators was generally kept fixed when the installed GMP facility area and capacity were constant, with values reported either in the literature or through interactions with experts. As a rule of thumb, it was considered that a minimum number of manufacturing operators in a GMP facility per team is 3. The number of teams is estimated by assuming that each manufacturing team can operate a given number of clean rooms in parallel. For simplicity, in most cases, it was assumed that each team can operate 2 clean rooms simultaneously.

When the installed capacity was dynamically changed, the number of manufacturing operators, $N_{labor,op}$, was increased according to the number of clean rooms each manufacturing team can process in parallel. Accordingly, the number of manufacturing operators is obtained by multiplying the number of operators in a team, $N_{labor,op/team}$, by the number of clean rooms operating in parallel in the facility N_{cr}, divided by the number of clean rooms per team $N_{cr/team,parallel}$.

$$N_{labor,op} = N_{labor,op/team} * \frac{N_{cr}}{N_{cr/team,parallel}} \tag{3.11}$$

Additionally, other personnel is required, namely supervisors and managers to oversee the facility, and Quality Control (QC), Quality Assurance (QA), and Qualified Person (QP) to verify the quality of the batches and of the process at different time points. The supervisors and managers are included in the $N_{labor,sup}$ category and the QC/QA/QP personnel in the $N_{labor,qc}$ category. The numbers of members in each team are calculated given ratios of these personnel categories to the manufacturing operators ($r_{sup/op}$ and $r_{qc/op}$, respectively).

$$N_{labor,sup} = N_{labor,op} * r_{sup/op} \tag{3.12}$$

$$N_{labor,qc} = N_{labor,op} * r_{qc/op} \tag{3.13}$$

The total numbers of personnel involved in manufacturing of the cell therapy are obtained by adding these three categories:

$$N_{labor} = N_{labor,op} + N_{labor,sup} + N_{labor,qc} \tag{3.14}$$

Labor Costs

The labor costs are considered based on the total operator time, based on the number of days the facility is in operation for the cell culture campaign (Eq. 3.15). It is considered that every worker, regardless of the type (operator, supervisor/manager, or QA/QC/QP), receives the same daily salary as a simplification. The rates included in this work include pension and overheads as a simplification as well. Where applicable, a Full-time Equivalent (FTE) is multiplied to account for the average ratio of paid hours by the total number of hours the labor is worked. Additionally, in case the labor is spread out through multiple projects in parallel, a ratio of the total working time of the operating labor spent in the stem cell culture project ($r_{project}$) is also considered.

$$COG_{labor} = N_{labor} * C_{worker/day} * FTE * r_{project} * t_{operation} \tag{3.15}$$

where $n_{workers}$ represents the number of workers in the facility, $p_{worker,day}$ represents the daily pay rate of each worker, and $t_{operation}$ the total operation time to satisfy the demand in the facility.

Utilization of consumables

Within unit operations of isolation, expansion, and differentiation, different vessels for cell culture can be used. The model has a database of 2D vessels (T-flasks, cell culture stacks) with different areas and culture medium volume requirements, starting at 25 cm^2 / 5ml and ending at 6360 cm^2 / 1300 ml. It also has a database of 3D technologies, for either suspension based cultures, like pluripotent stem cell aggregates, or adherent cell cultures, through the use of microcarriers. In the case of differentiation protocols, 6 well plates were also considered, in agreement with published protocols [271, 223]. The 3D vessels considered in this work have working volumes between 100 ml and 50 L, since this is the upper threshold for which efficient expansion of mesenchymal stem/stromal cells was reached in a bioreactor system with microcarriers [162].

The type of vessel selected for each step is done through an algorithm that minimizes the number of vessels to be seeded while reducing as much as possible the waste of cells upon seeding through different flasks. The type of flasks is determined through the following equation:

$$name\_vessel = vessel\_database(min\frac{N_{cells,total}}{N_{cells,vessel}}) \tag{3.16}$$

For adherent technologies or protocols, the number of cells to seed per vessels is determined in the basis of the available expansion area.

$$N_{cells,vessel} = d^{seeding} * a_{vessel} \tag{3.17}$$

In 3.17, $d^{seeding}$ is the seeding density per culture (in cells/cm^2), and a_{vessel} the total culture seeding area available per unit of the culture system in cm^2.

In the case of 3D adherent systems based in microcarriers, the total area is calculated such that:

$$a_{vessel} = a_{mc}^{mass} * c_{mc} * V_{culture,vessel} \tag{3.18}$$

In 3.18, a_{mc}^{mass} is the area per mass of microcarrier (in cm^2/g), c_{mc} is the mass per volume concentration of microcarriers used (g/mL) and $V_{culture,vessel}$ is the working volume of the vessel in mL.

For suspension cultures, like aggregates, the number of cells to seed per culture system is determined on the basis of a volume density $d^{seeding}$ in cells/mL and the working culture volume (Eq. 3.19):

$$N_{cells,vessel} = d^{seeding} * V_{culture,vessel} \tag{3.19}$$

The number of vessels of the type selected through Eq. 3.16 is then determined by dividing the total number of cells available for seeding by the number of cells to be seeded per flask, rounded to the lower nearest integer. The number of cells seeded is limited by the maximum number of flasks of the given type that can be seeded, taking into account limitations in incubator or bioreactor systems, i.e., dedicated equipment (Eq. 3.5), available in the facility.

$$N_{vessels} = min(\frac{N_{cells,total}}{N_{cells,vessel}}, N_{vessels/equip} * N_{equip}) \tag{3.20}$$

Often, the cells are cryopreserved in intermediate steps of the process, such as the establishment of master and working cell banks, in cryovials. Additionally, depending on the final product formulation, the cells for product formulation can either be cryopreserved or stored in bags for fresh cell infusion at the point of care. The number of cell storage containers (i.e., vials or bags, depending on the formulation) per storage step are calculating by dividing the total number of cells coming from the unit operation by the cell concentration in each storage container (in cells/volume) (c_{cells}), multiplied by the maximum volume of each container ($V_{container}$), and rounded to the nearest integer:

$$N_{containers} = \frac{N_{cells,total}}{c_{cells} * V_{container}} \tag{3.21}$$

For processes that require centrifugation, volume reduction, and/or affinity purification of cells, disposable centrifugation vials or purification columns are required. Three options were considered in the development of TESSEE:

1. For the sake of simplicity, a fixed consumables cost for the purification step was assumed [156] (Chapter 6).

2. A similar approach to the cell storage case was assumed for the centrifugation as the method and of choice for DSP (used in isolation and in smaller scale purification of MSC) (Chapters 4, 5, and 7).

3. In the development of the case studies, it was also considered that, for the affinity purification of differentiated cells, the number of columns for purification was obtained by dividing the total number of cells to be sorted by the maximum number of cells per purification column.

Mass balances

In this section, the step yield and considerations for each unit operation are described in more detail.

The isolation process is used in the case studies pertaining this thesis work to obtain MSC from different cell sources. For the sake of generalization, the population that is seeded after isolation from each cell source is a mixed population ($N_{mixedpop}$) containing MSC. The number of MSC (N_{MSC}) is then calculated from the ratio of MSC after the isolation process respective to the initial number of cells from the mixed population ($r_{MSC/mixedpop}$).

$$N_{MSC} = N_{mixedpop} * r_{MSC/mixedpop} \tag{3.22}$$

The expansion process is used across all case studies and the following equation is related to the number of cells at the end of each passage relatively to the number of cells in the beginning of each passage. Pasaging, i.e, performing expansion by seeding and harvesting the cells sequentially in different vessels, prevents cell accumulation to become a limiting factor in expansion and quality attributes of cell culture, as cells multiply during the culture process. The number of cells obtained per vessel at the end of a passage $N_{cells,f}$ is divided by the number of seeded cells $N_{cells,i}$ to obtain a fold increase FI. Keep in mind that the number of cells obtained at the end of each passage is reduced by the harvesting yield Y_h, as cell detachment from the vessels (i.e., harvesting) always involves a certain amount of loss of cell viability.

$$FI = \frac{N_{cells,f}/Y_h}{N_{cells,i}} \tag{3.23}$$

The fold increase obtained from literature data μ can be used to estimate daily growth rates of cell culture through a simple exponential growth curve. The calculation takes in account the period, in days, from the beginning and end of the exponential growth stage (Δ t).

$$\mu = \frac{\ln(FI)}{\Delta t} \tag{3.24}$$

While this was the model applied, for the sake of simplicity, to estimate the growth rates in the case studies presented in this thesis, other models were considered as well.

An ordinary differential equation (ODE) model assuming growth saturation and cell death should be used whenever data on cell growth at a given time ($N_{cells,t}$) from growth curves allows an accurate estimation of the three model parameters: μ and k_d, representing the specific daily growth and death rates, respectively, and $N_{cells,max}$, introduced to take into account the effect of cell confluence and growth saturation [272, 273]. These parameters can be estimated with appropriate curve fitting methods:

$$\frac{dN_{cells,t}}{dt} = \mu N_{cells,t} * \frac{N_{cells,max} - N_{cells,t}}{N_{cells,max}} - k_d * N_{cells,t} \tag{3.25}$$

In order to account for growth limiting substrate dynamics, a Monod kinetics where glucose is the limiting substrate was reported for MSC growth [274] and was also considered during the development of TESSEE. For case studies where data on metabolite consumption and production is available, es-

timation of rates with limiting substrate can provide additional information, aiming at optimizing culture media exchange protocols:

$$\mu = \mu_{max} * \frac{C_g}{K_g + C_g} \tag{3.26}$$

In equation 3.26, μ_{max} is the maximum daily growth rate, C_g is the concentration of substrate (in this case, glucose) in the culture medium (generally, in mol/L) and K_g is the half-rate concentration, that is, the substrate concentration for which μ is half of μ_{max}.

Finally, the growth rates influence the cell growth in time through an ODE such as 3.25, or simplified as:

$$\frac{dN_{cells,t}}{dt} = \mu * N_{cells,t} \tag{3.27}$$

When applicable, the number of cells of a given differentiated lineage, obtained from either pluripotent or multipotent stem cells, are obtained simply by multiplying the number of seeded stem cells in the beginning of the unit operation by the ratio of differentiated cells to the initial seeded stem cells, called the differentiation yield (Y_d). Note that the number of differentiated cells is obtained when the differentiation protocol ends. The total differentiation time can vary from a few weeks to a few months [222].

$$N_{cells,diff} = N_{cells,i} * Y_d \tag{3.28}$$

Finally, the number of cells obtained after downstream processing (volume reduction and purification) and the fill-finish of the product to the final formulation are obtained by multiplying the number of cells entering the downstream processing by the yield of these unit operations (Y_{vrp} and Y_{ff} respectively).

$$N_{cells,f} = N_{cells,i} * Y_{vrp} * Y_{ff} \tag{3.29}$$

After obtaining the final number of cells of each batch, or of the final process, the number of doses produced is simply obtained by dividing the number of cells by the target number of cells per dose.

$$N_{doses} = \frac{N_{cells,f}}{N_{cells,dose}} \tag{3.30}$$

Cost of Consumables

The disposable culture vessels consumable cost of goods (COG) associated with cell culture are simply calculated by a sum of the number of flasks of each category, multiplied by the costs of each flask, with a microcarrier based contribution whenever applicable (Eq. 3.31):

$$COG_{vessels} = \sum N_{vessels,i} * C_{vessel,i} + m_{mc} * C_{mc}^{mass} \tag{3.31}$$

$C_{vessel,i}$ represents the vector containing the unit cost of a particular vessel type, m_{mc} the total mass of microcarriers spent, and C_{mc}^{mass} the cost per gram of microcarrier. Consumable costs associated with

the vessels for storage $COG_{storage}$ are also considered, and the purification disposable consumables COG_{purif} as follows:

$$COG_{storage} = \sum N_{container,i} * C_{container,i} \tag{3.32}$$

$$COG_{purif} = N_{centrif} * C_{centrif} + N_{columns} * C_{columns} \tag{3.33}$$

The total consumable costs of a process are then the sum of these three cost components:

$$COG_{consumables} = COG_{vessels} + COG_{storage} + COG_{purif} \tag{3.34}$$

Utilization of reagents

In the case study where isolation of stem cells from a complex mixture is considered (Chapter 4), the mixed population of interest is separated from the cell source through density gradient centrifugation. In a more specific way, it is considered that isolation reagents in the initial isolation stage (before seeding of the mixed population into cell culture vessels) comprise only the density centrifugation volume. However, isolation processes for adipose tissue and umbilical cord matrix include protocols requiring enzymatic treatment [200, 273], for which the volume of enzymes could easily be added into the code. The volume of density gradient per stem cell donor is multiplied by the number of donors isolated in the process.

$$V_{dg} = \sum V_{dg,donor} * N_{donors} \tag{3.35}$$

The key reagent for cell culture is the culture media used for cell expansion. The volume of culture media per vessel in a given cell culture passage is calculated by adding the volume used for cell seeding, the volume used in media exchanges during the passage, and the volume used for formulation and inactivation of the harvesting reagent.

$$V_{cm,vessel} = V_{cm,seeding} + V_{cm,feeding} * N_{exchanges,media} + V_{cm,harvesting} \tag{3.36}$$

The total volume of culture media can be calculated by the sum of the culture media requirements of each type of vessel, multiplied by the number of vessels of that particular type used in cell culture. Note that culture media can be unit operation specific, as the media used for stem cell culture is different from the media used for differentiation of stem cells, for cell harvesting, cell wash between operations, and cryopreservation.

$$V_{cm} = \sum V_{cm,vessel,i} * N_{vessel,i} \tag{3.37}$$

In the end of each passage, a given volume for cell detachment from the cell culture vessels is used. The total volume of harvesting reagent is calculated in the same way as calculated above for the total utilization of culture media.

$$V_{hr} = \sum V_{hr,vessel,i} * N_{vessel,i} \tag{3.38}$$

Volume reduction and purification after cell culture requires washing the cells from the culture media. The cells are washed multiple times with a basal media, having a different formulation of the culture media. The volume of washing media is calculated by taking into account the possibility of more than one cycle of cell washing and purification:

$$V_{wm} = V_{wm,wash} * N_{washes} \tag{3.39}$$

Finally, cryopreservation buffers or buffer for fresh product formulation are required for cell storage of intermediate or final products. As a generalization, these are considered in the same category of formulation buffers:

$$V_{fb} = V_{cryo,buffer} * N_{cryovials} + V_{fresh,buffer} * N_{bags} \tag{3.40}$$

Reagent costs

The total costs of reagents are obtained by taking into account all reagents used in the multiple stages (Eq. 3.41):

$$COG_{reagents} = V_{cm} * C_{cm} + V_{dg} * C_{dg} + V_{hr} * C_{hr} + V_{wm} * C_{wm} + \sum V_{fb} * C_{fb} \tag{3.41}$$

Quality Control

The quality controls are assumed to have a fixed cost per batch produced, and the costs per dose are divided by the number of doses produced per batch. In the cases where intermediate banking steps are used, due to the establishment of master and working cell banks, intermediate quality controls are also input and multiplied by the number of MCB and WCB established during the whole culture process. The total quality control costs are given as 3.42:

$$COG_{QC} = C_{QC,batch} * N_{batch} + C_{QC,WCB} * N_{WCB} + C_{QC,MCB} * N_{MCB} \tag{3.42}$$

The quality controls are always associated with a given batch failure rate. If, for the considered batch, the quality controls are passed, all the calculated costs in the other categories are kept and the quality control costs divided by all the doses in that batch. However, if there is a batch failure, all the doses in that batch are discarded, and the full costs of producing that batch are equally divided by the doses in other batches that passed the quality controls.

Total costs of goods

The total COG of the process are obtained by adding all the contributions presented above:

$$COG_{total,process} = COG_{consumables,process} + COG_{reagents,process} + COG_{labor,process} + COG_{fe,process} + COG_{QC,process} \quad (3.43)$$

The cost of goods per batch are obtained by summing the costs associated directly with the batch size, such as direct expenditure of consumables and reagents, and the quality controls, with the indirect costs (labor, facility and equipment depreciation and operation, and quality controls).

$$COG_{direct,batch} = COG_{consumables,batch} + COG_{reagents,batch} + \frac{COG_{QC,process} * N_{doses,batch}}{N_{doses,process}} \quad (3.44)$$

$$COG_{indirect,batch} = \frac{(COG_{labor,process} + COG_{fe,process}) * t_{operation,batch}}{t_{operation,total}} \quad (3.45)$$

$$COG_{batch} = COG_{direct,batch} + COG_{indirect,batch} \quad (3.46)$$

Finally, the cost of goods per dose is obtained by dividing the total costs per batch by the number of doses produced in this batch.

$$COG_{dose} = \frac{COG_{batch}}{N_{doses,batch}} \quad (3.47)$$

3.4 Health Technology Assessment Model

3.4.1 Model workflow

The models for health technology assessment vary with the clinical application sought after, but they follow the same structure input wise. The health economics model is based on a cost-utility analysis. A cell therapy is chosen over the comparator standard of care as a result of showing a higher effectiveness in terms of quality of life of the patients, as measured by health state utility values, and a combination of either cost minimization or higher costs below a willingness to pay threshold (expressed in cost/quality – adjusted life years (QALY)). Similar to the Bioprocess Economics Model in the previous section, the model follows a generic workflow that can be adapted to any therapeutic indication (Figure 3.2):

1. The model receives as inputs both user specified values and database values from literature search and expert opinion. Database values include costs of the different therapeutic options, costs associated with general management in each health state to be modeled, probabilities of state transition and probabilities of additional health complications, costs of health complications, the initial utilities of each health state and decrements from complications. Age-specific mortality rates are also included in the database as calculated from life tables. User-specified inputs are related to the number of patients to simulate in the model run, the follow up time of each patient,

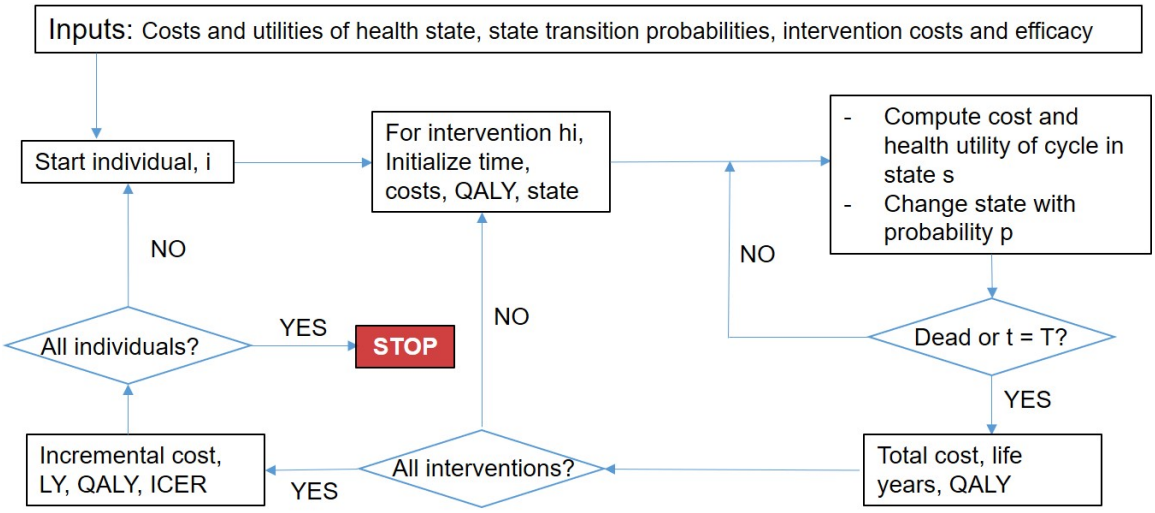

Figure 3.2: Generic microsimulation cost-utility flowchart.

the initial age at time of the follow-up, and the initial state the patient is on. The inputs have the option to be either deterministic or stochastic, when applicable. When the second option holds, for each run of the model, different values of the parameters are sampled.

2. In order to start the process, an individual is initialized and assessed for both therapeutic options considered in the model. This contains the the disease state transition Markov model, where patients move through health states in time with different state transition probabilities, as described in the next chapter for the respective case studies. Each disease state is associated with a health utility between 0 (death) and 1 (perfect health) and with costs of managing that health state. Over time, when the individual migrates through these states, the costs and utilities are accumulated to calculate the final costs and utilities for the patient and treatment option.

3. When the model finishes running, due to reaching the final number of individuals to process, the costs, utilities, and occurrence of related complications for each of the therapeutic options are stored for all individuals. The values provide a statistical distribution of the cost-effectiveness of the stem cell based therapy over a standard of care with varying patient outcomes.

In terms of the flow between the different modules of Python present in the source code of TESSEE, the model implementation is shown as follows:

1. The model receives as inputs both user specified values and database values from literature search and expert opinion (Section 3.5):

    - Database values include costs of the different therapeutic options, costs associated with general management in each health state to be modeled, probabilities of state transition and probabilities of additional health complications, costs of health complications, the initial utilities of each health state and decrements from complications. Age-specific mortality rates are also included in the database as calculated from life tables. All the database values are stored as attributes of the **Database()** class in the module file **"database.py"**

- User specified inputs are related to the number of patients to simulate in the model run, the follow up time of each patient, the initial age at time of the follow-up, and the initial state the patient is on. The inputs have the option to be either deterministic or stochastic, when applicable. When the second option holds, for each run of the model, different values of the parameters are sampled. These values are distributed appropriately by the **"main.py"** and **"individual.py"** modules.

2. In order to start the process, an instance of the **Individual()** class is called for both therapeutic options considered in the model. This class contains the the disease state transition Markov model, where patients move through health states in time with different state transition probabilities, as described in the next chapter for the respective case studies. Each disease state is associated with a health utility between 0 (death) and 1 (perfect health) and with costs of managing that health state. Over time, when the individual migrates through these states, the costs and utilities are accumulated to calculate the final costs and utilities for the patient and treatment option. The definition of the patient-specific model is on the **"individual.py"** module.

3. When the model finished running, due to reaching the final number of patients to process, the costs, utilities, and occurrence of related complications for each of the therapeutic options are stored for all the patients. This data is stored in CSV files using code contained on the **"main.py"** module. The values provide a statistical distribution of the cost-effectiveness of the stem cell based therapy over a standard of care with varying patient outcomes.

3.4.2 Model equations

The cost utility assessment in the end of the disease state modeling period performed by calculating the differences between costs and QALY between the new treatment and standard of care (Eqs. 3.48,3.49). More details in the calculation of costs and QALY for each case study are provided in the specific case studies of Chapters 6 and 7.

$$\Delta Cost = Cost_{new} - Cost_{standard} \tag{3.48}$$

$$\Delta QALY = QALY_{new} - QALY_{standard} \tag{3.49}$$

If the cost of new treatment is lower and effectiveness is higher, the new intervention is cost dominant. In the opposite case of higher costs and lower effectiveness, the standard of care is dominant and the new therapy would not be adopted. In the case of higher costs and effectiveness or lower costs and effectiveness, the decision of which therapy to adopt is not as straightforward. The decision in this case would be related to the values of the incremental cost effectiveness ratio (ICER) (Eq. 3.50):

$$ICER = \frac{\Delta Cost}{\Delta QALY} \tag{3.50}$$

3.5 Data acquisition

A comprehensive set of parameters and process configurations were included in the modeling exercises using this tool. While the general configuration and flow of cells in a GMP facility was general, process specific adaptations were required to better fit the case studies.

Most of the cell growth parameters were calculated from literature research and a thorough consultation of the process parameters used in each step of stem cell bioprocessing. Additionally, prices of reagents, consumables, quality controls, equipment and facility operation costs were collected and validated with experts and laboratory researchers.

For the health economics models, the specific disease state models for type 1 diabetes and cystic fibrosis were adapted from existing literature on the field. Values for the specific parameters were collected from either published manuscripts or reports from patient registries, and validated with expert clinicians.

The discussions pertaining the model and parameter validations included experts from the following academic, industrial and clinical centers:

- Stem Cell Engineering Research Group, Instituto Superior Técnico, Universidade de Lisboa, Portugal
- Department of Bioengineering, Instituto Superior Técnico, Universidade de Lisboa, Portugal
- Instituto de Medicina Molecular, Universidade de Lisboa, Portugal
- ECBio, Amadora, Portugal
- Newbiotechnic, Seville, Spain
- Eppendorf, Hamburg, Germany
- Harvard Stem Cell Institute, Cambridge, MA, USA
- Sentien Biotechnologies, Lexington, MA, USA
- Semma Therapeutics, Cambridge, MA, USA
- RoosterBio, Frederick, MD, USA
- Compass Biomedical, Cleveland, OH, USA
- Harvard Medical School, Boston, MA, USA
- Boston Children's Hospital, Boston, MA, USA
- Case Western Reserve University, Cleveland, OH, USA
- Joslin Diabetes Center, Boston, MA, USA

3.6 Choice of case studies

In the conception of the bioprocess modeling tool, the main aim was to enable the tool to be flexible enough to accurately model two of the main stem cell types in preclinical and clinical studies: mesenchymal stem/stromal cells (MSC), and pluripotent stem cells (PSC). Showcasing these two different stem cell types is compliant with the present market and regulatory trends. More information on these trends can be found in Chapter 2.

MSC were chosen due to the maturity of clinical trials, and the fact that they are adult stem cells, retrievable from diverse sources. Furthermore, their use avoids the ethical issues of PSC (in particular, for embryonic stem cells). PSC were selected as they have an additional regenerative potential that MSC do not have, as PSC can be differentiated into any cell type of the organism. Additionally, the discovery of the method of reprogramming differentiated cells into induced pluripotent stem cells (iPSC) opened new avenues in personalized medicine, while avoiding the ethical issues with embryo destruction.

Chapter 4 was conceptualized to comply with the research, industry, and regulatory trend for reduction of the use of animal components in human stem cell bioprocessing, namely culture media supplementation with fetal bovine serum (FBS). There are several formulations of human platelet lysate (hPL) in the market, supporting improved cell proliferation from FBS. As hPL is a more expensive supplement than FBS, this paper studied under which conditions would a process transfer to a xeno-free culture medium be cost-effective from the manufacturing standpoint. The inclusion of uncertainty in the growth curves, process times, and process costs would allow to pinpoint strategies for uncertainty reduction in the process transfer to a new culture medium.

Chapter 5 aimed at showcasing the abilities of the model for microcarrier based culture of MSC from two different cell sources, through economic modeling based on experimental data from the Stem Cell Engineering Research Group (SCERG). Scale-up of MSC culture by microcarrier-based culture has been reported in the literature and the modeling work showcases the trade-off between increased cell culture vessel costs and higher cell yields, and determine if the investment in the Vertical Wheel Bioreactor is cost-effective.

Chapter 6 was derived to showcase a more complete version of stem cell bioprocessing, allowing for modeing of pluripotent stem cell (PSC) based products. The choice of clinical application - type 1 diabetes was obtained in a combination of the considerable market size for the stem cell-based therapy, the envisioned clinical benefits by the elimination of insulin dependence and the avoidance of immunosuppression by an encasing device, and the accessibility to academic, industry, and clinical experts in the Boston area.

Chapter 7 aimed at modeling the cost-effectiveness of a possible anti-inflammatory, MSC-based, therapy for cystic fibrosis, undergoing a Phase I/II clinical trial. This project was devised after the collaboration with Compass Biomedical for two poster presentations through mutual introductions and was considered an innovative work, due to the fast-growing therapeutic research in cystic fibrosis, and by being the first report of early health technology assessment of cell therapies for this disease.

Chapter 4

Bioprocess economics assessment of process transfer to xeno-free culture media for patient-specific mesenchymal stem/stromal cell based therapies

Note: The contents of this chapter are adapted from the peer-reviewed article: C. Bandeiras, J. M. S. Cabral, S. N Finkelstein, F. C. Ferreira, Modeling biological and economic uncertainty on cell therapy manufacturing: the choice of culture media supplementation, Regenerative Medicine 13(8), 917-933 [275]

4.1 Outline

The aim of the studies presented in this chapter is to evaluate the cost-effectiveness of manufacturing of autologous cell therapy in xeno-free conditions. The expansion of bone marrow human mesenchymal stem/stromal cells (BM-hMSC), with culture media supplemented either with fetal bovine serum (FBS) or human platelet lysate (hPL) is assessed. This chapter presents the first case study using the bioprocess modeling capabilities of TESSEE (Section 3.3). Herein, it is illustrated how the model can be used for modeling manufacturing costs of stem cell therapies. The selected case study aims at answering the question of what is the acceptable price of a new culture media that promotes better expansion rates than the current standard of culture to obtain lower manufacturing costs per dose.

The biological variability is included in the model, namely establishing distribution curves for isolation and expansion of BM-MSC. This chapter discusses the effect of introducing donor, multi-passage, and

culture media variability on cell yields and process times. A case study was established for the use of adherent culture flasks at a scale-out campaign of 1000 doses of 75 million cells for autologous therapy. In this autologous therapy, each donor generates one clinically relevant dose.

The results obtained show that passage numbers in the expansion step are strongly associated with the isolation cell yield. Each additional passage drives additional costs per dose of $1,970 and $2,802 for FBS and hPL respectively. hPL decreases passage numbers in 94.5% of donors, while the process costs are lower in 97% of donors in comparison with FBS. The main drivers for this cost reduction are lower facility and labor contributions to the costs. Cost-savings are maintained when the inclusion of equipment and facility depreciation is considered. When a higher target number of cells per dose are also considered, hPL culture is also less expensive. This fact demonstrates that the number of cells obtained per passage step is the key cost driver.

These results, overall, show that, at the current price and promotion of proliferative abilities of BM-hMSC, hPL is a cost-effective culture media supplement for manufacturing of autologous BM-hMSC based therapies. The inclusion of biological uncertainty at the isolation and expansion steps made possible by TESSEE highlighted the importance of sustained improvement of isolation and expansion cell yields.

4.2 Methods

4.2.1 Model Overview

The discrete event simulation model was adapted from the tool described in 3.3 to determine the impact of donor, multi-passage and culture media associated variability on the manufacturing cost structure of autologous mesenchymal stem/stromal cell-based therapies. The tool was implemented in Python, comprising a database of resources and experimentally derived inputs.

The model is designed to perform calculations such that bone marrow aspirates queue for incubators and, once an incubator and operator are available, the density gradient centrifugation process to isolate mononuclear cells (MNC) starts, yielding a number of MNCs to be seeded into an appropriate adherent cell culture flask (eq. 3.22). The model selects for the optimal number and area of these flasks to seed cells with an appropriate initial density (eqs. 3.16 - 3.17) (Tables 4.1 to 4.3) [145]. The flasks undergo simulated media changes until reaching confluence, as specified by confluence times and yields of mesenchymal stem cells (MSC) per MNC seeded [276, 277]. After obtaining the initial MSC population, simulation of the expansion starts in order to multiply the cell number until the target number of cells is reached. The same process for optimal flask selection occurs and cells are incubated until reaching the appropriate harvesting density and confluence time. Then, calculations account for the cells to be removed from the flasks using a harvesting agent and re-seeded in new flasks to mimic the passaging process until the target number is reached. Afterward, the model simulates that cells are separated from the culture medium, undergo cell wash and concentration, and are then cryopreserved. Finally, release testing of the batch is considered.

Table 4.1: GMP facility and equipment related parameters

Parameter	Value	Reference
GMP facility area	400 sq. mt.	[270]
Number of workers	9	[270]
Number of incubators	8	[270]
Number of BSCs	4	[270]
Number of centrifuges	4	[270]
% clean room space	20%	[160]
Price clean room/sq. mt.	$5,815	[160]
Price non clean room/sq. mt.	$3,392	[160]
Facility depreciation period	15 years	[270]
CO^2 supply annual cost	$6,000	[270]
Other gases supply annual cost	$15,600	[270]
Additional lab supplies annual cost	$7,900	[270]
Requalification annual cost	$65,400	[270]
Maintenance annual cost	$52,800	[270]
Cleaning annual cost	$28,000	[270]
Garments annual cost	$2,000	[270]
Daily worker pay	$100	This work
Unit incubator price	$17,835	[5]
Unit BSC price	$17,000	[5]
Unit centrifuge price	$12,000	This work
Equipment depreciation period	5 years	[5]

Biological variability is an input in the model at the level of the number of MNC per bone marrow aspirate volume [277], the yield of MSC per MNC seeded [276], and the multi-passage harvesting densities at confluence [3]. The published experimental data was used to derive probabilistic distributions (Table 4.4) from which these parameters are sampled for each donor. These parameters will drive a Monte Carlo simulation method for stochastic simulation. The different resulting initial MSC population and the number of MSC per area at confluence will impact the number and area of culture flasks used for isolation and expansion that are calculated accordingly as a model variable. As a result, appropriate reagent volumes are input into the database and the different number of cells per passage will drive expansion processes occurring with varying numbers of passages, driving a range of process times that will impact the operational costs related to the facility and labor as well.

Throughout the simulated process, the operation times, occupancy times of equipment, and the amount of single-use expansion technologies and reagents used are stored into appropriate databases to allow for the final calculation of the manufacturing costs per dose (Figure 4.1). The cost structure has indirect costs components, related to the depreciation of facility materials and equipment, facility and equipment operational costs, and labor, and direct costs, comprising all the expenditure in reagents (culture medium, isolation reagents, cryopreservation medium, harvesting solution), single-use expansion technologies (consumables), and quality controls. The total manufacturing costs are calculated on a per dose basis within the same batch. The costs associated with doses that fail the quality controls

are distributed equally by the accepted batches.

Table 4.2: Cell processing parameters

Parameter	Value	Reference
Common across stages		
DMEM basal media/ml	\$0.04	This work
FBS/ml	\$2.38	This work
hPL/ml	\$4.28	This work
TrypLE (Harvesting agent)/ml	\$0.21	This work
PBS (buffer solution)/ml	\$0.08	[278]
Isolation		
Volume bone marrow	10 ml	[279]
Volume Ficoll Paque	20 ml	[276]
Ficoll Paque/ml	\$0.39	This work
Volume PBS	\$10 ml per wash + 10 ml initial BM dilution	[276]
Number of washes	2	[276]
Time initial centrifugation	30 min	[276]
Time centrifugation/wash	10 min	[276]
Time for MSC isolation	9 days hPL, 12 days FBS	[277]
Seeding density MNC	200,000 cells/cm^2	[272]
Expansion		
Maximum no. passages	5	This work
Passage time	6 days	[278]
Number cells/dose	75 million	This work
Number doses/donor	1	[51]
Seeding density/passage	5,000 cells/cm^2	[278]
Harvesting yield	0.9	[6]
Harvesting time	14 min	This work
Downstream Processing		
Number of washes	2	[278]
Volume reduction and washing time	4h	[10]
Volume reduction yield	0.8	[10]
Cell concentration	12.5 million/ml	This work
Fill finish time	2h	[10]
Cryovial volume	2 ml	This work
Unit price cryovial	\$1.27	This work
Cryomedium/ml	\$2.68	This work
Ratio cryomedium/basal medium	0.5	[56]
Release Testing		
Pass/release ratio	0.9	[29]
Price quality control testing/donor	\$10,000	[5]
Quality control time	7 days	This work

Table 4.3: Characteristics of expansion technologies used in this work to simulate 2D expansion. Times and maximum unit numbers referenced from [5]

Name	Area (cm^2)	Unit price ($)	Media (ml)	Harvesting reagent (ml)	Seed time (h)	Feed time (h)	Harvest time (h)	Max no. units per worker	Max no. units per incubator
T25	25	1.65	5	1.75	0.04	0.04	0.05	10	100
T75	75	4.58	15	3.5	0.04	0.04	0.05	10	100
T175	175	7.38	35	7	0.04	0.04	0.05	10	100
T225	225	8.55	45	9	0.04	0.04	0.05	10	100
Cellstack1	636	33.89	130	25	0.15	0.15	0.06	1	60
Cellstack2	1272	60.12	260	50	0.15	0.15	0.06	1	60
Cellstack5	3180	131.96	650	125	0.20	0.20	0.16	1	24
Cellstack10	6360	142.72	1300	250	0.25	0.25	0.25	1	12

Table 4.4: Cell processing stochastic parameters

Parameter	Probability distribution type	Probability distribution profile	Reference
No. MNCs/ml bone marrow	Triangular	2.03,6.87,11.71e6	[276]
MSC/MNC, FBS	Triangular	0.05,0.10,0.20	[277]
MSC/MNC, hPL	Triangular	0.05,0.10,0.20	[277]

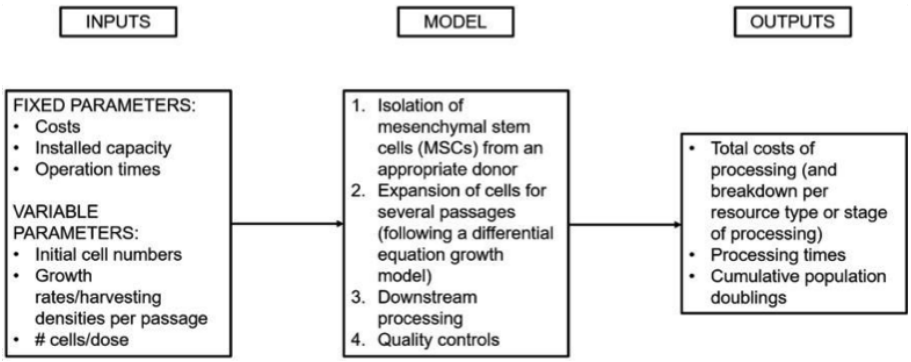

Figure 4.1: Inputs and Outputs of the model.

4.2.2 Case study definition

The case study baseline scenario encompasses the simulation of a process transfer from an animal-based culture to a xeno-free culture in a GMP facility manufacturing setting for a prospective autologous mesenchymal stem/stromal cell-based therapy. Clinical trial information for the only approved autologous MSC based product (Hearticellgram) reports doses of 1 million cells/kg, yielding 72 +/- 0.9 million cells per patient [51]. A therapeutic dose of 75 million cells per dose will be simulated accordingly, as an average patient weight of 75 Kg was adopted. We assume a scale-out manufacturing scheme, where several donors are processed in parallel while there is equipment availability. The study will be parameterized using a study reporting the multi-passage expansion of BM-MSC with DMEM + 10% FBS and with DMEM + 10% hPL using several donors (Table 4.5) [3]. To estimate growth rates and isolation yields, we used studies related to the yield of MSC per seeded MNC obtained from the isolation of bone marrow aspirates using the Ficoll-Paque density method [276, 277]. In the isolation step, 9 to 12 days of duration were simulated, according to the experimental data [277]. Relatively to the expansion step,

simulations will consider up to 5 passages, with each passage taking 6 days to complete, and a seeding density of 5000 cells/cm^2. The purification and volume reduction takes 4 hours and the final product formulation takes 2 hours [10]. Finally, a complete release testing takes 7 days before the product is shipped for administration.

To account for donor, multi-passage and culture media variability on isolation yields and expansion growth rates, 1000 donors will be simulated and parameterized through sampling from the aforementioned probabilistic distributions. In the base line scenario, the isolation yields and growth rates of BM-MSC with either FBS or hPL supplementation will be derived from the experimental studies directly and the current market prices of the two supplements will be used for comparison, with hPL being considered twice as expensive per volume as FBS [280, 281]. Probabilistic distributions of the total costs per dose and numbers of passages will be derived, reflecting the different numbers of steps required to reach the demand per dose and how the different variable factors affect the costs of manufacturing. Due to batch-to-batch variability verified in different commercial formulations of these culture media supplements and consequent possible impact on the biological parameters, key model drivers (isolation yield, isolation time, multi-passage harvesting density, price of hPL, labor rate, equipment depreciation and number of cells per dose) were varied to determine the robustness of the cost-effectiveness of the process transfer. Due to the diverse nature of the parameters, the sensitivity analysis was conducted by normalizing the parameter variability. Each parameter had a 25% increment or decrement for the nominal value to assess what are the parameters that influence the most the distributions of the cost of goods for both culture media formulations.

Table 4.5: Growth rates (mean & 95% CI) calculated from harvesting densities derived from [278] (n=1000)

Passage number	Growth rate, FBS(day^{-1})	Growth rate, hPL(day^{-1})
1	0.18 (0.16-0.21)	0.27 (0.26-0.29)
2	0.19 (0.17-0.21)	0.30 (0.29-0.31)
3	0.20 (0.17-0.24)	0.29 (0.27-0.30)
4	0.18 (0.17-0.19)	0.18 (0.11-0.24)
5	0.18 (0.17-0.19)	0.18 (0.11-0.24)

4.3 Results

4.3.1 Impact of culture media supplement on isolation and expansion manufacturing cost variability and processing times

The biological variability inputs from the culture with hPL vs FBS stem from two major contributions: (i) a higher ratio of isolated MSC per number of seeded MNC and faster isolation times [277], and (ii) higher numbers of cells at the confluence and faster growth rates through several passages in planar expansion [282, 220]. From the sampled donors, we created a distribution of the number of MNC per

donor with an average number per donor of 68.8 million cells (95% CI: 30.8 – 106.7) (Figure 4.2A). For the simulation of the isolation of MSC from 10 ml of bone marrow aspirate using the Ficoll-Paque density gradient method, the FBS group yielded, on average, 6.0 million P0 MSC (95% CI: 2.2-14.5), while the hPL group yielded an average of 9.54 million P0 MSC (95% CI: 3.32-21.7) (Figure 4.2B). 89% of the simulated donors were computed to have an increase in the yield of P0 MSC. On average, the MSC yield per donor with hPL was 1.72 times higher than with FBS (95% CI: 0.77-3.34). Given the different number of cells obtained after isolation (i.e at P0), is expected that the sequential passages of MSCs to achieve the final dose of 75 million cells per patient will start with more cells with hPL than with FBS for most of the donors (Figure 4.2C).

For hPL based cell culture, fewer passages are needed to reach the final target number of cells relative to FBS based cell culture. This is a consequence of the higher numbers of cells at the end of each passage, combined with the higher initial numbers of MSC for expansion. For isolation and cultures with hPL, the 75 million cells are obtained between one and four passages, with 79% of donors reaching the final dose in two passages, while for isolation and cultures with FBS reaching the same number of cells took two or more passages, with 61.5% of donors reaching the final cell number after four passages (Figure 4.3A). By analyzing the difference in the number of passages necessary to achieve the final cell demand, the majority of the donors reached the final cell number with hPL in two passages less than with FBS (54.6%). Only 5.5% of the donors did not experience any difference in the number of passages required (Figure 4.3B). The number of passages required to expand the cells to the final dose is strongly negatively correlated with the initial number of cells at isolation, in particular for FBS cultures (R^2 = -0.86 for FBS vs R^2 = -0.68 for hPL) (Figures 4.3C, D). However, the harvesting densities at passage 1 and the number of passages required to expand the cells in both culture media supplements did not show any meaningful correlation (Figures 4.3E, F), suggesting that the initial cells after isolation are a key factor to drive faster processing in the xeno-free culture.

The integration of the biological aspects and variability of cell culture in the model allows the translation of their impact on manufacturing decisions by calculation of variable process costs. The calculations show that the stochastic nature of cell isolation and expansion rates and its impact on the processing times will lead to considerable differences in the total costs of the process (Figure 4.4A). Bioprocessing of autologous BM-MSC using FBS as a culture medium supplement has a calculated average total cost per dose of $24883 (95% CI: $21365 - $27421) while the same process with hPL as a supplement has an average estimated cost of $20947 (95% CI: $18033 - $23423). The peaks of the cost distributions are in agreement with the distributions of the number of passages per donor (Fig. 4.3B). For the hPL, the most frequent cluster of CoG/donor (approximately $20,000/donor) is for donor that took 2 passages with hPL to reach the target cell number. For FBS cultures, the peak cluster of CoG/donor of about $25,500/donor is for donor taking 4 passages to reach the target number of cells.

Out of all sourced cell samples from different donors, it is estimated that there are savings in total process costs for 97.1% of the cases when processed with hPL supplementation. On average, calculated processing costs of the cells from the same donor with hPL implies a reduction by 0.84 fold relatively to culture using FBS (95% CI: 0.77-1.00) (Figure 4.4B). This cost reduction is connected to the lower

number of passages required to expand the cells. The peak cluster around a hPL/FBS cost ratio per donor of 0.8 is composed of donors for which the use of hPL resulted in a saving of 2 to 3 passages in processing relative to FBS.

There is also a very strong correlation between the total number of passages required and the total costs (R^2 = 0.99 for FBS, R^2 = 0.93 for hPL), with an average increase in the total costs with an additional passage of $1970 for FBS and of $2802 for hPL (Figure 4.4C). The ratio of the costs per donor with hPL relative to FBS shows that, if no passages are saved, there is virtually no reduction in the final process costs (mean: 1.00, 95% CI: 0.95 – 1.01) (Figure 4.4D). This happens for donors for which the use of

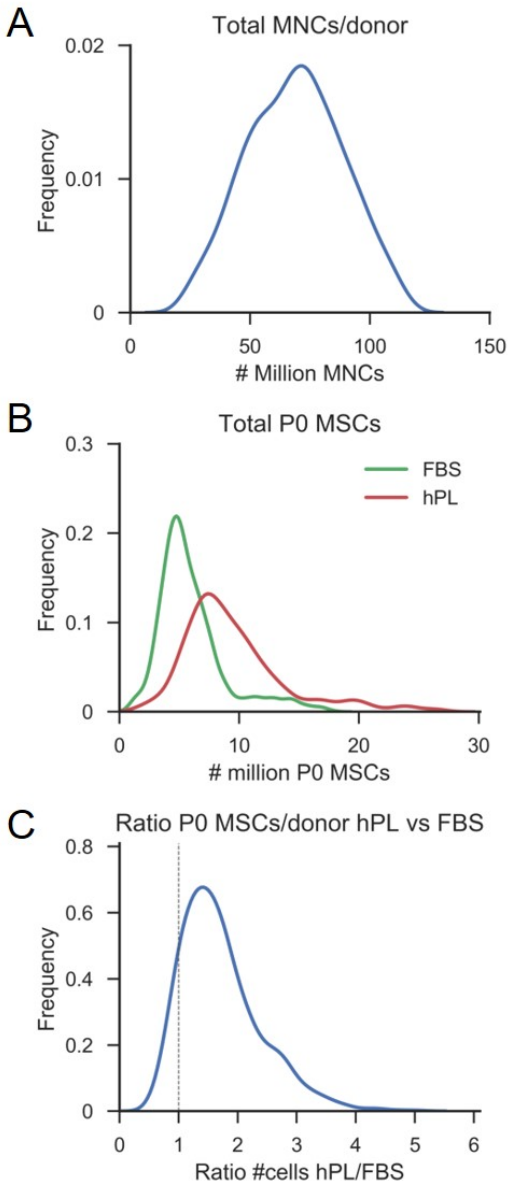

Figure 4.2: Probability density functions related to the isolation of bone marrow mesenchymal stem/stromal cells (BM-MSCs) with the Ficoll-Paque density gradient method. A – Distribution of total MNC/donor from 10ml of bone marrow. Results derived from experimental data [276]. B - Total BM-MSC after isolation (passage 0 - P0) for FBS (green) and hPL (red) culture media supplementation. Ratios of MSC per initial MNC seeded were derived from [277]. C – Ratio of P0 BM-MSC cells obtained with hPL vs FBS per donor. 1000 donors were simulated.

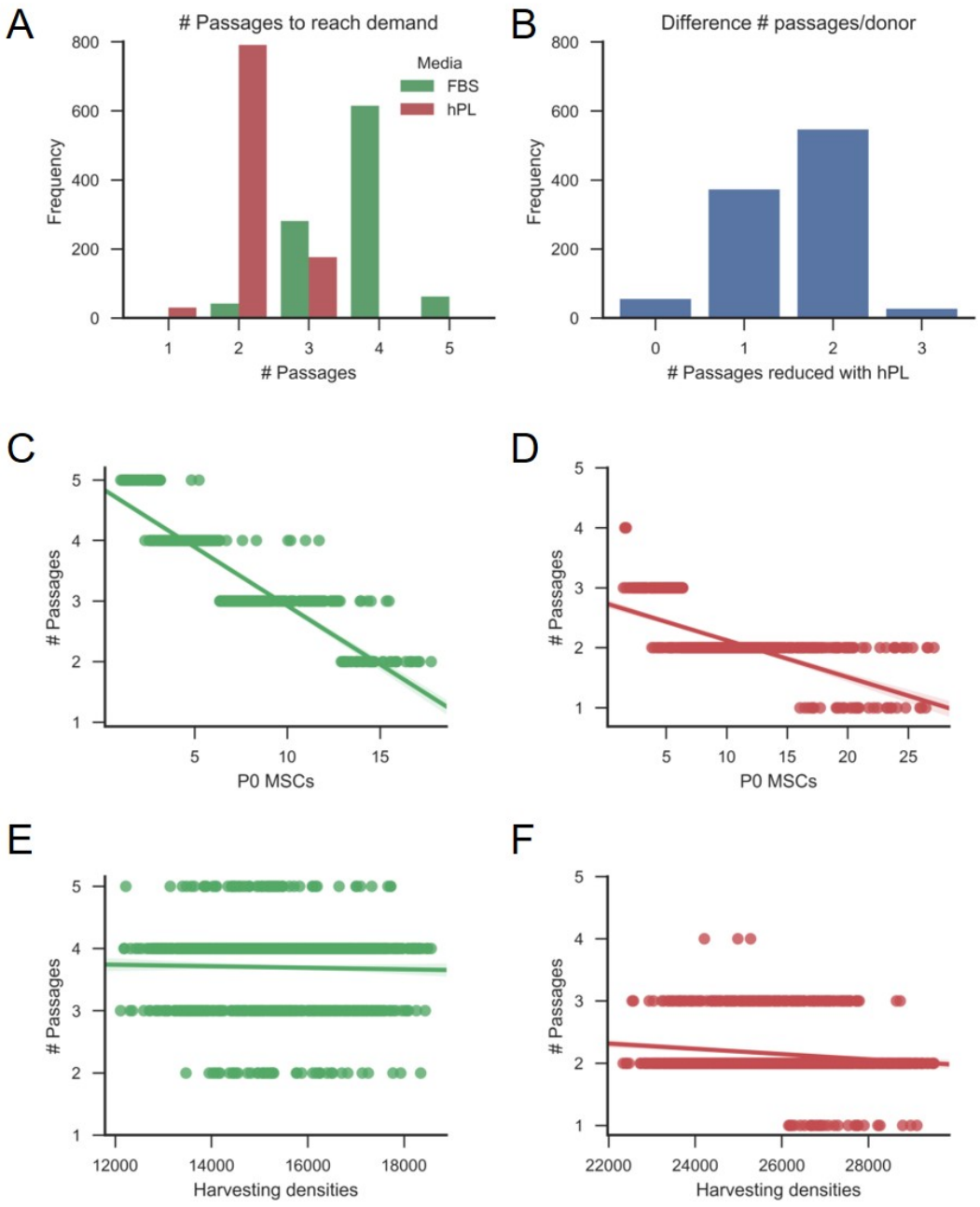

Figure 4.3: Impact of culture media supplementation in the number of expansion passages required to reach a dose of 75 million cells per donor. A – Passage numbers required per donor to expand the cells to the dose of 75 million cells with FBS (green) or hPL (red). B – Number of passages per donor saved with the process change to hPL. C, D – Correlation of the number of MSCs after isolation with the number of passages required to expand the cells to the final dose for FBS (green) and hPL (red). E,F – Correlation of the harvesting densities per donor after 1 expansion passage with the number of passages required to expand the cells to the final dose for FBS (green) and hPL (red). Data from simulations for 1,000 donors.

hPL and FBS results in either 2 or 3 passages to reach the target cell number. The reduction in costs is strongly associated with the number of passages saved per donor, with the most common case of two passages saved per donor occurring in manufacturing cells with hPL with 20% relative cost savings compared to FBS (Mean ratio: 0.8, 95% CI 0.77-0.85). This case is associated mostly with donors

needing 4 passages to reach the target cell number with FBS, and had the expansion operation reduced to 2 passages with hPL.

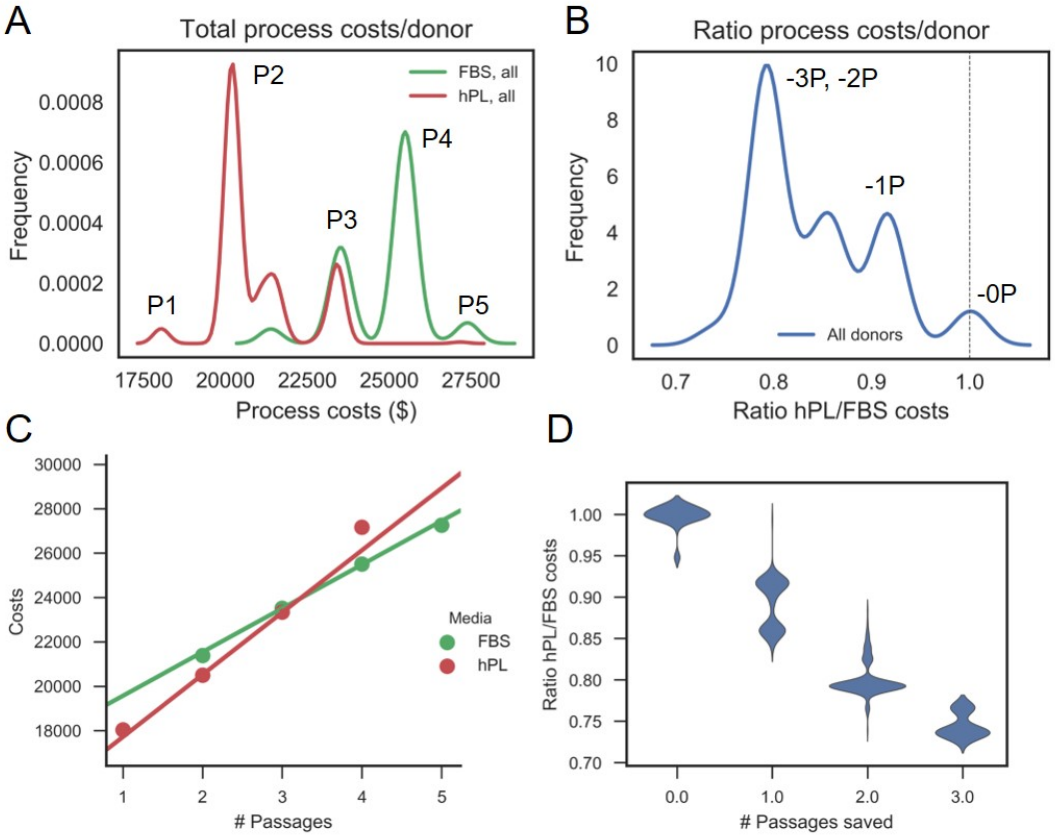

Figure 4.4: Impact of culture media supplementation on the cost of goods (CoGs) per dose. A – Frequency distribution of the processing costs of 1000 donors with FBS (green) or hPL (red) until reaching the final dose of 75 million cells per donor. B – Ratio of hPL vs FBS processing costs per donor. C – Linear model fitting of the mean CoG/dose and the number of passages to reach the target cell dose/donor. D – Distribution of the ratio of hPL/FBS CoG/dose per donor for each number of passages saved per donor with the process transfer to hPL.

Due to the expensive quality controls that have to be performed for every dose, the main fraction of operational costs is occupied by the quality controls in each donor. The ratio of total costs ranges from approximately 0.41 (95% CI: 0.37 – 0.47) for FBS to 0.48 (95% CI: 0.43 – 0.55) for hPL (Figure 4.5A). This shift toward a higher relative contribution of quality controls for the cost structure in the xeno-free cultures is related to lower facility and labor costs. Facility and labor costs make up for 27% and 16% of costs, on average, for cultures with hPL, rendering them important cost drivers. This is actually a specificity of an autologous therapy, and therefore a limitation of our model imposed by the selected case study. In absolute terms, donors cultured with hPL have average facility and equipment depreciation and operational costs of $5692, which is a significant reduction from the average $8016 facility costs for FBS. (Figure 4.5B). A similar pattern is seen for the labor costs, with a reduction from the average labor costs of $4596 for donors cultured with FBS to $3264 labor costs for hPL. However, on the other hand, the consumables costs, related to the vessels used for cell expansion, culture media, and other reagents, are very similar on average between the two different culture supplements ($1984 for FBS vs $1913 for

hPL).

The cost savings per dose divided by the number of passages saved by the culture with hPL, facility, and labor costs are always lower in the hPL culture, with a very strong linear association (R^2 = -0.97) (Figure 4.5C). Regardless, the number of passages saved per donor with the transfer from FBS to hPL still holds. This is a consequence of the fact that the isolation time was three days shorter. The cost savings become higher with the number of passages averted, since each passage means, under this dataset, six days of operation. However, for consumable costs, there is not such a clear linear relationship between the ratios and the number of passages (R^2 = -0.55) (Figure 4.5D). When no passages or one passage is avoided, on average, the consumables costs are higher for hPL than for FBS, due to the more expensive culture medium and the use of higher areas and more expensive expansion flasks. On average, only after two passages saved does hPL start to be cost saving, with apparent stabilization of the ratio at approximately 80% of consumable costs with FBS.

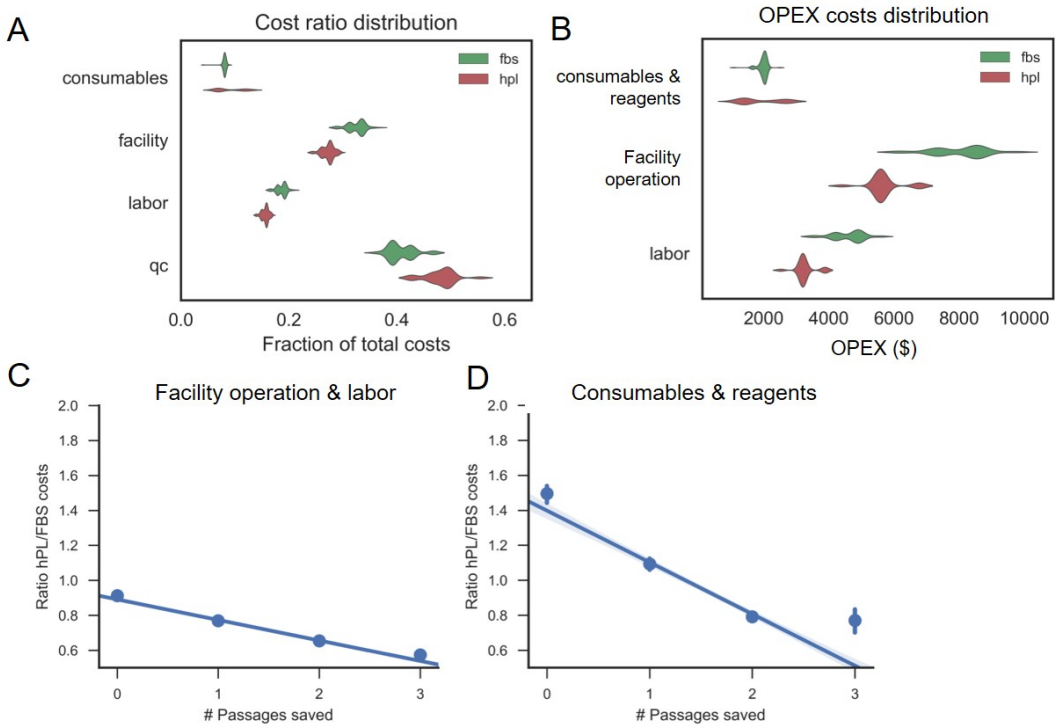

Figure 4.5: Breakdown of the cost of goods per dose by process resource. A – Violin plots of the distribution of total costs ratios for FBS (green) and hPL (red) per operational resource: consumables and reagents, facility and equipment depreciation and operational costs, labor costs, and quality control costs. B – Total OPEX. The costs accounted for in OPEX are the consumables and reagents, facility operational costs, and labor costs. C – Linear correlation between the ratio of hPL vs FBS facility and labor costs per number of passage saved per donor when switching to hPL. D – Linear correlation between the ratio of hPL vs FBS consumables and reagents costs per number of passages saved per donor. 1,000 donors were simulated.

4.3.2 Cost-effectiveness of process transfer is maintained with higher cell numbers per dose and assuming fully depreciated equipment

The variability in the costs per manufactured dose derived from the donor and multi-passage cell numbers at confluence showcased the additional costs of manufacturing when more passages are required to reach the number of cells per dose and the different process times, causing batch timing issues [278].

A large portion of these additional costs comes from the operational costs of higher processing times. A conservative assumption for the baseline scenario was made such as the facility and equipment were not yet fully depreciated. Here, an additional scenario in which manufacturing in a facility with fully depreciated equipment was considered. In this case, benefits on overall cost through the use of hPL are more modest. Still, labor costs will be sensitive to processing times (and passages) reduced by the use of hPL (Figure 4.5C). In the absence of depreciation costs, the impact of the supplement cost on the overall cost structure increases (Figure 4.5D). The depreciated equipment process configuration decreased the average total processing costs per dose to $19402 (95% CI: $17367 - $21070) for FBS and $17195 (95% CI: $15192 – 19052) for hPL. With depreciated equipment, the percentage of donors from which manufacturing therapeutic cell doses is estimated to be more expensive with hPL rose from 5% to 8%. (Figure 4.6A-B).

Autologous therapies may use higher cell numbers per dose (from 2-5 million cells/kg) or more doses per patient than the numbers considered in the baseline case study [283, 284]. Two additional scenarios that imply an increase in facility scale were assessed: manufacture of MSCs with doses of 150 million and 300 million cells (Figures 4.6C-F). For these numbers of cells, the costs of processing have a considerable increase to values above $30000 per donor. While for the 150 million cells/dose assumption, there is not a relevant impact on the number of donors for which hPL processing is more expensive (1 to 3%, undepreciated vs depreciated), for the higher dose of 300 million cells/dose there is a considerable number of donors with more expensive hPL based processing, starting at 16% for the non depreciated case and reaching 24% for the depreciated case. This increase is related to the higher numbers of passages required to produce the cells. With depreciated equipment, the relative facility contribution is decreased, decreasing the cost-effectiveness of process transfer. Therefore, when doses have high cell numbers, at the current prices of hPL and FBS, it is critical to control the relative proliferative advantages of hPL to ensure robust cost-effectiveness.

4.3.3 Multi-passage harvesting density is the key cost driver for xeno-free process cost effectiveness

To bring additional insights into the decision rationale brought by the model, sensitivity analyses were conducted to vary some of the inputs used.

1. Isolation and expansion of cells: Importantly, the model calculates costs taking into account the biological features of the cells, therefore sensitivity analysis for the effects of isolation and expansion yields were analyzed as a function of the number of cells obtained per surface area, as a

consequence of the cell size at confluence [220]. Additionally, the time of isolation was also varied.

2. Media supplement costs: The effect of media supplement used on overall costs is important, mainly as a result of different processing times (and passages) and consequent changes in facilities and labor costs. While the media costs represent just a small fraction of the overall cost, it is still an important parameter to address due to possible market fluctuations.

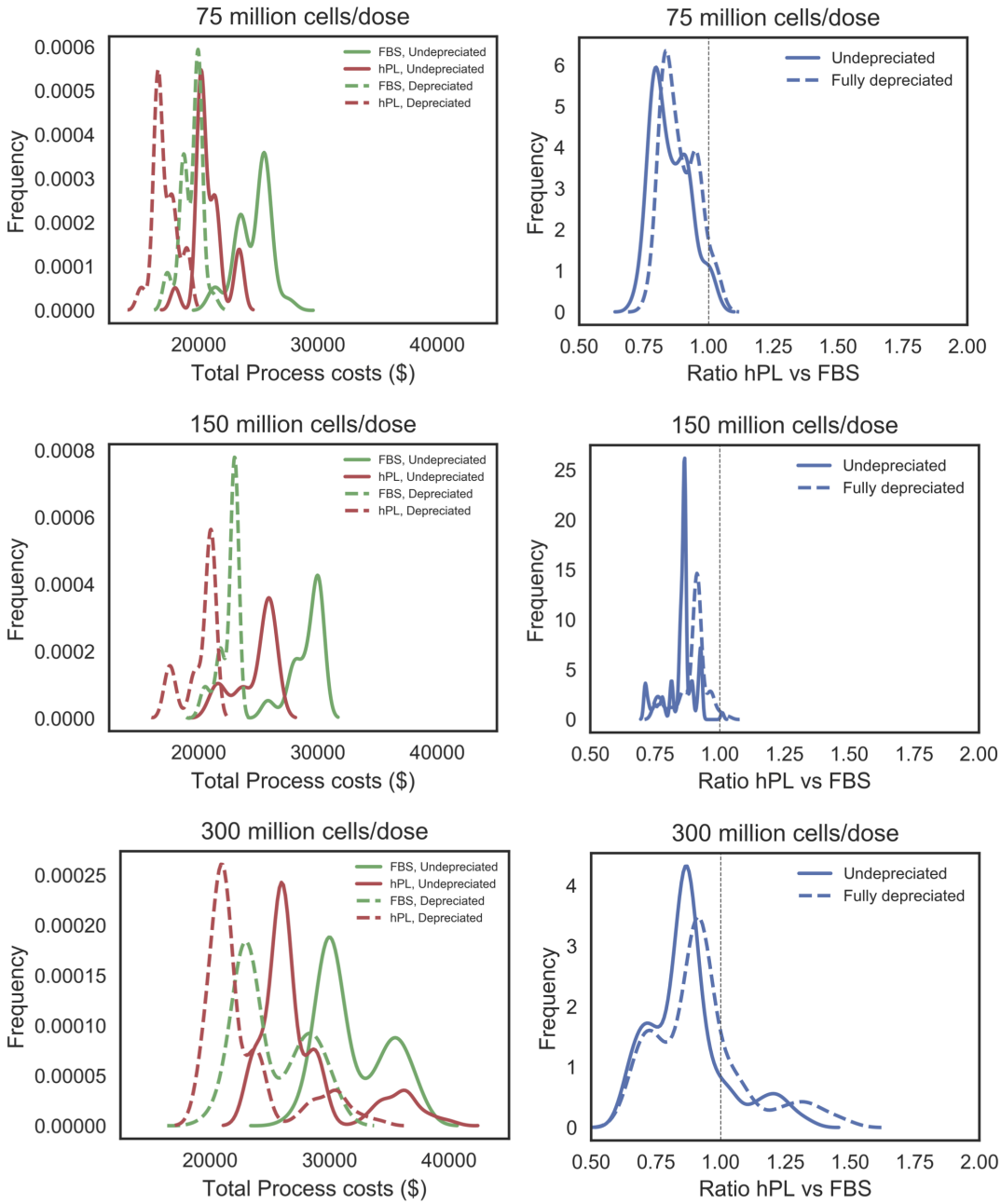

Figure 4.6: Total cost of goods (CoG) per dose for FBS (green) and hPL (red) culture media supplementation for different dose sizes and capital investment depreciation considerations. A, C, and E – Frequency distributions of the costs of processing 75 (A), 150 (C) and 300 (E) million cells/donor for FBS (green) or hPL (red), with undepreciated (solid) or fully depreciated (dashed) equipment and facility. B, D, and F - Frequency distributions of the ratio of CoG/dose per donor when using hPL vs FBS as a culture media supplement. 1,000 donors were simulated.

3. The contribution of labor was further assessed considering a lower labor pay rate since labor is one of the main cost drivers and is more pronounced in hPL cultures due to lower passage numbers than in FBS.

A 25% increase or decrease in these factors was assumed to evaluate the impact on the costs per donor of processing with hPL relatively to the baseline (Figure 4.7).

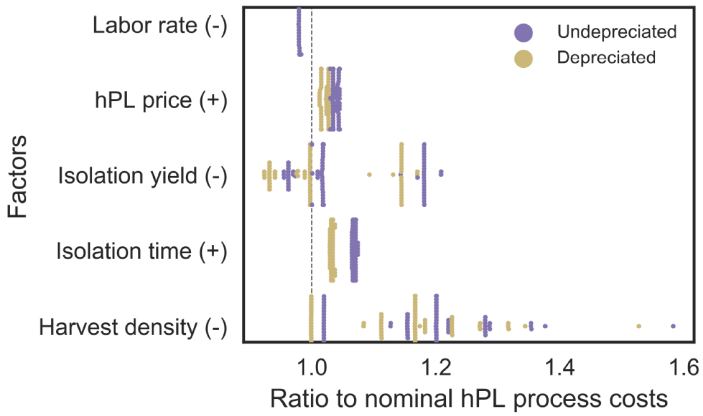

Figure 4.7: Sensitivity analysis of key process cost drivers, accounting and not accounting for the capital investment depreciation cost contribution, for the CoG/dose using hPL as a culture medium supplement. Key process cost drivers were increased (+) or decreased (-) by 25% for both non depreciated (purple) and depreciated (yellow) facility and equipment manufacturing scenarios. Points represent individual donors. 1,000 donors were simulated.

hPL promotes the growth of MSCs of smaller size and therefore a higher number of cells are isolated when sub-confluence is reached in P0 [220]. Despite the fact that the number of passages that cells undergo is highly correlated to the number of P0 MSCs after isolation, a decrease in 25% of this factor did not show a significant impact in costs, with an increase of 5% (-4 to 18 %) with depreciation and 2% (-7 to 14%) with fully depreciated equipment. The rationale for this is related to the fact that, as long as the proliferative potential is maintained, the number of cells required would be reached in the same number of passages. The main impact of the reduced isolation yield is on the type of flask selected for passage 1, pointing towards lower areas and cheaper consumable costs in this first expansion step. Interestingly, the impact of an increase of the isolation time by 25% has a more homogeneous effect on the cost structure than the yield, but both average to similar values.

The factor with the most relevant impact on the cost structure is the multi-passage harvest density, where a decrease of 25% in the number of cells at confluence per area yields increases in the processing costs of 18% (95% CI: 2%-35%) with undepreciated equipment and 15% with fully depreciated equipment (95% CI: 1%-32%). This factor, in combination with the number of MSCs at P0, reduced the need for additional passages to obtain the desired number of cells for a clinical dose (Figure 2). Cells that undergo fewer passages are more likely to retain their multipotency and therapeutic potential [285]. The underlying assumption taken in this model is supported, for bone marrow MSC, by several studies in the literature stating that growth with hPL yields smaller cells than with FBS, making this supplement more attractive from a proliferative point of view in adherent technologies, since more cells are yielded

per area [286, 287, 288, 289]. Regardless of the changes in the parameters performed within the considered range of 25% of the nominal value, all donors still reach the final cell number and thus there are no changes in batch failure rates. Note that batch failures are driven from cells failing the potency and/or sterility testing.

In the baseline scenario for the autologous process considered, culture medium costs are a small fraction of the total manufacturing costs and it is not expected that fluctuations in the ratio of hPL and FBS prices per volume affect the cost-effectiveness of the xeno-free process transfer for autologous therapies. In fact, an increase of the price per volume of hPL by 25% had a minimal (2-4%) effect on the costs of processing per donor, assuming that all biological factors are kept constant. Therefore, for low doses, the process is robust to fluctuations in the price of hPL as long as the supplement batches retain the quality attributes for improved proliferation. Due to the relatively low cell numbers and the fact that only one dose is required per donor, the culture medium volumes used are low in comparison with allogeneic therapies, aimed at a scale economy. In an allogeneic process, the media costs are generally the most relevant cost contributor per dose [5, 11] and the impact of the price of the supplement would be probably more relevant. In future work, the impact of hPL vs FBS as a supplement for allogeneic mesenchymal stem/stromal cell therapies should be the object of analysis.

A decrease in labor rate (i.e, daily worker pay) has a minimal impact of 2% on costs. This analysis points to the relevance of the selection of hPL batches with strong proliferative abilities while retaining the quality attributes required to comply with quality controls and ensure process comparability with FBS. Under this autologous process, the variability in the ability to generate smaller cells and more numbers per passage comparatively to FBS would be more detrimental to the cost-effectiveness of the process transfer to hPL than fluctuations in price. This is a direct result of decreasing processing times when using hPL and thus of costs with facility and labor.

4.4 Discussion

The results of this modeling study support the cost-effectiveness of the use of human platelet lysate as a xeno-free culture media supplement for manufacturing autologous MSC based therapies. The cost-effectiveness comes as a result of the superior proliferative performance in isolation and expansion of MSC cultured with hPL comparatively to FBS, yielding considerable cost savings. However, additional considerations for the establishment of a xeno-free process need to be taken into account in combination with manufacturing costs.

- **Cell potency and safety:** Decisions concerning manufacture process should be taken relatively early on the development of a cell-based therapy, preferable before a Phase III clinical trial, as effects on changes in cell potency and safety with process specificity may be a concern [11]. All of the analyses were conducted assuming comparability between the two culture media supplements in terms of quality controls. Quality controls for release testing of MSC are related to safety, identity, purity and potency [290, 291]. While some studies claim that hPL does not modify the immunomodulatory characteristics and the multipotency of MSC [286, 287, 289, 292], others show

that immunomodulatory activity decreases, along with surface marker modifications, in BM-MSC cultured with hPL [185, 293, 294]. Therefore, in addition to cost, the decision of the manufacturing process to be selected should also consider the therapeutic action of the obtained cells.

- **Batch Failure:** When a donor fails the quality controls in autologous therapy, it means that the patient will not be treated. Then, before any process transfer is considered for an autologous therapy, quality comparability has to be guaranteed. For that reason, sensitivity analysis to batch failure rates was not performed. However, in an allogeneic setting, the failure of quality controls will have less impact on treating the patients and more so on the cost distribution. Eventual future studies on xeno-free process transfer for allogeneic therapies should include this comparison. Multi-criteria decision models for autologous therapies would allow addressing the quality attributes of the process and the final product in a quantitative manner [28, 156].

- **Cell source:** While this analysis was performed with BM-MSC, which involve a particularly tedious and expensive collection method, other types of MSC with less invasive collection methods, such as adipose tissue-derived MSC (AT-MSC) or umbilical cord matrix/Wharton's Jelly MSC (UCM-MSC/WJ-MSC), have been isolated and expanded with hPL with improvement in the proliferative potential with lower cell size while retaining potency attributes [295, 215, 296, 297, 298].

- **hPL as a xeno-free alternative for culture media supplementation:** hPL has the caveats of being dependent on donor samples, high batch to batch variability, poor definition of its components and the possible transmission of viruses. The sterility of hPL could be improved with pathogen inactivation methods without detriment to cell potency, while supplement variability could be reduced with pooling of samples from different donors [287, 288, 296]. In order to minimize the negative impact of these caveats, chemically defined serum-free/xeno-free media have gained relevance for MSCs processing with comparable proliferation potential to serum containing media [293, 296, 273, 299]. However, the yield of MSC after isolation is not yet comparable [300] and this factor might impair the cost-effectiveness of a fully serum-free/xeno-free process transfer. The application of the methodology described in this work could provide technological and economical cues to improve the cost-effectiveness of bioprocessing of less invasive MSC sources under chemically defined media.

- **Cryopreserved vs fresh products:** The fact that, in autologous therapies, cells from each donor have different proliferative and morphological attributes results in variable processing times. The different processing times required to manufacture doses from different donors that may start processing at the same time can create batch timing issues that can entail additional operational costs related to supply chain management [278]. These issues are particularly noticeable under the current paradigm for the administration of fresh cell products for infusion. The creation of off-the-shelf stem cell therapies that come from cryobanks is gaining momentum with the recent approval of the first MSC based therapy of the kind in Europe. However, the negative impact of cryopreservation on cell quality attributes after thawing limits this approach [55]. We followed an optimistic view for cryopreservation of manufactured doses to mitigate the batch timing issues that are associated

with a manufacturing campaign under the scale-out system such as the one approved. However, for fresh products, the simulation of the proliferative abilities per donor after pre-screening would help plan for parallel manufacturing of batches with similar processing times to optimize resource utilization.

To the best of current knowledge, this is one of two studies addressing the impact of two different culture media formulations for bioprocessing of BM-MSC. The study by Harrison and colleagues [186] compares the planar expansion of BM-MSC, comparing Serum-containing media (SCM), as a formulation of DMEM + 5% FBS, with Serum-free media (SFM). The serum-free, xeno-free medium of choice was Irvine PRIME-XV xeno-free MSC medium. While the SFM is considered to be about 9 times more expensive per volume unit than the SCM, the superior multipassage proliferative abilities when the SCM is used for expansion, obtained for 3 BM-MSC donors, result in the use of SCM being a cost-effective choice for obtaining 2,500 doses/year of 7.5 million BM-MSC/dose. While both studies support the conclusion that there are cost-effective culture media formulation alternatives to FBS supplementation, the present study differs from the study by Harrison and colleagues [186] in key study assumptions:

- This study addresses the comparison between FBS and a serum-containing, xeno-free culture media, while the study in [186] does not address the possibility of using a xeno-free supplement. Both hPL and Irvine PRIME-XV xeno-free MSC medium show higher proliferation abilities for BM-MSC than FBS. An interesting follow-up study for both the present study and the study in [186] would be the comparison between hPL and several serum-free, xeno-free media.

- The study in [186] only addresses variability at the multipassage expansion level explicitly, with the number of cells to start the expansion set at a constant number (875,000 cells/donor). Furthermore, it is not clear if, in the SFM case, the BM-MSC cells were isolated in a SFM culture, for a full serum-free, xeno-free culture. It was shown experimentally, for another serum-free, xeno-free culture medium, that the isolation yield of BM-MSC was significantly compromised [300]. The present study includes variability at the isolation level per simulated donor, and the xeno-free media supports increased yield of MSC after isolation.

- Due to limitations in the proliferative abilities of cultures with SCM in the study of Harrison and colleagues, the two culture media formulations were compared for a dose of 7.5 million cells, 10 times lower than the doses simulated in the present study.

- The study in [186] is aimed at allogeneic expansion of BM-MSC to fulfill an annual demand of 2,500 doses, with varying lot sizes, depending on the expansion capabilities obtained for a specific donor with each culture medium formulation. In the present study, autologous therapies, with one dose per donor, are simulated.

- While expansion data from 3 donors in [186] is input in the simulations, to address the CoG obtained to meet the annual demand of 2,500 doses, using each of these 3 donors for an allogeneic process, the present study samples, for 1,000 simulated donors, different isolation yield and multipassage growth rates on an autologous process.

- The study from Harrison and colleagues addresses process drivers that were not considered in this study, such as the comparison between a manual and an automated planar expansion of BM-MSC, and the costs of fresh vs cryopreserved MSC products.

4.5 Conclusion

The costs of bioprocessing of MSC therapies are very high in comparison with those of small drug molecules and biologics. Previous work points out the contributions to the total cost of the maintenance of expensive GMP-complying facilities and equipment, high costs of culture media and other reagents, labor-intensive tasks and expensive quality control testing [5, 145, 3].

In the case of autologous cell therapies, relatively low cell numbers are required. In that sense, these therapies are amenable to parallel, scale-out processing. Still, quality control costs are very high, since they are required for each prepared dose that the patient requires [8, 53]. In addition to these hurdles, biological variability in the number of BM-MSC after isolation and in the number of cells at confluence per donor render additional uncertainty to the costs of manufacturing. A new bioprocess and bioeconomics model for MSC manufacturing simulation embracing the biological variability was developed and used for a specific case study.

The case study consisted on evaluating the impact, on the total process costs of autologous BM-MSC therapies of replacing FBS by hPL, as an example of a xeno-free alternative, in culture medium supplementation. The use of hPL promotes the isolation of a higher number of cells after their isolation from bone marrow and after multi-passage growth, which translate in the need of lower passages to achieve the targeted therapeutic dose of cells per patient required. The decrease in the number of passages, in turn, results in cost savings of 16%, on average, per donor compared with supplementation with FBS. The impact of additional passages required to achieve the therapeutic dose creates a multimodal cost distribution with average additional costs per passage per donor of $1970 for FBS and $2802 on average for hPL.

The findings of biological variability in process times and resource consumption and, finally, in process costs per donor, will have an impact on the profit margins once a fixed price for therapy reimbursement is set. However, the supplementation with hPL reduces this variability in comparison with FBS, with the advantage of rendering a robust process cost wise to fluctuations in hPL supplement price, as long as the higher proliferative potential and the generation of more cells per passage at confluence, due to smaller cell size, are maintained and combined with comparable potency and sterility attributes. The modeling methodology, integrating biological variability can help to better plan for the impact of process changes before the start of a clinical trial to design more robust processes, both biologically and economically. However, the proliferative and economic benefits of a process transfer should always be studied as a part of a framework including regulatory guidelines and identification of key potency attributes for the specific clinical indication.

Bioprocess economics decisional tools, like the one described throughout this thesis, are powerful tools to assess the impact of changes in technology and how process decisions should be made to

ensure profitability, while quality attributes and regulatory demands are met. With regulatory agencies encouraging a shift from animal-based methods to xeno-free cultures, the economic model presented allows the determination of the full costs of MSC bioprocessing, assuming a xeno-free supplement and encourages steps to reduce variability in the efficacy of the supplements for autologous based cell culture, since the donor's own cells are the products. It highlights how the need for additional unit operations increases the costs of manufacturing significantly and how determining the worst-case scenarios might help in planning for possible profitability under a set reimbursement price. Cost-efficient processes that retain quality attributes make it more likely that stem cell therapies will reach the clinic.

Additional work, also described on this thesis, show how this tool can be used with different types of stem cells (Chapter 6), under allogeneic, 3D configurations (Chapter 5), and incorporate health economics modeling for a specific clinical indication (Chapters 7 - 6) or to contribute to plan clinical trials (Chapter 7).

Chapter 5

Bioprocess economics assessment of process transfer of expansion of human mesenchymal stem/stromal cells to the Vertical-Wheel Bioreactor System

Note: The contents of this chapter are adapted from the peer-reviewed article: D. S. Pinto, C. Bandeiras, C.A.V. Rodrigues, M. A. Fuzeta, S-H Jung, R-J Tseng, C-Y Shen, W. Milligan, B. Lee, F. C. Ferreira, C. L. da Silva, J. M. S. Cabral, Expansion of Human Mesenchymal Stem/Stromal Cells in the Vertical-Wheel™ Bioreactor System: An Experimental and Economic Approach, Biotechnology Journal [301]

5.1 Outline

As previously mentioned, mesenchymal stromal cells (MSC) hold great promise for tissue engineering applications and cell-based therapies. Large numbers of doses are however required for clinical purposes under an allogeneic, off-the-shelf manufacturing scheme. Therefore, in this chapter, TESSEE is upgraded to answer the challenges of manufacturing MSC on a large scale for allogeneic therapy.

A serum- and xenogeneic-free (S/XF) microcarrier-based culture system was established in the Stem Cell Engineering Research Group for the expansion of human UCM-MSC and AT-MSC using the Vertical-Wheel™ system (PBS-0.1 MAG, PBS Biotech). The culture medium supplement, in line with the previous chapter, is human platelet lysate (hPL). TESSEE is used to model this system as a means to compare the manufacturing costs of the process transfer from traditional T-flask culture to PBS-0.1 MAG in the last expansion step, for both cell sources.

These culture systems aim at providing scale-up of MSC expansion to meet the dose requirements of allogeneic cell therapies. However, the paradigm of manufacturing is different. Instead of obtaining a target number of cells per dose for one donor, the aim is to maximize the number of cells expanded after five passages from the same donor. In this scheme, it is desirable to obtain the maximum number of doses possible to provide therapies for several patients. The scale-up paradigm brings new operational challenges. Here, intermediate banking steps (master and working cell banks) need to be modeled to replicate the usual processes. Like the previous chapter, the final product is assumed to be cryopreserved. The two cell sources considered in this chapter, umbilical cord matrix, and adipose tissue, are less invasive sources of collection of MSC than bone marrow.

The experimental results used for modeling show UCM and AT MSC expanded to maximum cell densities of 5.3 +/- 0.4 x 10^5 cell/mL (n=3) and 3.6 +/- 0.7 x 10^5 cell/mL (n=3), respectively, after 7 days of culture. Based on the experimental data, it is assumed that they maintain their identity, according to standard criteria.

An economic evaluation of the process transfer from T-flasks to PBS-0.1 MAG showed a reduction in the costs associated with the production of a dose for an average 70 kg-adult patient (i.e. 70 million cells). Costs decreased from $17,0k to $11,1k for UCM-MSC and from $21,5k to $11,1k for AT MSC, proving that the transition to Vertical-Wheel^{TM} reactors provides a cost-effective alternative for MSC expansion. Overall, the present work reports the establishment of a scalable and cost-effective culture platform for the manufacturing of UCM and AT-MSC in an S/XF microcarrier-based system.

This chapter marked the expansion of the TESSEE modeling framework to allogeneic process flowsheet modeling, introducing intermediate banking steps, and a dynamic utlization of the bank vials to explore the full installed capacity in the last expansion step. Since different process components impact the number of cells obtained per expansion run, the model allows for a variable number of cells per batch and number of batches produced from a single donor.

5.2 Methods

5.2.1 Experimental Data Collection

Culture of previously isolated and expanded human MSC from adipose tissue (AT-MSC) and umbilical cord matrix (UCM-MSC) was performed by Diogo Pinto, Ph.D. under the scope of his Ph.D. thesis. Briefly, cells were cultured in DMD + 5% (v/v) UltraGRO^{TM}-PURE, a human platelet lysate (hPL) based supplement, in either 2D (T-175 flasks) and 3D conditions (PBS-0.1 MAG vertical wheel bioreactors). In 3D conditions, plastic microcarriers (Pall SoloHill) were incubated with cells to provide adhesion support for MSC culture. The culture parameters were inputs of the modeling approach. Additional details can be found elsewhere [301].

5.2.2 Model Overview

The bioprocess economics tool reported in 3.3 was used for cost of goods modeling. Briefly, the tool accounts for the isolation, expansion, downstream processing and quality controls, with different operation times and reagent requirements on a simulated GMP facility. Such tool was modified to account for the expansion of UCM and AT MSC considering an allogeneic setting, as well as to include intermediate banking steps and allow estimation of cell expansion in the VW system. The isolation yields, growth rates, seeding densities and harvesting densities are modeled as inputs for each expansion scheme based on the experimental data presented in this study for each cell source.

The model was expanded to consider the possibility of intermediate banking steps, including a master cell bank (MCB) that is then used to generate one, or more, working cell banks (WCB), from which cells are used to perform final expansion steps and generate product batches for purification, final product fomulation, and release testing. Intermediate quality control steps were introduced at the end of MCB and WCB banking simulations as well.

5.2.3 Case Study Definition

A therapeutic dose of 1 million cells/kg was considered, in agreement with typical doses in clinical trials using MSC as therapeutic interventions [169]. Doses containing 70 million cells (i.e. average adult patient weighting 70 kg) were used as a proxy.

The economic evaluation of the VW system is hereby performed against the use of planar cell cultivation technology (T-175 flasks), the current standard system for MSC expansion. The model was not set to deliver a specific yield, and the output is calculated instead. This value is determined in terms of the number of doses of 70 million cells possible to obtain from a single donor of either AT-MSC or UCM-MSC following two different process options. Therefore, each process corresponds to the cells expanded from one single donor. Such cells are first used to prepare an MCB, and from this, a WCB is established using planar technology (i.e. T-flasks). The WCB is prepared to maximize facility capacity use. Then the WCB is completed used in planar or bioreactor batches according to the process evaluated. The model workflow is described in detail as follows:

1. **Master cell bank (MCB):**

   A master cell bank (MCB) is prepared by expanding cells isolated from one donor of a specific tissue source (adipose tissue or umbilical cord matrix) using 2D tissue culture flasks, Passage 1 (P1) cells. The number of cells of the MCB is dependent on the tissue source.

   Based on a panel of standard tests for MSC, a fixed cost per MCB is assumed for quality control, regardless of the number of cells of the MCB [30]. When MCB cells pass the quality control, these are further expanded to prepare a Working cell bank (WCB), otherwise, these are discarded.

2. **Working cell bank (WCB):**

   The cells on the MCB are then further expanded to prepare the WCB, using T-175 flasks for two passages (P2 and P3). The model algorithm calculates the number of cells from the MCB to be

used, Passage 2 (P2), in order to use the facility full capacity, i.e. four incubators with 24 T-175 flasks each, in the second of these two expansion steps, i.e. Passage 3. The cells obtained after these two expansion steps using T-175 comprise the WCB.

Again, a fixed cost per WCB is assumed for quality control regardless of the number of cells of the WCB. When WCB cells pass the quality control, these are used for the different expansion batches, otherwise, these are discarded and a new WCB needs to be prepared using the remaining MCB cells.

3. **Batches:**

   The cells in the WCB are then used for further expansion (P4) using T-175 and the obtained cells in this step are then used for seeding several batches of either planar or VW systems. The model algorithm calculates the number of cells from the WCB to be used, when seeding each type of expansion technology, in order that each batch uses the maximum GMP facility capacity, i.e. four incubators, each fitting 24 T-Flasks (4200 cm^2) or 6 VW bioreactors (4320 cm^2), for the final expansion passage (P5). The number of batches corresponds to the number of repetitions of these two culture steps until to spend all the WCB cells.

4. **Downstream processing and dose release:**

   The total cells obtained after each batch, which number varies with cell source and expansion technology used, undergo downstream processing that includes centrifugation for removal of microcarriers from the cell suspension when applicable, washing the cells from the culture media, volume reduction, and fill-finish in cryovials with a proper final formulation buffer. In this process, benchtop centrifuges are used.

   Based on a panel of standard tests for MSC, a fixed cost per batch is assumed for quality control for release testing, regardless of the number of cells per batch [30]. When a batch of cells passes the quality control, these are qualified as manufactured doses, otherwise, these are discarded.

   As mentioned, steps 3-4 are repeated, generating more final product cells, until no more WCB cells (P3) remain in the bank. When the MCB and WCB cells are totally spent, the process ends.

5. **Model outputs:**

   The model calculates, for each process, the total number of P5 cells obtained from one donor, the total number of cells per batch, and the total number of batches of final product. It is important to emphasize that the number of batches is defined by the number of repetitions of Steps 4-5.

   The number of cells per dose was assumed to be 70 million cells/dose based on an average patient weight of 70 kg and a dosage of 1 million cells/kg. The total number of doses per batch and the total number of doses obtained in the process, for each combination of expansion technology and cell source, are obtained by dividing the number of cells calculated by the number of cells in a dose (70 million cells/dose).

The total costs per dose are obtained by dividing the sum of total process costs by the number of doses produced. The total process costs are obtained by considering several categories (consumables, labor, quality controls, and facility costs).

The Consumables category includes the disposable components of the process, such as single-use cell culture flasks (T-175) and bioreactor disposable vessel (PBS-0.1MAG), microcarriers, and other reagents, such as isolation, culture and centrifugation media, and harvesting agents. Note that the PBS costs include a disposable PBS vessel and the microcarriers, which contributes to the consumables associated with the use of this expansion technology.

The Consumables costs for wet materials are obtained by multiplying the total volume of culture medium, buffers and harvesting agent by the cost per volume of each reagent. The costs for disposable consumables include the disposable vessels for cell expansion (T-175 and PBS-0.1MAG), microcarriers for expansion support in PBS-0.1MAG, and accessories, such as cryovials. The total cost is determined by accounting for the total number of units used in the process and multiplying by the unit cost.

The Labor costs include the contribution of the manufacturing personnel, with a fixed daily rate, multiplied by total the duration of the process.

The Facility costs include the fixed and operational costs related to the GMP facility and the equipment required for cell culture processing (incubators, biosafety cabinets (BSC), and benchtop centrifuges). These fixed and operational costs are input on a daily basis and included in the costs proportionally to the duration of the process.

The Testing contribution is obtained by multiplying the number of tests for MCB, WCB, and final product release incurred during the process, by the unit costs of each of these tests.

The parameters associated with the setup of the modeling case study are depicted in Tables 5.1 and 5.2.

Table 5.1: Characteristics of expansion systems. The parameters work as inputs of the bioprocess economics model and are derived from the characteristics of the experimental process.

Parameter	T-175 flask	PBS-0.1 MAG
Culture medium volume (ml)	35	100
Harvesting reagent volume (ml)	7	20
Mass of microcarriers (g)	-	2
Type of microcarrier	-	Plastic SoloHill
Incubator capacity	24	6
Expansion area (cm^2)	175	720
Seeding density (cells/cm^2)	3000	6944
Consumables unit costs ($)	7.38	181.55
Microcarrier cost ($/g)	-	3.00
Ancillary equipment costs ($)	-	2306.25
DSP yield (%)	90	75

Table 5.2: Key facility, labor, quality control and reagent assumptions for the bioprocess economics modeling

Parameter	Value	Reference
GMP facility area	180 sq. mt.	This work
% clean room area	20	This work
No. clean rooms	1	This work
No of incubators	4	This work
No. of Biosafety Cabinets (BSC)	1	This work
No. of centrifuges	1	This work
Incubator unit cost ($)	10,000	This work
BSC unit cost ($)	10,500	This work
Centrifuge unit cost ($)	8,500	This work
Facility depreciation period	15 years	[270]
Equipment depreciation period	5 years	[5]
No. operators	4	This work
Daily worker rate	$100	This work
Quality control cost, MCB	$100,000/batch	Expert opinion
Quality control cost, WCB	$10,000/batch	Expert opinion
Quality control cost, final	$10,000/batch	Expert opinion
Culture media cost/ml	$0.34	This work
Harvesting reagent cost/ml	$0.21	This work
No. cells/dose	70 million	This work
No. P0 cells	5 million AT MSC 500,000 UCM MSC	This work
Batch failure rate/QC	10%	[29]

5.3 Results

The economic model developed by our group 4 was used to determine the economic feasibility of the process. A total of 5 passages (around 10-13 population doublings) were considered for the model to maximize cell numbers in the cell banks, without compromising cell quality (Table 5.3) [302]. The calculated number of cells expanded from a single donor after 5 passages (with intermediate MCB and WCB steps) was higher both for UCM-MSC (1.84 vs 1.97 x10^9 cells) and for AT-MSC (3.49 vs. 2.24 x 10^9 cells), when using PBS-0.1 MAG in comparison with the planar culture system (Figure 5.1A). The higher number of cells needed to seed the PBS-0.1MAG system for a full expansion capacity led to a higher number of cells per batch, where an increase from 245 to 460 million cells per batch for UCM-MSC and from 172 to 388 million cells per batch for AT-MSC was simulated, when introducing the PBS 0.1 MAG in the final expansion stage (Figure 5.1B). The number of total final product batches is reduced with the transition to PBS-0.1MAG from 13 to 9 (AT-MSC) and from 8 to 4 (UCM-MSC). Finally, the number of

total doses of 70 million cells produced increased from 26 to 45 (AT-MSC) and from 23 to 25 (UCM-MSC) (Table 5.3).

Table 5.3: Total processing costs, number of batches per process, and total doses obtained for each process

Parameter	Cell Source	T-175	VWR
Total process costs	AT MSC	$559,730	$499,657
	UCM MSC	$391,906	$278,081
# of batches	AT MSC	13	9
	UCM MSC	8	4
Total costs/batch	AT MSC	$43,056	$55,517
	UCM MSC	$48,988	$69,520
# of doses	AT MSC	26	45
	UCM MSC	23	25
# of doses/batch	AT MSC	2	5
	UCM MSC	3	8
Total costs per dose	AT MSC	$21,258	$11,103
	UCM MSC	$17,039	$11,123
Cumulative Population Doublings	AT MSC	9.70	9.93
	UCM MSC	12.70	12.94

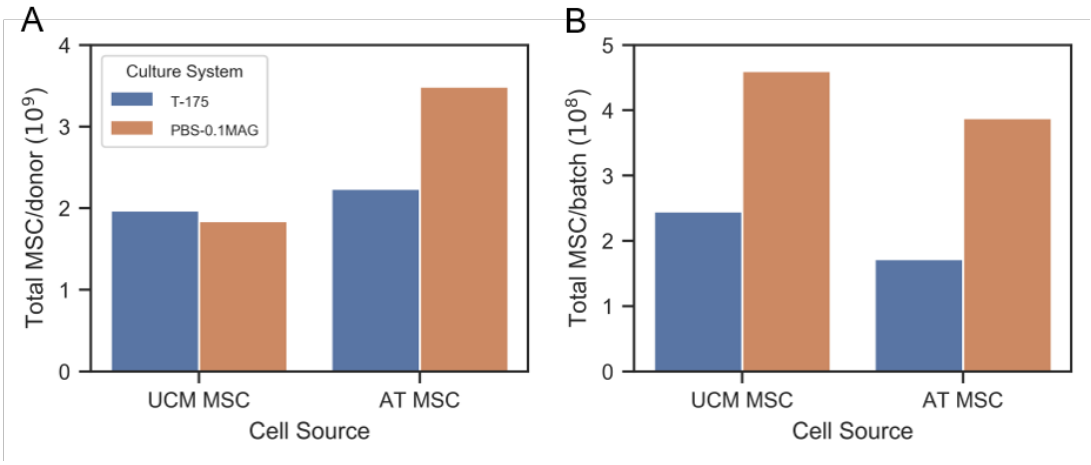

Figure 5.1: Total predicted number of umbilical cord matrix- and adipose tissue-derived mesenchymal stromal cells expanded in T-175 flasks vs PBS-0.1 MAG system, per donor and batch. A - Total predicted number of umbilical cord matrix (UCM)- and adipose tissue (AT)-derived mesenchymal stromal cells (MSC) expanded from a single donor using T-175 flasks (blue) vs PBS-0.1 MAG (orange) systems. B - Total predicted number UCM-MSC and AT-MSC expanded from a single batch using T-175 flasks (blue) vs PBS-0.1 MAG (orange) systems.

The utilization of PBS 0.1 MAG also leads to a reduction in the total process costs of 11% and 30% for UCM-MSC and AT-MSC, respectively (Table 5.4). Costs per dose decrease from $17.0 K to $11.1 K for UCM-MSC and from $21.5 K to $11.1 K for AT-MSC (Figure 5.2.A). Moreover, the reduction of the quality control costs per dose (testing) and labor contribution, are important factors leading to cost reduction

(Figure 5.2.B-C, Tables 5.4-5.5). In absolute values, the higher contributors for cost reduction are labor and testing, in agreement with the increase in cell output provided by the VW system when compared with the use of T-175 flasks. As the seeding density of PBS-0.1MAG is considerably higher than for T-175, more WCB cells are seeded to initiate the expansion cycle. This leads to faster consumption of the full WCB capacity, resulting in lower numbers of batches in the PBS-0.1MAG expansion (Table 5.3). However, each batch of the PBS-0.1MAG has higher cell numbers (Figure 5.1B). The release testing costs are fixed per batch, regardless of the number of cells per batch. Thus, with fewer batches and, therefore, fewer release testings required, the PBS-0.1 MAG expansion offers a reduction in the relative release testing contribution. The consumable costs of the total process are higher for the VWR system, in agreement with the higher unit costs of PBS-0.1MAG, and the total consumable costs per dose of final product also show an absolute reduction, associated to the higher cell yield with the VWR system (Table 5.4). However, the relative contribution of consumable costs to the cost structure per dose is increased, as well as the quality control relative cost contribution (Figure 5.2.D-E).

Table 5.4: Total process costs per category for adipose tissue-derived mesenchymal stromal cells and umbilical cord matrix mesenchymal stromal cells.

	AT MSC		UCM MSC	
	T-175	VWR	T-175	VWR
Consumables	$101,459	$126,233	$56,923	$43,124
Labor	$156,000	$110,800	$103,600	$57,600
Equipment and facility	$62,271	$52,624	$41,354	$27,357
Testing	$240,000	$210,000	$190,000	$150,000

Table 5.5: Total number of cells from the working cell bank (WCB) used to seed each final product batch and total number of batches obtained from each WCB.

	T-175		VWR	
	# 10^6 cells	# batches	# 10^6 cells	# batches
AT MSC	13.5	13	31	9
UCM MSC	9.5	8	21.5	4

5.4 Discussion

The costs of goods per dose obtained within the scope of this study ($11,000 - $21,000) are within the range of costs of goods obtained in other MSC bioprocess modeling studies [27, 144, 186]. Given that the final prices of commercially available ATMPs are in a range of $500 - $850,000 per dose [27, 103, 105], interventions aimed at reducing the costs of goods per dose are key to ensure sustainability of cell based products under reimbursement constraints [103].

The higher cell seeding density requirements of microcarrier based technologies is a consequence of the suboptimal MSC adhesion rates in microcarriers and impacts the process operation [219]. For AT MSC, the number of WCB vials (500,000 cells each) needed to see the last expansion cycle increase

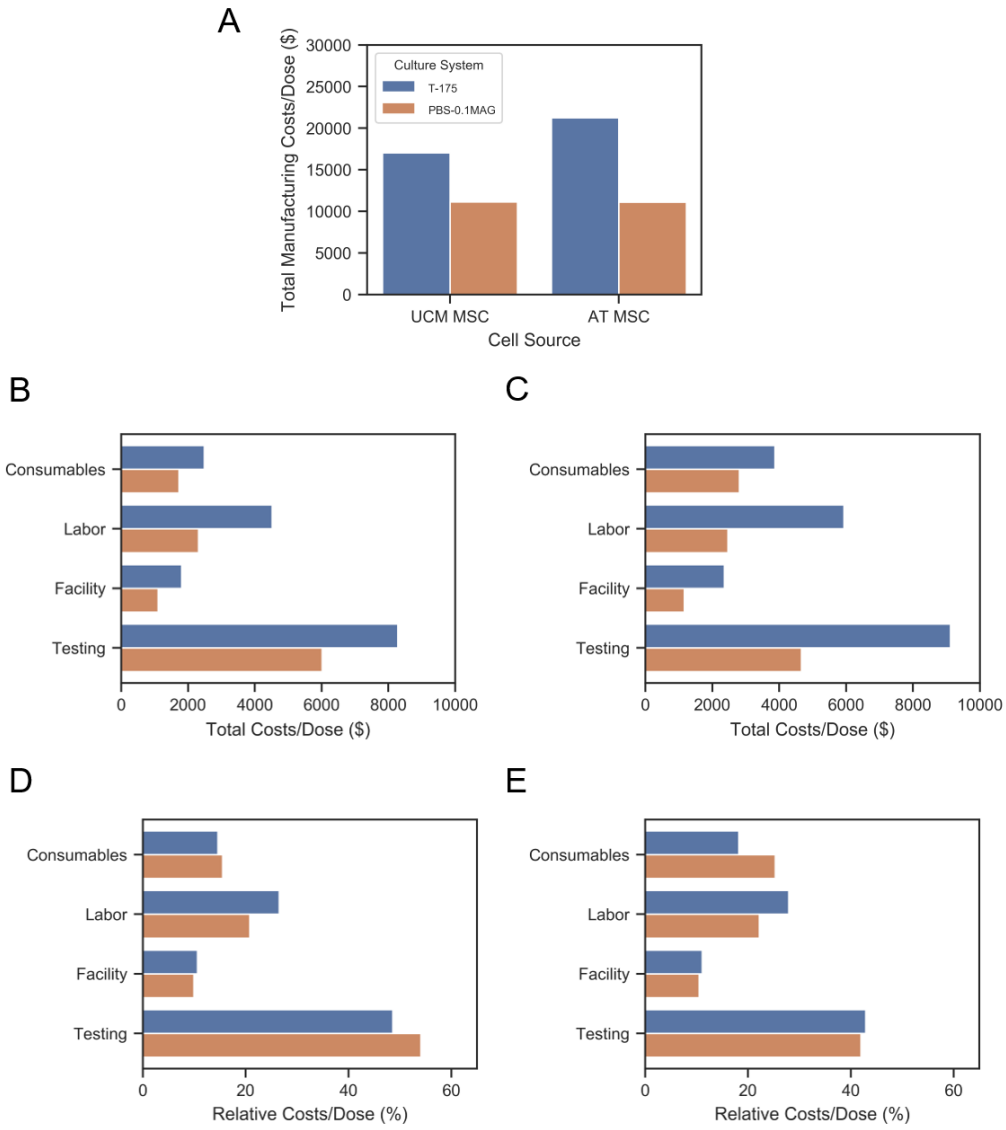

Figure 5.2: Total predicted manufacturing costs per dose and relative contribution of consumables, labor, depreciation, and testing, for the cost of goods per dose and for the percentage of costs, considering the expansion of adipose tissue- and umbilical cord matrix-derived mesenchymal stromal cells using T-175 flasks vs PBS-0.1 MAG system. A - Total predicted manufacturing costs per dose for umbilical cord matrix (UCM)- and adipose tissue (AT)-derived mesenchymal stromal cells (MSC) manufacturing using T-175 flasks (blue) vs PBS-0.1 MAG system (orange). Relative contribution of consumables, labor, depreciation, and testing for the total cost of goods per dose (B,C [$]) and for the percentage of costs (D,E, [%]) for UCM MSC (B,D) and AT MSC (C,E) manufacturing in T-175 flasks (blue) vs PBS-0.1 MAG system (orange).

from 27 to 62 with the process transfer from T-175 to PBS-0.1MAG, while for UCM MSC the number of WCB vials used increases from 19 to 43. Only 4 or 9 batches are sufficient to exhaust the WCB vials of UCM or AT MSC, respectively, using the PBS-0.1MAG; while 8 or 13 batches are required for complete use of the WCB vials of UCM MSC or AT MSC (Tables 5.3, 5.5). Further technological improvements at the level of initial adhesion to microcarriers would offer shorter times to attain confluence.

In the current setup, the main cost driver is the quality controls. A fixed cost was assumed, irrespec-

tive of the number of MCB, WCB, and final batch vials. However, the scale of the banks simulated in this process is fairly small. The simulations yielded 2-20 million cells per MCB and 70-200 million cells per WCB, while MCB containing 500 – 5,000 million cells and WCB containing 500 – 5,000 million cells were already reported [56]. Therefore, it is estimated that, in future studies concerning the scalability of expansion in bioreactors of higher volumes and in larger GMP facilities, the relative contribution of the quality controls to the cost structure will decrease.

The increase in total consumable costs in the microcarrier-based culture poses challenges in the scalability supply and cost of consumables [5]. Additionally, other challenges are related with the need to guarantee scalability of the proliferative benefits across higher volume platforms, and that quality attributes are maintained [186, 248, 254]. Finally, a current bottleneck of scalability is the volumes handled by current DSP systems [28, 27, 10], for which DSP with microcarrier-based systems is generally less effective than for planar technologies [30].

5.5 Conclusion

The economic evaluation presented in this Chapter supports the process transition to vertical wheel bioreactors in a cost-effective manner, as long as safety and clinically meaningful quality attributes are similar to planar technologies. This analysis provides positive indications for the scalability to higher volumes (i.e. PBS-3, PBS-80, and PBS-500, with maximum working volumes of 3L, 80L, and 500L, respectively) in order to obtain clinically meaningful MSC numbers for clinical translation in a controlled and closed system.

The cost savings per dose held for both AT-MSC and UCM-MSC, two types of MSC seen as more sustainable and less invasive as the most traditional BM-MSC. In both systems, it was assumed that the cell quality attributes were equivalent in T-175 and PBS-0.1 MAG culture. The transfer of quality attributes to reactor-based culture is a concern in the development of therapeutic products expanded in such configurations [303]. The development of specific potency assays for the envisioned clinical indications of MSC from either adipose tissue or umbilical cord matrix is required to provide more information to update the cost-effectiveness estimations.

This chapter provided advancement in the development of TESSEE from Chapter 4 due to the implementation of intermediate banking steps and introduction of a choice of microcarrier based culture in bioreactors. As this process was not developed, at this moment, with a specific prospective clinical application, the application of TESSEE here was purely in bioprocess economics.

The next chapters of this thesis will present a further advancement of TESSEE in the determination of bioprocess costs of allogeneic therapies, but with a specific clinical indication in mind. In Chapter 7, an allogeneic MSC therapy for cystic fibrosis will be evaluated from both the bioprocess and health economics standpoint. The same framework is enlarged in Chapter 6 to include process steps for manufacturing of a pluripotent stem cell (PSC) based therapy for type 1 diabetes (T1D).

Chapter 6

Bioprocess and early health economic modeling of pluripotent stem cell (PSC) derived beta cell loaded devices for insulin secretion in type 1 diabetes

Note: The contents of this chapter are adapted from the peer-reviewed article: C. Bandeiras, J. M. S. Cabral, R. A. Gabbay, S. N. Finkelstein, F. C. Ferreira, Bringing stem cell based therapies for type 1 diabetes to the clinic: early insights from bioprocess economics and cost effectiveness analysis, Biotechnology Journal 14(8):1800563 [304]

6.1 Outline

In this chapter, the manufacturing of an allogeneic cell-based product is again considered, but not from MSC. Instead, pluripotent stem cells (PSC) are considered as starting cells to be used in the manufacturing process. The use of PSC brings forth new model challenges, such as the need to include not only an expansion stage but also a differentiation stage. Moreover, PSC culture protocols are longer than for MSC and involve more expensive culture media. Furthermore, in order to ensure that only differentiated cells are present in the therapeutic products, as undifferentiated PSC can cause teratomas *in vivo*, a purification step is required in downstream processing (DSP). One of the most common purification systems to collect the cell population of interest is magnetic activated cell sorting MACS, a process based on cell surface antigens that bind to specific magnetically-activated beads coated with specific antibodies.

Here, TESSEE was upgraded to combine a bioprocess decision support tool was combined with a disease state transition model, allowing to assess the cost-effectiveness of a stem cell-based therapy against a standard of care.

The therapeutic case study evaluated in this chapter is the development of stem cell-based therapy for type 1 diabetes (T1D). Differentiation of PSC into functional beta cells and their transplantation, encapsulated in semipermeable devices for protection from immune response, could provide insulin independence for T1D patients. Importantly, this approach would address limitations on sourcing beta cells from pancreatic donors and it would reduce clinical complications that most patients managed on Intensive Insulin Therapy (IIT) eventually face. However, bottlenecks of PSC manufacturing hinder the long-term cost-effectiveness and accessibility of these therapies. Optimization of these parameters can be informed by computational models such as TESSEE.

PSC were simulated to be expanded in T-flasks and cell stacks, and aggregated for differentiation in 6-well plates, according to experimental protocols [271, 305]. Cost-effectiveness of the stem cell-based therapy against IIT was assessed in quality-adjusted life-years (QALY). The model was used for process optimization of batch size and annual demand, reducing manufacturing costs per patient from $430,000 to $160,000. The simulations show that the reagents were the process resource with a higher impact on costs, while differentiation was the most expensive process step. This study estimates that cell therapy would improve the quality of life, in comparison with IIT, for 96% of the patients. Cost savings were achieved for 2% of the population through prevention of renal disease. The therapy was determined to be cost-effective for 3.4% of patients when a willingness to pay (WTP) threshold of up to $150,000/QALY was considered. A 75% cost reduction of the cell therapy price increased cost-effectiveness likelihood to 51% at $100,000/QALY. This study highlighted, with quantitative computational data, the need for scalable manufacturing platforms for stem cell therapies to reduce the cost of goods, as well as to prioritizing access to the therapy to patients with an increased likelihood of costly complications.

6.2 Methods

6.2.1 Case Study Definition

This work focused on the early health technology assessment of a stem cell-based implantable therapy for type 1 diabetes, with devices containing pluripotent stem cell (PSC) derived islet cells. Each device contains approximately 100 million islet cells [306]. The device consists on the cells encased in a semipermeable membrane allowing nutrient flux but protecting the cells from immune response. Each patient is transplanted with 5 devices, for a total final dose per patient of 500 million cells. A first pilot-scale scenario was considered, with 1 patient per batch, 5 patients/year. Then, a scenario of 50 patients, 250 devices/year was derived in agreement with a Phase I/II clinical trial (NCT02239354), with 1 patient/batch. For such simulation, several batches are processed in parallel and there was a staggering of the utilization of the purification equipment, aiming at reduction of costs. These two cases were fresh products and a made-to-order scenario was adopted. Further optimization of utilization of the equipment capacity was performed through a case with 50 patients/year, 10 patients/batch. This strategy aimed at cryopreserved, off-the-shelf products.

The early assessment comprised a bioprocess economics model and a disease state cost-utility

analysis. The bioprocess economics model was used to calculate the cost of goods (CoG) of the stem cell-based devices and these costs of goods were then linked to the clinical cost-effectiveness through a disease state model comparing stem cell-based therapy with IIT.

6.2.2 Bioprocess economics model implementation

The bioprocess economics model presented in Chapter 3 was reported elsewhere for mesenchymal stem/stromal cells (MSC) (Chapters 4 - 7) [275, 301]. Briefly, this model encompassed the expansion of pluripotent stem cells in vials from a working cell bank (WCB). In the base case scenario, the WCB contains iPSC. Cells from WCB vials were expanded for 4 passages. The model was expanded to include cell aggregation and differentiation protocols as previously reported for T1D [305, 307, 308, 271] (Figure **??**). This work aims at modeling a facility operating 336 days/year. The manufacturing process for each batch of stem cell-based devices takes 42 days in total, with 12 days for expansion of PSC from a WCB, followed by 30 days for differentiation of PSC into beta cells, and with downstream processing and final product formulation on day 42.

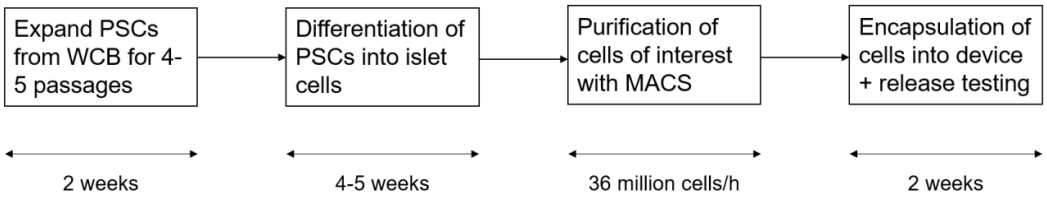

Figure 6.1: Bioprocess model of PSC-derived beta cell-loaded devices. Modified from [308]

Cost and mass balance inputs drove the calculation of the total CoG per dose, as well as the cost of goods breakdown per resource and per process stage (Table 6.1 and Table 6.2).

The number of cells per PSC bank and the cost per million cells were derived from published estimates [150]. The PSC expansion parameters were an average of a range of scalable expansion runs of MCB and WCB PSC in 2D cell culture flasks (T-flasks and cell factories) [271]. A differentiation yield of PSC into islet cells of 80% was assumed, based on a range of values from differentiation protocols [305]. We simulated a DSP strategy using magnetic-activated cell sorting (MACS). This technique was previously reported for purification of beta cells from a complex mixture [309], as well as for the positive selection of pancreatic and endoderm progenitors derived from stem cells [310, 311, 312]. A DSP yield of 20% was used for model runs, based on the yield from the purification of beta cells from cadaveric pancreatic donors [309]. (Table 6.1). The reagent costs were adapted from the several media formulations used for cell expansion, aggregation and differentiation (Table 6.1). The facility dimensions were varied in order to supply the annual demands and batch sizes [5, 10, 6, 156, 147]. A nominal batch failure rate at the release testing stage of 30% was included, accounting for the several different batch failure step rates (banking, expansion, differentiation, and release testing). This estimate was provided for the manufacturing of PSC-derived islet cells after discussions with experts. The costs of failed batch runs were spread out by the total passed runs. Additionally, a sensitivity analysis to evaluate

Table 6.1: Key facility, labor, quality control and reagent assumptions for the bioprocess economics modeling.

Parameter	Value	Reference
Scenario Set up		
No. cells/device	100 x 10^6	[306]
No. cells/patient	500 x 10^6	[12]
Max No. batches/year	50	This work
Max No. patients/batch	10	This work
Lang Factor	8	This work
Facility depreciation period	15 years	This work
Equipment depreciation period	5 years	This work
Max No. incubators/facility	10	This work
Max No. incubators/clean room	2	This work
Max No. incubators/BSC	2	This work
Max No. incubators/MACS	2	This work
Expansion system	Cell culture flasks	[271]
Differentiation system	6-well plates	[271]
Max No. expansion system/incubator	12-100	[5]
Max No. differentiation system/incubator	600	[6]
Costs		
Facility operating costs/year ($)	188,000	Derived from [270]
Incubator unit cost ($)	16,000	[5]
BSC unit cost ($)	15,300	[5]
MACS unit cost ($)	50,000	[156]
Expansion media cost ($/ml)	0.76	Derived from [271]
Differentiation media cost ($/ml)	0.21 - 4.32 (stage dependent)	Derived from [305]
Harvesting reagent cost ($/ml)	0.24	Derived from [271]
PSC from WCB/10^6 cells ($)	1,500	Derived from [150]
Encapsulation device cost ($)	400	This work
Mass balance		
Expansion seeding density (cells/cm^2)	50,000	[271]
Expansion growth rate (day^{-1})	0.53 - 0.69 (stage dependent)	Derived from [271]
Differentiation seeding density (cells/ml)	1 x 10^6	[271]
Differentiation yield	0.80	Derived from [305]
Max No. cells/MACS sorting	3.5 x 10^{10}	[156]
MACS yield	0.2	Derived from [309]
Batch failure rate	0.3	This work

the reduction in CoG caused by changing specific inputs to the best possible case was performed for the three manufacturing strategies. Namely, as a best-case banking scenario, allogeneic ESC cells are considered to reduce the costs required with reprogramming and establishment of an iPSC bank. The best-case parameter choice is depicted in Table 6.3.

Table 6.2: Summary of the equations used to compute the different cost categories included in the cost of goods per batch, per dose (i.e., stem cell-based device), and per patient. Table modified from [313]

Cost category		Value
Direct	Consumables	f(utilization/batch)
	Banking	No. initial cells/batch * PSC from WCB cost
	Reagents	f(utilization/batch)
	Quality Controls	QC cost/batch
Indirect	Equipment acquisition cost	No. Incubators * Incubator cost + No. BSC * BSC cost + No. MACS * MACS cost
	Equipment depreciation	(Equipment acquisition cost/ Equipment depreciation period) / No. batches/year
	Fixed capital investment (FCI)	(Equipment acquisition cost * Lang factor)
	Facility depreciation	FCI / Facility depreciation period / No. batches/year
	Operating costs	Annual facility operating costs / No. batches/year
	Labor costs	(No. workers * Annual cost/worker) / No. batches/year
Cost of goods/batch		Direct costs + Indirect costs
Cost of goods/dose		Cost of goods/batch / No. doses/batch
Cost of goods/patient		Cost of goods/dose * No. doses/patient

Table 6.3: Comparison of the baseline scenario and the best-case scenario used in the sensitivity analysis

Parameter	Operating Case		Best Case	
	Value	Reference	Value	Reference
Banking/10^6 cells ($)	1,500	[150]	375	[314]
Expansion rates/passage (day^{-1})	0.53 - 0.69	[271]	0.57 - 0.70	[271]
Max No.cells/MACS	3.5 x 10^{10}	[156]	1.2 x 10^{11}	[315]
MACS yield (%)	20	[309]	86	[312]
Differentiation yield (%)	80	[305]	95	[305]
Differentiation media ($)	0.21-4.32	[308]	0.21	[308]

6.2.3 Disease state model implementation

A discrete state-transition Markov model for the cost-effectiveness of beta cell transplantation for T1D was employed. The model was implemented in Python for compatibility with the bioprocess model and slightly modified from published models [316, 12, 19, 317]. The comparator therapy was IIT. In this model (Figure 6.2), five states were defined for the beta cell transplant model: (i) Full insulin independence, (ii) partial graft function without complications (insulin dependent but producing other relevant factors for

glucose control), (iii) graft failure without complications, (iv) diabetes-related complications (after graft failure), and (v) death. The IIT arm had three states: (i) IIT without complications, (ii) diabetes-related complications, and (iii) death.

A 20-year follow-up was modeled. The model was run considering a sample of 1000 hypothetical patients, with probabilities of complications and state transition sampled from data on transplantation of cadaveric donor islets. The key assumptions of the health economics study are depicted in Table 6.5 and the key model equations are summarized in Table 6.4.

The main parameters of the model are the probability of patients moving between states, the costs associated with the therapies and diabetes-related complications, and utilities representing a score in the 0-1 range for the quality of life of a year associated with each health state [12, 317]. Initially, a patient undergoing IIT had a utility weight of 0.71, in agreement with patients with hypoglycemia unawareness. A patient with partial graft function had a utility of 0.81, as a T1D patient without complications, but requiring insulin administration. Patients with full graft function had a utility of 0.91, similar to healthy young adults [316, 317]. Note that the model assumed equivalent clinical effectiveness and graft failure rates to cadaveric islets and that the cohort of patients is considered to not have any diabetes-related complications at the time of the start of follow-up. It was considered that patients could suffer complications from 5 main groups: hypoglycemia, cardiovascular, neuropathy, nephropathy, and ophthalmological [318]. Each complication was computed with increased medical costs and a utility decrement per patient of up to -0.29 [319, 320]. In the case of graft failure, a new transplant may be performed to ensure long term insulin independence [12, 317]. As a modification from previous cost-effectiveness analyses approaches in the field, we assumed that no immunosuppression was required for these transplants. The lack of immunosuppression requirement is related to encapsulation that protects the cells from both alloimmune and autoimmune attack [316, 19, 317]. Yearly costs and quality of life scores (i.e. utility weights) associated with each state were computed. Moreover, patients could move through states according to event probabilities [318, 317]. All input costs are expressed in 2017 United States Dollars (USD). When required, input costs were adjusted to 2017 USD using the Consumer Price Index [321]. While running the model for the follow-up period, costs and utilities were discounted at an annual rate of 3% [12, 317, 322].

After the follow-up period, the total direct medical costs were computed, as well as a sum of the utilities per year yielding the total quality-adjusted life years (QALY). The cost-effectiveness of the new treatment was assessed as an incremental cost-effectiveness ratio (ICER), a ratio of the total difference in costs to the difference in QALY between the two therapies. Stem cell-based therapy was cost-effective if it was below a given willingness to pay (WTP) threshold in cost/QALY. In order to stratify the patients that could benefit the most from stem cell-based therapy, due to the type of complications averted using stem cell-based therapy in comparison with IIT, the number of patients with complications averted and type of complications averted in typical WTP threshold was evaluated as well.

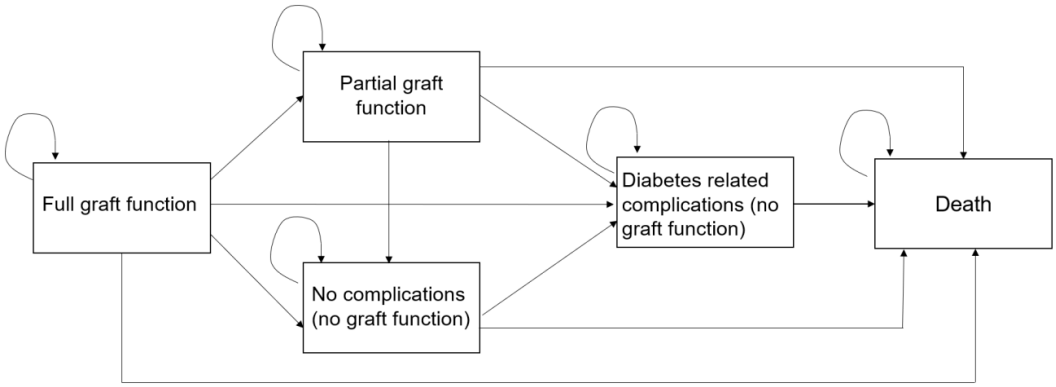

Figure 6.2: Disease state model of type 1 diabetes, with or without graft. Modified from [317].

Table 6.4: Summary of the equations used to compute the total costs, quality adjusted life years, and incremental cost-effectiveness ratios (ICER) in the disease state model. The calculation follows the same structure as [12, 19]

Parameter		Value
Costs	Therapy costs	Annual costs * Years in therapy
	Transplant costs	One time + Annual follow up costs * Years of follow up
	Medical complications	One time + Annual complication costs * Years of follow up
	Total direct medical costs	Therapy costs + Medical complications + Transplant costs (when applicable)
Utilities	Quality-adjusted life years (QALY)	Sum(utility/year)
Incremental cost-effectiveness ratio (ICER)		Δ costs / Δ QALY

6.3 Results

6.3.1 Increase of annual demand and batch size offer bioprocess cost savings

For the first pilot of 5 patients a year, with 1 patient/batch, 10 million WCB PSC were required to start the PSC expansion process. After expansion, 4.79 billion cells were obtained, with an estimated 2.87 billion islet cells were obtained. The purification process yielded 767 million islet cells. The total processing time per batch was 42 days. The total CoG per stem cell-based device were $85,446, yielding a total CoG per patient of $427,231. Increasing the demand to 50 doses/year, but maintaining the strategy of 1 patient/batch, slightly reduced the CoG per stem cell-based device to $71,763 and the CoG per patient to $358,818. The 16% decrease of cost with the increase in the annual demand was due to a more efficient distribution of indirect costs across multiple batches processed in parallel.

We estimated that only 25% of the expansion capacity per incubator, 30% of the differentiation capacity per incubator, and 14% of the MACS sorting capacity per equipment were utilized per batch. In order to allow more efficient use of the equipment, 65 million PSC cells from the WCB were seeded to

Table 6.5: Key cost, utility and disease state transition probabilities for the health economics modeling of type 1 diabetes progression.

Parameter	Value	Reference
Cost insulin/year	$9,601	[323]
Stem cell-based device price/patient	(CoG/patient) / 0.25	Derived from [324]
Transplantation procedure costs	$25,330	Derived from [324]
Probability of complications	0.001 - 0.03 25% less with partial graft 45% less with full graft	[318, 317]
Costs of complications	Event cost: $0-30,181 Yearly follow up: $185-220,187 Variable with complications	[318]
Graft failure probability	0-30%, time dependent	[316]
Health state base utility weights	0.71 (insulin) 0.91 (transplant)	[316]
# initial complications	0	[316]
Initial patient age	18-35 years	[316]
Utility decrement with complications	0.08 - 0.29 Variable with complications	[319, 320]
Hazard ratio mortality	2.4 with hypoglicemia 7.16 with other complications	[317]
Timespan of analysis	20 years	[316]

start the process. A batch consisting of cells coming from a single MACS equipment yielded enough cells for 10 patients. When considering 50 patients/year, 10 patients/batch, the process resulted in CoG per stem cell-based device of $32,744 (CoG per patient of $163,720). These costs represent a 54% reduction from the 50 patients/year, 1 patient/batch scenario (Figure 6.3A). As manufacturing costs of cadaveric islets per patient are in the order of $80,000, these manufacturing strategies resulted still in higher manufacturing costs per patient than cadaveric islets [324].

In the 5 patients/year, 1 patients/batch setting, 46% of costs were attributed to the reagents (expansion and differentiation media, harvesting and purification reagents, final formulation buffers). This was, by far, the highest contribution in direct process costs. The other direct costs, identified as banking, consumables, and quality controls costs, account for 4%, 3% and 8% of the total costs per dose, respectively. Regarding the indirect costs, the labor costs were 32% of the total costs per dose, and the facility associated costs (building and equipment operational and depreciation costs) contributed to 8% of total costs. The increase in annual demand to 50 patients led to a noticeable reduction in the indirect costs contribution per dose, as the labor costs were 9% of the total costs per dose and facility costs were 3% of these costs. This was a result of parallel processing of different batches, spreading the indirect costs over several batches. Note that the facility was dimensioned, in this case, such that a maximum of 10 batches could be processed in parallel. It is worthwhile noticing that the absolute values of direct costs per dose (banking, consumables, reagents and quality controls) increased in the 50 patients/year case. This was a result of the inclusion of the costs of failed batch runs. For 50 patients/year, increasing the batch size to 10 patients/batch further decreased the indirect costs contribution, with labor accounting

for 9% of costs and the facility for 2% of the costs. The reagent costs accounted for 82% of the total dose costs (Figure 6.3B). Regarding the process stages, the main share of costs was attributed to the differentiation stage for every process configuration (between 74 to 87% of total costs per dose, depending on process configuration). The differentiation stage involved media exchange daily or every other day, resulting in large volumes of culture media spent [307, 308]. The costs of generation of banking vials accounted for 3-6% of the total cost breakdown. Downstream processing accounted for 1-3% of costs. This is not unsurprising since the process was dimensioned for the maximum number of cells out of the differentiation step to not surpass the maximum number of cells per MACS equipment. Therefore, there are no waiting times for equipment, or the need to use several MACS equipment in parallel to process a single batch. The cost contribution of expansion was 3-11% of total costs, with the costs decreasing with the increased annual demand and batch size, as these costs were spread over a higher number of doses (Figure 6.3C).

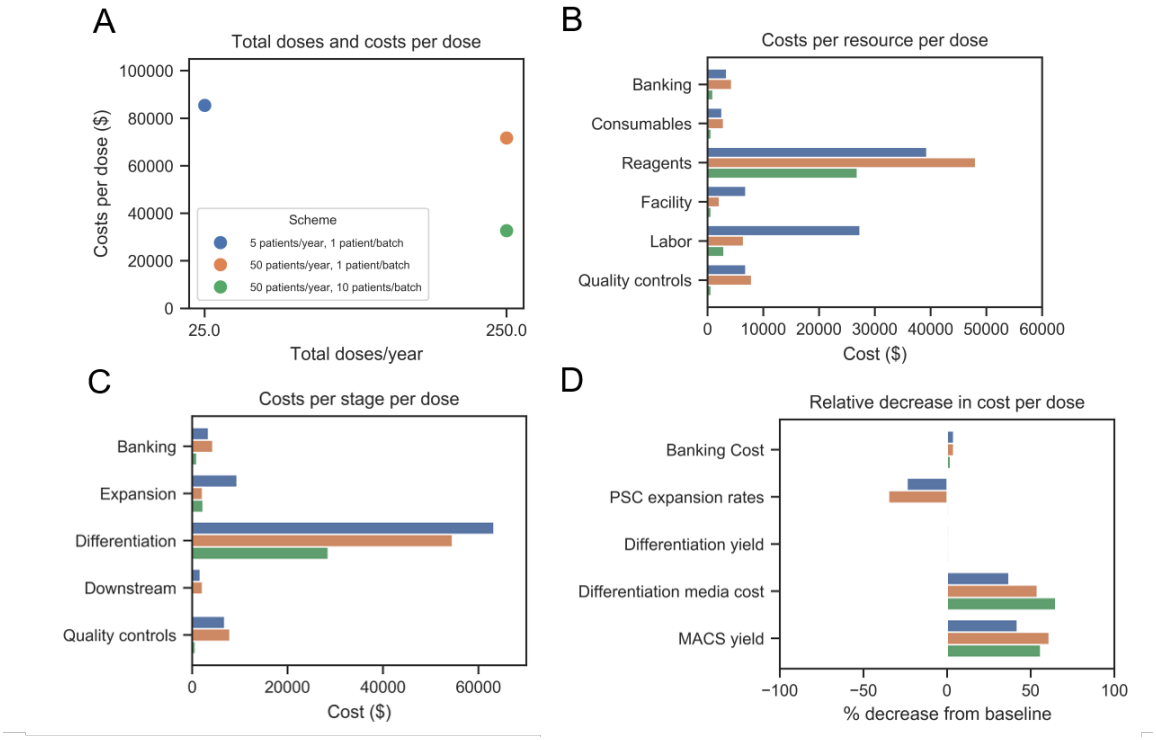

Figure 6.3: Impact of the annual demand for PSC-derived, beta cell-loaded devices, in the cost of goods (CoG) involved in manufacturing devices for each individual with type 1 diabetes (T1D). Each individual received 5 devices per transplant, leading to a final dose of 500 million beta cells per individual. A – CoG vs the number of devices produced per year and the number of individuals considered per process batch. B - Breakdown of CoG per process resource. C - Breakdown of costs per process stage. D – Sensitivity analysis of the total costs per dose when improving process parameters to a best-case scenario. Parameter values are described in Table 6.3.

6.3.2 Media costs and downstream yield are key factors to optimize

Figure 6.3D illustrates the changes in CoG in response to the change in input parameters to their best-case values. When increasing the expansion growth rates to the best possible case, the CoG for the 1

patient/batch case increased 24-35%. For the process with 10 patients/batch, a minor cost reduction of 1% was achieved. The increases in expansion growth rates resulted in a lower number of WCB cells necessary to seed the expansion stage to reach full incubator capacity. Under the increased expansion yields, 7.5 million cells from the bank were required to start the expansion, instead of 10 million in the baseline case for 1 patient/batch. For 10 patients/batch, the number of WCB cells required was reduced from 35 to 25 million cells.

The differentiation yield was increased to 95% as a best-case scenario but its effects were negligible, as the baseline case operated with a considerably high differentiation yield of 80%. However, as reagent costs and the differentiation unit operation were major cost contributors, the reduction of the differentiation media costs had a major impact, as CoG per device were reduced by 37-65%. Assuming the best-case DSP scenario, for which the reported MACS yield was 86% (Table 6.3), the reductions in the cost per dose were 42-61%. Therefore, the optimization of downstream processing systems (assuming consistent differentiation yields of PSC into islet cells), would be a key strategy to increase the batch size and reduce costs per device. Cell vials sourcing cost was also evaluated on this sensitivity analysis. The reduction to a best-case cost of $375 per million cells led to a small decrease in the costs per dose of 2-4%.

By applying the reported improvements in DSP yield and media costs to the cheapest initial scenario (50 patients/year, 10 patients/batch), the cost of goods per dose would decrease to approximately $12,000/dose, with a total manufacturing cost per patient of $60,000. In this fashion, the CoG per patient for stem cell-based devices would be lower than for cadaveric islets.

6.3.3 Cost-effectiveness of the cell loaded devices is related to prevention of complications

The bioprocess economics model results provided inputs for the price per patient of stem cell-based devices needed for the transplantation arm of the disease state model. Considering the manufacturing strategy of 50 patients/year, 10 patients/batch, the final price per transplant per patient was assumed as $650,000 (such that CoG if 25% of the final price) [110]. The stem cell-based therapy yielded improved life outcomes. The model calculated an increase of 3.73 QALY per patient, on average, in comparison with IIT, over a 20-year timespan. However, the transplant is, overall, a more costly treatment due to high upfront costs. Direct medical costs over a 20-year timespan were, on average, 4 times higher than for IIT (Table 6.6). Each patient underwent between 1 and 3 transplantations (of 5 stem cell-based devices each) in the timespan of the analysis.

Table 6.6: Mean and 95% confidence intervals for the costs and QALY for the two T1D therapeutic options calculated using the disease state transition model.

Therapy	20-year costs	QALY
Insulin intensive therapy	$319,981 ($148,227-$1,518,940)	9.61 (4.84-10.88)
Islet cell device	$582,002 ($353,357-$818,625)	13.24 (8.37-13.94)

Figure 6.4A depicts the individual QALY and costs increments analysis using the stem cell-based therapy vs IIT. 96.4% of the patients had higher QALY with stem cell-based therapy. The transplant was a cost-saving alternative for only 1.6% of the patients, as they showed as well lower direct medical costs in comparison with IIT. For these patients, end-stage renal disease was averted with the transplantation, irrespective of the occurrence of other complications (Table 6.7).

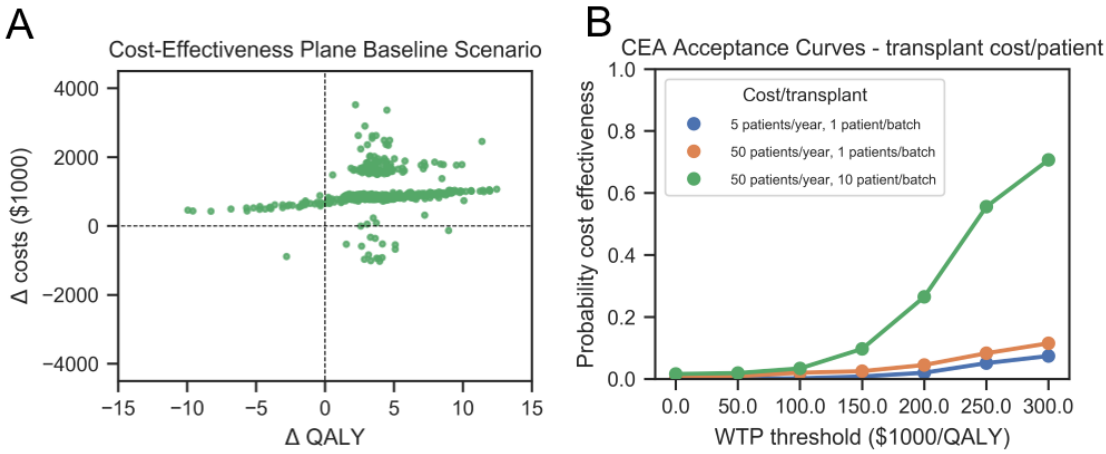

Figure 6.4: Long-term cost-effectiveness of transplantation of PSC-derived, beta cell-loaded devices for type 1 diabetes (T1D) management. A - Cost-effectiveness acceptance plane (difference in costs vs difference in QALY) after a 20 year follow up period from the transplant, assuming a price per transplant of $650,000 (considering that the manufacturing costs per patient of the 50 patients/year, 10 patients/batch scheme represent 25% of the final transplant price per patient). Points are 1,000 randomly sampled individual patients. B - Cost-effectiveness acceptance probability curve relative to the willingness to pay (WTP) thresholds employed by the payer for transplants using devices manufactured under the 5 patients/year, 1 patient/batch ($1.7M final transplant price), 50 patients/year, 1 patient/batch ($1.45M final transplant price) and the 50 patients/year, 10 patients/batch ($650,000 final transplant price) strategies. Probabilities are calculated as the ratio of the number of patients with an incremental cost-effectiveness ratio (ICER) for stem cell-based therapy below each WTP threshold by the total number of patients.

The cost-effectiveness for the patients with higher cost and QALY under the transplantation scheme is dependent on the ICER and the willingness to pay (WTP) threshold. At a WTP threshold of $50,000/QALY, stem cell-based therapy is cost-effective for only 1.9% of the patients. Within this group, the correlation with the type of complications averted by cell therapy was not as pronounced. For 75% of the patients for which cost-effectiveness was achieved at $50,000/QALY, more than one complication was averted by the transplantation of stem cell-based devices (Table 6.7). The complication averted with the highest frequency was End-Stage Renal Disease (ESRD) (35.2%), followed by Congestive Heart Failure (CHF) (14.8%). At the WTP threshold of $50,000/QALY, the probability of cost efficiency is only marginally affected by the stem cell therapy final price. While the cost-effectiveness probability for the 50 patients/year, 10 patients/batch, at this threshold, is low, it represents an improvement from the manufacturing strategies with 1 patient/batch. The final prices per transplant per patient (calculated considering that the manufacturing costs in Figure 6.3 represent 25% of the final price) are $1.7M for the 5 patients/year scenario and $1.45M for the 50 patients/year case. For these two scenarios, the transplant would not be cost-effective for any patient at the $50,000/QALY threshold.

Considering the $100,000/QALY threshold, the intervention is cost-effective for about 3.4% of the

Table 6.7: Percentage of patients with complications averted per patient per type and per cost-effectiveness group. Disease incidences and costs per complication type were input from [318]. Complication percentages calculated using the health economics model.

Complication	Cost saving	Cost effective, $50,000/QALY	Cost effective, $100,000/QALY	Cost effective, $150,000/QALY
Hypoglicemia				
Inpatient	0	0	0	4.8
Outpatient	0	3.7	0	0
Cardiovascular				
Stroke	0	0	6.7	11.1
PVD	0	3.7	0	3.2
AMI	0	3.7	0	1.5
CHF	0	14.8	13.3	25.4
Neuropathy				
Amputation	0	0	0	0
Foot ulcer	0	7.4	6.7	9.5
Gangrene	12.5	12.9	13.3	4.8
Nephropathy				
ESRD	100	35.2	13.3	1.6

patients in the baseline scenario. At such ICER, the price of the cell loaded device plays a more significant role. For the 1 patient/batch manufacturing scenarios, the cost-effectiveness probability at $100,000/QALY ranged from 0.2% (5 patients/year) to 2% (50 patients/year). 60% of patients had complications averted by the utilization of stem cell-based devices, with the most common averted complications being ESRD, gangrene, and CHF (avoided in 13.3% of patients for each complication). At $150,000/QALY, 13.2% of the patients show cost-effectiveness with the transplant for the 50 patients/year, 10 patients/batch case. At this threshold, cost-effectiveness probabilities for the other scenarios are 0.8% (5 patients/year, 1 patient/batch) and 2.5% (50 patients/year, 1 patient/batch). The most commonly averted complications are CHF (25.4% of patients) and non-proliferative retinopathy (15.8% of patients). 60% of the patients with ICER between $100,000 and $150,000/QALY had complications averted. Therefore, at high WTP thresholds, the avoidance of high-cost complications became gradually less relevant for ensuring cost-effectiveness. For the manufacture strategies of 1 patient/batch, the cost-effectiveness probability was still very low at high WTP thresholds of $300,000/QALY, with only 10% of the patients for which the transplant would be cost-effective in comparison with IIT. The 50 patient/year, 10 patient/batch strategy indicates, at high WTP thresholds, a vast improvement from the 1 patient/batch strategies, as 70% of patients would benefit from a cost-effective transplant at the $300,000/QALY threshold (Figure 6.4B).

A sensitivity analysis was performed to identify strategies to increase the likelihood of cost-effectiveness. At $50,000/QALY, reduction of the transplant costs between 25% and 75% for 50 patients/year, 10 patients/batch strategy would increase the probability of cost-effectiveness to 2.2%-3.1% of the patient population, respectively. At the $100,000/QALY threshold, a more relevant improvement in cost-effectiveness probability to up to 51.7% of the patients was achieved (Figure 6.5A), by reducing the

selling price to 75% of the nominal value.

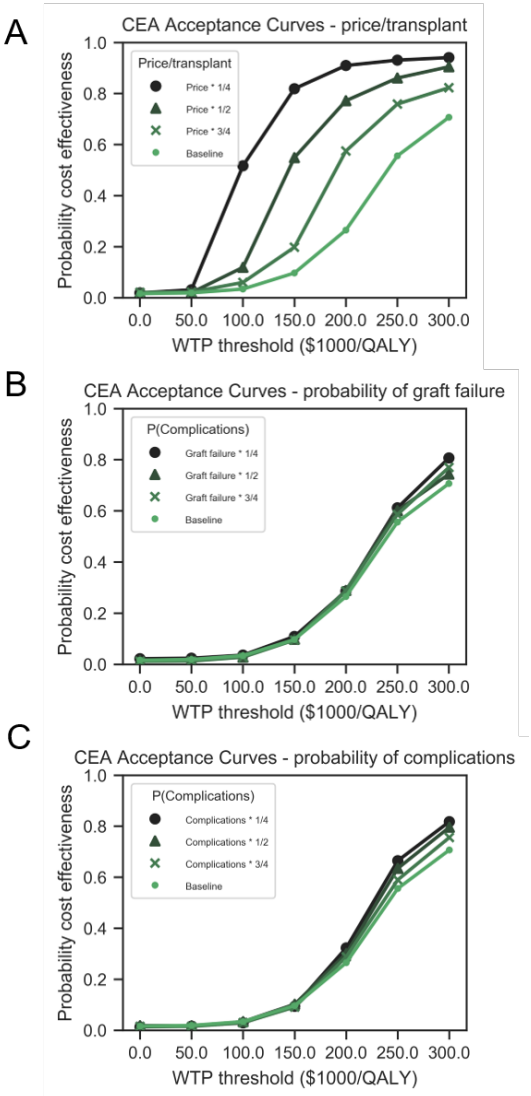

Figure 6.5: Effect of variation of key cost-effectiveness analysis drivers on the cost-effectiveness acceptance curves for PSC-derived, beta-cell loaded devices. Cost-effectiveness acceptance curves where key model parameters are reduced by 25, 50 and 75% of the nominal value, assuming a baseline price per patient of $650,000 (equivalent to the 50 patients/year, 10 patients/batch strategy). Probabilities are calculated as the ratio of the number of patients with an incremental cost-effectiveness ratio (ICER) for stem cell-based therapy below each WTP threshold by the total number of patients. A – Price per patient. B – Probability of diabetes-related complications when the graft is functional. C – Probability of graft failure.

At $50,000/QALY, further reductions in the probability of diabetes-related complications by a functional graft increased the probability of cost-effectiveness to only 2.4%. For the higher thresholds, the differences due to further reductions in graft failure probabilities remained non-significant. This was a considerably more modest increase in the probability of cost-effectiveness than provided by the reduction of manufacturing costs (Figure 6.5B). The final analyzed parameter was the annual graft failure probabilities. At $100,000/QALY, 75% reduction of the annual graft failure probabilities does not increase the cost-effectiveness probability (Figure 6.5C). The differences between groups became only relevant at the threshold of $300,000/QALY, for which a reduction of 75% in the probability of complica-

tions increased the cost-effectiveness probability from 70% to 81.8%. Overall, stem cell-based therapy can further benefit from cost reductions to ensure cost-effectiveness and robustness to reimbursement prices.

6.4 Discussion

The modeling results provide support for long-term cost-effectiveness of stem cell-based devices as therapies for T1D. The estimated possible price per transplant with the manufacturing scenarios simulated in the bioprocess economics model is significantly reduced with the scaling-up of the process from $1.7M to $650,000. While the direct medical costs in this study differ from previously published literature, our conclusions are analogous to those of earlier health technology assessments of stem cell-based beta cell devices [12, 19].

In order to reduce CoG per dose, a scale-up approach, where batches have high numbers of doses, is desired. However, a key limiting factor in scaling-up production of cell therapies is the DSP [10, 9, 147]. In our model, the current low DSP yield reported for MACS purification of islet cells limited the batch size, as a theoretical maximum of just above 5 billion differentiated islet cells (i.e., enough doses for 10 patients) can be obtained per MACS cycle [309, 156, 147]. Increasing the MACS yield to values reported for affinity purification processes for Pancreatic Progenitors PP and Definitive Endoderm (DE) [310, 311, 312] offered significant cost-savings per dose. Current clinical trials do not employ an affinity purification step and encapsulate the pancreatic progenitors assuming that a very high differentiation efficiency is sufficient to minimize the occurrence of teratomas. This strategy would reduce costs and allow higher batch sizes. However, recent animal studies show that teratomas may occur in stem cell-based devices and that a purification step is advisable for safety [36]. In order to overcome the scalability and yield limitations of MACS, economic assessment of other DSP systems evaluated for PSC and PSC-derived differentiated cell types, such as Aqueous Two-Phase Separation (ATPS) and tangential flow filtration TFF [9, 325], could be a future strategy to increase the annual demand and batch size without compromising the facility footprint.

The total costs of manufacturing per patient obtained with the different strategies are above the range presented on a recent study on the CoG modeling of stem cell-derived devices containing pancreatic progenitors [12]. It is important to note that the mentioned study differs from the analysis presented in this work in three key points: (i) the stem cell-based devices contain pancreatic progenitors, with a higher differentiation yield and a faster differentiation process than the ones reported for terminally differentiated beta cells; (ii) it does not take into account the contribution of the cell bank vials in the process, and does not explicitly address downstream processing bottlenecks; (iii) does not consider the impact of possible longer times that pancreatic progenitor-based devices might take to secrete insulin *in vivo* than beta cell-based devices [326]. As a 4-5 week process to obtain terminally differentiated islets was simulated, differentiation costs dominate the cost breakdown. The costs of differentiation can be mitigated by the development of more efficient directed differentiation and media exchange protocols at a larger scale. The scalability of the process to 3D suspension platforms, such as spinners [305, 308, 327]

and bioreactors [230, 328], either in aggregate or microcarrier based platforms, could improve both the expansion and differentiation rates and yields by providing a more similar environment to the native niche, combined with better metabolite and growth factor control [329, 330, 331, 332].

While the stem cell-based therapy would bring an added quality of life to most patients, the transplantation has very high upfront costs in comparison with the continuous administration of insulin. The finding that the therapy would be cost saving for patients for whom ESRD is avoided is consistent with the current clinical development of devices allowing direct vascularization for treatment of patients with a high risk of ESRD [141, 333]. The development of predictive models of diabetes-related complications [334, 335] would help optimize the allocation of resources of these high value, high-cost therapies under budget limitations. The cell-loaded device price is one of the critical factors influencing the probability of cost-effectiveness, and increased likelihood of reimbursement by healthcare payers in budget-constrained scenarios. The positive effect of price on the increase of cost-effectiveness acceptance probability, as evaluated in the sensitivity analysis, is particularly noticeable at a threshold of $100,000/QALY and a price reduction to 25% of the baseline value. A previous study, focused on the United Kingdom healthcare system and using a headroom method approach, recommended reimbursement at a threshold of GBP 20,000 ($26,089)/QALY for the new therapy as cost-effective [19]. For that threshold and the manufacturing costs calculated by our model, the new therapy would be only cost-effective for up to 2% of the patients, eliciting the need for reduction of complications and associated clinical costs. A similar ratio is noticed at a threshold of $50,000/QALY as well. This fact elicits the need for even larger cost reductions associated with the transplantation for the prospective therapy to be adopted over insulin under more strict healthcare spending scenarios. The present study was conducted from a US payer perspective, a market for which cost-effectiveness does not determine recommendations for reimbursement by each healthcare payer. Still, most of the interventions recommended by the American Diabetes Association were cost-effective at $50,000/QALY [336]. The use of our analysis, updated with country-specific healthcare utilization costs, would be particularly useful for decisions in markets for which cost-effectiveness analysis is a key factor of recommendation for reimbursement.

This study aimed at providing cues for initial manufacturing strategies and how the manufacturing costs and the treatment cost-effectiveness influence each other. The study is limited to the scale of manufacturing and reports costs per run, in order to access key bottlenecks in the process. The process costs are dependent on the scale of operation and this tool can be used for the design processes of facilities of different dimensions. Design process considerations include not only scale but also decisions concerning centralized vs de-centralized manufacturing schemes [12]. Additionally, supply chain considerations that will increase the costs are not included in this analysis. Finally, the lack of clinical trial data on efficacy and effectiveness is also a model limitation. The first clinical trials in this field are still in progress. However, the findings of this work create an initial framework for optimizing the manufacturing of stem cell-based devices aiming at improved health outcomes and reduced costs.

6.5 Conclusion

This study demonstrates that manufacturing parameter optimization would result in costs in the range of cadaveric islets for transplantation, given a more optimal utilization of manufacturing resources. Moreover, cost-effectiveness at WTP thresholds between $50,000 and $150,000/QALY could be improved by the reduction of cell loaded device costs, together with the reduction of diabetes-related complications and sustainable, long-term cell loaded device engraftment. The reduction of cell loaded device costs of manufacturing is related to more optimal PSC expansion, differentiation and purification protocols. The findings suggest an increased need for research in the field, in order to provide safe, cost-effective, curative approaches for T1D.

This chapter is a mark on the development of TESSEE in two ways. First, the development of the model for manufacturing of therapies derived from pluripotent stem cells provides a more versatile platform for evaluation of prospective stem cell therapies. However, more importantly, this was the first chapter where a custom disease state model, as a link between manufacturing and cost-effectiveness, was presented.

In this chapter, the uncertainty was present at the level of the cost-effectiveness analysis. Unlike Chapter 4, where the bioprocess model has different degrees of biological uncertainty, the expansion rates per donor were kept constant in this case study for simplicity.

The inclusion of uncertainty at both the bioprocess and health economics model is a focus of the last results chapter of this thesis. On Chapter 7, the modeling of manufacturing of a MSC therapy for cystic fibrosis includes intra donor varaibility in the growth rates. Additionally, different effectiveness outcomes for a prospective therapy provide a more complete view for the development of this therapy, currently in Phase 1 clinical trials.

Chapter 7

Bioprocess and early health economic modeling of mesenchymal stem/stromal cells (MSC) as therapeutic agents for cystic fibrosis

Note: The contents of this chapter are contained in a manuscript in preparation: C. Bandeiras, J.R. Koc, J.F. Chmiel, G.S. Sawicki, J.M.S. Cabral, F.C. Ferreira, S.N. Finkelstein, Bioprocess and early health economic modeling of mesenchymal stem/stromal cells (MSC) as therapeutic agents for cystic fibrosis, Value in Health

7.1 Outline

This chapter introduces a real clinical case study application of TESSEE for informing on the viability of a prospective clinical trial using MSC as a therapy. Therefore, in this chapter, as the manufacturing protocol is defined by protocol used in real practice for this case, the main focus is on a scenario analysis for cost-effectiveness of a MSC therapy.

The framework presented throughout this thesis is adapted in this chapter for modeling an allogeneic, just-in-time manufacturing scenario for MSC therapies for cystic fibrosis CF individuals. The modeling of the manufacturing protocol of MSC doses is in agreement with the Phase 1 clinical trial being modeled (NCT02866721). MSC doses of 1, 3 and 5 million cells/kg were considered. Cost-effectiveness of the stem cell-based therapy against modulator-only was assessed in quality-adjusted-life-years (QALY).

Manufacturing costs per dose, under a just-in-time scenario, range from $9,352 to $12,834, depending on the final dose. Considering one MSC infusion per patient per year, and that manufacturing costs are 20% of the therapy list price, effectiveness assumptions of 10-75% reduction of pulmonary exacerbation and function decay through MSC administration yielded reduction in mortality rates up to 10% and

of transplantation rates up to 8%. Average QALY gains per patient of up to 0.83 QALY were achieved, with a very high variability within the cohort. These gains of quality of life yielded at an average of $2 million additional costs per patient, limiting cost-effectiveness. However, robustness of QALY gains would ensure that MSC therapies would be cost-effective at thresholds of $100,000 and $150,000/QALY, under effectiveness of 50 and 75%, on an outpatient setting. This study highlighted the need for robust effectiveness of MSC therapies in a synergistic effect with disease modulators for CF, while reduction of manufacturing costs could improve the likelihood of cost-effectiveness for more budget limited scenarios.

The application of TESSEE to a real clinical trial setting highlighted in this chapter is customizable and reproducible, being a viable asset for early health technology assessment. Using this approach, it is possible to determine combined effectiveness, technical, and economic constraints and innovations that need to be taken into account for the economic feasibility of a prospective approved therapy using current manufacturing protocols.

7.2 Methods

7.2.1 Bioprocess economics model implementation

For this case study, the bioprocess economics model of TESSEE was slightly adapted to simulate manufacturing of an allogeneic, just-in-time fresh product containing bone marrow mesenchymal stem/stromal cells (BM-MSC), in agreement with a protocol used for manufacturing of the cell product for a phase 1 clinical trial toward anti inflammatory therapy for CF patients (NCT02866721). The simulated process encompasses only expansion, downstream processing and fill-finish of the fresh product, starting the process by thawing previously isolated BM-MSC (Figure 7.1). Three doses were simulated (1, 3 and 5 million cells/kg) and expansion is simulated according to previously published growth rates of BM-MSC in 2D culture in T-flasks, using human platelet lysate (hPL) as the culture medium supplement (PLUS^{TM}, Compass Biomedical, Cleveland, OH). Preliminary, deterministic modeling results showed that expansion costs are dose and patient weight dependent and range from $2,500 for 65 million cells to $6,000 for 425 million cells per patient [337]. This analysis will be extended using additional donor and multi passage variability and a representative distribution of patient weights [338]. The cells are expanded until a final number is reached and then subjected to a protocol of successive washing and volume reduction to purify the cells from media components and prepare them for final administration. The process timeframe and the culture operations (cell seeding, media exchange, harvesting from culture flasks, cell washing and final formulation) drive cost of goods simulations for 1,000 patients. Key model inputs and parameter distributions are depicted in Tables 7.1 - 7.3.

7.2.2 Disease state model implementation

A discrete state transition Markov model for analyzing the cost-effectiveness of Cystic Fibrosis Transmembrane Conductance Regulator (CFTR) modulators was implemented, based on previously published models for CF disease progression, and modified to include prospective assumptions on the

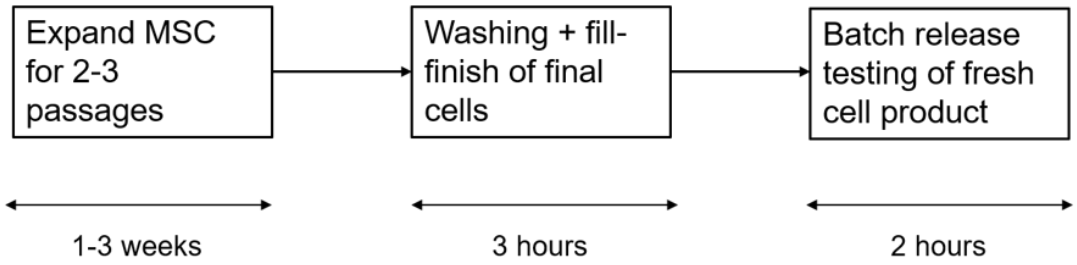

Figure 7.1: Bioprocess modeling scheme for simulation of costs of manufacturing mesenchymal stem/stromal cell (MSC) as a fresh therapeutic product for cystic fibrosis.

treatment regimes and clinical effectiveness of MSC therapy, together with ivacaftor as a disease modulator [339, 340, 341]. The comparator is modulator therapy with ivacaftor, in combination with other standard of care therapies.

Table 7.1: GMP facility and equipment related parameters

Parameter	Value	Reference
GMP facility area	3,000 sq. ft.	This work
% clean room space	50%	This work
Price clean room/sq. ft.	$600	[160]
Price non-clean room/sq. ft.	$350	[160]
Facility depreciation period	15 years	[270]
Facility installation costs	$1,45M	This work
Annual maintenance costs	$47,750	This work
Annual requalification costs	$65,400	[270]
Annual quality assurance costs	$3,200	This work
Annual gas supply costs	$21,600	[270]
Annual cleaning costs	$28,000	[270]
Annual additional supply costs	$9,900	[270]
No. incubators	12	This work
No. BSC	6	This work
No. centrifuges	6	This work
Unit incubator price	$16,000	This work
Unit BSC price	$15,300	This work
Unit centrifuge price	$12,000	This work
Equipment depreciation period	5 years	[270]
Factor facility occupation with stem cell manufacturing	1/6 years	This work
Total workers	6: - 3 manufacturing - 1 supervisor - 1 head of production - 1 QA/QC specialist	This work
Full-time equivalent (FTE) factor	0.8	This work
Factor worker occupation with stem cell manufacturing	0.33	This work
Manufacturing worker pay/day	$272	This work

Table 7.2: Cell processing parameters

Parameter	Value	Reference
Common across stages		
DMEM basal media/ml	\$0.04	This work
Culture media supplement/ml	\$3.00	This work
TrypLE (Harvesting agent)/ml	\$0.21	This work
Isolation		
Cost MCB/vial	\$1,100	This work
No. cells/MCB vial	2 x 10^6	This work
Expansion		
Maximum no. passages	3	This work
No. cells/dose	1, 3 or 5 x 10^6/kg	This work
No. doses/patient	1	This work
No. patients/batch	2	This work
Seeding density/passage	4857 cells/cm^2	This work
Time to confluence	4-6 days	This work
Harvesting yield	0.9	[6]
Harvesting time	14 min	This work
Downstream Processing		
Number of washes	3	[278]
Total DSP time	3h	This work
Volume reduction yield	0.8	[10]
Cost wash medium/ml	\$0.59	This work
Cell concentration	4 x 10^6/ml	This work
Fresh cell bag volume	100 ml	This work
Unit price cell bag	\$8.5	This work
Cost finish medium/ml	\$0.64	This work
Release Testing		
Pass/release ratio	0.9	[29]
Price quality control testing/batch	\$11,300	This work
Time release testing	2 hours	This work

Table 7.3: Intra donor growth rates (mean & range) per passage

Passage no.	Growth rate (day^{-1})
1	0.52 (0.32-0.61)
2	0.48 (0.29-0.71)
3	0.48 (0.27-0.49)

In this model, 5 states were defined, corresponding to the three definitions of lung disease, according to the levels of Forced Expiratory Volume in 1 second (FEV_1): mild ($FEV_1 > 70\%$), moderate ($40\% < FEV_1 < 70\%$) and severe ($FEV_1 < 40\%$), lung transplantation, and death (Figure 7.2). It is hypothesized that MSCs will reduce lung function decay and the rate of pulmonary exacerbations. The effectiveness

measure used is quality adjusted life years (QALY), affected by decrements in the utility of the patients by the decreased of FEV_1 [340], and the occurence of Pulmonary Exacerbations (PEx). The MSC therapy will be administered once a year. The wholesale price is calculated from the costs of goods determined by the bioprocess model, assuming that CoG are 20% of the final reimbursement price. This value is derived from the estimates of current CoG and reimbursement price in the United States of Chimeric Antigen Receptor T-Cells (CAR-T) therapies [342]. Finally, in order to account for differences in inpatient and outpatient procedures, different hospital markups in the prices of the MSC infusion are applied on top of the reimbursement price. In agreement with markups considered for a recent analysis on the inpatient and outpatient administration of CAR-T therapies, an hospital markup of 76% will be added if the MSC are administered through an inpatient procedure, while a markup of 28% is considered for an outpatient procedure [122]. The key modeling inputs and assumptions are depicted in Tables 7.4 - 7.5.

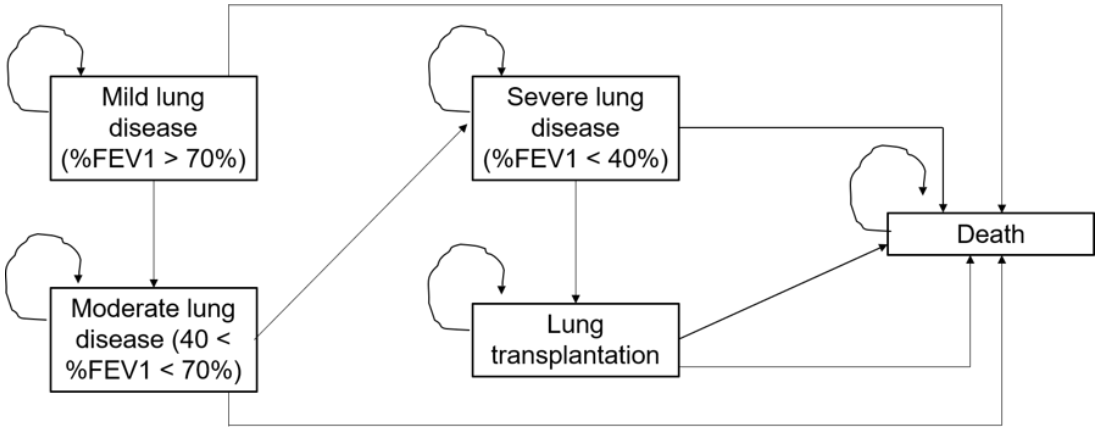

Figure 7.2: Disease state model of cystic fibrosis, with or without MSC infusion. Modified from [339].

7.3 Results

7.3.1 Bioprocess Economics

In order to supply enough cells, after 3 passages, for two patients/batch, an initial number of 5 million MCB cells is seeded in the first passage to obtain two final doses of 1 million cells/kg, under a distribution of patient weights. This value is increased to 15 million cells for the final doses of 3 million cells/kg and to 25 million cells when the final patient dose is 5 million cells/kg. In average, the cost of goods for each batch of 2 patients increase from $18,704 for the 1 million cells/kg dose to $25,669 for the 5 million cells/kg doses. These values are in agreement with the range of values presented in other works focused on modeling of CoG of MSC manufacturing [275]. These costs are largely dominated by the quality control contribution of $11,300 per batch. Since each batch supplies 2 patients, the CoG/dose per patient range from $9,352 to $12,834, depending on the final dose/kg (Table 7.6). Given that a final price for which CoG are estimated as 20% of the final reimbursement price, prices of the MSC therapy per patient dose are in the range of $46,750 - $64,170. This is the estimated price of the MSC therapy per year that will be administered in the clinical setting to the patients, before the inpatient or outpatient

Table 7.4: Initial states and disease state transition probabilities for the health economics modeling of cystic fibrosis progression.

Parameter	Value	Reference
Initial States		
Initial age	25	[343]
Analysis time span	25 years	This work
% patients, mild	46	[338]
% patients, moderate	36	[338]
% patients, severe	17	[338]
Probabilities (modulator arm)		
Death, baseline	Age-specific, CF population	[344]
Death, post-transplant	Calculated year-wise	[345]
PEx, mild	0.18	Derived from [343] and [340]
PEx, moderate	0.32	Derived from [343] and [340]
PEx, severe	0.38	Derived from [343] and [340]
State transition, 1st year	0	Derived from [340]
Mild to moderate, no PEx (1+ years)	0.015	Derived from [343] and [340]
Moderate to severe, no PEx (1+ years)	0.014	Derived from [343] and [340]
Severe to transplant, no PEx (1+ years)	0.647	[340]
Mild to moderate, with PEx (1+ years)	0.035	Derived from [343] and [340]
Moderate to severe, with PEx (1+ years)	0.031	Derived from [343] and [340]
Severe to transplant, no PEx (1+ years)	0.647	[340]

procedure markups.

7.3.2 Adverse clinical outcomes

Under the baseline scenario of using the modulator therapy only, after the follow up period of 25 years, an estimated 55% of the patients did not survive. Additionally, an estimated 9.6% of the patients underwent transplantation during the follow up period. Furthermore, the prevalence of pulmonary exacerbations is noticeable. On average, each patient had 4.4 years with one or more PEx occurences (Figure 7.3A). A combined reduction of the probability of PEx and the probability of state transition to states with lower quality of life of 10%, enabled by the prospective MSC, has a minor impact on the mortality rate (3% reduction from the modulator only therapy), on the transplantation rate (0.5% reduction) and on the number of years with PEx per patient (average reduction of 0.4 years). An increase of the reduction of the rates of PEx and of disease aggravation to up to 75% reduces the overall mortality to 46% of the cohort. However, the impact of the MSC therapy at these levels of clinical effectiveness would reduce the rate of transplantation in the cohort to 1.5% only, and the average number of years with PEx to

Table 7.5: Key costs and utilities for the health economics modeling of cystic fibrosis progression.

Parameter	Value	Reference
Costs (2016 USD)		
Modulator/year	$285,528	Derived from [340]
Disease management, mild/year	$25,367	[340]
Disease management, moderate/year	$33,462	[340]
Disease management, severe/year	$57,210	[340]
PEx, mild	$48,015	[340]
PEx, moderate	$76,322	[340]
PEx, severe	$109,371	[340]
Lung transplant	$905,191	[340]
Post-transplant, 1st year	$273,665	[340]
Post-transplant, 2+ years	$109,913	[340]
MSC price/year	CoG/dose * 5	Derived from [342]
MSC inpatient markup	72%	[122]
MSC outpatient markup	28%	[122]
	Utilities	
Mild	0.86	[343]
Moderate	0.81	[343]
Severe	0.64	[343]
Post-transplant	0.83	[343]
PEx	-0.17	[343]

Table 7.6: Cost of goods (CoG)/dose of manufacturing of the MSC therapy from 1,000 manufacturing model sample runs.

Dose (10^6 cells/kg)	MSC_i (10^6)	MSC_f (10^6)	Total CoG/batch	Total CoG/patient
1	5	137 (97-199)	$18,704 ($15,520 - $19,686)	$9,352 ($7,760 - $9,843)
3	15	413 (296-590)	$22,270 ($17,031 - $24,325)	$11,135 ($8,515 - $12,162)
5	25	690 (469-981)	$25,669 ($17,903 - $28,789)	$12,834 ($8,951 - $14,394)

1. Therefore, as long as a significant synergistic effect of the MSC therapy with the modulator therapy would be proven, the reduction of mortality and costly adverse clinical outcomes of cystic fibrosis justifies the clinical effectiveness of the MSC therapy.

7.3.3 Cost-effectiveness analysis

On average, after a 25-year follow-up period, the total costs of managing cystic fibrosis per patient are $8,278,795, with an average of 10.71 QALY. The treatment in combination with MSC with 10% additional effectiveness in reduction of PEx and pulmonary decay rates generates, in average, an additional 0.06

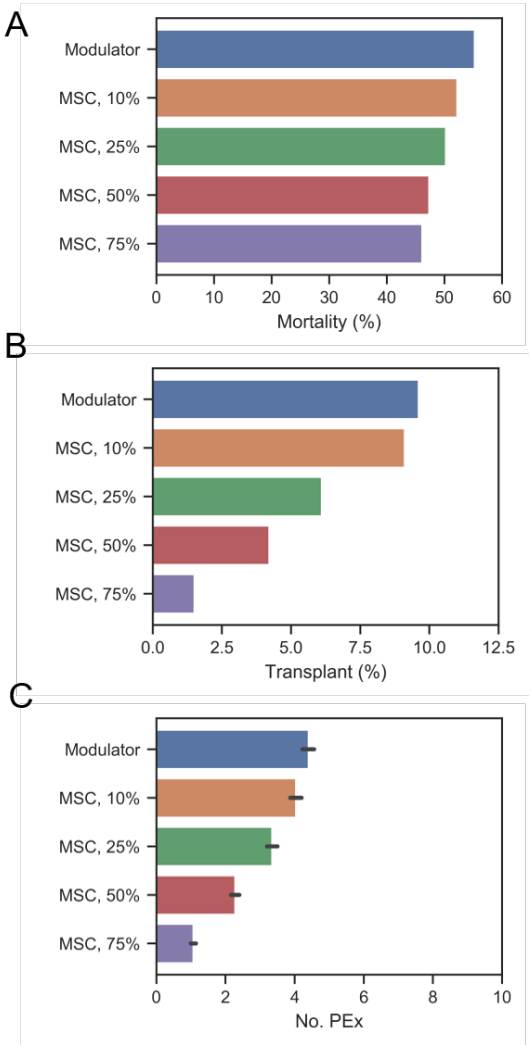

Figure 7.3: Scenario analysis of the reduction of the rate of pulmonary exacerbations (PEx) and state transition associated with the decay of pulmonary function by the MSC therapy in health outcomes for cystic fibrosis (CF) individuals. Mean (with 95% confidence intervals) for the population of 1,000 simulated individuals. A – Mortality rates per therapeutic scheme. B – Population transplantation rates per therapeutic scheme. C – Number of years per patient with, at least, 1 PEx event, per therapeutic scheme.

QALY per patient, a very modest increase at a cost increase per patient of over $2,000,000 for every MSC dose and administration setting. As the effectiveness of MSC as a therapeutic agent increases, an average additional 0.83 QALY are gained per patient with an additional effectiveness of 75%. However, on average, there is not a significant change in the treatment costs with the additional effectiveness, as the disease management costs, per patient, increase between $105,000 and $611,088, depending on the dose and administration regime. It is noticeable that the increase in the costs per MSC dose, as the number of cells per dose increases, for the same clinical effectiveness, leads to an average increase in total costs of approximately $600,000 per patient when the dose of 3 million cells/kg is used over the 1 million cells/kg dose, and an increase of $515,000 when the dose is increased from 3 to 5 million cells/kg. Finally, administration of the therapy in an outpatient setting would provide cost savings between $276,000 and $1,298,000 per patient in comparison with the administration in the inpatient

setting, for the same clinical effectiveness of MSC. However, it is worthwhile noting that there is a very large variability in the cohort, given the significant mortality associated with CF and the different stages of disease per patient at the beginning of the analysis.

Table 7.7: Mean direct medical costs per patient after 25 years of follow-up.

	1 x 10^6 MSC/kg		3 x 10^6 MSC/kg		5 x 10^6 MSC/kg	
	Inpatient	Outpatient	Inpatient	Outpatient	Inpatient	Outpatient
MSC, 10%	$M 10.4	$M 10.1	$M 11.1	$M 10.3	$M 11.7	$M 10.4
MSC, 25%	$M 10.5	$M 9.9	$M 11.2	$M 10.4	$M 11.5	$M 10.9
MSC, 50%	$M 10.8	$M 10.2	$M 11.2	$M 10.4	$M 11.8	$M 11.0
MSC, 75%	$M 10.8	$M 10.2	$M 11.4	$M 11.0	$M 11.9	$M 11.1
Modulator	$M 8.3					

Table 7.8: Mean quality-adusted life years (QALY) per patient after 25 years of follow-up

Therapy	QALY
MSC, 10%	10.77
MSC, 25%	10.98
MSC, 50%	11.37
MSC, 75%	11.54
Modulator	10.71

The average incremental cost-effectiveness ratios (ICER) for all the different configurations (dose, administration setting, and clinical effectiveness) are in the range of 2 – 8 million $/QALY (Figure 7.4). The distribution of ICER in the population have consistently lower values when the administration of the therapy is considered in an outpatient setting. Additionally, there is a trend, for the different clinical effectiveness, of the increase of the cost per QALY with the increase of the number of cells per dose, given that the cell therapy has increased costs. Finally, a trend of reduction of the average cost per QALY is shown when the clinical effectiveness of the MSC therapy is improved, consistent with the finding of higher incremental QALY per patient with the increase of effectiveness.

The dataset shows considerable variability. Therefore, an analysis of the probability of cost effectiveness acceptance per WTP threshold would bring additional insights on how the different factors will affect the possible reimbursement and policy recommendations in the area of cell therapies for cystic fibrosis. In Figure 7.5, it is shown that, while, for a 10% increase of clinical effectiveness when MSC are introduced, the percentage of patients for which the MSC therapy is cost-effective saturates at 51%, an increase of the clinical effectiveness increases this acceptance to a limit of 63% of the population. The change from an inpatient to an outpatient setting does not significantly modify the percentage for which the therapy is cost-effective under, virtually, no budget limitations. The change to an outpatient setting slightly increases the cost-effectiveness acceptance ratio at $1,000,000/QALY from 4.5 to 9.3%.

An estimated 60% of the simulated population showed increased QALY with the administration of

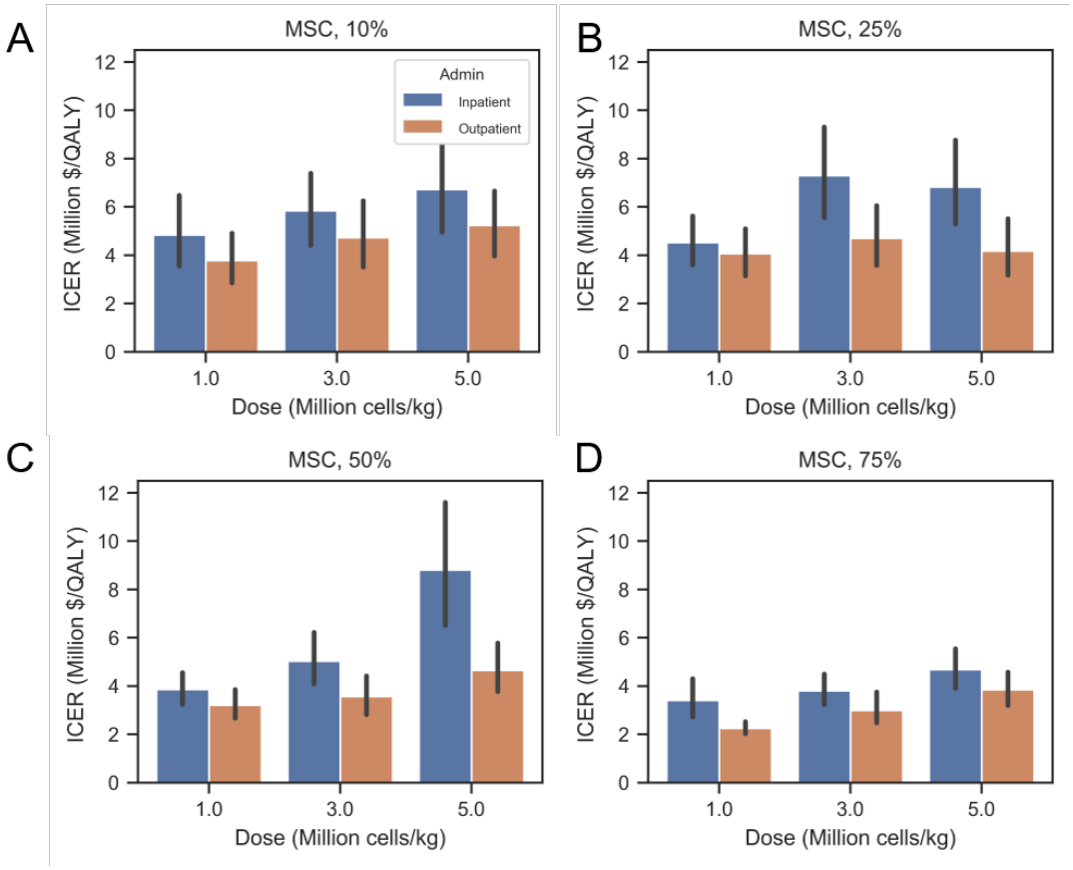

Figure 7.4: Scenario analysis of the reduction of the rate of pulmonary exacerbations (PEx) and state transition associated with the decay of pulmonary function by the MSC therapy on the distribution of incremental cost-effectiveness ratio (ICER) of the MSC based therapy over the modulator only therapy on a cohort of cystic fibrosis (CF) individuals. Mean (with 95% confidence intervals) ICER for the population of 1,000 simulated individuals, accounting for the three MSC doses, and the inpatient vs outpatient setting for a clinical effectiveness of the MSC therapy of 10% (A), 25% (B), 50% (C) and 75% (D).

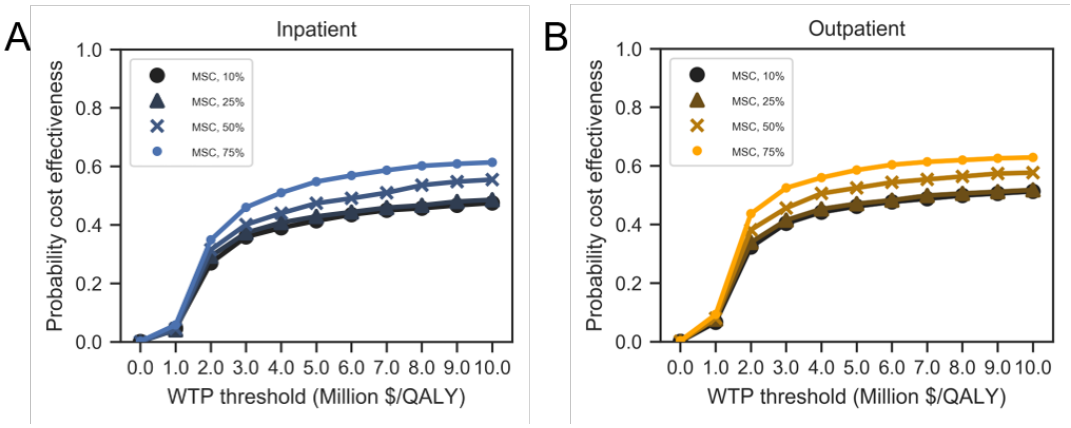

Figure 7.5: Cost-effectiveness acceptance curves for different clinical administration scenarios and clinical effectiveness of the MSC therapy. Probability of cost effectiveness for a therapy with a dose of 1 million cells/kg, simulated for 1,000 individuals, in an inpatient (A) or outpatient (B) setting. Each curve represents a scenario of the reduction of the rate of pulmonary exacerbations (PEx) and state transition associated with the decay of pulmonary function by the MSC therapy from 10 to 75% of the rates of PEx and state transition for the comparator treatment.

the MSC therapy. However, the ICER are much higher than the typically evaluated thresholds of cost-effectiveness (between $25,000-150,000/QALY). Given the average increase in QALY through the lifespan, Table 7.9 shows the unit price per dose that the MSC therapy should have and the manufacturing costs per dosage, assuming CoG of sales and the hospital markup percentages like the baseline scenario. Note that this unit price considers an administration scheme of one MSC infusion per year. The clinical effectiveness and the willingness to pay threshold for reimbursement have a major impact in the allowable unit price, ranging from $3,000 per dose to $124,500 per dose.

Table 7.9: Threshold analysis of allowable MSC unit prices to guarantee cost-effectiveness of the MSC based therapy.

	Unit price to achieve $50,000/QALY	Unit price to achieve $100,000/QALY	Unit price to achieve $150,000/QALY
MSC, 10%	$3,000	$6,000	$9,000
MSC, 25%	$13,500	$27,000	$40,500
MSC, 50%	$33,000	$66,000	$99,000
MSC, 75%	$41,500	$83,000	$124,500

When considering that CoG are 20% of sales and the hospital markups of 76 and 28% for inpatient and outpatient administration, respectively, it is noticeable that some of the unit prices are compatible with the current manufacturing configurations. Given the estimated 95% confidence interval for the manufacturing of doses of 1 million cells/kg, 95% of the manufactured doses would have a CoG below the threshold deemed necessary for cost-effectiveness at $100,000/QALY (outpatient administration with 50% effectiveness of the MSC therapy, or 75% effectiveness of the MSC therapy, irrespective of the administration scheme), and at $150,000/QALY, with a clinical effectiveness of either 50% or 75% in the reduction of PEx and pulmonary function decay rates. In the case that the most effective dose is of 3 million cells/kg, 95% of the manufactured doses would have costs compatible with the 50% effectiveness at $150,000/QALY, outpatient setting, and for 75% effectiveness ($100,000/QALY, outpatient and $150,000/QALY, both settings). Finally, a most effective dose of 5 million cells/kg would only be cost effective at $150,000/QALY if the effectiveness is 50% on an outpatient setting, or for an effectiveness of 75%. While these values provide some cues about the feasibility of the current manufacturing process for cost-effectiveness of the prospective MSC therapy, the fact that a high percentage of reduction of the rates of PEx and pulmonary decay is required and the fact that the QALY outcomes are highly variable in the estimated population cohort elicit the need to identify groups of patients that would benefit the most from this therapy (Table 7.10).

7.4 Discussion

Modulator therapies for cystic fibrosis revolutionized the care for patients with specific CFTR mutations. In the United States, three modulator therapies: Ivacaftor (Kalydeco®), lumacaftor/ivacaftor (Orkambi®) and tezacaftor/ivacaftor (Symdeko®), have been approved as of April 2019 [340]. In combination, these therapies provide treatment for approximately 50% of CF individuals. Two triple combi-

Table 7.10: Threshold analysis of allowable MSC unit prices to guarantee cost-effectiveness of the MSC based therapy.

	$50,000/QALY		$100,000/QALY		$150,000/QALY	
	Inpatient	Outpatient	Inpatient	Outpatient	Inpatient	Outpatient
10%	$340.91	$468.75	$681.82	$937.50	$1,022.73	$1,406.25
25%	$1,534.09	$2,109.38	$3,068.18	$4,218.75	$4,602.27	$6.328.13
50%	$3,750.00	$5,156.25	$7,500.00	$10,312.50	$11,250.00	$15,468.75
75%	$4,715.91	$6,484.38	$9,431.82	$12,968.75	$14,147.73	$19,452.13

nation therapies are currently in clinical trials and showed good safety and efficacy profiles in Phase 2 clinical trials. If these triple combination modulators are approved, 90% of CF patients might benefit from these treatments [346]. While these therapies show noticeable clinical effectiveness through the reduction of the rate of pulmonary exacerbations and reduced rate of decay of pulmonary function, further effectiveness could be reached by better antimicrobial clearance and restoration of healthy epithelium. Mesenchymal stem/stromal cells are hypothesized to have a positive effect on these two fronts after pre-clinical studies showed a positive impact [37, 347]. However, cell therapies have high manufacturing costs that often results in approved therapies with very high costs and that are only cost-effective at a very high effectiveness [122, 342, 275]. The purpose of this study was to perform an early health technology assessment (HTA) of an MSC based therapy for reduced inflammation in CF individuals, under the dose regimes performed at a Phase I clinical trial. In agreement with the clinical trial design, we assumed only adult patients would receive the therapy as a simplification, with yearly MSC infusions for a follow-up period of 25 years. Under varying dose, administration regimes, and clinical effectiveness, the results of our study showed that MSC therapy, upon effectiveness, has the potential of reducing mortality, transplantation rates, and the number of pulmonary exacerbations, coupled with better quality of life outcomes. However, in average, for all the parameter combinations, each additional QALY gained was associated with extremely high costs ($2-8 million). This incremental cost effectiveness ratio (ICER) is well beyond the most common cost-effectiveness thresholds evaluated in the health economics literature in the US ($50,000 - $150,000/QALY) [340, 343, 339, 348, 341].

The disease state model used herein is similar to disease state models used to evaluate the cost-effectiveness of modulator therapies over the best supporting care [340, 343, 339, 348, 341]. All these studies showed that, while the modulator therapies have a considerable increase in QALY, the high cost of these therapies (in the range of $250,000 - $350,000/year per patient) does not allow cost-effectiveness in thresholds between $50,000 - $500,000/QALY [340]. It was estimated that, for the current modulator therapies to be cost-effective in the United States, the list price would need to be reduced to values between 18-58% of the current price [340]. These therapies were approved in the United States and, as of 2017, were prescribed for therapeutic uses for about 60% of the eligible population [349]. The conclusions of our study, comparing MSC + modulators with the modulator only arm, are affected by factors such as the health states of the starting cohort, the low state transition probabilities achieved already with the modulator therapy, and high mortality in the cohort. Furthermore, the model

hereby used assumes a simplified structure [343], where the FEV1% decay with time is not explicitly modeled, in opposition to other literature contributions [340, 343, 339, 348, 341]. Further work could involve exploring specific groups with higher FEV1% decay rates, different age populations, and varying clinical effectiveness of the modulator for a more complete overview of the factors in play.

Under the current manufacturing scheme for the MSC therapy, assuming a fresh product for infusion and doses of 1, 3 or 5 million cells/kg, the costs per dose are in the range of costs obtained for other processes using cell culture flasks for expansion of MSC [275, 301, 5, 30]. These costs are compatible with cost-effectiveness of MSC therapy for patients who have an average QALY gain of 0.8 QALY, or higher, at the thresholds of $100,000/QALY and $150,000/QALY. Such values are obtained when MSC therapies are effective at reducing the rate of PEx and of pulmonary function decay by 50 or 75%, and under the assumption that CoG are 20% of sales and with additional markups for the inpatient and outpatient setting. As the outpatient setting administration results in lower ancillary costs for MSC infusion, ensuring that MSC infusion can be performed, with maintenance of efficacy and supply chain viability, in an outpatient setting, would be ideal. However, reduction of manufacturing costs would enable a solution for less expensive therapies and make cost-effectiveness at $50,000/QALY possible. Since only two doses are produced per batch, reduction of manufacturing costs would be made possible by increasing the number of doses per batch, hence diluting quality control costs over a higher number of doses. Since administration of several fresh infused products simultaneously would be infeasible in small centers, a solution for this would be to generate off-the-shelf, cryopreserved MSC products, at a larger scale, on a centralized facility. However, potency and quality concerns of cryopreserved MSC products need to be addressed before exploring this strategy [350].

While MSC therapies have shown promise in pre-clinical models of cystic fibrosis, the clinical efficacy of MSC therapies in Phase 2 clinical trials for other pulmonary diseases, such as chronic obstructive pulmonary disorder (COPD) and idiopathic pulmonary fibrosis (IPF) have been very limited under the treatment administration regimes investigated in such trials [351, 352, 353]. A recent in vitro study showed that the brochoalveolar lavage fluid (BALF) of patients with CF is detrimental to MSC survival [354]. However, other studies showcased immunomodulatory properties of MSC and MSC extracellular vesicles [355, 37, 347]. A compromise between an ideal administration regime of MSC, or MSC based products for maximum potency and the costs of administration and management of disease under such conditions will provide additional cues for early prediction of cost-effectiveness of MSC therapy.

7.5 Conclusion

Early HTA of MSC therapies for cystic fibrosis, under different conditions of effectiveness, dose regimes, and administration setting, showcased that MSC could be useful, at a 75% additional PEx and pulmonary decay rate reduction from the modulator therapies, to reduce mortality rates, the number of patients requiring transplants in a population, and the number of years where PEx occur. An average increase in QALY of 0.06 – 0.83 per patient is obtained by varying the rate of PEx and pulmonary decay rate from 10 to 75% of the nominal modulator values. However, these values come at average incre-

mental costs of over $2 million. The cohort shows high variability in incremental QALY that is detrimental for the widespread effectiveness of MSC based therapies. However, on average, MSC based therapies, at the current manufacturing paradigm, are priced at values that are consistent with cost effectiveness at willingness to pay thresholds of $100,000/QALY and $150,000/QALY, while ensuring a clinical effectiveness of 50-75% reduction of PEx and pulmonary function decay rates, and assuming an outpatient administration scenario is plausible. These results highlight the need for assessing robustness of clinical effectiveness in cystic fibrosis patients in order to enable cost-effectiveness, while reduction of manufacturing costs could enable cost-effectiveness in more budget constrained scenarios.

This final results chapter showcases the usefulness of TESSEE as a model and framework for early health technology assessment of stem cell therapies in early-stage clinical trials. In this case, the support for cost-effectiveness and economic feasibility of the current manufacturing scenario is limited by the assumption that the therapy would have a very high clinical effectiveness, and that lower numbers of cells per dose would be sufficient to reach this threshold. The reduction of the simulated prices for the MSC therapy, made technical possible by the use of other manufacturing paradigms, would eventually enable cost-effectiveness of the MSC therapy under less optimistic clinical effectiveness scenarios.

This flexible approach can be customized to any other stem cell-based therapies, and contribute for early dialogue between manufacturers and health technology assessment bodies in different countries towards sustainable pricing and reimbursement strategies after a successful clinical trial.

Chapter 8

Conclusions

The work herein presented aims at describing the development of an open source tool for early economic evaluation of stem cell based therapies, accounting for both bioprocess and health economics paradigms. The tool was highly customizable for each of the manufacturing and therapeutic challenges described in this thesis. Furthermore, probabilistic modeling was captured by taking into account donor to donor variability, culture media and expansion technology induced variation in cell growth rates, and the probabilities of suffering from disease related complications with the prospective stem cell therapy in comparison with the standards of care. This tool was developed with the open source programming language Python, allowing for an easy customization and transition for modeling the key components of stem cell bioprocessing and disease modeling, and fast computational times due to the discrete event simulation paradigm. The tool herein described (TESSEE) is available on a public repository on GitHub and licensed for use under the GNU GPL license 3.0.

8.1 Achievements

The usefulness of this tool was demonstrated through customization of operations in different scenarios and commercially and academically relevant case studies using different manufacturing paradigms. First of all, a scale-out autologous manufacturing scheme was modeled, allowing parallel processing of different donors at the same time for more efficient utilization of GMP facilities (Chapter 4). This manufacturing scheme is similar to the allogeneic, just-in-time manufacturing scheme used for modeling a clinical trial involving mesenchymal stem/stromal cells (MSC) for treatment of cystic fibrosis (Chapter 7). Finally, for cost reduction and higher scale of distribution, an allogeneic, scale-up approach was modeled, allowing an efficient cyclic utilization of master cell banks (MCB) and working cell banks (WCB) for maximization of the total number cells per dose derived from a single donor (Chapter 5). These approaches were combined for modeling of manufacturing of differentiated beta cells from pluripotent stem cells for type 1 diabetes (Chapter 6).

Relatively to the process transfer of a more traditional 2D culture for expansion of MSC, supplemented with fetal bovine serum (FBS), human platelet lysate (hPL) was investigated as an alternative.

hPL supplemented media increases the growth rates and number of BM-MSC at confluence per passage. However, this media supplement is currently more expensive than FBS. The analysis in Chapter 4 proved that, for a set of 1000 different simulated donors, with isolation and growth rates sampled from probabilistic distributions derived from experimental data from the literature, hPL allowed for less expensive overall processing of BM-MSC to reach a target dose of 70 million cells per donor. The higher number of cells per passage obtained with hPL supplementation makes less passages necessary to obtain the target dose. This fact has positive consequences on the time dependent manufacturing costs, such as facility and equipment operational costs and depreciation, and labor. Furthermore, the manufacturing of cells with less passages might promote the formulation of therapeutic products with a more primitive multipotency state and the retention of critical quality attributes.

In a culture process with hPL supplementation, a xeno-free process transfer to a 3D manufacturing platform was evaluated for two less invasive sources of MSC: adipose tissue (AT) and umbilical cord matrix (UCM) (Chapter 5). The 3D platform chosen to model was the vertical wheel bioreactor, a new type of stirred bioreactor that uses a vertical wheel impeller (instead of the typical horizontal impellers), aiming at reducing the shear stress and nutrient gradients found with horizontal impellers. Experimental data from the Stem Cell Engineering Research Group (performed by Dr. Diogo Pinto) proved that cell culture in these bioreactors improved the cell density at confluence in comparison with 2D flasks. While the bioreactor platforms are more expensive than traditional culture flasks and have higher culture media requirements, the higher cell yield in the end of a expansion process with the bioreactors drove a reduction of the costs per dose in an allogeneic setting. However, the fact that a higher seeding density is currently required for 3D platforms, due to suboptimal adhesion of MSC in microcarriers, is a factor that needs to be optimized to drive further cost reduction and scalability of 3D culture of MSC in bioreactors.

Aiming at establishing a link between cost effectiveness analysis and bioprocess economics, two clinical challenges were derived to determine what would be a compatible effectiveness and price for reimbursement, under given willingness to pay thresholds. The application of disease state modeling in the stem cell therapy field is underexplored, since there are very few approved therapies based on either MSC or PSC. The developed open source modeling tool allows an easy transition between cost data from the manufacturing perspective and the input of profit margins at reimbursement and the probabilistic modeling of different patients undergoing transition between stages of disease over time.

In order to show the capabilities of the modeling approach to a process with more unit operations, such as the differentiation of pluripotent stem cells into terminally differentiated cells and the inclusion in a device for implantation, bioprocess modeling of pluripotent stem cell derived beta cell manufacturing and the early health technology assessment of a encapsulated device for type 1 diabetes was considered (Chapter 6). While the reported purification yield per process run of differentiated beta cells is low and the simulated manufacturing costs are high (estimated between $163,720 - $427,231 / patient, for a demand/patient of 500 million beta cells per transplant), the therapy could be cost-effective over a long time span due to the prevention of type 1 diabetes complications while improving the quality of life of patients. On the bioprocess side, modeling unveiled the high reprogramming and banking costs, together with low yields of purification of differentiated cells, as cost and yield limiting steps that require additional

technological innovation. On the disease modeling side, for a small subset of patients (2%), despite the high upfront cost of the beta cell loaded device, the therapy is cost saving due to the prevention of end stage renal disease and cost-effective at thresholds of $50,000 and $100,000/QALY for patients suffering from cardiac and neuropathic complications. Therefore, future work on predictive models of clinical complications could effectively direct patient groups toward such an high cost therapy for added value.

Finally, the modeling of a phase 1 clinical trial of a MSC therapy aiming at reducing inflammation in cystic fibrosis patients incorporated uncertainty in both the bioprocess and health economics modeling (Chapter 7). This study aimed at establishing a parameter space in the prospective price of the therapy and its clinical effectiveness. As a proxy to predict clinical effectiveness, rates of reduction of pulmonary exacerbation and pulmonary decay were reduced until 75% of the value of the standard of care. The manufacturing cost of goods of doses of 1, 3 and 5 million cells/kg are within the range of costs determined in chapters 4 and 5. Assuming that the costs of goods are 20% of the final price of the therapy, it was determined that the current manufacturing configuration and price assumption would be compatible with cost-effectiveness at $100,000/QALY. However, the high variability of clinical outcomes (in terms of QALY) limits this assumption. Furthermore, optimization of manufacturing, either by using a cryopreserved product, increasing scale, or adopting new expansion technologies for the cells, would allow cost-effectiveness at stricter willingness to pay thresholds.

The case studies used to demonstrate the applicability of TESSEE as a tool complement the existing contributions in the field of bioprocess and health economics modeling for prospective stem cells. The pre-existing literature in the field addressed industrially relevant case studies for different annual demands of doses, doses per lot, and number of cells per dose, aimed at therapeutic applications or drug screening applications [5, 30, 10, 27, 186, 12, 6, 147]. Our case studies builds from the mentioned studies by placing a specific focus on the impact of biological drivers for process variability, being at the donor, cell source, or process component levels. Additionally, up to date, the framework implemented in this thesis is the first open source model in the field, flexible enough to accomodate other relevant case studies. Relatively to the only study combining bioprocess economics modeling with an explicit disease state model to address long-term cost-effectiveness of a prospective therapy [12], while both this study and Chapter 6 address the application of stem cell-based therapies for Type 1 Diabetes management, the study reported in this thesis adds a more complete bioprocess modeling overview, by addressing key process bottlenecks and cost drivers. Additionally, the long-term cost-effectiveness analysis showcased specific groups of patients for which it is demonstrated that the therapy would be cost-effective by the prevention of specific diabetes complications, suggesting precision and personalized medicine applications of these therapies in clinical development.

While bioprocessing configurations and costs, and the estimated disease progression and long-term cost-effectiveness, are only a few of the factors behind approval, reimbursement, and commercialization of stem cell therapies, taking into account as early as possible parameters related to these factors could inform in strategies and technological innovation that will help bring safer and more affordable stem cell based therapies to the clinic.

8.2 Future Work

The tool and conceptual framework presented in this thesis was well received in academic and industry meetings and conferences. All the discussions involved in this thesis helped devise some suggestions for future work in the development and utilization of the tool. Additionally, a few limitations will be discussed and suggestions for future analyses that could help overcome these issues are herein presented.

8.2.1 Data Collection and Parameter Estimation:

One of the main difficulties when applying this model to literature data was the lack of comprehensive multipassage growth data that would inform about all the parameters necessary to address a full implementation of biological variability: seeding and harvesting densities, time to confluence, number of cells in the beginning of passage, and number of cells after isolation from a given source. When not available, the growth rates were calculated from assumptions on these parameters. For a more comprehensive modeling scenario, isolation data and multipassage growth data from different cell sources, culture media, and expansion platforms should be collected and/or provided in parallel with the modeling work.

The equations used to model cell growth are a simple exponential growth curve. The rationale for using a simple model is related to the inability to find studies with time curves for each expansion passage, for both 2D and 3D platforms. With limited time data points, it was not possible to perform reproducible curve fitting. However, the metabolite concentrations, such as glucose, oxygen, ammonia and lactate influence cell viability and quality. Spatiotemporal data on these metabolite concentrations will help promote a more complete assessment of critical process attributes and how nutrient and shear stress gradients can influence the yield and quality of the cells, and its impact on process costs.

When using random sampling for biological variability for key parameter inputs through the Monte Carlo method in this study, two issues were identified. First, for most of the key input parameters, a triangular distribution was used for simplicity, due to the limited replicates of experiments using the same protocols. Second, the possibility of correlation between the distributions of key process parameters needs to be further addressed. In future studies, the shape of parameter distributions should be investigated, by promoting studies with more experimental data replicates, and estimating a posteriori parameter distributions using Bayesian methods for a more accurate model of real bioprocess data. Including built-in methods for parameter distribution estimation that can derive the distributions from input data would be a desirable feature to make TESSEE a more powerful tool. Additionally, correlations between data from different unit operations need to be addressed.

Relatively to more complete modeling of specific bioprocess unit operations, one of the most solicited issues in future work is a more comprehensive modeling of quality controls. While some quality control assays are not standardized, the definition of quality control costs and rates is modeled simply through a batch failure rate within values reported in the literature and by experts. For different cell sources, types, and bioprocess components, an interesting link to establish would be a relationship between cell dose and quality attributes, in order to optimize the cell doses in a more quantitative manner before a clinical

trial.

8.2.2 Modeling scenarios:

In the health economics models, the bioprocessing of stem cells can be linked to any therapeutic challenge desired by an end-user of this tool. While this analysis was performed using a cost utility analysis, with utilities being addressed as influencing the quality adjusted life years of a patient with the stem cell therapy vs standard of care, QALY have been criticized as a simplistic measurement by different researchers. Therefore, analysis accounting for other measures of effectiveness, such as life years, disability adjusted life years, and number of complications averted, should also be performed. Additionally, this analysis was carried from the payer perspective, accounting only for direct medical costs. Other measures of how valuable a therapy can be also include indirect costs, such as the loss of income due to morbidity of a therapeutic challenge. The inclusion of societal costs in this analysis could enhance the understanding of the impact of stem cell therapies, once approved, in the healthcare systems and patients.

A key limitation of the case studies considered in this thesis is the fact that the cost-effectiveness analyses were performed only from a United States payer perspective. The United States are the country with the highest healthcare expenditure per capita [356]. Additionally, the costs of manufacturing cell therapies have been shown to vary considerably across different manufacturing site locations and countries [342]. The case studies using TESSEE, and the database of GMP facility and health care costs, needs to be updated in further studies to include country-specific preferences.

Stem cell therapies, as high cost and value therapies, are also amenable toward precision and personalized medicine. As budget constraints are always present in the health care budgets, directing the expensive treatments toward the patients that will benefit the most from them is fundamental. The development of predictive models of disease markers and the probability of suffering from certain complications that are avoided by stem cell based therapies will enhance the clinical delivery once the product is approved, but not only. These models, derived from patient registries in real-world data, will help manufacturers have a more precise understanding of the market size and the target groups that should be addressed in clinical trials. These predictive models may also be linked to the tool in the future, using machine learning and artificial intelligence algorithms to extract the key features determining disease progression and risk from medical data.

Furthermore, the relative infancy of the stem cell therapy field results in limited clinical trial and commercial process data for model calibration and validation. The development of the tool took into account suggestions from industry, academic, and medical experts, taking into account regulatory and operational constraints. While the costs of goods from the bioprocess model are within the ranges reported in the literature in the field, the findings from the cost-effectiveness analyses have limited validation at the moment due to the lack of long-term clinical trial efficacy data. Currently, the model inputs are subject to a large number of theoretical assumptions by assuming some costs and efficacy data from analogous therapies. The validation of these findings is dependent on the future availability of this data for specific

clinical challenges and modeling assumptions may need to be refined accordingly.

8.2.3 Tool dissemination:

The utilization of this tool is also connected with the determination of the key process and clinical delivery parameters requiring technological innovation. Therefore, this tool can be used by decision makers to draft science policy proposals and decide on key areas to fund research and development on. Future work is necessary in the societal and policy impact of customizable decision support tools for different therapeutic challenges involving stem cells and other regenerative medicine strategies.

Finally, this tool was developed for open source in order to provide free educational content to everyone who wants to learn more about early health technology assessment and stem cell manufacturing from a cost effectiveness perspective. The promotion of this tool for educational purposes in different settings is also a future goal, targeting academic labs and students at first, while this tool can also be used in commercial settings.

In order to create a community of users of TESSEE for educational purposes, a graphical user interface (GUI) is fundamental to improve the user experience and remove the requirement for minimal programming knowledge. Under the scope of this thesis, the implementation of the models for several case studies was accomplished. However, for dissemination, the development of a GUI is a key future step to be considered.

The creation of a community of stakeholders and users in the fields of regenerative medicine manufacturing and clinical deployment towards cost-effective healthcare in this area is one of the future desired outputs of this thesis. Open source collaborative frameworks in value-based healthcare, such as the Innovation and Value Initiative (IVI) [357], can inspire the development of this community around TESSEE. This open framework can be complemented by lessons of communities of users of frameworks in process modeling, such as Biosolve [358], Simul8 [359], and Arena [360].

List of Publications and Presentations

Articles in Peer-Reviewed Journals:

- C. Bandeiras, J. M. S. Cabral, S. N. Finkelstein, and F. C. Ferreira. Modeling biological and economic uncertainty on cell therapy manufacturing: the choice of culture media supplementation. Regenerative medicine, 13(8):917–933, 2018 [275]
- D. S. Pinto, C. Bandeiras, C.A.V. Rodrigues, M. A. Fuzeta, S-H Jung, R-J Tseng, C-Y Shen, W. Milligan, B. Lee, F. C. Ferreira, C. L. da Silva, J. M. S. Cabral, Expansion of Human Mesenchymal Stem/Stromal Cells in the Vertical-Wheel^{TM} Bioreactor System: An Experimental and Economic Approach. Biotechnology Journal, 14(8):1800716, 2019 [301]
- C. Bandeiras, J. M. S. Cabral, R. A. Gabbay, S. N. Finkelstein, F. C. Ferreira, Bringing stem cell based therapies for type 1 diabetes to the clinic: early insights from bioprocess economics and cost effectiveness analysis, Biotechnology Journal, 14(8):1800563 [304]
- C. Bandeiras, J. M. S. Cabral, A. J. Hwa, R. A. Gabbay, S. N. Finkelstein, F. C. Ferreira, Economics of beta cell replacement therapy, Current Diabetes Reports 19:75, 2019 [361]
- C. Bandeiras, J. Reese Koç, J. F. Chmiel, G. S. Sawicki, J. M. S. Cabral, F. C. Ferreira, S. N. Finkelstein, Bioprocess and early health economic modeling of mesenchymal stem/stromal cells (MSC) as therapeutic agents for cystic fibrosis, Value in Health (in preparation)

Conference proceedings:

- C. Bandeiras, J. M. S. Cabral, S. N. Finkelstein, and F. C. Ferreira. TESSEE - Tool for Early Stem Cell Economic Evaluation, Mediterranean Conference on Medical and Biological Engineering and Computing, 1919-1932 [362]
- C. Bandeiras, J.R. Koc, Y. Ma, M. Samberg, J.M.S. Cabral, S. N. Finkelstein, and F.C. Ferreira. Cost-effectiveness analysis of allogeneic, just-in-time expansion of mesenchymal stem cells with PLUS^{TM} human platelet lysate for a clinical trial. Cytotherapy 20(5), S60 [337]
- C. Bandeiras, C. A. V. Rodrigues, J. M. S. Cabral, F. C. Ferreira, and S. N. Finkelstein. Effects of culture media and suspension expansion technologies in mesenchymal stem cell manufacturing - a computational bioprocess and bioeconomics study. Scale-up and Manufacturing of Cell-based therapies V, January 15-19, San Diego, USA, 2017.

Oral communications:

- C. Bandeiras, J. M. S. Cabral, S. N. Finkelstein, and F. C. Ferreira. A model for bioeconomics of manufacturing of pluripotent stem cell (PSCs) based therapies. ESBES2018 – 12th European Symposium on Biochemical Engineering Sciences, September 9-12, Lisbon, Portugal, 2018.

Poster communications:

- C. Bandeiras, J. M. S. Cabral, S. N. Finkelstein, and F. C. Ferreira. Open-source early health technology assessment in regenerative medicine with TESSEE, IEEE-EMBS International Students Conference (ISC), November 22-24, Magdeburg, Germany, 2019

- C. Bandeiras, J. M. S. Cabral, S. N. Finkelstein, and F. C. Ferreira. TESSEE - Tool for Early Stem Cell Economic Evaluation, 3rd Stem Cell Community Day - Eppendorf, November 21, Cascais, Portugal, 2019

- C. Bandeiras, J. M. S. Cabral, S. N. Finkelstein, and F. C. Ferreira. TESSEE - Tool for Early Stem Cell Economic Evaluation, MEDICON2019 - Mediterranean Conference on Medical and Biological Engineering and Computing, September 26-28, Coimbra, Portugal, 2019 - **Best Student Paper Award**

- C. Bandeiras, TESSEE - Tool for Early Stem Cells Economic Evaluation. Encontro Ciência 2019, July 8-10, Lisbon, Portugal, 2019.

- C. Bandeiras, TESSEE - Tool for Early Stem Cells Economic Evaluation. PhD Open Days - Instituto Superior Tecnico 2019, April 9-10, Lisbon, Portugal, 2019.

- C. Bandeiras, J.R. Koc, Y. Ma, M. Samberg, J.M.S. Cabral, S. N. Finkelstein, and F.C. Ferreira. Cost-effectiveness analysis of allogeneic, just-in-time expansion of mesenchymal stem cells with PLUS human platelet lysate for a clinical trial. ISCT2018 – International Society for Cellular Therapy Annual Meeting, May 2-5, Montreal, Canada, 2018.

- C. Bandeiras, Y. Ma, M. Samberg, J.M.S. Cabral, S. N. Finkelstein, and F.C. Ferreira. Cost-effectiveness analysis analysis of expansion of bone marrow mesenchymal stem cells (BM-MSCs) and adipose stem cells (ASCs) with PLUS^{TM} human platelet lysate (hPL). Bioprocess International 2017, September 25-27, Boston, USA, 2017.

- C. Bandeiras, J.M.S. Cabral, S. N. Finkelstein, and F.C. Ferreira. A comprehensive bioprocess and bioeconomics model for scale-up and scale-out of manufacturing of mesenchymal stem cells (MSCs) based therapies. ISSCR2017 - International Society for Stem Cell Research 2017 Annual Meeting, June 14-17, Boston, USA, 2017.

- C. Bandeiras, C. A. V. Rodrigues, J. M.S. Cabral, F. C. Ferreira, and S. N. Finkelstein. Effects of culture media and suspension expansion technologies in mesenchymal stem cell manufacturing - a computational bioprocess and bioeconomics study. Scale-up and Manufacturing of Cell-based therapies V, January 15-19, San Diego, USA, 2017.

- C. Bandeiras, S. N. Finkelstein, J. M. S. Cabral and F. C. Ferreira. A new model and decision support tool for stem cell manufacturing: bioprocess and bioeconomics perspectives. 2016 MIT Portugal Annual Conference, June 30, Braga, Portugal, 2016.

Editorial and opinion pieces:

- C. Bandeiras, J. M. Cabral, S. N. Finkelstein, and F. C. Ferreira. Logical process designs for stem cell manufacturing: computational support tools for improved cost-effectiveness. RegMedNet, 2017.
- C. Bandeiras, Hunting for computational approaches for stem cells at ISSCR2017. The Niche, 2017

Invited Lectures:

- C. Bandeiras, Early Health Technology Assessment of Stem Cell Therapies: Applications for Type 1 Diabetes, BioMAN Summit 2019, December 11-12, Cambridge, MA, USA, 2019
- C. Bandeiras, Economics of Cell Therapies and Regenerative Medicine, Instituto Superior de Engenharia de Lisboa, April 11, Lisbon, Portugal, 2019
- C. Bandeiras, Stem cell manufacturing for therapeutic development in type 1 diabetes. Principles and Practice of Drug Development (PPDD2018), Massachusetts Institute of Technology, October 24, Cambridge, MA, USA, 2018
- C. Bandeiras, Stem cell bioprocessing and manufacturing - Decision making perspectives. Biomaterials Technology, Instituto Superior Tecnico, December 2, Lisbon, Portugal, 2016

Bibliography

[1] K. Coopman and N. Medcalf. From production to patient: challenges and approaches for delivering cell therapies. StemBook/© The Authors, 2014.

[2] L. Foley and M. Whitaker. Concise review: cell therapies: the route to widespread adoption. *Stem cells translational medicine*, 1(5):438–447, 2012.

[3] T. R. Heathman, A. W. Nienow, M. J. McCall, K. Coopman, B. Kara, and C. J. Hewitt. The translation of cell-based therapies: clinical landscape and manufacturing challenges. *Regenerative medicine*, 10(1):49–64, 2015.

[4] Clinicaltrials.gov. Accessed: 2018-10-18.

[5] A. S. Simaria, S. Hassan, H. Varadaraju, J. Rowley, K. Warren, P. Vanek, and S. S. Farid. Allogeneic cell therapy bioprocess economics and optimization: Single-use cell expansion technologies. *Biotechnology and bioengineering*, 111(1):69–83, 2014.

[6] M. Jenkins, J. Bilsland, T. E. Allsopp, S. V. Ho, and S. S. Farid. Patient-specific hipsc bioprocessing for drug screening: Bioprocess economics and optimisation. *Biochemical engineering journal*, 108:84–97, 2016.

[7] F. Dos Santos, P. Andrade, C. da Silva, and J. Cabral. Scaling-up ex vivo expansion of mesenchymal stem/stromal cells for cellular therapies. In *Mesenchymal Stem Cell Therapy*, pages 1–14. Springer, 2013.

[8] N. M. Mount, S. J. Ward, P. Kefalas, and J. Hyllner. Cell-based therapy technology classifications and translational challenges. *Phil. Trans. R. Soc. B*, 370(1680):20150017, 2015.

[9] C. L. Darkins and C.-F. Mandenius. Design of large-scale manufacturing of induced pluripotent stem cell derived cardiomyocytes. *Chemical Engineering Research and Design*, 92(6):1142–1152, 2014.

[10] S. Hassan, A. S. Simaria, H. Varadaraju, S. Gupta, K. Warren, and S. S. Farid. Allogeneic cell therapy bioprocess economics and optimization: downstream processing decisions. *Regenerative medicine*, 10(5):591–609, 2015.

[11] S. Hassan, H. Huang, K. Warren, B. Mahdavi, D. Smith, S. Jong, and S. S. Farid. Process change evaluation framework for allogeneic cell therapies: impact on drug development and commercialization. *Regenerative medicine*, 11(3):287–305, 2016.

[12] K. Wallner, R. G. Pedroza, I. Awotwe, J. M. Piret, P. A. Senior, A. J. Shapiro, and C. McCabe. Stem cells and beta cell replacement therapy: a prospective health technology assessment study. *BMC endocrine disorders*, 18(1):6, 2018.

[13] C. Bandeiras, C. A. Rodrigues, J. Cabral, F. C. Ferreira, and S. N. Finkelstein. Effects of culture media and suspension expansion technologies in mesenchymal stem cell manufacturing-a computational bioprocess and bioeconomics study. 2017.

[14] M. J. IJzerman, H. Koffijberg, E. Fenwick, and M. Krahn. Emerging use of early health technology assessment in medical product development: a scoping review of the literature. *PharmacoEconomics*, 35(7):727–740, 2017.

[15] B. Jönsson. Bringing in health technology assessment and cost-effectiveness considerations at an early stage of drug development. *Molecular oncology*, 9(5):1025–1033, 2015.

[16] M. J. McCall and D. J. Williams. Developing cell therapies: Enabling cost prediction by value systems modeling to manage developmental risk. *Journal of Commercial Biotechnology*, 19(2), 2013.

[17] C. Pandya, S. Hashmi, N. Khera, M. A. Gertz, A. Dispenzieri, W. Hogan, M. Siddiqui, K. Noyes, and S. K. Kumar. Cost-effectiveness analysis of early vs. late autologous stem cell transplantation in multiple myeloma. *Clinical transplantation*, 28(10):1084–1091, 2014.

[18] K. Schulman, E. Stadtmauer, S. Reed, H. Glick, L. Goldstein, J. Pines, J. Jackman, S. Suzuki, M. Styler, P. Crilley, et al. Economic analysis of conventional-dose chemotherapy compared with high-dose chemotherapy plus autologous hematopoietic stem-cell transplantation for metastatic breast cancer. *Bone marrow transplantation*, 31(3):205, 2003.

[19] P. R. Archibald and D. J. Williams. Using the cost–effectiveness of allogeneic islet transplantation to inform induced pluripotent stem cell-derived β-cell therapy reimbursement. *Regenerative medicine*, 10(8):959–973, 2015.

[20] E. Hanna, J. Dorey, S. Aballéa, P. Auquier, and M. Toumi. Will stem cells for heart failure be the next sofosbuvir issue? *Value in Health*, 19(7):A656, 2016.

[21] E. J. Culme-Seymour, K. Mason, L. Vallejo-Torres, C. Carvalho, L. Partington, C. Crowley, N. J. Hamilton, E. C. Toll, C. R. Butler, M. J. Elliott, et al. Cost of stem cell-based tissue-engineered airway transplants in the united kingdom: case series. *Tissue Engineering Part A*, 22(3-4):208–213, 2015.

[22] H. McAteer, E. Cosh, G. Freeman, A. Pandit, P. Wood, and R. Lilford. Cost-effectiveness analysis at the development phase of a potential health technology: examples based on tissue engineering

of bladder and urethra. *Journal of tissue engineering and regenerative medicine*, 1(5):343–349, 2007.

[23] T. S. de Windt, J. C. Sorel, L. A. Vonk, M. M. Kip, M. J. Ijzerman, and D. B. Saris. Early health economic modelling of single-stage cartilage repair. guiding implementation of technologies in regenerative medicine. *Journal of tissue engineering and regenerative medicine*, 11(10):2950–2959, 2017.

[24] M. J. IJzerman, T. Wissing, E. de Koning, and D. Stamatialis. Early health economic evaluation of bioartificial organs: Involving users in the design of the bioartificial pancreas for diabetes. In *Biomedical Membranes And (Bio) artificial Organs*. World Scientific, 2017.

[25] K. Thavorn, S. Van Katwyk, M. Krahn, D. Coyle, and L. McIntyre. The early bird catches the worm: Measuring the potential value of mesenchymal stem cells therapy for septic shock using the early health economic evaluation. *Value in Health*, 20(9):A799–A800, 2017.

[26] A. Nagpal, R. Milte, S. W. Kim, S. Hillier, M. A. Hamilton-Bruce, J. Ratcliffe, and S. A. Koblar. Economic evaluation of stem cell therapies in neurological diseases: a systematic review. *Value in Health*, 2018.

[27] T. D. P. Chilima, F. Moncaubeig, and S. S. Farid. Impact of allogeneic stem cell manufacturing decisions on cost of goods, process robustness and reimbursement. *Biochemical Engineering Journal*, 2018.

[28] T. P. Chilima, T. Bovy, and S. Farid. Designing the optimal manufacturing strategy for an adherent allogeneic cell therapy. *Bioprocess Int*, 14:24–32, 2016.

[29] A. G. Lopes, A. Sinclair, and B. Frohlich. Cost analysis of cell therapy manufacture: Autologous cell therapies, part 2. *BioProcess Int*, 16(3), 2018.

[30] A. Mizukami, T. D. P. Chilima, M. D. Orellana, M. A. Neto, D. T. Covas, S. S. Farid, and K. Swiech. Technologies for large-scale umbilical cord-derived msc expansion: Experimental performance and cost of goods analysis. *Biochemical Engineering Journal*, 135:36–48, 2018.

[31] B. Lee, Y. Hashimura, S. Jung, and R. Wesselschmidt. Scale up of pluripotent stem cell cultivation and directed differentiation in a novel single-use bioreactor system. *Cytotherapy*, 20(5):S93, 2018.

[32] X. Yuan, A.-C. Tsai, I. Farrance, J. A. Rowley, and T. Ma. Aggregation of culture expanded human mesenchymal stem cells in microcarrier-based bioreactor. *Biochemical engineering journal*, 131: 39–46, 2018.

[33] C. A. Rodrigues, T. P. Silva, D. E. Nogueira, T. G. Fernandes, Y. Hashimura, R. Wesselschmidt, M. M. Diogo, B. Lee, and J. M. Cabral. Scalable culture of human induced pluripotent cells on microcarriers under xeno-free conditions using single-use vertical-wheel^{TM} bioreactors. *Journal of Chemical Technology & Biotechnology*.

[34] G. Iskrov, S. Dermendzhiev, T. Miteva-Katrandzhieva, and R. Stefanov. Health economic data in reimbursement of new medical technologies: importance of the socio-economic burden as a decision-making criterion. *Frontiers in pharmacology*, 7:252, 2016.

[35] M. Flume, M. Bardou, S. Capri, O. Sola-Morales, D. Cunningham, L.-A. Levin, M. J. Postma, and N. Touchot. Approaches to manage 'affordability'of high budget impact medicines in key eu countries. *Journal of market access & health policy*, 6(1):1478539, 2018.

[36] P. J. Neumann and G. D. Sanders. Cost-effectiveness analysis 2.0. *N Engl J Med*, 376(3):203–5, 2017.

[37] M. T. Sutton, D. Fletcher, S. K. Ghosh, A. Weinberg, R. Van Heeckeren, S. Kaur, Z. Sadeghi, A. Hijaz, J. Reese, H. M. Lazarus, et al. Antimicrobial properties of mesenchymal stem cells: therapeutic potential for cystic fibrosis infection, and treatment. *Stem cells international*, 2016, 2016.

[38] S. Kent, F. Becker, T. Feenstra, A. Tran-Duy, I. Schlackow, M. Tew, P. Zhang, W. Ye, S. Lizheng, W. Herman, et al. The challenge of transparency and validation in health economic decision modelling: a view from mount hood. *Pharmacoeconomics*, pages 1–8, 2019.

[39] J. T. Cohen, P. J. Neumann, and J. B. Wong. A call for open-source cost-effectiveness analysis. *Annals of internal medicine*, 167(6):432–433, 2017.

[40] Y. Avior, I. Sagi, and N. Benvenisty. Pluripotent stem cells in disease modelling and drug discovery. *Nature reviews Molecular cell biology*, 17(3):170, 2016.

[41] M. P. Lutolf, P. M. Gilbert, and H. M. Blau. Designing materials to direct stem-cell fate. *Nature*, 462(7272):433, 2009.

[42] J. L. Sterneckert, P. Reinhardt, and H. R. Schöler. Investigating human disease using stem cell models. *Nature Reviews Genetics*, 15(9):625, 2014.

[43] H. Hui, Y. Tang, M. Hu, and X. Zhao. Stem cells: general features and characteristics. In *Stem Cells in Clinic and Research*. InTech, 2011.

[44] R. S. Mahla. Stem cells applications in regenerative medicine and disease therapeutics. *International journal of cell biology*, 2016, 2016.

[45] N. Malik. Allogeneic versus autologous stem-cell therapy. *BioPharm International*, 25(7):36–40, 2012.

[46] P. Hourd, A. Chandra, N. Medcalf, and D. J. Williams. Regulatory challenges for the manufacture and scale-out of autologous cell therapies. In *StemBook [Internet]*. Harvard Stem Cell Institute, 2014.

[47] Q. A. Rafiq, K. Coopman, and C. J. Hewitt. Scale-up of human mesenchymal stem cell culture: current technologies and future challenges. *Current Opinion in Chemical Engineering*, 2(1):8–16, 2013.

[48] A. Trounson and N. D. DeWitt. Pluripotent stem cells progressing to the clinic. *Nature reviews Molecular cell biology*, 17(3):194, 2016.

[49] N. Escacena, E. Quesada-Hernández, V. Capilla-Gonzalez, B. Soria, and A. Hmadcha. Bottlenecks in the efficient use of advanced therapy medicinal products based on mesenchymal stromal cells. *Stem cells international*, 2015, 2015.

[50] D. Niederwieser, H. Baldomero, J. Szer, M. Gratwohl, M. Aljurf, Y. Atsuta, L. F. Bouzas, D. Confer, H. Greinix, M. Horowitz, et al. Hematopoietic stem cell transplantation activity worldwide in 2012 and a swot analysis of the worldwide network for blood and marrow transplantation group including the global survey. *Bone marrow transplantation*, 51(6):778, 2016.

[51] J.-W. Lee, S.-H. Lee, Y.-J. Youn, M.-S. Ahn, J.-Y. Kim, B.-S. Yoo, J. Yoon, W. Kwon, I.-S. Hong, K. Lee, et al. A randomized, open-label, multicenter trial for the safety and efficacy of adult mesenchymal stem cells after acute myocardial infarction. *Journal of Korean medical science*, 29 (1):23–31, 2014.

[52] Y.-B. Park, C.-W. Ha, C.-H. Lee, Y. C. Yoon, and Y.-G. Park. Cartilage regeneration in osteoarthritic patients by a composite of allogeneic umbilical cord blood-derived mesenchymal stem cells and hyaluronate hydrogel: Results from a clinical trial for safety and proof-of-concept with 7 years of extended follow-up. *Stem cells translational medicine*, 6(2):613–621, 2017.

[53] P. Hourd, P. Ginty, A. Chandra, and D. J. Williams. Manufacturing models permitting roll out/scale out of clinically led autologous cell therapies: regulatory and scientific challenges for comparability. *Cytotherapy*, 16(8):1033–1047, 2014.

[54] K. Muroi, K. Miyamura, M. Okada, T. Yamashita, M. Murata, T. Ishikawa, N. Uike, M. Hidaka, R. Kobayashi, M. Imamura, et al. Bone marrow-derived mesenchymal stem cells (jr-031) for steroid-refractory grade iii or iv acute graft-versus-host disease: a phase ii/iii study. *International journal of hematology*, 103(2):243–250, 2016.

[55] J. Galipeau and L. Sensébé. Mesenchymal stromal cells: Clinical challenges and therapeutic opportunities. *Cell stem cell*, 22(6):824–833, 2018.

[56] S. Viswanathan, A. Keating, R. Deans, P. Hematti, D. Prockop, D. F. Stroncek, G. Stacey, D. J. Weiss, C. Mason, and M. S. Rao. Soliciting strategies for developing cell-based reference materials to advance mesenchymal stromal cell research and clinical translation. *Stem cells and development*, 23(11):1157–1167, 2014.

[57] D. Ilic and C. Ogilvie. Concise review: Human embryonic stem cells—what have we done? what are we doing? where are we going? *Stem Cells*, 35(1):17–25, 2017.

[58] M. Mandai, A. Watanabe, Y. Kurimoto, Y. Hirami, C. Morinaga, T. Daimon, M. Fujihara, H. Akimaru, N. Sakai, Y. Shibata, et al. Autologous induced stem-cell–derived retinal cells for macular degeneration. *New England Journal of Medicine*, 376(11):1038–1046, 2017.

[59] A. Akabayashi, E. Nakazawa, and N. S. Jecker. Japan must tighten up clinical trial of stem cells for heart failure. *Nature*, 560(7719):431, 2018.

[60] D. Normille. First-of-its-kind clinical trial will use reprogrammed adult stem cells to treat parkinson's. Science. 2018-07-30.

[61] T. Kikuchi, A. Morizane, D. Doi, H. Magotani, H. Onoe, T. Hayashi, H. Mizuma, S. Takara, R. Takahashi, H. Inoue, et al. Human ips cell-derived dopaminergic neurons function in a primate parkinson's disease model. *Nature*, 548(7669):592–596, 2017.

[62] D. Garcia-Olmo and D. A. Schwartz. Cumulative evidence that mesenchymal stem cells promote healing of perianal fistulas of patients with crohn's disease–going from bench to bedside. *Gastroenterology*, 149(4):853–857, 2015.

[63] P.-O. Carlsson, E. Schwarcz, O. Korsgren, and K. Le Blanc. Preserved β-cell function in type 1 diabetes by mesenchymal stromal cells. *Diabetes*, 64(2):587–592, 2015.

[64] V. R. Dasari, K. K. Veeravalli, and D. H. Dinh. Mesenchymal stem cells in the treatment of spinal cord injuries: A review. *World journal of stem cells*, 6(2):120, 2014.

[65] D. Karussis, C. Karageorgiou, A. Vaknin-Dembinsky, B. Gowda-Kurkalli, J. M. Gomori, I. Kassis, J. W. Bulte, P. Petrou, T. Ben-Hur, O. Abramsky, et al. Safety and immunological effects of mesenchymal stem cell transplantation in patients with multiple sclerosis and amyotrophic lateral sclerosis. *Archives of neurology*, 67(10):1187–1194, 2010.

[66] H. J. Kim, S. W. Seo, J. W. Chang, J. I. Lee, C. H. Kim, J. Chin, S. J. Choi, H. Kwon, H. J. Yun, J. M. Lee, et al. Stereotactic brain injection of human umbilical cord blood mesenchymal stem cells in patients with alzheimer's disease dementia: a phase 1 clinical trial. *Alzheimer's & Dementia: Translational Research & Clinical Interventions*, 1(2):95–102, 2015.

[67] N. K. Venkataramana, S. K. Kumar, S. Balaraju, R. C. Radhakrishnan, A. Bansal, A. Dixit, D. K. Rao, M. Das, M. Jan, P. K. Gupta, et al. Open-labeled study of unilateral autologous bone-marrow-derived mesenchymal stem cell transplantation in parkinson's disease. *Translational Research*, 155(2):62–70, 2010.

[68] T. G. Fernandes and J. M. Cabral. Stem-cell microscale platforms for toxicology screening. *Stem Cells in Birth Defects Research and Developmental Toxicology*, pages 285–308, 2018.

[69] T. Hamazaki, N. El Rouby, N. C. Fredette, K. E. Santostefano, and N. Terada. Concise review: induced pluripotent stem cell research in the era of precision medicine. *Stem Cells*, 35(3):545–550, 2017.

[70] B. Ho, N. Pek, and B.-S. Soh. Disease modeling using 3d organoids derived from human induced pluripotent stem cells. *International journal of molecular sciences*, 19(4):936, 2018.

[71] M. Völkner, M. Zschätzsch, M. Rostovskaya, R. W. Overall, V. Busskamp, K. Anastassiadis, and M. O. Karl. Retinal organoids from pluripotent stem cells efficiently recapitulate retinogenesis. *Stem Cell Reports*, 6(4):525–538, 2016.

[72] R. Morizane, A. Q. Lam, B. S. Freedman, S. Kishi, M. T. Valerius, and J. V. Bonventre. Nephron organoids derived from human pluripotent stem cells model kidney development and injury. *Nature biotechnology*, 33(11):1193, 2015.

[73] M. A. Lancaster and J. A. Knoblich. Generation of cerebral organoids from human pluripotent stem cells. *Nature protocols*, 9(10):2329, 2014.

[74] P. Hoang, J. Wang, B. R. Conklin, K. E. Healy, and Z. Ma. Generation of spatial-patterned early-developing cardiac organoids using human pluripotent stem cells. *Nature protocols*, 13(4):723, 2018.

[75] P. Guye, M. R. Ebrahimkhani, N. Kipniss, J. J. Velazquez, E. Schoenfeld, S. Kiani, L. G. Griffith, and R. Weiss. Genetically engineering self-organization of human pluripotent stem cells into a liver bud-like tissue using gata6. *Nature communications*, 7:10243, 2016.

[76] L. Bruens and H. J. Snippert. Expanding the tissue toolbox: Deriving colon tissue from human pluripotent stem cells. *Cell stem cell*, 21(1):3–5, 2017.

[77] C. Miranda, T. Fernandes, M. Diogo, and J. Cabral. Towards multi-organoid systems for drug screening applications. *Bioengineering*, 5(3):49, 2018.

[78] Research and Markets. The global market for stem cells. 2016.

[79] Markets and Markets. Stem cell therapy market by type (allogeneic, autologous), therapeutic application (musculoskeletal, wound & injury, cvd, surgery, and agvhd), cell source (adipose tissue, bone marrow, neural, embryo/cord blood derived, ipscs) - global forecasts to 2021, . 2016.

[80] G. V. Research. Stem cells market analysis by product (adult stem cells, hesc, induced pluripotent stem cells), by application (regenerative medicine, drug discovery), by technology, by therapy, and segment forecasts, 2018 - 2025, . 2017.

[81] B. Research. Induced pluripotent stem cells: Global markets, . 2017.

[82] Markets and Markets. High throughput screening market by technology (cell-based assays, lab on a chip, bioinformatics), application (target identification, primary screening, toxicology), product (reagent, instruments, software, service), end user - global forecast to 2023, . 2016.

[83] BioInformant. Stem cell research products – opportunities, tools, and technologies. 2016.

[84] A. Elsanhoury, R. Sanzenbacher, P. Reinke, and M. Abou-El-Enein. Accelerating patients' access to advanced therapies in the eu. *Molecular Therapy-Methods & Clinical Development*, 7:15–19, 2017.

[85] D. G. Coppens, M. L. De Bruin, H. G. Leufkens, and J. Hoekman. Global regulatory differences for gene-and cell-based therapies: Consequences and implications for patient access and therapeutic innovation. *Clinical Pharmacology & Therapeutics*, 103(1):120–127, 2018.

[86] S. de Wilde, D. G. Coppens, J. Hoekman, M. L. de Bruin, H. G. Leufkens, H.-J. Guchelaar, and P. Meij. Eu decision-making for marketing authorization of advanced therapy medicinal products: a case study. *Drug discovery today*, 2018.

[87] J. Hoekman, W. Boon, J. Bouvy, H. Ebbers, J. de Jong, and M. De Bruin. Use of the conditional marketing authorization pathway for oncology medicines in europe. *Clinical Pharmacology & Therapeutics*, 98(5):534–541, 2015.

[88] A. Hubert, J. Barry, and C. Vieira. Proposed solutions to further improve the regulatory landscape for atmps in europe.

[89] R. A. Charo and D. Sipp. Rejuvenating regenerative medicine regulation. *New England Journal of Medicine*, 378(6):504–505, 2018.

[90] D. Sipp. Conditional approval: Japan lowers the bar for regenerative medicine products. *Cell Stem Cell*, 16(4):353–356, 2015.

[91] C. McCabe and D. Sipp. Undertested and overpriced: Japan issues first conditional approval of stem cell product. *Cell Stem Cell*, 18(4):436–437, 2016.

[92] J. O. Lim. Regulation policy on cell-and tissue-based therapy products in korea. *Tissue Engineering Part A*, 21(23-24):2791–2796, 2015.

[93] J. A. Smith and D. A. Brindley. Conditional approval pathways: the "special" case of global regenerative medicine regulation, 2017.

[94] D. Y. Wohn. Korea okays stem cell therapies despite limited peer-reviewed data, 2012.

[95] P. J. Neumann, J. T. Cohen, and M. C. Weinstein. Updating cost-effectiveness—the curious resilience of the $50,000-per-qaly threshold. *New England Journal of Medicine*, 371(9):796–797, 2014.

[96] L. Vallejo-Torres, B. García-Lorenzo, I. Castilla, C. Valcárcel-Nazco, L. García-Pérez, R. Linertová, E. Polentinos-Castro, and P. Serrano-Aguilar. On the estimation of the cost-effectiveness threshold: why, what, how? *Value in Health*, 19(5):558–566, 2016.

[97] P. J. Neumann and J. T. Cohen. Qalys in 2018—advantages and concerns. *JAMA*, 2018.

[98] A. I. Caplan, C. Mason, and B. Reeve. The 3rs of cell therapy. *Stem cells translational medicine*, 6(1):17–21, 2017.

[99] J. Jørgensen and P. Kefalas. Reimbursement of licensed cell and gene therapies across the major european healthcare markets. *Journal of market access & health policy*, 3(1):29321, 2015.

[100] M. Abou-El-Enein, A. Elsanhoury, and P. Reinke. Overcoming challenges facing advanced therapies in the eu market. *Cell Stem Cell*, 19(3):293–297, 2016.

[101] L. P. Garrison, T. Jackson, D. Paul, and M. Kenston. Value-based pricing for emerging gene therapies: the economic case for a higher cost-effectiveness threshold. *Journal of managed care & specialty pharmacy*, 25(7):793–799, 2019.

[102] I. Brannon and A. T. Lo Sasso. Properly valuing investment in the development of gene replacement therapy. *Available at SSRN 3373135*, 2019.

[103] Y. Y. Lipsitz, W. D. Milligan, I. Fitzpatrick, E. Stalmeijer, S. S. Farid, K. Y. Tan, D. Smith, R. Perry, J. Carmen, A. Chen, et al. A roadmap for cost-of-goods planning to guide economic production of cell therapy products. *Cytotherapy*, 19(12):1383–1391, 2017.

[104] N. Cuende, J. E. Rasko, M. B. Koh, M. Dominici, and L. Ikonomou. Cell, tissue and gene products with marketing authorization in 2018 worldwide. *Cytotherapy*, 20(11):1401–1413, 2018.

[105] E. Seoane-Vazquez, V. Shukla, and R. Rodriguez-Monguio. Innovation and competition in advanced therapy medicinal products. *EMBO molecular medicine*, 11(3):e9992, 2019.

[106] V. Shukla, E. Seoane-Vazquez, S. Fawaz, L. Brown, and R. Rodriguez-Monguio. The landscape of cellular and gene therapy products: Authorization, discontinuations, and cost. *Human Gene Therapy Clinical Development*, 30(3):102–113, 2019.

[107] A. Shahryari, M. Saghaeian Jazi, S. Mohammadi, H. Razavi Nikoo, Z. Nazari, E. S. Hosseini, I. Burtscher, S. J. Mowla, and H. Lickert. Development and clinical translation of approved gene therapy products for genetic disorders. *Frontiers in Genetics*, 10:868, 2019. ISSN 1664-8021. doi: 10.3389/fgene.2019.00868. URL `https://www.frontiersin.org/article/10.3389/fgene.2019.00868`.

[108] S. Viswanathan and T. Bubela. Current practices and reform proposals for the regulation of advanced medicinal products in canada. *Regenerative medicine*, 10(5):647–663, 2015.

[109] E. Hanna, C. Rémuzat, P. Auquier, and M. Toumi. Gene therapies development: slow progress and promising prospect. *Journal of market access & health policy*, 5(1):1265293, 2017.

[110] R. Grant, M. Curtis, and M. Brown. Planning for commercial scale of cell therapy and regenerative medicine products, part 2: Clinical efficacy, reimbursement, and needle-to-needle logistics. *BioProcess International, Oct*, 2015.

[111] B. P. Dodson and A. D. Levine. Challenges in the translation and commercialization of cell therapies. *BMC biotechnology*, 15(1):70, 2015.

[112] T. Bubela, C. McCabe, P. Archibald, H. Atkins, S. E. Bradshaw, P. Kefalas, M. Mujoomdar, C. Packer, J. Piret, M. Raxworthy, et al. Bringing regenerative medicines to the clinic: the future for regulation and reimbursement. *Regenerative medicine*, 10(7):897–911, 2015.

[113] P. B. Bach. National coverage analysis of car-t therapies—policy, evidence, and payment. *New England Journal of Medicine*, 379(15):1396–1398, 2018.

[114] K. Elverum and M. Whitman. Delivering cellular and gene therapies to patients: solutions for realizing the potential of the next generation of medicine. *Gene therapy*, pages 1–8, 2019.

[115] Going into hospital as an inpatient or outpatient. `https://www.nhs.uk`. Accessed: 2019-11-18.

[116] G. Bai and G. F. Anderson. A more detailed understanding of factors associated with hospital profitability. *Health Affairs*, 35(5):889–897, 2016.

[117] L. N. Newcomer. Those who pay have a say: A view on oncology drug pricing and reimbursement. *The oncologist*, 21(7):779–781, 2016.

[118] M. S. Corbett, A. Webster, R. Hawkins, and N. Woolacott. Innovative regenerative medicines in the eu: a better future in evidence? *BMC medicine*, 15(1):49, 2017.

[119] A. Towse and E. Fenwick. Uncertainty and cures: discontinuation, irreversibility, and outcomes-based payments: what is different about a one-off treatment? *Value in Health*, 22(6):677–683, 2019.

[120] C. Morrison. Fresh from the biotech pipeline—2016, 2017.

[121] A. Yip and R. M. Webster. The market for chimeric antigen receptor t cell therapies. *Nature reviews. Drug discovery*, 17(3):161, 2018.

[122] I. for Clinical and E. Review. Chimeric antigen receptor t-cell therapy for b- cell cancers: Effectiveness and value - final evidence report, . 2018-03-23.

[123] Kymriah secures novel outcomes-based deal in germany. `https://mapbiopharma.com/home/2019/03/kymriah-secures-novel-outcomes-based-deal-in-germany/`, . Accessed: 2019-11-18.

[124] U.s. approves novartis cell therapy for lymphoma. `https://www.reuters.com/article/us-novartis-pharmaceuticals/u-s-approves-novartis-cell-therapy-for-lymphoma-idUSKBN1I24GP`, . Accessed: 2019-11-18.

[125] C. A. for Drugs and T. in Health. Tisagenlecleucel for acute lymphoblastic leukemiaand diffuse large b-cell lymphoma:recommendations, . 2019-01-15.

[126] Novartis leukaemia drug approved in switzerland. `https://www.swissinfo.ch/eng/kymriah_novartis-leukaemia-drug-approved-in-switzerland/44490894`, . Accessed: 2019-11-18.

[127] A. G. M. S. A. Committee. Application no. 1519 – tisagenlecleucel (ctl019) for treatment of refractory cd19-positive leukaemia and lymphoma. 2019-04-15.

[128] Novartis gets approval to sell kymriah in japan for $306,000. https://www.reuters.com/article/us-novartis-kymriah-japan/novartis-gets-approval-to-sell-kymriah-in-japan-for-306000-idUSKCN1SL057, . Accessed: 2019-11-18.

[129] C. A. for Drugs and T. in Health. Axicabtagene ciloleucel for adults with relapsed or refractory large b-cell lymphoma, . 2019-08-15.

[130] P. B. Bach, S. A. Giralt, and L. B. Saltz. Fda approval of tisagenlecleucel: promise and complexities of a $475 000 cancer drug. *Jama*, 318(19):1861–1862, 2017.

[131] R. Rubin. Medicare to cover car t-cell therapies. *Jama*, 322(12):1133–1133, 2019.

[132] N. I. for Health and C. Excellence. Tisagenlecleucel for treating relapsed or refractory diffuse large b-cell lymphoma after 2 or more systemic therapies. 2018-09-19.

[133] P. Kefalas, O. Ali, J. Jørgensen, N. Merryfield, T. Richardson, A. Meads, L. Mungapen, and M. Durdy. Establishing the cost of implementing a performance-based, managed entry agreement for a hypothetical car t-cell therapy. *Journal of market access & health policy*, 6(1):1511679, 2018.

[134] C. Hildreth. Pricing of approved cell therapy products – stem cells, car-t, and more. BioInformant. 2017-10-22.

[135] Alofisel (darvadstrocel) in national health service (nhs) - united kingdom. https://www.sps.nhs.uk/medicines/darvadstrocel/. Accessed: 2018-12-11.

[136] T. T. Yu, P. Gupta, V. Ronfard, A. A. Vertès, and Y. Bayon. Recent progress in european advanced therapy medicinal products and beyond. *Frontiers in bioengineering and biotechnology*, 6, 2018.

[137] Will value-based pricing be a trump card for takeda's alofisel? https://www.pharmaceutical-technology.com/comment/crohns-disease-drug/. Accessed: 2019-11-19.

[138] Japan poised to allow 'reprogrammed' stem-cell therapy for damaged corneas. https://www.nature.com/articles/d41586-019-00860-0, . Accessed: 2019-11-19.

[139] J. Takahashi. Preparing for first human trial of induced pluripotent stem cell-derived cells for parkinson's disease: an interview with jun takahashi. *Regenerative medicine*, 14(2):93–95, 2019.

[140] 'reprogrammed' stem cells approved to mend human hearts for the first time. nature.com/articles/d41586-018-05278-8, . Accessed: 2019-11-19.

[141] P. Senior and J. Pettus. Stem cell therapies for type 1 diabetes: current status and proposed road map to guide successful clinical trials. *Diabetic Medicine*, 2018.

[142] D. Crow. Could ipscs enable “off-the-shelf” cell therapy? *Cell*, 177(7):1667–1669, 2019.

[143] H. M. Blau and G. Q. Daley. Stem cells in the treatment of disease. *New England Journal of Medicine*, 380(18):1748–1760, 2019.

[144] A. Mizukami and K. Swiech. Mesenchymal stromal cells: From discovery to manufacturing and commercialization. *Stem Cells International*, 2018, 2018.

[145] M. J. Jenkins and S. S. Farid. Human pluripotent stem cell-derived products: Advances towards robust, scalable and cost-effective manufacturing strategies. *Biotechnology journal*, 10(1):83–95, 2015.

[146] A. DePalma. Stem cell manufacturing: It’s all about scale. *Genetic Engineering & Biotechnology News*, 38(1):1–22, 2018.

[147] B. D. Weil, M. J. Jenkins, S. Uddin, D. G. Bracewell, D. Wellings, S. S. Farid, and F. Veraitch. An integrated experimental and economic evaluation of cell therapy affinity purification technologies. *Regenerative medicine*, 12(4):397–417, 2017.

[148] M. S. Rao, Y. Pei, T. Y. Garcia, S. Chew, T. Kasai, T. Hisai, H. Taniguchi, T. Takebe, D. A. Lamba, and X. Zeng. Illustrating the potency of current good manufacturing practice–compliant induced pluripotent stem cell lines as a source of multiple cell lineages using standardized protocols. *Cytotherapy*, 20(6):861–872, 2018.

[149] Induced pluripotent stem cell (ipsc) core laboratory - yale stem cell center. `https://medicine.yale.edu/stemcell/coreservices/corelabs/hicore/ipsc/`. Accessed: 2019-11-20.

[150] E. Neofytou, C. G. O’Brien, L. A. Couture, and J. C. Wu. Hurdles to clinical translation of human induced pluripotent stem cells. *The Journal of clinical investigation*, 125(7):2551–2557, 2015.

[151] P. Karagiannis. Clinical potential of induced pluripotent stem cells. In *Medical Applications of iPS Cells*, pages 3–12. Springer, 2019.

[152] C. A. Bravery. Do human leukocyte antigen-typed cellular therapeutics based on induced pluripotent stem cells make commercial sense? *Stem cells and development*, 24(1):1–10, 2014.

[153] Y. Jang, J. Choi, N. Park, J. Kang, M. Kim, Y. Kim, and J. H. Ju. Development of immunocompatible pluripotent stem cells via crispr-based human leukocyte antigen engineering. *Experimental & molecular medicine*, 51(1):3, 2019.

[154] D. C. Kirouac and P. W. Zandstra. The systematic production of cells for cell therapies. *Cell stem cell*, 3(4):369–381, 2008.

[155] L. Sensebé, P. Bourin, and K. Tarte. Good manufacturing practices production of mesenchymal stem/stromal cells. *Human gene therapy*, 22(1):19–26, 2010.

[156] M. J. Jenkins and S. S. Farid. Cost-effective bioprocess design for the manufacture of allogeneic car-t cell therapies using a decisional tool with multi-attribute decision-making analysis. *Biochemical Engineering Journal*, 137:192–204, 2018.

[157] M. S. Inamdar, L. Healy, A. Sinha, and G. Stacey. Global solutions to the challenges of setting up and managing a stem cell laboratory. *Stem Cell Reviews and Reports*, 8(3):830–843, 2012.

[158] D. Holbrook. Controlling contamination: the origins of clean room technology. *History and Technology*, 25(3):173–191, 2009.

[159] M. Abou-El-Enein, G. Bauer, and P. Reinke. The business case for cell and gene therapies. *Nature biotechnology*, 32(12):1192, 2014.

[160] J.-F. Denault, A. Coquet, and V. Dodelet. Construction and start-up costs for biomanufacturing plants. *BioProcess International, Feb*, 2008.

[161] M. R. Placzek, I.-M. Chung, H. M. Macedo, S. Ismail, T. M. Blanco, M. Lim, J. M. Cha, I. Fauzi, Y. Kang, D. C. Yeo, et al. Stem cell bioprocessing: fundamentals and principles. *Journal of the Royal Society interface*, 6(32):209–232, 2009.

[162] A. C. Schnitzler, A. Verma, D. E. Kehoe, D. Jing, J. R. Murrell, K. A. Der, M. Aysola, P. J. Rapiejko, S. Punreddy, and M. S. Rook. Bioprocessing of human mesenchymal stem/stromal cells for therapeutic use: current technologies and challenges. *Biochemical Engineering Journal*, 108:3–13, 2016.

[163] F. dos Santos, A. Campbell, A. Fernandes-Platzgummer, P. Z. Andrade, J. M. Gimble, Y. Wen, S. Boucher, M. C. Vemuri, C. L. da Silva, and J. M. Cabral. A xenogeneic-free bioreactor system for the clinical-scale expansion of human mesenchymal stem/stromal cells. *Biotechnology and Bioengineering*, 111(6):1116–1127, 2014.

[164] Q. A. Rafiq, K. M. Brosnan, K. Coopman, A. W. Nienow, and C. J. Hewitt. Culture of human mesenchymal stem cells on microcarriers in a 5 l stirred-tank bioreactor. *Biotechnology letters*, 35 (8):1233–1245, 2013.

[165] V. Jossen, S. C. Kaiser, C. Schirmaier, J. Herrmann, A. Tappe, D. Eibl, A. Siehoff, C. v. den Bos, and R. Eibl. Modification and qualification of a stirred single-use bioreactor for the improved expansion of human mesenchymal stem cells at benchtop scale. *Pharmaceutical Bioprocessing*, 2(4):311–322, 2014.

[166] T. R. Heathman, A. W. Nienow, Q. A. Rafiq, K. Coopman, B. Kara, and C. J. Hewitt. Agitation and aeration of stirred-bioreactors for the microcarrier culture of human mesenchymal stem cells and potential implications for large-scale bioprocess development. *Biochemical Engineering Journal*, 136:9–17, 2018.

[167] M. J. Osiecki, T. D. Michl, B. K. Babur, M. Kabiri, K. Atkinson, W. B. Lott, H. J. Griesser, and M. R. Doran. Packed bed bioreactor for the isolation and expansion of placental-derived mesenchymal stromal cells. *PloS one*, 10(12):e0144941, 2015.

[168] C. A. Rodrigues, T. G. Fernandes, M. M. Diogo, C. L. da Silva, and J. M. Cabral. Stem cell cultivation in bioreactors. *Biotechnology advances*, 29(6):815–829, 2011.

[169] C. Ikebe and K. Suzuki. Mesenchymal stem cells for regenerative therapy: optimization of cell preparation protocols. *BioMed research international*, 2014, 2014.

[170] G. Chen, D. R. Gulbranson, Z. Hou, J. M. Bolin, V. Ruotti, M. D. Probasco, K. Smuga-Otto, S. E. Howden, N. R. Diol, N. E. Propson, et al. Chemically defined conditions for human ipsc derivation and culture. *Nature methods*, 8(5):424, 2011.

[171] K. G. Chen, B. S. Mallon, R. D. McKay, and P. G. Robey. Human pluripotent stem cell culture: considerations for maintenance, expansion, and therapeutics. *Cell stem cell*, 14(1):13–26, 2014.

[172] C. McKee and G. R. Chaudhry. Advances and challenges in stem cell culture. *Colloids and Surfaces B: Biointerfaces*, 159:62–77, 2017.

[173] B. C. Heng, C. M. Cowan, and S. Basu. Comparison of enzymatic and non-enzymatic means of dissociating adherent monolayers of mesenchymal stem cells. *Biological procedures online*, 11 (1):161, 2009.

[174] K. Tsuji, M. Ojima, K. Otabe, M. Horie, H. Koga, I. Sekiya, and T. Muneta. Effects of different cell-detaching methods on the viability and cell surface antigen expression of synovial mesenchymal stem cells. *Cell transplantation*, 26(6):1089–1102, 2017.

[175] R. Bajpai, J. Lesperance, M. Kim, and A. V. Terskikh. Efficient propagation of single cells accutase-dissociated human embryonic stem cells. *Molecular Reproduction and Development: Incorporating Gamete Research*, 75(5):818–827, 2008.

[176] J. Beers, D. R. Gulbranson, N. George, L. I. Siniscalchi, J. Jones, J. A. Thomson, and G. Chen. Passaging and colony expansion of human pluripotent stem cells by enzyme-free dissociation in chemically defined culture conditions. *Nature protocols*, 7(11):2029, 2012.

[177] R. H. Croze, D. E. Buchholz, M. J. Radeke, W. J. Thi, Q. Hu, P. J. Coffey, and D. O. Clegg. Rock inhibition extends passage of pluripotent stem cell-derived retinal pigmented epithelium. *Stem cells translational medicine*, 3(9):1066–1078, 2014.

[178] X.-S. Yue, M. Fujishiro, C. Nishioka, T. Arai, E. Takahashi, J.-S. Gong, T. Akaike, and Y. Ito. Feeder cells support the culture of induced pluripotent stem cells even after chemical fixation. *PloS one*, 7(3):e32707, 2012.

[179] S. Llames, E. García-Pérez, A. Meana, F. Larcher, and M. del Río. Feeder layer cell actions and applications. *Tissue Engineering Part B: Reviews*, 21(4):345–353, 2015.

[180] G. Yu, Y. Kamano, F. Wang, H. Okawa, H. Yatani, and H. Egusa. Feeder cell sources and feeder-free methods for human ips cell culture. In *Interface Oral Health Science 2014*, pages 145–159. Springer, 2015.

[181] R. L. Wesselschmidt and P. H. Schwartz. The stem cell laboratory: design, equipment, and oversight. In *Human Pluripotent Stem Cells*, pages 3–13. Springer, 2011.

[182] G. M. Rodrigues, C. A. Rodrigues, T. G. Fernandes, M. M. Diogo, and J. M. Cabral. Clinical-scale purification of pluripotent stem cell derivatives for cell-based therapies. *Biotechnology journal*, 10 (8):1103–1114, 2015.

[183] M. Silva, L. Daheron, H. Hurley, K. Bure, R. Barker, A. J. Carr, D. Williams, H.-W. Kim, A. French, P. J. Coffey, et al. Generating ipscs: translating cell reprogramming science into scalable and robust biomanufacturing strategies. *Cell Stem Cell*, 16(1):13–17, 2015.

[184] B. Cunha, C. Peixoto, M. M. Silva, M. J. Carrondo, M. Serra, and P. M. Alves. Filtration methodologies for the clarification and concentration of human mesenchymal stem cells. *Journal of Membrane Science*, 478:117–129, 2015.

[185] V. Jossen, C. van den Bos, R. Eibl, and D. Eibl. Manufacturing human mesenchymal stem cells at clinical scale: process and regulatory challenges. *Applied microbiology and biotechnology*, pages 1–14, 2018.

[186] R. P. Harrison, N. Medcalf, and Q. A. Rafiq. Cell therapy-processing economics: small-scale microfactories as a stepping stone toward large-scale macrofactories. *Regenerative medicine*, 13 (2):159–173, 2018.

[187] R. Haddock, S. Lin-Gibson, N. Lumelsky, R. McFarland, K. Roy, K. Saha, J. Zhang, and C. Zylberberg. Manufacturing cell therapies: the paradigm shift in health care of this century. *National Academy of Medicine*, 2017.

[188] J. Rowley, E. Abraham, A. Campbell, H. Brandwein, and S. Oh. Meeting lot-size challenges of manufacturing adherent cells for therapy. *BioProcess Int*, 10(3):7, 2012.

[189] M. Daniszewski, D. E. Crombie, R. Henderson, H. H. Liang, R. C. Wong, A. W. Hewitt, and A. Pébay. Automated cell culture systems and their applications to human pluripotent stem cell studies. *SLAS TECHNOLOGY: Translating Life Sciences Innovation*, page 2472630317712220, 2017.

[190] S. Sullivan, G. N. Stacey, C. Akazawa, N. Aoyama, R. Baptista, P. Bedford, A. Bennaceur Griscelli, A. Chandra, N. Elwood, M. Girard, et al. Quality control guidelines for clinical-grade human induced pluripotent stem cell lines. *Regenerative medicine*, 13(7):859–866, 2018.

[191] J. J. Bara, R. G. Richards, M. Alini, and M. J. Stoddart. Concise review: Bone marrow-derived mesenchymal stem cells change phenotype following in vitro culture: implications for basic research and the clinic. *Stem cells*, 32(7):1713–1723, 2014.

[192] C. T. Vangsness Jr, H. Sternberg, and L. Harris. Umbilical cord tissue offers the greatest number of harvestable mesenchymal stem cells for research and clinical application: a literature review of different harvest sites. *Arthroscopy: The Journal of Arthroscopic & Related Surgery*, 31(9): 1836–1843, 2015.

[193] M. F. Pittenger. Mesenchymal stem cells from adult bone marrow. In *Mesenchymal Stem Cells*, pages 27–44. Springer, 2008.

[194] L. Xu and G. Li. Circulating mesenchymal stem cells and their clinical implications. *Journal of Orthopaedic Translation*, 2(1):1–7, 2014.

[195] E. M. Fennema, A. J. Renard, A. Leusink, C. A. van Blitterswijk, and J. de Boer. The effect of bone marrow aspiration strategy on the yield and quality of human mesenchymal stem cells. *Acta orthopaedica*, 80(5):618–621, 2009.

[196] U. D. Wankhade, M. Shen, R. Kolhe, and S. Fulzele. Advances in adipose-derived stem cells isolation, characterization, and application in regenerative tissue engineering. *Stem cells international*, 2016, 2016.

[197] B. A. Bunnell, M. Flaat, C. Gagliardi, B. Patel, and C. Ripoll. Adipose-derived stem cells: isolation, expansion and differentiation. *Methods*, 45(2):115–120, 2008.

[198] E. Oberbauer, C. Steffenhagen, C. Wurzer, C. Gabriel, H. Redl, and S. Wolbank. Enzymatic and non-enzymatic isolation systems for adipose tissue-derived cells: current state of the art. *Cell Regeneration*, 4(1):7, 2015.

[199] J. A. Aronowitz, R. A. Lockhart, and C. S. Hakakian. Mechanical versus enzymatic isolation of stromal vascular fraction cells from adipose tissue. *Springerplus*, 4(1):713, 2015.

[200] I. N. Simões, J. S. Boura, F. dos Santos, P. Z. Andrade, C. M. Cardoso, J. M. Gimble, C. L. da Silva, and J. M. Cabral. Human mesenchymal stem cells from the umbilical cord matrix: Successful isolation and ex vivo expansion using serum-/xeno-free culture media. *Biotechnology journal*, 8 (4):448–458, 2013.

[201] J. Hua, J. Gong, H. Meng, B. Xu, L. Yao, M. Qian, Z. He, S. Zou, B. Zhou, and Z. Song. Comparison of different methods for the isolation of mesenchymal stem cells from umbilical cord matrix: proliferation and multilineage differentiation as compared to mesenchymal stem cells from umbilical cord blood and bone marrow. *Cell biology international*, 38(2):198–210, 2014.

[202] P. Swamynathan, P. Venugopal, S. Kannan, C. Thej, U. Kolkundar, S. Bhagwat, M. Ta, A. S. Majumdar, and S. Balasubramanian. Are serum-free and xeno-free culture conditions ideal for large scale clinical grade expansion of wharton's jelly derived mesenchymal stem cells? a comparative study. *Stem cell research & therapy*, 5(4):88, 2014.

[203] G. Guo, F. von Meyenn, F. Santos, Y. Chen, W. Reik, P. Bertone, A. Smith, and J. Nichols. Naive pluripotent stem cells derived directly from isolated cells of the human inner cell mass. *Stem cell reports*, 6(4):437–446, 2016.

[204] F. A. Khan, D. Almohazey, M. Alomari, and S. A. Almofty. Isolation, culture, and functional characterization of human embryonic stem cells: Current trends and challenges. *Stem cells international*, 2018, 2018.

[205] V. K. Singh, M. Kalsan, N. Kumar, A. Saini, and R. Chandra. Induced pluripotent stem cells: applications in regenerative medicine, disease modeling, and drug discovery. *Frontiers in cell and developmental biology*, 3:2, 2015.

[206] D. Hockemeyer and R. Jaenisch. Induced pluripotent stem cells meet genome editing. *Cell stem cell*, 18(5):573–586, 2016.

[207] I. J. Fox, G. Q. Daley, S. A. Goldman, J. Huard, T. J. Kamp, and M. Trucco. Use of differentiated pluripotent stem cells in replacement therapy for treating disease. *Science*, 345(6199):1247391, 2014.

[208] S. Ruiz, A. J. Lopez-Contreras, M. Gabut, R. M. Marion, P. Gutierrez-Martinez, S. Bua, O. Ramirez, I. Olalde, S. Rodrigo-Perez, H. Li, et al. Limiting replication stress during somatic cell reprogramming reduces genomic instability in induced pluripotent stem cells. *Nature communications*, 6: 8036, 2015.

[209] R. Trokovic, J. Weltner, P. Noisa, T. Raivio, and T. Otonkoski. Combined negative effect of donor age and time in culture on the reprogramming efficiency into induced pluripotent stem cells. *Stem cell research*, 15(1):254–262, 2015.

[210] P. Wuchter, K. Bieback, H. Schrezenmeier, M. Bornhäuser, L. P. Müller, H. Bönig, W. Wagner, R. Meisel, P. Pavel, T. Tonn, et al. Standardization of good manufacturing practice–compliant production of bone marrow–derived human mesenchymal stromal cells for immunotherapeutic applications. *Cytotherapy*, 17(2):128–139, 2015.

[211] K. Cooper and C. Viswanathan. Establishment of a mesenchymal stem cell bank. *Stem cells international*, 2011, 2011.

[212] R. Hass, C. Kasper, S. Böhm, and R. Jacobs. Different populations and sources of human mesenchymal stem cells (msc): a comparison of adult and neonatal tissue-derived msc. *Cell Communication and Signaling*, 9(1):12, 2011.

[213] A. Dudakovic, E. Camilleri, S. M. Riester, E. A. Lewallen, S. Kvasha, X. Chen, D. J. Radel, J. M. Anderson, A. A. Nair, J. M. Evans, et al. High-resolution molecular validation of self-renewal and spontaneous differentiation in clinical-grade adipose-tissue derived human mesenchymal stem cells. *Journal of cellular biochemistry*, 115(10):1816–1828, 2014.

[214] H. J. Jin, Y. K. Bae, M. Kim, S.-J. Kwon, H. B. Jeon, S. J. Choi, S. W. Kim, Y. S. Yang, W. Oh, and J. W. Chang. Comparative analysis of human mesenchymal stem cells from bone marrow, adipose tissue, and umbilical cord blood as sources of cell therapy. *International journal of molecular sciences*, 14(9):17986–18001, 2013.

[215] C. Siciliano, M. Ibrahim, G. Scafetta, C. Napoletano, G. Mangino, L. Pierelli, G. Frati, and E. De Falco. Optimization of the isolation and expansion method of human mediastinal–adipose tissue derived mesenchymal stem cells with virally inactivated gmp-grade platelet lysate. *Cytotechnology*, 67(1):165–174, 2015.

[216] K. Schallmoser, C. Bartmann, E. Rohde, A. Reinisch, K. Kashofer, E. Stadelmeyer, C. Drexler, G. Lanzer, W. Linkesch, and D. Strunk. Human platelet lysate can replace fetal bovine serum for clinical-scale expansion of functional mesenchymal stromal cells. *Transfusion*, 47(8):1436–1446, 2007.

[217] S. Wang, X. Qu, and R. C. Zhao. Clinical applications of mesenchymal stem cells. *Journal of hematology & oncology*, 5(1):19, 2012.

[218] M. Mendicino, A. M. Bailey, K. Wonnacott, R. K. Puri, and S. R. Bauer. Msc-based product characterization for clinical trials: an fda perspective. *Cell stem cell*, 14(2):141–145, 2014.

[219] A. M. de Soure, A. Fernandes-Platzgummer, C. L. da Silva, and J. M. Cabral. Scalable microcarrier-based manufacturing of mesenchymal stem/stromal cells. *Journal of biotechnology*, 236:88–109, 2016.

[220] T. R. Heathman, A. Stolzing, C. Fabian, Q. A. Rafiq, K. Coopman, A. W. Nienow, B. Kara, and C. J. Hewitt. Scalability and process transfer of mesenchymal stromal cell production from monolayer to microcarrier culture using human platelet lysate. *Cytotherapy*, 18(4):523–535, 2016.

[221] R. Krawetz, J. T. Taiani, S. Liu, G. Meng, X. Li, M. S. Kallos, and D. E. Rancourt. Large-scale expansion of pluripotent human embryonic stem cells in stirred-suspension bioreactors. *Optimization*, 2016.

[222] C. Kropp, D. Massai, and R. Zweigerdt. Progress and challenges in large-scale expansion of human pluripotent stem cells. *Process Biochemistry*, 59:244–254, 2017.

[223] C. C. Miranda, T. G. Fernandes, J. F. Pascoal, S. Haupt, O. Brüstle, J. M. Cabral, and M. M. Diogo. Spatial and temporal control of cell aggregation efficiently directs human pluripotent stem cells towards neural commitment. *Biotechnology journal*, 10(10):1612–1624, 2015.

[224] Y. Y. Lipsitz, P. D. Tonge, and P. W. Zandstra. Chemically controlled aggregation of pluripotent stem cells. *Biotechnology and bioengineering*, 2018.

[225] C. A. Rodrigues, M. Branco, D. E. Nogueira, T. P. Silva, A. R. Gomes, M. M. Diogo, and J. M. Cabral. Bioreactors for human pluripotent stem cell expansion and differentiation. In *Bioreactors for Stem Cell Expansion and Differentiation*, pages 25–45. CRC Press, 2018.

[226] B. M. Davis, E. R. Loghin, K. R. Conway, and X. Zhang. Automated closed-system expansion of pluripotent stem cell aggregates in a rocking-motion bioreactor. *SLAS TECHNOLOGY: Translating Life Sciences Innovation*, 23(4):364–373, 2018.

[227] G. Srinivasan, D. Morgan, D. Varun, N. Brookhouser, and D. A. Brafman. An integrated biomanufacturing platform for the large-scale expansion and neuronal differentiation of human pluripotent stem cell-derived neural progenitor cells. *Acta biomaterialia*, 74:168–179, 2018.

[228] S. M. Badenes, T. G. Fernandes, C. S. Cordeiro, S. Boucher, D. Kuninger, M. C. Vemuri, M. M. Diogo, and J. M. Cabral. Defined essential 8^{TM} medium and vitronectin efficiently support scalable xeno-free expansion of human induced pluripotent stem cells in stirred microcarrier culture systems. *PloS one*, 11(3):e0151264, 2016.

[229] A. J. Want, A. W. Nienow, C. J. Hewitt, and K. Coopman. Large-scale expansion and exploitation of pluripotent stem cells for regenerative medicine purposes: beyond the t flask. *Regenerative medicine*, 7(1):71–84, 2012.

[230] A. L. Rodrigues, C. A. Rodrigues, A. R. Gomes, S. F. Vieira, S. M. Badenes, M. M. Diogo, and J. M. Cabral. Dissolvable microcarriers allow scalable expansion and harvesting of human induced pluripotent stem cells under xeno-free conditions. *Biotechnology journal*, page 1800461, 2018.

[231] D. Paull, A. Sevilla, H. Zhou, A. K. Hahn, H. Kim, C. Napolitano, A. Tsankov, L. Shang, K. Krumholz, P. Jagadeesan, et al. Automated, high-throughput derivation, characterization and differentiation of induced pluripotent stem cells. *Nature methods*, 12(9):885, 2015.

[232] S. Ting, A. Chen, S. Reuveny, and S. Oh. An intermittent rocking platform for integrated expansion and differentiation of human pluripotent stem cells to cardiomyocytes in suspended microcarrier cultures. *Stem cell research*, 13(2):202–213, 2014.

[233] H. Kempf, R. Olmer, C. Kropp, M. Rückert, M. Jara-Avaca, D. Robles-Diaz, A. Franke, D. A. Elliott, D. Wojciechowski, M. Fischer, et al. Controlling expansion and cardiomyogenic differentiation of human pluripotent stem cells in scalable suspension culture. *Stem cell reports*, 3(6):1132–1146, 2014.

[234] Y. Zhang, C. Pak, Y. Han, H. Ahlenius, Z. Zhang, S. Chanda, S. Marro, C. Patzke, C. Acuna, J. Covy, et al. Rapid single-step induction of functional neurons from human pluripotent stem cells. *Neuron*, 78(5):785–798, 2013.

[235] J. Chal, M. Oginuma, Z. Al Tanoury, B. Gobert, O. Sumara, A. Hick, F. Bousson, Y. Zidouni, C. Mursch, P. Moncuquet, et al. Differentiation of pluripotent stem cells to muscle fiber to model duchenne muscular dystrophy. *Nature biotechnology*, 33(9):962, 2015.

[236] R. Santos, K. C. Vadodaria, B. N. Jaeger, A. Mei, S. Lefcochilos-Fogelquist, A. P. Mendes, G. Erikson, M. Shokhirev, L. Randolph-Moore, C. Fredlender, et al. Differentiation of inflammation-responsive astrocytes from glial progenitors generated from human induced pluripotent stem cells. *Stem cell reports*, 8(6):1757–1769, 2017.

[237] N. Gunhanlar, G. Shpak, M. Van Der Kroeg, L. Gouty-Colomer, S. T. Munshi, B. Lendemeijer, M. Ghazvini, C. Dupont, W. Hoogendijk, J. Gribnau, et al. A simplified protocol for differentiation of electrophysiologically mature neuronal networks from human induced pluripotent stem cells. *Molecular psychiatry*, 2017.

[238] T. P. Dias, S. N. Pinto, J. I. Santos, T. G. Fernandes, F. Fernandes, M. M. Diogo, M. Prieto, and J. M. Cabral. Biophysical study of human induced pluripotent stem cell-derived cardiomyocyte structural maturation during long-term culture. *Biochemical and biophysical research communications*, 499 (3):611–617, 2018.

[239] G. M. Rodrigues, T. Gaj, M. M. Adil, J. Wahba, A. T. Rao, F. K. Lorbeer, R. U. Kulkarni, M. M. Diogo, J. M. Cabral, E. W. Miller, et al. Defined and scalable differentiation of human oligodendrocyte precursors from pluripotent stem cells in a 3d culture system. *Stem cell reports*, 8(6):1770–1783, 2017.

[240] J. A. Heslop, T. G. Hammond, I. Santeramo, A. Tort Piella, I. Hopp, J. Zhou, R. Baty, E. I. Graziano, B. Proto Marco, A. Caron, et al. Concise review: workshop review: understanding and assessing the risks of stem cell-based therapies. *Stem cells translational medicine*, 4(4):389–400, 2015.

[241] J. J. Cunningham, T. M. Ulbright, M. F. Pera, and L. H. Looijenga. Lessons from human teratomas to guide development of safe stem cell therapies. *Nature biotechnology*, 30(9):849, 2012.

[242] A. S. Lee, C. Tang, M. S. Rao, I. L. Weissman, and J. C. Wu. Tumorigenicity as a clinical hurdle for pluripotent stem cell therapies. *Nature medicine*, 19(8):998, 2013.

[243] Q. A. Rafiq and F. Masri. Downstream processing for cell-based therapies. *BioPharm International*, 30(4), 2017.

[244] B. Cunha, T. Aguiar, M. M. Silva, R. J. Silva, M. F. Sousa, E. Pineda, C. Peixoto, M. J. Carrondo, M. Serra, and P. M. Alves. Exploring continuous and integrated strategies for the up-and downstream processing of human mesenchymal stem cells. *Journal of biotechnology*, 213:97–108, 2015.

[245] N. Willoughby, H. Bock, M. Hoeve, S. Pells, C. Williams, G. McPhee, P. Freile, D. Choudhury, and P. De Sousa. A scalable label-free approach to separate human pluripotent cells from differentiated derivatives. *Biomicrofluidics*, 10(1):014107, 2016.

[246] G. Moll, S. Geißler, R. Catar, L. Ignatowicz, M. J. Hoogduijn, D. Strunk, K. Bieback, and O. Ringdén. Cryopreserved or fresh mesenchymal stromal cells: only a matter of taste or key to unleash the full clinical potential of msc therapy? In *Biobanking and Cryopreservation of Stem Cells*, pages 77–98. Springer, 2016.

[247] K. W. Yong, W. K. Z. Wan Safwani, F. Xu, W. A. B. Wan Abas, J. R. Choi, and B. Pingguan-Murphy. Cryopreservation of human mesenchymal stem cells for clinical applications: current methods and challenges. *Biopreservation and biobanking*, 13(4):231–239, 2015.

[248] T. Lambrechts, M. Sonnaert, J. Schrooten, F. P. Luyten, J.-M. Aerts, and I. Papantoniou. Large-scale mesenchymal stem/stromal cell expansion: a visualization tool for bioprocess comparison. *Tissue Engineering Part B: Reviews*, 22(6):485–498, 2016.

[249] M. Sachidananda, J. Erkoyuncu, D. Steenstra, and S. Michalska. Discrete event simulation modelling for dynamic decision making in biopharmaceutical manufacturing. *Procedia CIRP*, 49:39–44, 2016.

[250] R. Misener, M. C. Allenby, M. Fuentes-Garí, K. Gupta, T. Wiggins, N. Panoskaltsis, E. N. Pistikopoulos, and A. Mantalaris. Stem cell biomanufacturing under uncertainty: a case study in optimizing red blood cell production. *AIChE Journal*, 64(8):3011–3022, 2018.

[251] K. S. Ng, J. A. Smith, M. P. McAteer, B. E. Mead, J. Ware, F. O. Jackson, A. Carter, L. Ferreira, K. Bure, J. A. Rowley, et al. Bioprocess decision support tool for scalable manufacture of extracellular vesicles. *Biotechnology and bioengineering*, 2018.

[252] K. E. Glen, E. A. Cheeseman, A. J. Stacey, and R. J. Thomas. A mechanistic model of erythroblast growth inhibition providing a framework for optimisation of cell therapy manufacturing. *Biochemical Engineering Journal*, 133:28–38, 2018.

[253] R. Rekhi, J. A. Smith, Z. Arshad, M. Roberts, C. Bountra, I. Bingham, K. Bure, and D. A. Brindley. Decision-support tools for monoclonal antibody and cell therapy bioprocessing: Current landscape and development opportunities. *Bioprocess International*, 13(11), 2015.

[254] C. Lam, E. Meinert, A. Alturkistani, A. R. Carter, J. Karp, A. Yang, D. Brindley, and Z. Cui. Decision support tools for regenerative medicine: Systematic review. *Journal of Medical Internet Research*, 20(12):e12448, 2018.

[255] S. Brailsford and N. Hilton. A comparison of discrete event simulation and system dynamics for modelling health care systems. 2001.

[256] B. Jerry. *Discrete event system simulation*. Pearson Education India, 2005.

[257] N. Matloff. Introduction to discrete-event simulation and the simpy language. *Davis, CA. Dept of Computer Science. University of California at Davis. Retrieved on August*, 2(2009), 2008.

[258] J. J. Caro, J. Möller, J. Karnon, J. Stahl, and J. Ishak. *Discrete event simulation for health technology assessment*. Chapman and Hall/CRC, 2015.

[259] L. Stothers. Cost-effectiveness analyses. In *Clinical Research Methods for Surgeons*, pages 283–296. Springer, 2006.

[260] F. A. Sonnenberg and J. R. Beck. Markov models in medical decision making: a practical guide. *Medical decision making*, 13(4):322–338, 1993.

[261] University of birmingham: Introduction to decision modeling. `https://www.economicsnetwork.ac.uk`. Accessed: 2019-11-22.

[262] M. C. Weinstein, J. E. Siegel, M. R. Gold, M. S. Kamlet, and L. B. Russell. Recommendations of the panel on cost-effectiveness in health and medicine. *Jama*, 276(15):1253–1258, 1996.

[263] G. D. Sanders, P. J. Neumann, A. Basu, D. W. Brock, D. Feeny, M. Krahn, K. M. Kuntz, D. O. Meltzer, D. K. Owens, L. A. Prosser, et al. Recommendations for conduct, methodological practices, and reporting of cost-effectiveness analyses: second panel on cost-effectiveness in health and medicine. *Jama*, 316(10):1093–1103, 2016.

[264] M. Sculpher. Quality-adjusted life years (qalys) – help or hindrance in supporting health care decision making?, 2015.

[265] A. J. Wailoo, M. Hernandez-Alava, A. Manca, A. Mejia, J. Ray, B. Crawford, M. Botteman, and J. Busschbach. Mapping to estimate health-state utility from non–preference-based outcome measures: an ispor good practices for outcomes research task force report. *Value in Health*, 20(1):18–27, 2017.

[266] A. Beresniak. Are qalys a relevant and justifiable outcome measure for health economic evaluations?, 2015.

[267] A. Beresniak, A. Medina-Lara, J. P. Auray, A. De Wever, J.-C. Praet, R. Tarricone, A. Torbica, D. Dupont, M. Lamure, and G. Duru. Validation of the underlying assumptions of the quality-adjusted life-years outcome: results from the echoutcome european project. *Pharmacoeconomics*, 33(1):61–69, 2015.

[268] D. S. Shepard. Cost-effectiveness in health and medicine. by mr gold, je siegel, lb russell, and mc weinstein (eds). new york: Oxford university press, 1996. *The journal of mental health policy and economics*, 2(2):91–92, 1999.

[269] J. Novais, N. Titchener-Hooker, and M. Hoare. Economic comparison between conventional and disposables-based technology for the production of biopharmaceuticals. *Biotechnology and bioengineering*, 75(2):143–153, 2001.

[270] M. A. El-Enein. *The Economics of Manufacturing Clinical-grade Advanced Therapy Medicinal Products (ATMPs)*. PhD thesis, Medizinische Fakultät Charité-Universitätsmedizin Berlin, 2014.

[271] T. C. Schulz, H. Y. Young, A. D. Agulnick, M. J. Babin, E. E. Baetge, A. G. Bang, A. Bhoumik, I. Cepa, R. M. Cesario, C. Haakmeester, et al. A scalable system for production of functional pancreatic progenitors from human embryonic stem cells. *PloS one*, 7(5):e37004, 2012.

[272] F. Dos Santos, P. Z. Andrade, J. S. Boura, M. M. Abecasis, C. L. Da Silva, and J. M. Cabral. Ex vivo expansion of human mesenchymal stem cells: a more effective cell proliferation kinetics and metabolism under hypoxia. *Journal of cellular physiology*, 223(1):27–35, 2010.

[273] J. G. Carmelo, A. Fernandes-Platzgummer, M. M. Diogo, C. L. da Silva, and J. M. Cabral. A xeno-free microcarrier-based stirred culture system for the scalable expansion of human mesenchymal

stem/stromal cells isolated from bone marrow and adipose tissue. *Biotechnology journal*, 10(8): 1235–1247, 2015.

[274] G. Higuera, D. Schop, F. Janssen, R. van Dijkhuizen-Radersma, T. van Boxtel, and C. A. van Blitterswijk. Quantifying in vitro growth and metabolism kinetics of human mesenchymal stem cells using a mathematical model. *Tissue Engineering Part A*, 15(9):2653–2663, 2009.

[275] C. Bandeiras, J. M. Cabral, S. N. Finkelstein, and F. C. Ferreira. Modeling biological and economic uncertainty on cell therapy manufacturing: the choice of culture media supplementation. *Regenerative medicine*, 13(8):917–933, 2018.

[276] N. Y. Naung, S. Suttapreyasri, S. Kamolmatyakul, and T. Nuntanaranont. Comparative study of different centrifugation protocols for a density gradient separation media in isolation of osteoprogenitors from bone marrow aspirate. *Journal of oral biology and craniofacial research*, 4(3): 160–168, 2014.

[277] M. Juhl, J. Tratwal, B. Follin, R. H. Søndergaard, M. Kirchhoff, A. Ekblond, J. Kastrup, and M. Haack-Sørensen. Comparison of clinical grade human platelet lysates for cultivation of mesenchymal stromal cells from bone marrow and adipose tissue. *Scandinavian journal of clinical and laboratory investigation*, 76(2):93–104, 2016.

[278] T. R. Heathman, Q. A. Rafiq, A. K. Chan, K. Coopman, A. W. Nienow, B. Kara, and C. J. Hewitt. Characterization of human mesenchymal stem cells from multiple donors and the implications for large scale bioprocess development. *Biochemical engineering journal*, 108:14–23, 2016.

[279] S. Wakitani, T. Okabe, S. Horibe, T. Mitsuoka, M. Saito, T. Koyama, M. Nawata, K. Tensho, H. Kato, K. Uematsu, et al. Safety of autologous bone marrow-derived mesenchymal stem cell transplantation for cartilage repair in 41 patients with 45 joints followed for up to 11 years and 5 months. *Journal of Tissue Engineering and Regenerative Medicine*, 5(2):146–150, 2011.

[280] Thermo fisher scientific. `https://www.thermofisherhttps://www.thermofisher.com/order/catalog/product/16140071?SID=srch-srp-16140071`. Accessed: 2018-02-01.

[281] Stem cell technologies. `https://www.stemcell.com/human-platelet-lysate.html`. Accessed: 2018-02-01.

[282] M. Baker. Reproducibility: Respect your cells!, 2016.

[283] D. K. Packham, I. R. Fraser, P. G. Kerr, and K. R. Segal. Allogeneic mesenchymal precursor cells (mpc) in diabetic nephropathy: a randomized, placebo-controlled, dose escalation study. *EBioMedicine*, 12:263–269, 2016.

[284] R. T. Maziarz, T. Devos, C. R. Bachier, S. C. Goldstein, J. F. Leis, S. M. Devine, G. Meyers, J. L. Gajewski, J. Maertens, R. J. Deans, et al. Single and multiple dose multistem (multipotent adult progenitor cell) therapy prophylaxis of acute graft-versus-host disease in myeloablative allogeneic

hematopoietic cell transplantation: a phase 1 trial. *Biology of Blood and Marrow Transplantation*, 21(4):720–728, 2015.

[285] V. Turinetto, E. Vitale, and C. Giachino. Senescence in human mesenchymal stem cells: functional changes and implications in stem cell-based therapy. *International journal of molecular sciences*, 17(7):1164, 2016.

[286] T. R. Heathman, A. Stolzing, C. Fabian, Q. A. Rafiq, K. Coopman, A. W. Nienow, B. Kara, and C. J. Hewitt. Serum-free process development: improving the yield and consistency of human mesenchymal stromal cell production. *Cytotherapy*, 17(11):1524–1535, 2015.

[287] S. Castiglia, K. Mareschi, L. Labanca, G. Lucania, M. Leone, F. Sanavio, L. Castello, D. Rustichelli, E. Signorino, M. Gunetti, et al. Inactivated human platelet lysate with psoralen: a new perspective for mesenchymal stromal cell production in good manufacturing practice conditions. *Cytotherapy*, 16(6):750–763, 2014.

[288] J. Pierce, E. Benedetti, A. Preslar, P. Jacobson, P. Jin, D. F. Stroncek, and J.-a. Reems. Comparative analyses of industrial-scale human platelet lysate preparations. *Transfusion*, 57(12):2858–2869, 2017.

[289] E. Fernandez-Rebollo, B. Mentrup, R. Ebert, J. Franzen, G. Abagnale, T. Sieben, A. Ostrowska, P. Hoffmann, P.-F. Roux, B. Rath, et al. Human platelet lysate versus fetal calf serum: these supplements do not select for different mesenchymal stromal cells. *Scientific reports*, 7(1):5132, 2017.

[290] J. Carmen, S. R. Burger, M. McCaman, and J. A. Rowley. Developing assays to address identity, potency, purity and safety: cell characterization in cell therapy process development. *Regenerative medicine*, 7(1):85–100, 2012.

[291] M. Radrizzani, S. Soncin, V. L. Cicero, G. Andriolo, S. Bolis, and L. Turchetto. Quality control assays for clinical-grade human mesenchymal stromal cells: methods for atmp release. In *Mesenchymal Stem Cells*, pages 313–337. Springer, 2016.

[292] V. Becherucci, L. Piccini, S. Casamassima, S. Bisin, V. Gori, F. Gentile, R. Ceccantini, E. De Rienzo, B. Bindi, P. Pavan, et al. Human platelet lysate in mesenchymal stromal cell expansion according to a gmp grade protocol: a cell factory experience. *Stem cell research & therapy*, 9(1):124, 2018.

[293] A. Oikonomopoulos, W. K. Van Deen, A.-R. Manansala, P. N. Lacey, T. A. Tomakili, A. Ziman, and D. W. Hommes. Optimization of human mesenchymal stem cell manufacturing: the effects of animal/xeno-free media. *Scientific reports*, 5:16570, 2015.

[294] H. Abdelrazik, G. M. Spaggiari, L. Chiossone, and L. Moretta. Mesenchymal stem cells expanded in human platelet lysate display a decreased inhibitory capacity on t-and nk-cell proliferation and function. *European journal of immunology*, 41(11):3281–3290, 2011.

[295] A. M. de Soure, A. Fernandes-Platzgummer, F. Moreira, C. Lilaia, S.-H. Liu, C.-P. Ku, Y.-F. Huang, W. Milligan, J. M. Cabral, and C. L. da Silva. Integrated culture platform based on a human platelet lysate supplement for the isolation and scalable manufacturing of umbilical cord matrix-derived mesenchymal stem/stromal cells. *Journal of tissue engineering and regenerative medicine*, 11(5): 1630–1640, 2017.

[296] M. Cimino, R. Gonçalves, C. Barrias, and M. Martins. Xeno-free strategies for safe human mesenchymal stem/stromal cell expansion: supplements and coatings. *Stem cells international*, 2017, 2017.

[297] A. Mizukami, M. S. de Abreu Neto, F. Moreira, A. Fernandes-Platzgummer, Y.-F. Huang, W. Milligan, J. M. Cabral, C. L. da Silva, D. T. Covas, and K. Swiech. A fully-closed and automated hollow fiber bioreactor for clinical-grade manufacturing of human mesenchymal stem/stromal cells. *Stem Cell Reviews and Reports*, 14(1):141–143, 2018.

[298] F. Petry, J. R. Smith, J. Leber, D. Salzig, P. Czermak, and M. L. Weiss. Manufacturing of human umbilical cord mesenchymal stromal cells on microcarriers in a dynamic system for clinical use. *Stem cells international*, 2016, 2016.

[299] S. Jung, A. Sen, L. Rosenberg, and L. A. Behie. Human mesenchymal stem cell culture: rapid and efficient isolation and expansion in a defined serum-free medium. *Journal of tissue engineering and regenerative medicine*, 6(5):391–403, 2012.

[300] S. Gottipamula, K. Ashwin, M. S. Muttigi, S. Kannan, U. Kolkundkar, and R. N. Seetharam. Isolation, expansion and characterization of bone marrow-derived mesenchymal stromal cells in serum-free conditions. *Cell and tissue research*, 356(1):123–135, 2014.

[301] D. de Sousa Pinto, C. Bandeiras, M. de Almeida Fuzeta, C. A. V. Rodrigues, S. Jung, Y. Hashimura, R. J. Tseng, W. Milligan, B. Lee, F. C. Ferreira, C. L. da Silva, and J. M. S. Cabral. [Scalable Manufacturing of Human Mesenchymal Stromal Cells in the Vertical-Wheel^{TM} Bioreactor System: An Experimental and Economic Approach]. *Biotechnol J*, page e1800716, Apr 2019.

[302] S. Jung, K. M. Panchalingam, L. Rosenberg, and L. A. Behie. Ex vivo expansion of human mesenchymal stem cells in defined serum-free media. *Stem cells international*, 2012, 2012.

[303] J. Hupfeld, I. H. Gorr, C. Schwald, N. Beaucamp, K. Wiechmann, K. Kuentzer, R. Huss, B. Rieger, M. Neubauer, and H. Wegmeyer. Modulation of mesenchymal stromal cell characteristics by microcarrier culture in bioreactors. *Biotechnology and bioengineering*, 111(11):2290–2302, 2014.

[304] C. Bandeiras, J. M. S. Cabral, R. A. Gabbay, S. N. Finkelstein, and F. C. Ferreira. Bringing stem cell-based therapies for type 1 diabetes to the clinic: early insights from bioprocess economics and cost-effectiveness analysis. *Biotechnology journal*, page 1800563, 2019.

[305] A. D. Agulnick, D. M. Ambruzs, M. A. Moorman, A. Bhoumik, R. M. Cesario, J. K. Payne, J. R. Kelly, C. Haakmeester, R. Srijemac, A. Z. Wilson, et al. Insulin-producing endocrine cells differentiated

in vitro from human embryonic stem cells function in macroencapsulation devices in vivo. *Stem cells translational medicine*, 4(10):1214–1222, 2015.

[306] V. So, L. Martinson, C. Green, and M. Scott. 3-dimensional large capacity cell encapsulation device, Nov. 25 2014. US Patent D718,468.

[307] J. R. Millman, C. Xie, A. Van Dervort, M. Gürtler, F. W. Pagliuca, and D. A. Melton. Generation of stem cell-derived β-cells from patients with type 1 diabetes. *Nature communications*, 7: ncomms11463, 2016.

[308] F. W. Pagliuca, J. R. Millman, M. Gürtler, M. Segel, A. Van Dervort, J. H. Ryu, Q. P. Peterson, D. Greiner, and D. A. Melton. Generation of functional human pancreatic β cells in vitro. *Cell*, 159 (2):428–439, 2014.

[309] G. A. Martens, V. De Punt, and G. Stangé. Cd99 as surface anchor for human islet endocrine cell purification. *Journal of tissue engineering and regenerative medicine*, 12(1):e171–e176, 2018.

[310] C. Davenport, U. Diekmann, and O. Naujok. A quick and efficient method for the purification of endoderm cells generated from human embryonic stem cells. *JoVE (Journal of Visualized Experiments)*, (109):e53655, 2016.

[311] K. F. Cogger, A. Sinha, F. Sarangi, E. C. McGaugh, D. Saunders, C. Dorrell, S. Mejia-Guerrero, Y. Aghazadeh, J. L. Rourke, R. A. Screaton, et al. Glycoprotein 2 is a specific cell surface marker of human pancreatic progenitors. *Nature communications*, 8(1):331, 2017.

[312] H. Liu, H. Yang, D. Zhu, X. Sui, J. Li, Z. Liang, L. Xu, Z. Chen, A. Yao, L. Zhang, et al. Systematically labeling developmental stage-specific genes for the study of pancreatic β-cell differentiation from human embryonic stem cells. *Cell research*, 24(10):1181, 2014.

[313] T. D. Pereira Chilima. *Decisional Tools for Enabling Successful Manufacture and Commercialisation of Cell Therapy Products*. PhD thesis, UCL (University College London), 2019.

[314] L. Jacquet, E. Stephenson, R. Collins, H. Patel, J. Trussler, R. Al-Bedaery, P. Renwick, C. Ogilvie, R. Vaughan, and D. Ilic. Strategy for the creation of clinical grade hesc line banks that hla-match a target population. *EMBO molecular medicine*, 5(1):10–17, 2013.

[315] C. A. Keever-Taylor, S. M. Devine, R. J. Soiffer, A. Mendizabal, S. Carter, M. C. Pasquini, P. N. Hari, A. Stein, H. M. Lazarus, C. Linker, et al. Characteristics of clinimacs® system cd34-enriched t cell-depleted grafts in a multicenter trial for acute myeloid leukemia-blood and marrow transplant clinical trials network (bmt ctn) protocol 0303. *Biology of Blood and Marrow Transplantation*, 18 (5):690–697, 2012.

[316] J. Beckwith, J. A. Nyman, B. Flanagan, R. Schrover, and H.-J. Schuurman. A health economic analysis of clinical islet transplantation. *Clinical transplantation*, 26(1):23–33, 2012.

[317] K. Wallner, A. J. Shapiro, P. A. Senior, and C. McCabe. Cost effectiveness and value of information analyses of islet cell transplantation in the management of 'unstable'type 1 diabetes mellitus. *BMC endocrine disorders*, 16(1):17, 2016.

[318] J. Zhu, P. Kahn, J. Knudsen, S. N. Mehta, and R. A. Gabbay. Predictive model for estimating the cost of incident diabetes complications. *Diabetes technology & therapeutics*, 18(10):625–634, 2016.

[319] J. Smith-Palmer, J. P. Bae, K. S. Boye, K. Norrbacka, B. Hunt, and W. J. Valentine. Evaluating health-related quality of life in type 1 diabetes: a systematic literature review of utilities for adults with type 1 diabetes. *ClinicoEconomics and outcomes research: CEOR*, 8:559, 2016.

[320] P. McEwan, H. Bennett, J. Fellows, J. Priaulx, and K. Bergenheim. The health economic value of changes in glycaemic control, weight and rates of hypoglycaemia in type 1 diabetes mellitus. *PloS one*, 11(9):e0162441, 2016.

[321] A. Dunn, S. D. Grosse, and S. H. Zuvekas. Adjusting health expenditures for inflation: a review of measures for health services research in the united states. *Health services research*, 53(1): 175–196, 2018.

[322] A. E. Attema, W. B. Brouwer, and K. Claxton. Discounting in economic evaluations. *PharmacoEconomics*, 36(7):745–758, 2018.

[323] D. Care. Economic costs of diabetes in the us in 2017. *Diabetes Care*, 41:917, 2018.

[324] S. Moassesfar, U. Masharani, L. Frassetto, G. Szot, M. Tavakol, P. Stock, and A. Posselt. A comparative analysis of the safety, efficacy, and cost of islet versus pancreas transplantation in nonuremic patients with type 1 diabetes. *American Journal of Transplantation*, 16(2):518–526, 2016.

[325] B. Cunha, R. J. Silva, C. Correia, A. Koshkin, P. M. Alves, M. Serra, C. Peixoto, and M. J. Carrondo. Finding the design space of a filtration-based operation for the concentration of human pluripotent stem cells. *Journal of Membrane Science*, 542:399–407, 2017.

[326] T. Robert, I. De Mesmaeker, G. M. Stangé, K. G. Suenens, Z. Ling, E. J. Kroon, and D. G. Pipeleers. Functional beta cell mass from device-encapsulated hesc-derived pancreatic endoderm achieving metabolic control. *Stem cell reports*, 10(3):739–750, 2018.

[327] C. C. Miranda, T. G. Fernandes, M. M. Diogo, and J. M. Cabral. Scaling up a chemically-defined aggregate-based suspension culture system for neural commitment of human pluripotent stem cells. *Biotechnology journal*, 11(12):1628–1638, 2016.

[328] S. M. Badenes, T. G. Fernandes, C. C. Miranda, A. Pusch-Klein, S. Haupt, C. A. Rodrigues, M. M. Diogo, O. Brüstle, and J. M. Cabral. Long-term expansion of human induced pluripotent stem cells in a microcarrier-based dynamic system. *Journal of Chemical Technology & Biotechnology*, 92 (3):492–503, 2017.

[329] R. Sambathkumar, A. Migliorini, and M. C. Nostro. Pluripotent stem cell-derived pancreatic progenitors and β-like cells for type 1 diabetes treatment. *Physiology*, 33(6):394–402, 2018.

[330] Q. Zhou and D. A. Melton. Pancreas regeneration. *Nature*, 557(7705):351, 2018.

[331] Y. Y. Lipsitz, C. Woodford, T. Yin, J. H. Hanna, and P. W. Zandstra. Modulating cell state to enhance suspension expansion of human pluripotent stem cells. *Proceedings of the National Academy of Sciences*, 115(25):6369–6374, 2018.

[332] H. M. Shahjalal, A. A. Dayem, K. M. Lim, T.-i. Jeon, and S.-G. Cho. Generation of pancreatic β cells for treatment of diabetes: advances and challenges. *Stem cell research & therapy*, 9(1):355, 2018.

[333] D. Ilic. Latest developments in the field of stem cell research and regenerative medicine compiled from publicly available information and press releases from nonacademic institutions 1 january–28 february 28 2018. *Regenerative medicine*, 13(4):361–370, 2018.

[334] A. J. Karter, E. M. Warton, K. J. Lipska, J. D. Ralston, H. H. Moffet, G. G. Jackson, E. S. Huang, and D. R. Miller. Development and validation of a tool to identify patients with type 2 diabetes at high risk of hypoglycemia-related emergency department or hospital use. *JAMA internal medicine*, 177(10):1461–1470, 2017.

[335] K. R. Marino, R. L. Lundberg, A. Jasrotia, L. S. Maranda, M. J. Thompson, B. A. Barton, L. C. Alonso, and B. U. Nwosu. A predictive model for lack of partial clinical remission in new-onset pediatric type 1 diabetes. *PloS one*, 12(5):e0176860, 2017.

[336] Y. Zhong, P.-J. Lin, J. T. Cohen, A. N. Winn, and P. J. Neumann. Cost-utility analyses in diabetes: a systematic review and implications from real-world evidence. *Value in Health*, 18(2):308–314, 2015.

[337] C. Bandeiras, J. Koc, Y. Ma, M. Samberg, S. Finkelstein, and F. Ferreira. Cost effectiveness analysis of allogeneic, just-in-time expansion of mesenchymal stem cells with plus^{TM} human platelet lysate for a clinical trial. *Cytotherapy*, 20(5):S60, 2018.

[338] E. A. Knapp, A. K. Fink, C. H. Goss, A. Sewall, J. Ostrenga, C. Dowd, A. Elbert, K. M. Petren, and B. C. Marshall. The cystic fibrosis foundation patient registry. design and methods of a national observational disease registry. *Annals of the American Thoracic Society*, 13(7):1173–1179, 2016.

[339] P. Dilokthornsakul, M. Patidar, and J. D. Campbell. Forecasting the long-term clinical and economic outcomes of lumacaftor/ivacaftor in cystic fibrosis patients with homozygous phe508del mutation. *Value in Health*, 20(10):1329–1335, 2017.

[340] I. for Clinical and E. Review. Modulator treatments for cystic fibrosis: Effectiveness and value - final evidence report and meeting summary, . 2018-06-07.

[341] P. Whiting, M. Al, L. Burgers, M. Westwood, S. Ryder, M. Hoogendoorn, N. Armstrong, A. Allen, H. Severens, and J. Kleijnen. Ivacaftor for the treatment of patients with cystic fibrosis and the g551d mutation: a systematic review and cost-effectiveness analysis. 2014.

[342] R. P. Harrison, E. Zylberberg, S. Ellison, and B. L. Levine. Chimeric antigen receptor–t cell therapy manufacturing: modelling the effect of offshore production on aggregate cost of goods. *Cytotherapy*, 2019.

[343] D. Sharma, S. Xing, Y.-T. Hung, R. N. Caskey, M. L. Dowell, and D. R. Touchette. Cost-effectiveness analysis of lumacaftor and ivacaftor combination for the treatment of patients with cystic fibrosis in the united states. *Orphanet journal of rare diseases*, 13(1):172, 2018.

[344] T. MacKenzie, A. H. Gifford, K. A. Sabadosa, H. B. Quinton, E. A. Knapp, C. H. Goss, and B. C. Marshall. Longevity of patients with cystic fibrosis in 2000 to 2010 and beyond: survival analysis of the Cystic Fibrosis Foundation patient registry. *Ann. Intern. Med.*, 161(4):233–241, Aug 2014.

[345] A. L. Stephenson, J. Sykes, Y. Berthiaume, L. G. Singer, S. D. Aaron, G. A. Whitmore, and S. Stanojevic. Clinical and demographic factors associated with post-lung transplantation survival in individuals with cystic fibrosis. *J. Heart Lung Transplant.*, 34(9):1139–1145, Sep 2015.

[346] B. W. Ramsey, G. P. Downey, and C. H. Goss. Update in Cystic Fibrosis. *Am. J. Respir. Crit. Care Med.*, Mar 2019.

[347] A. Carbone, R. Zefferino, E. Beccia, V. Casavola, S. Castellani, S. Di Gioia, V. Giannone, M. Seia, A. Angiolillo, C. Colombo, M. Favia, and M. Conese. Gap Junctions Are Involved in the Rescue of CFTR-Dependent Chloride Efflux by Amniotic Mesenchymal Stem Cells in Coculture with Cystic Fibrosis CFBE41o- Cells. *Stem Cells Int*, 2018:1203717, 2018.

[348] P. Dilokthornsakul, R. N. Hansen, and J. D. Campbell. Forecasting US ivacaftor outcomes and cost in cystic fibrosis patients with the G551D mutation. *Eur. Respir. J.*, 47(6):1697–1705, 06 2016.

[349] C. F. Foundation. 2017 patient registry annual data report. 2018-08.

[350] G. Moll, J. J. Alm, L. C. Davies, L. von Bahr, N. Heldring, L. Stenbeck-Funke, O. A. Hamad, R. Hinsch, L. Ignatowicz, M. Locke, H. Lonnies, J. D. Lambris, Y. Teramura, K. Nilsson-Ekdahl, B. Nilsson, and K. Le Blanc. Do cryopreserved mesenchymal stromal cells display impaired immunomodulatory and therapeutic properties? *Stem Cells*, 32(9):2430–2442, Sep 2014.

[351] D. J. Weiss, R. Casaburi, R. Flannery, M. LeRoux-Williams, and D. P. Tashkin. A placebo-controlled, randomized trial of mesenchymal stem cells in COPD. *Chest*, 143(6):1590–1598, Jun 2013.

[352] X. Liu, Q. Fang, and H. Kim. Preclinical Studies of Mesenchymal Stem Cell (MSC) Administration in Chronic Obstructive Pulmonary Disease (COPD): A Systematic Review and Meta-Analysis. *PLoS ONE*, 11(6):e0157099, 2016.

[353] A. Tzouvelekis, R. Toonkel, T. Karampitsakos, K. Medapalli, I. Ninou, V. Aidinis, D. Bouros, and M. K. Glassberg. Mesenchymal Stem Cells for the Treatment of Idiopathic Pulmonary Fibrosis. *Front Med (Lausanne)*, 5:142, 2018.

[354] S. Abreu, J. Dearborn, N. Gasek, C. dos Santos, M. Wargo, P. Rocco, and D. Weiss. Cystic fibrosis bronchoalveolar lavage fluid lead to human mesenchymal stromal cell death. *Cytotherapy*, 20(5): S25–S26, 2018.

[355] A. Zulueta, M. Colombo, V. Peli, M. Falleni, D. Tosi, M. Ricciardi, A. Baisi, G. Bulfamante, R. Chiaramonte, and A. Caretti. Lung mesenchymal stem cells-derived extracellular vesicles attenuate the inflammatory profile of Cystic Fibrosis epithelial cells. *Cell. Signal.*, 51:110–118, Nov 2018.

[356] World health organization global health expenditure database - current health expenditure per capita (current us$). `https://data.worldbank.org/indicator/SH.XPD.CHEX.PC.CD`. Accessed: 2019-12-04.

[357] Ivi - innovation and value initiative. `https://www.thevalueinitiative.org/`. Accessed: 2019-12-04.

[358] Biopharm services - biosolve software. `https://biopharmservices.com/software/`. Accessed: 2019-12-04.

[359] Simul8 simulation software - visual process simulation modeling. `https://www.simul8.com/`. Accessed: 2019-12-04.

[360] Arena simulation software. `https://www.arenasimulation.com/`. Accessed: 2019-12-04.

[361] C. Bandeiras, A. J. Hwa, J. M. Cabral, F. C. Ferreira, S. N. Finkelstein, and R. A. Gabbay. Economics of beta-cell replacement therapy. *Current diabetes reports*, 19(9):75, 2019.

[362] C. Bandeiras, J. M. S. Cabral, S. N. Finkelstein, and F. C. Ferreira. Tessee–tool for early stem cells economic evaluation. In *Mediterranean Conference on Medical and Biological Engineering and Computing*, pages 1919–1932. Springer, 2019.